Analysis and Design
of Orthotropic Steel Bridges

Miklós Iványi

Miklós M. Iványi

The book has been published in the framework of the

Leonardo Program of the European Union

TEMPUS SJEP 12116 (1997-2000)

"Continuing Education for the Steel Industry in Hungary: Towards European Union"

Research and Educational material: During the preparation of this book every effort has been made that it contains reliable data and information, however the Authors and the Publisher can not take responsibility for the validity of the information and for the consequences of the other use of the information contained in this book.

Preface

Orthotropic steel bridges are commonly used in long-span steel bridges in many parts of the world, especially in Central Europe. Their popularity is based on the fact, that very light structures with high rigidity and small amount of material can be constructed. The analysis and construction work of orthotropic steel bridges, however, are complicated and require special skills, which make such structures very suitable to be discussed at final year bridge engineering courses.

The first main Chapter of the book gives an overview on the theory of orthotropic plates. In the second Chapter, methods of analysis are discussed. The third Chapter deals with limit states and modelling of the different parts of an orthotropic structure. The fourth Chapter discusses the construction of such structures. The fifth Chapter deals with the refurbishment problems of orthotropic steel bridges. The sixth Chapter discusses the design of steel bridges according to Eurocode 3, and during three examples shows the application of these design rules. The extracts in the Appendixes help the understanding of the application of design rules.

The primary audience for this book is the post-graduate students, and research and design professionals working in the field of structural engineering. It is assumed that the reader has background knowledge of steel design.

Budapest - Pécs, August 2011.

Em. Prof. Dr. Miklós Iványi, PhD, DSc

Pollack Mihály Faculty of Engineering,

University of Pécs, Hungary

Dr. Miklós M. Iványi, PhD

Pollack Mihály Faculty of Engineering,

University of Pécs, Hungary

UVATERV Co.

Table of Contents

1 Introduction

1.1 Characteristics of Materials and Structures

We assume in discussing the structural behaviour of engineering materials they hold certain idealized natural physical properties. It is assumed that the material is a *perfectly elastic solid* which will proceed its initial form completely after unloading. Mathematically, this elastic property is described by Hooke's law. Further, we assume that it is *homogeneous* [Troitsky, 1987].

A solid, which shows identical elastic behaviour in all directions, is called *isotropic*. Actually, this is an idealization of physical properties, because very seldom do such material bodies or structural materials exist.

Physically, most structural materials, such as, for example, steel, are composed of crystals of various kinds, as well as orientations and elastic properties in all directions. However, in considering relatively small sizes of crystals and their random distribution, it may be assumed that the elastic behaviour of one piece of material is expressed by the average of elastic properties of all crystals. On the basis of this approximation, the material is considered to be isotropic.

Apart from homogeneous and isotropic materials, modern construction also uses materials with definitely expressed differences in elastic properties in different directions. Such materials are called *anisotropic*.

Sometimes the fabrication methods make it necessary to consider anisotropic conditions for structural materials. Some sheets of metal show a marked anisotropy, depending on the direction of rolling. Consequently, such sheets show different elastic properties in different directions.

In such case, where a body possesses different elastic properties in only two perpendicular or orthogonal directions, it is called *orthogonal-anisotropic*, or in short, *orthotropic*. Therefore, orthotropy is only a particular case of anisotropy. Orthotropy, due to the physical structure of the material itself, is called "*natural orthotropy*" [Troitsky, 1987].

For the structural design of orthotropic elements, which are in a state of elastic deformation, it is necessary to determine theoretically those stresses and deformations in the orthotropic solids, or to solve the problem of the theory of elasticity of such orthotropic solids.

1.2 Historical Development of Orthotropic Plate

1.2.1 First stiffened steel plates as bridge decks

Stiffened steel plates have been used for many years in steel construction, for instance in ship building, hydraulic structures such as gates, locks, etc. The term 'orthotropic plate' used in association with bridge decks originates from the invention of a particular type of stiffened steel plate for the deck of steel road bridges which led to a patent in 1948 [Patentschrift, 1948]. The 'orthotropic plate' according to this patent was more than just a stiffened light weight steel deck, because various such decks were already built before the patent [MAN, 1957]. A 'bridge with an orthotropic plate' according to the patent meant a new approach to bridge design by which steel weights of pre-war bridge designs, Fig. 1.1, could be reduced by up to 50% [Sedlacek, 1992].
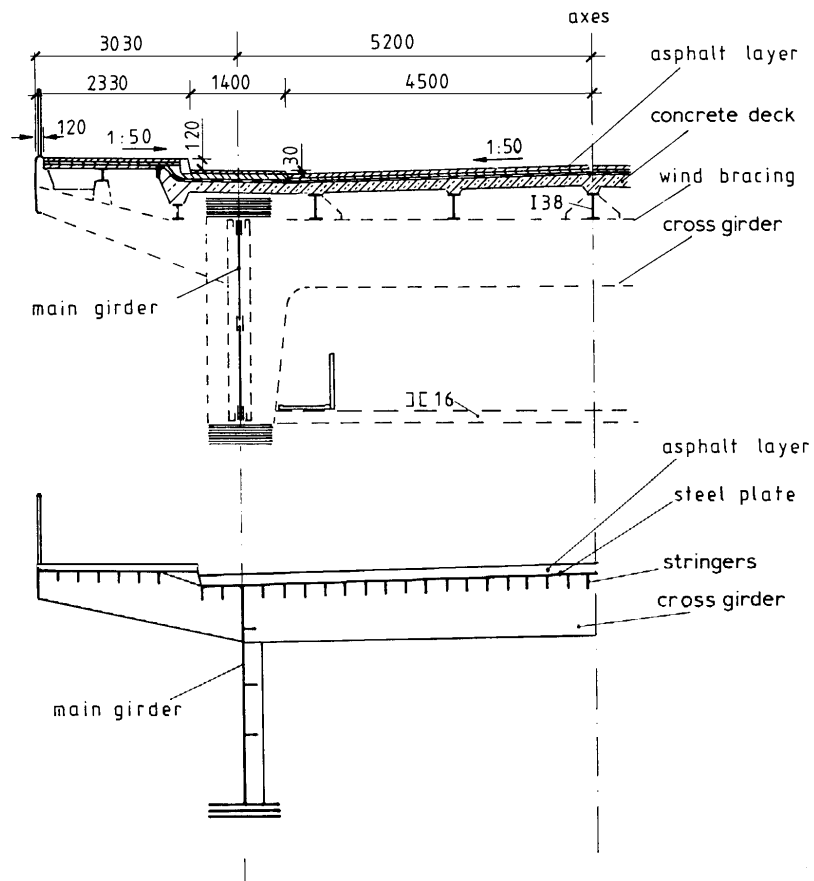
Figure 1.1 Traditional prewar bridge design with independent main girders, transverse beams, longitudinal girders and bridge deck and steel bridge with an orthotropic deck.

The main features of this breakthrough for steel bridges were:

– the deck plate forms an integral part of the main girders and cross girders and of the continuous longitudinal stringers by acting as part of their top flanges;
– the distance between the cross girders is smaller than 1/3 of the distance between the main girders allowing considerable advantage to be taken of the application of the theory of the *ortho*gonal–aniso*tropic* (orthotropic) plates to the design of the transverse and longitudinal girders, Fig. 1.2.
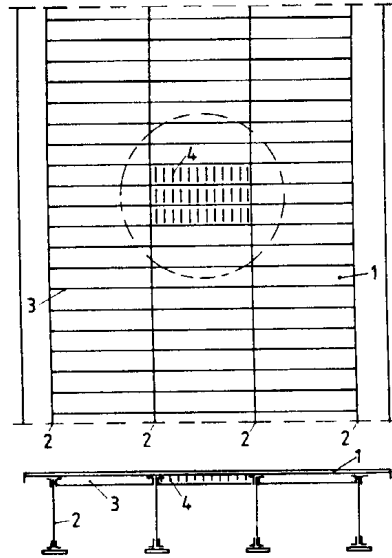
Figure 1.2 Bridge with an orthotropic plate according to the patent [Patentschrift, 1948].

The application rules associated with this patent were based on a minimum weight optimisation study. The original application rules in principle are still valid today with only small modifications caused by the change in the ratio of fabrication costs to material costs.

Stiffened steel deck plates used for road bridges are normally welded structures. The first deck was constructed in 1936, Fig. 1.3 [Schaechterle and Leonhardt, 1936]. The plate thickness was 10 mm, the distance between the longitudinal stringers made of I 457/152 was 51 cm and the distance between transverse beams was 1.09 m. All welds were hand welded fillet welds and took a lot of fabrication time. The main costs arose from the after-weld straightening procedure, which was needed because the weld shrinkage was not well controlled in those days.

As a result of this experience it was felt that larger spacings of the longitudinal stringers with the consequent reduction of weld-volume would improve the economy. This however led to damage to the asphalt layer [Roloff, 1942]. Hence it was necessary to return to smaller stringer spacings, which are now considered to be sufficient if the ratio of the distance, d, to the plate thickness, t, is such that $d/t < 25$, where the minimum thickness t is 12 mm.

In spite of this apparently regressive step the stiffened deck plates became more economical due to the introduction of automatic welding and a better understanding and control of shrinkage effects by the use of appropriate welding sequences, Fig. 1.4 [Pelikan, W. and Esslinger, M., 1957].

The first profiles for the stringers of orthotropic plates were open profiles such as angles, flat bars, or bulb fiats such as those used in ship building, Fig 1.5. For effective operation of these open sections the cross girders were spaced in the range of 0.9-1.9 m centres. The stringers normally ran continuously through the webs of the cross girders, Fig. 1.6, and the welded joints of the stringers were located at the points of contraflexure and detailed as illustrated in Fig. 1.7.

3

Due to the heavy costs of fabricating a deck with ship building profiles used as stringers, which were welded on both sides at the cross girder web intersections and other detailing solutions had to be found as indicated in Fig. 1.8, which made better allowance for the tolerances in the assembly and reduced the weld lengths.
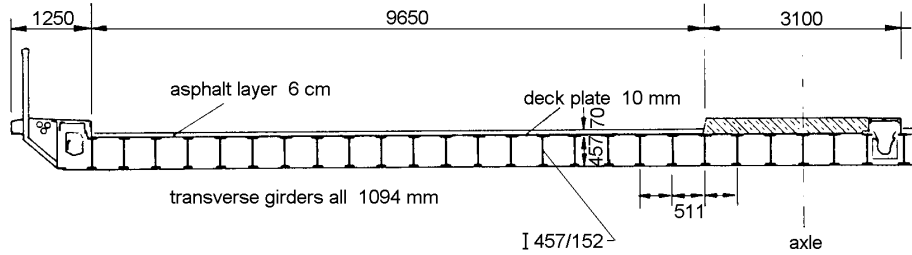
Figure 1.3 Stiffened steel deck of the highway bridge at Kircheim/Teck (Germany) built in [Schaechterle and Leonhardt, 1936].
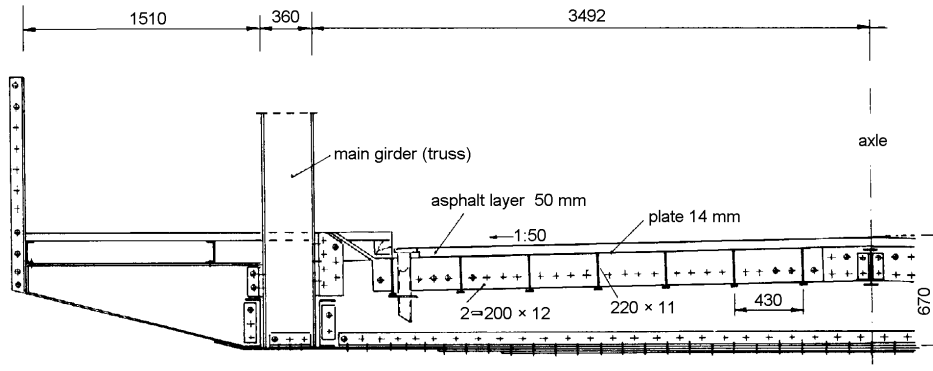
Figure 1.4 Stiffened steel deck with ship building profiles (Hasenhub Brodge in Meppen, Germany), 1947, [MAN, 1957].
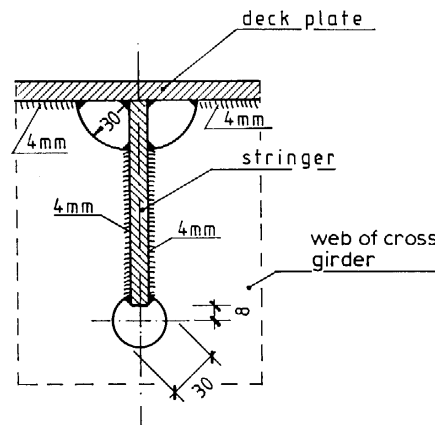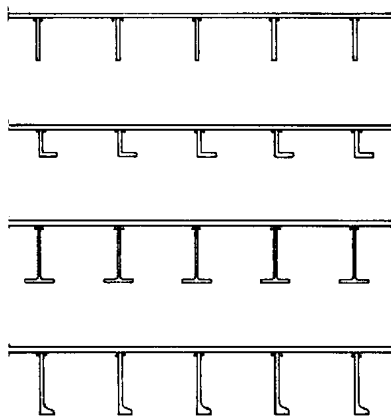
Figure 1.5 Open profiles for longitudinal stiffeners   **Figure 1.6** Stringers running through the webs of the cross girders [MAN, 1957].

4
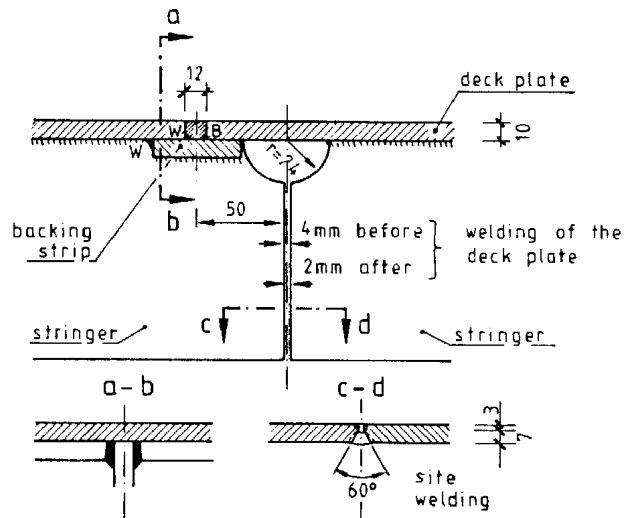
Figure 1.7 Detailing of the welded joints, [MAN, 1957].
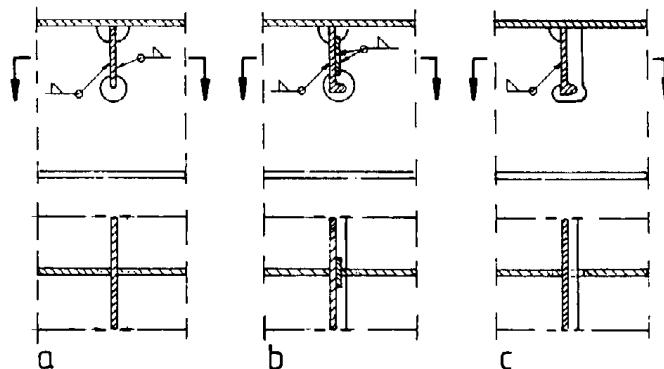
Figure 1.8 Development of the detailing of the connection between stringers and webs of cross girders, [Kunert, 1967].

1.2.2 First closed section stringers

In 1954 the first orthotropic decks with closed section stringers were constructed, Fig. 1.9.
    The advantages of this system were:

- — - the span lengths of the stringers were increased to 2.40 m and hence the number of costly hand welded intersections in the cross girders was reduced;
- — - the volume of the welds could be reduced by 50% by using one side welding only to the thin hollow closed stringers;
- — - advantage could be taken of the torsional rigidity in improving the local distribution of the deck.

5
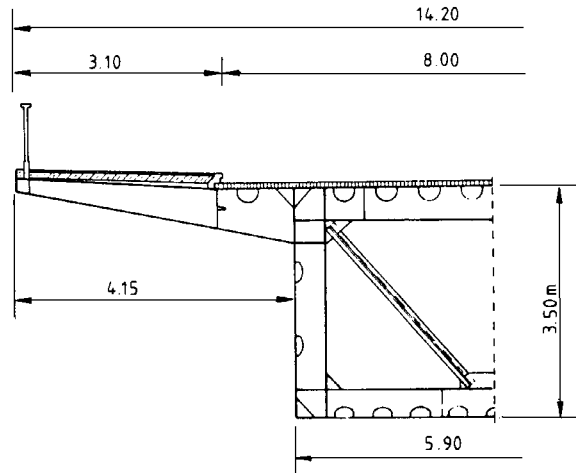
Figure 1.9 Orthotropic plate deck with closed section stringers (Weser-bridge Porta, Germany),
[Dörnen, 1955].

The disadvantage however appeared to be the lack of an economical welded joint solution for the stringers. The joints were either bolted, or the stringers were welded to each side of the web of the transverse beams, with large shrinkage effects being induced and thus a tendency to weld cracking. For some bridges this procedure later led to damage by crack propagation due to heat induced strains when the hot asphalt surfacing was put into place or due to traffic loads [Wolchuk, 1990] [Günther, 1985].

Further attempts were therefore undertaken to improve the detailing of orthotropic plate decks with closed stringers such as providing stringers running continuously through the webs of the cross girders and developing economic full welded joints.
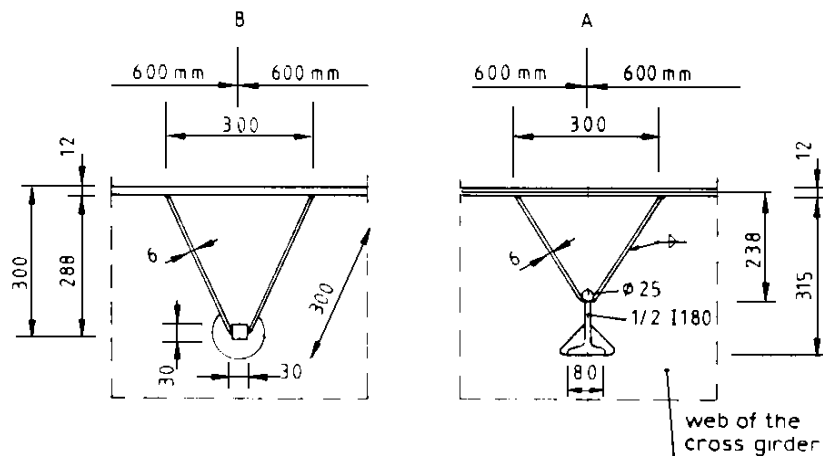
Figure 1.10 Champagne-glass profiles for longitudinal stringers, [Sedlacek, 1972].

6

The first step in this direction was represented by the development of 'champagne-glass-ribs' in the early 1960s, Fig. 1.10, built up of plates and rolled or other profiles. By increasing the bending resistance it was possible to extend the span lengths of the longitudinal stringers to up to 3.60 m and to adjust the chord profile to the local needs. At the crossings with the webs of the cross girders the flange sections ran continuously through whereas the plates were welded to the web plates, Fig. 1.11. The welded joint nominally was detailed as shown in Fig. 1.12, where tolerance problems and shrinkage effects accounted for by the 'window-joint-technique'.

The disadvantage of these built up stringers were the high welding costs as well as the tendency to cracking at the stringer-cross girder intersections caused by restraints to shrinkage resulting from the accumulation of welds in that zone.
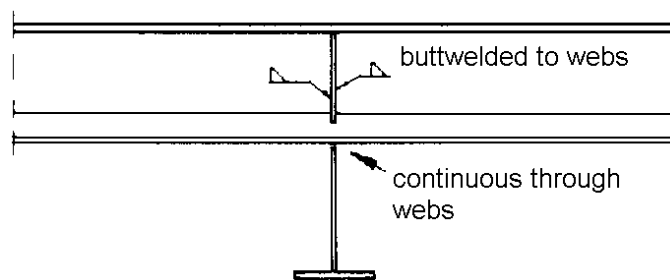
Figure 1.11 Detailing of the intersection between 'champagne-glass profiles' and the webs of cross girders.
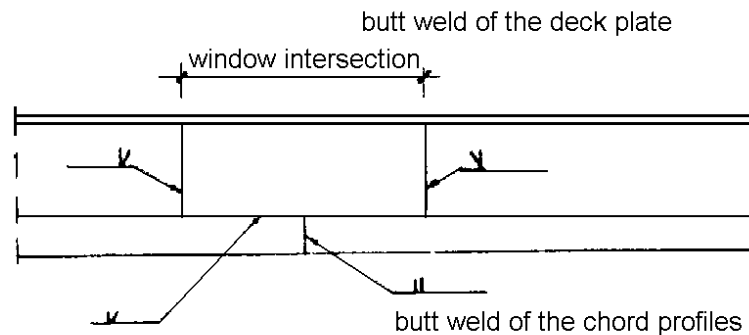
Figure 1.12 Welded joint of champagne-glass profiles with window-joint-technique.

1.2.3 Present standard of construction

In the late 1960s a breakthrough was achieved by the development of cold forming plants for sheet piling profiles in the steel industry. In these plants it was possible to produce long trapezoidal or vee shaped stringers from coils with acceptable geometries at acceptable prices. These profiles allowed cross girder spacings of up to 5 m to be achieved. By running the stringers through cross girder webs significant savings in the assembly and fabrication of deck panels were made possible, Fig. 1.13 [Sedlacek, 1972].
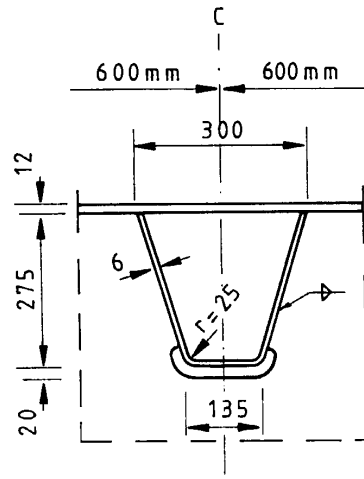
Figure 1.13 Detailing of the crossing of the hollow section stringers with the webs of the cross girders, [Sedlacek, 1972].

The cut outs in the cross girders' webs at the intersections were shaped such that the tolerances on the shapes of the hollow sections could be accounted for and sufficient fatigue resistance at the welds achieved. Using this technique a great amount of assembly and welding could be done automatically, Fig. 1.14. An economical solution for the welded joints the stringers was obtained using the 'window-joint-technique' as indicated in Fig. 1.15 [Kahmann, 1973].
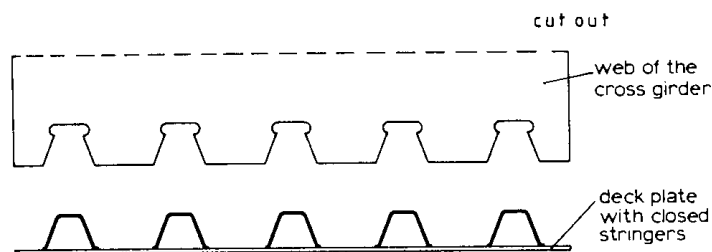
Figure 1.14 Assembly of the orthotropic plate.

These technical developments of the 'orthotropic plate' deck now provide the standard solution for road bridges and by slight modification of the cut outs, Fig. 1.16, also enable stiffened decks with closed ribs to be used for railway bridges. Fabrication costs could be further reduced by using similar construction also for the stiffened bottom flanges of box girders or for the webs of such girders with modifications only to the shape and spacing of the ribs.

Even in the case of bridges curved in plan orthogonal rib stiffening can be maintained by polygonal approximation using the 'window joint-technique' and where access of the window joints is restricted site welding can be carried out by separating the window-intersection-piece into two halves.

8
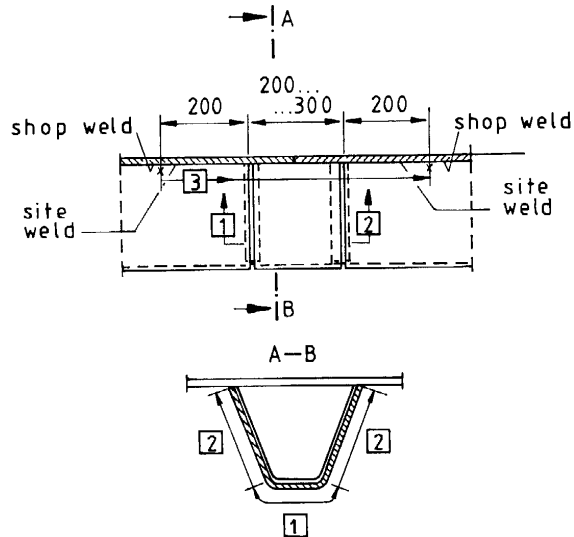
Figure 1.15 Welding sequence for the welded joint of the hollow section stringers with 'window-joint-technique', [Kahmann, 1973].
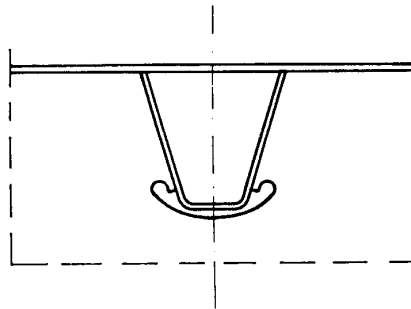
Figure 1.16 Improved cut out for orthotropic decks for railway bridges.

The trend to greater span lengths of closed section stringers however has been limited by the following factors:

- The production of deep trapezoidal ribs gives rise to tolerance problems and hence increases the assembly costs.
- Deep ribs lead to larger cut outs in the webs of the cross girders, Fig. 1.17, and produce a significant reduction of the shear resistance that cannot easily be compensated by the bending stiffness of the deck plate.
- Last but not least, the traffic loads on long span stiffeners may cause deflections, Fig. 18 [Günther et al., 1987], associated with large local transverse curvatures in the deck plate which may cause cracking of the asphalt surfacing. Experience of such surfacing cracks on orthotropic decks with large stringer spans has been used to formulate a requirement

9

for a minimum rib stiffness to prevent cracking of the surfacing. This can control the stringer design in many cases.

Using the above design criteria span lengths of stringers are normally limited to 3.50 – 4.50 m.
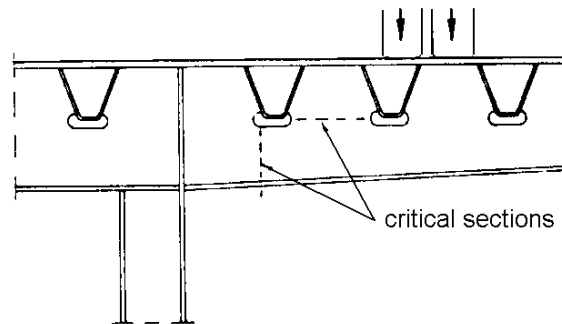
Figure 1.17 Critical sections for the shear and local bonding in the web of the cross girders.
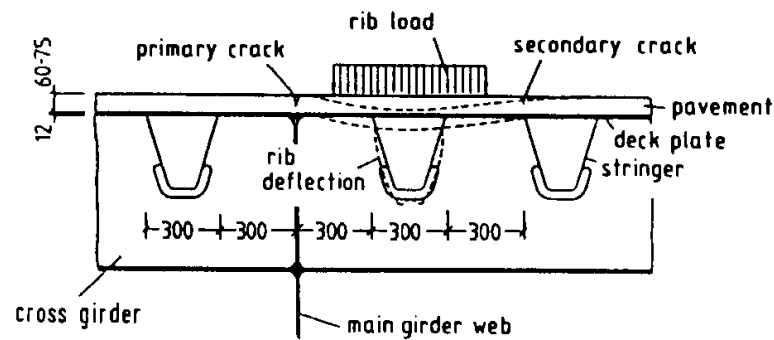
Figure 1.18 Potential positions of cracks in the asphalt layer, [Günther et al., 1987].

1.3 Introduction to Behaviour of Plated Structures

Plates are very important elements in steel structures. They can be assembled into complete members by the basic rolling process (as hot rolled sections), by folding (as cold formed sections) and by welding. The efficiency of such sections is due to their use of the high in-plane stiffness of one plate element to support the edge of its neighbour, thus controlling the out-of-plane behaviour of the latter [ESDEP, 1994].

The size of plates in steel structures varies from about 0.6 mm thickness and 70 mm width in a corrugated steel sheet, to about 100 mm thick and 3 m width in a large industrial or offshore structure. Whatever, the scale of construction the plate panel will have a thickness t that is much smaller than the width b, or length a. As will be seen later, the most important geometric

parameter for plates is b/t and this will vary, in an efficient plate structure, within the range 30 to 250.

1.3.1 Basic behaviour of a plate panel

Understanding of plate structures has to begin with an understanding of the modes of behaviour of a single plate panel.

1.3.1.1 Geometric and boundary conditions with different actions

The important geometric parameters are thickness t, width b (usually measured transverse to the direction of the greater direct stress) and length a, see Fig. 1.19.a. The ratio b/t, often called the plate slenderness, influences the local buckling of the plate panel; the aspect ratio a/b may also influence buckling patterns and may have a significant influence on strength.

(a) Single plate panel

(b) In-plane action, pre-buckling

(c) Out-of-plane action, small displacements

(d) In-plane action, post-buckling

(e) Out-of-plane action, large displacements
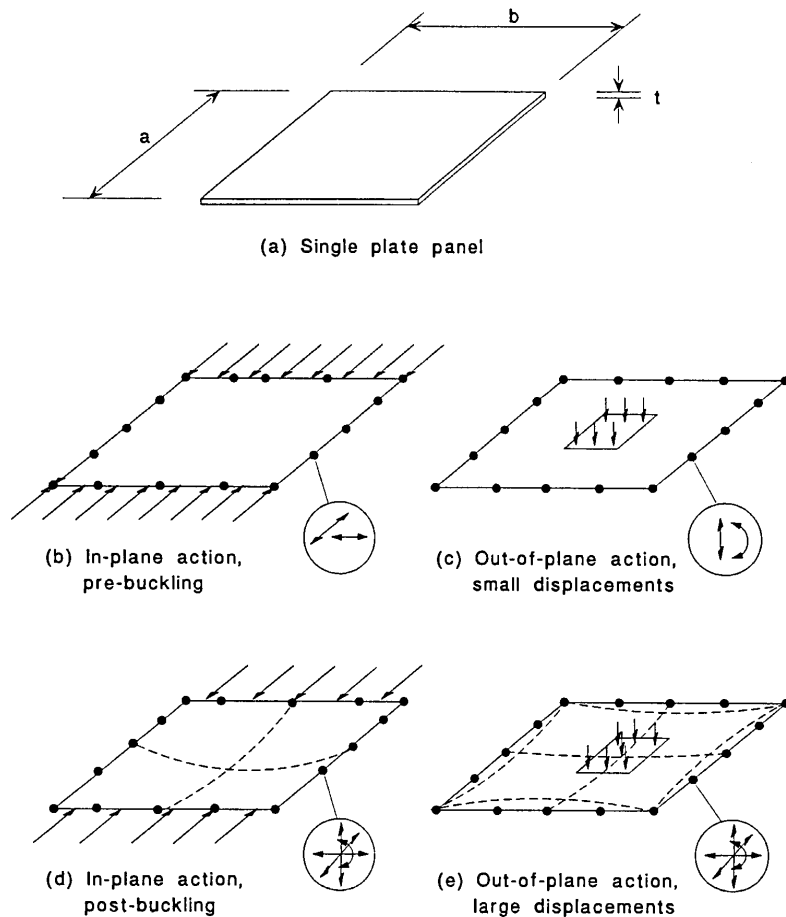
Figure 1.19 Significant boundary conditions for plate panels.

11

In addition to the geometric proportions of the plate, its strength is governed by its boundary conditions. Fig. 1.19 shows how response to different types of actions is influenced by different boundary conditions. Response to in-plane actions that do not cause buckling of the plate is only influenced by in-plane, plane stress, boundary conditions, Fig. 1.19.b. Initially, response to out-of-plane action is only influenced by the boundary conditions for transverse movement and edge moments, Fig. 1.19.c. However, at higher actions, responses to both types of action conditions are influenced by all four boundary conditions. Out-of plane conditions influence the local buckling, see Fig. 1.19.d; in-plane conditions influence the membrane action effects that develop at large displacements (> t) under lateral actions, see Fig. 1.19.e.

(a) In-plane actions

As shown in Fig. 1.20.a, the basic types of in-plane actions to the edge of a plate panel are the distributed action that can be applied to a full side, the patch action or point action that can be applied locally.

When the plate buckles, it is particularly important to differentiate between applied displacements, see Fig. 1.20.b and applied stresses, see Fig. 1.20.c. The former permits a redistribution of stress within the panel; the more flexible central region sheds stresses to the edges giving a valuable post buckling resistance. The latter, rarer case leads to an earlier collapse of the central region of the plate with in-plane deformation of the loaded edges.
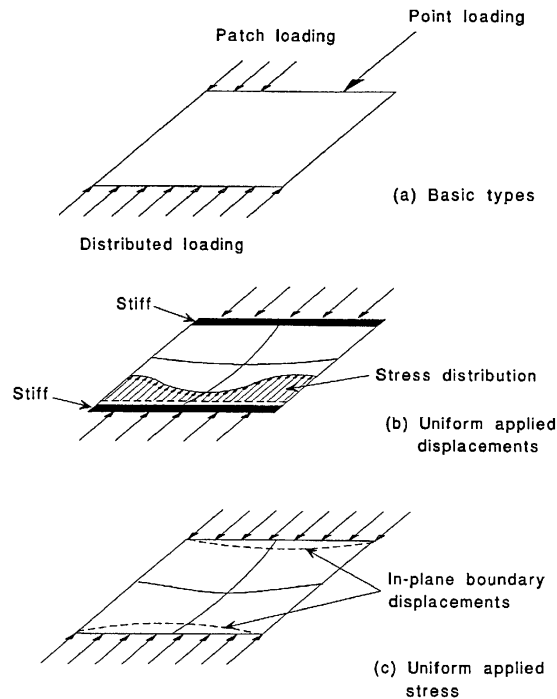
Figure 1.20 Types of in-plane actions.

(b) Out-of-plane actions

Out-of-plane loading may be:

- uniform over the entire panel, see for example Fig. 1.21.a, the base of a water tank,
- varying over the entire panel, see for example Fig. 1.21.b, the side of a water tank,
- a local patch over part of the panel, see for example Fig. 1.21.c, a wheel toad on a bridge deck.

(a) Uniformly distributed loading   (b) Variable distributed loading

(c) Patch loading
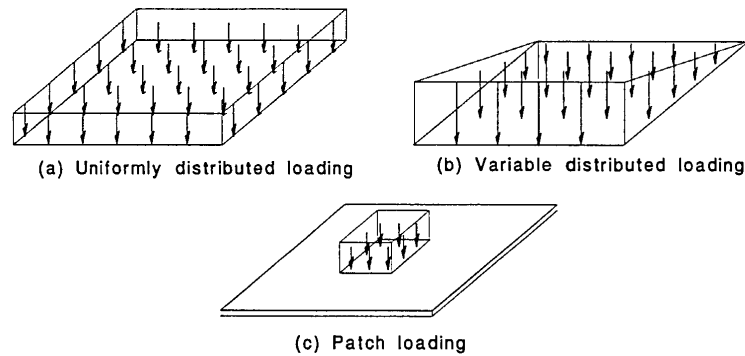
Figure 1.21 Types of out-of-plane actions.

1.3.1.2 Determination of plate panel actions

In some cases, for example in Fig. 1.22.a, the distribution of edge actions on the panels of a plated structure is self-evident. In other cases the in-plane flexibilities of the panels lead to distributions of stresses that cannot be predicted from simple theory. In the box girder shown in Fig. 1.22.b, the in-plane shear flexibility of the flanges leads to in-plane deformation of the top flange. Where these are interrupted, for example at the change in direction of the shear at the central diaphragm, the resulting change in shear deformation leads to a non-linear distribution of direct stress across the top flange; this is called **shear lag**.

In members made up of plate elements, such as the box girder shown in Fig. 1.23, many of the plate components are subjected to more than one component of in-plane action effect. Only panel A does not have shear coincident with the longitudinal compression.

If the cross-girder system EFG, was a means of introducing additional actions into the box, there would also be transverse direct stresses arising from the interaction between the plate and the stiffeners.

1.3.1.3 Variations in buckled mode

I.   Aspect ratio a/b

In a long plate panel, as shown in Fig. 24, the greatest initial inhibition to buckling is the transverse flexural stiffness of the plate between unloaded edges. (As the plate moves more into the post-buckled regime, transverse membrane action effects become significant as the plate deforms into a non-developable shape, i.e. a shape that cannot be formed just by bending).

(a) Box column

(b) Box girder at internal support
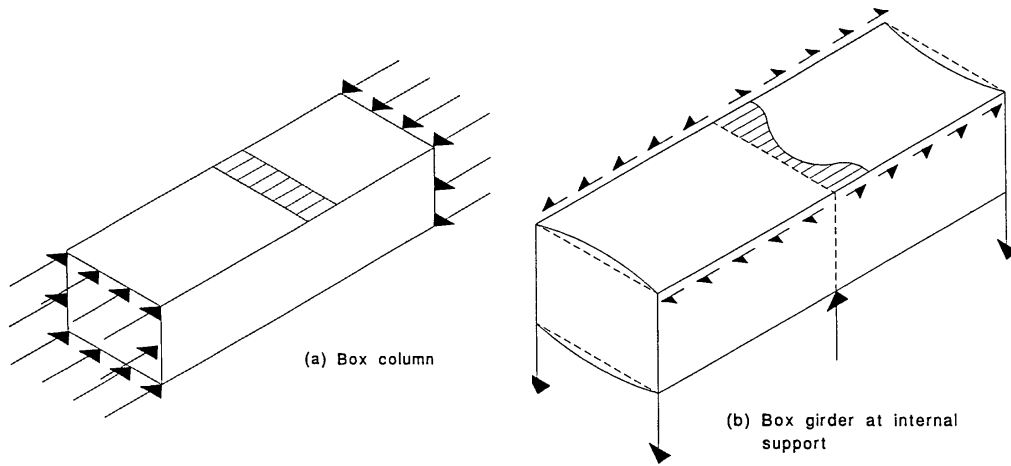
Figure 1.22 Effect of shear lag on distribution of stresses in plated structures.

A
Compression

B
Compression & shear

C
Compression & shear

D
Tension & shear
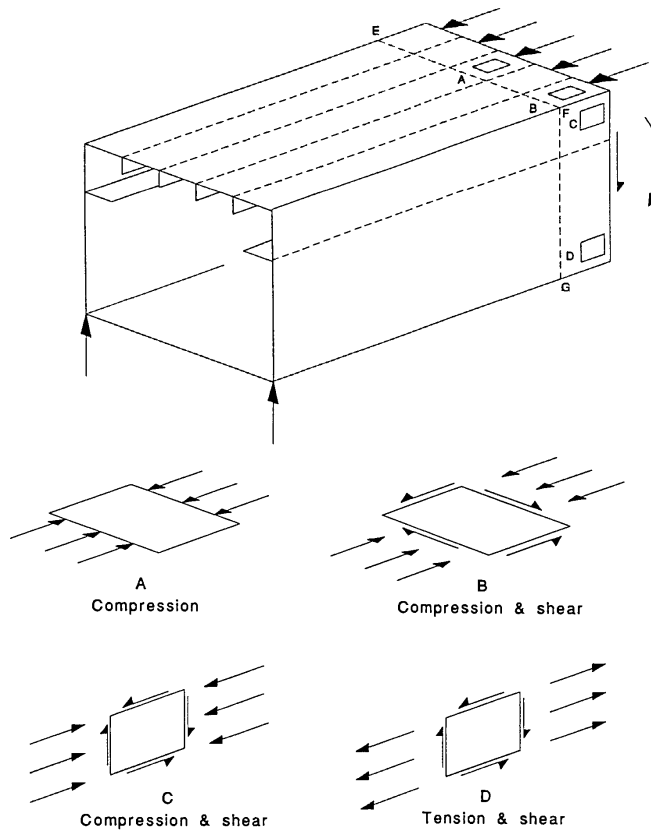
Figure 1.23 Examples of components of action on plate panels in a box girder.

m = Number of half waves
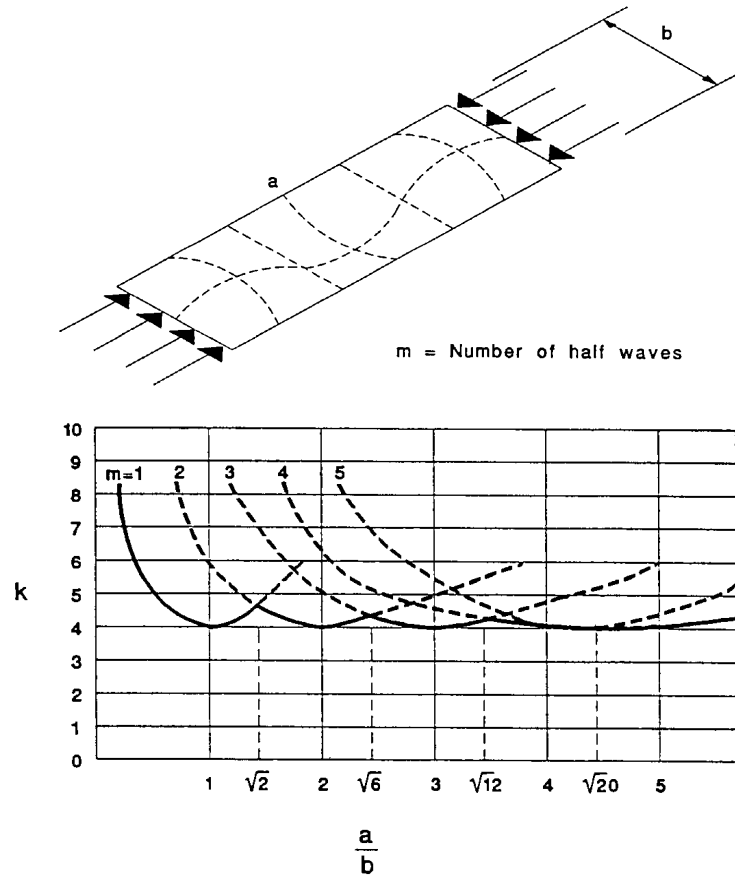
Figure 1.24 Variations in buckled mode with aspect ratio for a plate panel in longitudinal compression.

As with any instability of a continuous medium, more than one buckled mode is possible, in this instance, with one half wave transversely and in half waves longitudinally. As the aspect ratio increases the critical mode changes, tending towards the situation where the half wave length $a/m = b$. The behaviour of a long plate panel can therefore be modelled accurately by considering a simply-supported, square panel.

II.   Bending conditions

As shown in Fig. 1.25, boundary conditions influence both the buckled shapes and the critical stresses of elastic plates. The greatest influence is the presence or absence of simple supports, for example the removal of simple support to one edge between case 1 and case 4 reduces the buckling stress by a factor of 4.0/0.425 or 9.4. By contrast introducing rotational restraint to one edge between case 1 and case 2 increases the buckling stress by 1.35.

15

$$\sigma_{cr} = k \cdot \frac{\pi^2 E t^2}{12 \left(1 - \nu^2\right) b^2}$$
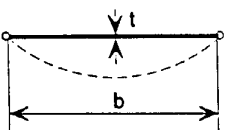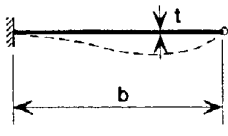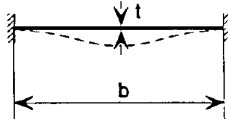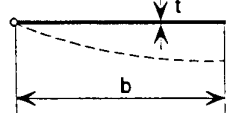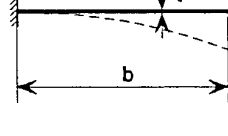
Case	Description of support at the unloaded edges		k
1	Both edges simply supported		4.00
2	One edges simply supported, the other fixed		5.42
3	Both edges fixed supported		6.97
4	One edges simply supported, the other free		0.425
5	One edge fixed, the other free		1.277

Figure 1.25 Coefficients for plate buckling in compression for various boundary conditions.

III.   Interaction of modes

Where there is more than one action component, there will be more than one mode and therefore there may be interaction between the modes. Thus in Fig. 1.26.b(i) the presence of low transverse compression does not change the mode of buckling. However, as shown in Fig. 1.26.b(ii), high transverse compression will cause the panel to deform into a single half wave. (In some circumstances this forcing into a higher mode may increase strength; for example, in case 26.b(ii), predeformation/transverse

compression may increase strength in longitudinal compression.) Shear buckling as shown in Fig. 1.26.c is basically an interaction between the diagonal, destabilising compression and the stabilising tension on the other diagonal.

Where buckled modes under the different action effects are similar, the buckling stresses under the combined actions are less than the addition of individual action effects. Fig. 1.27 shows the buckling interactions under combined compression, and uniaxial compression and shear.

(a) Uniaxial compression

(bi) Biaxial compression, longitudinal compression predominating

(bii) Biaxial compression, transverse compression predominating

(c) Shear
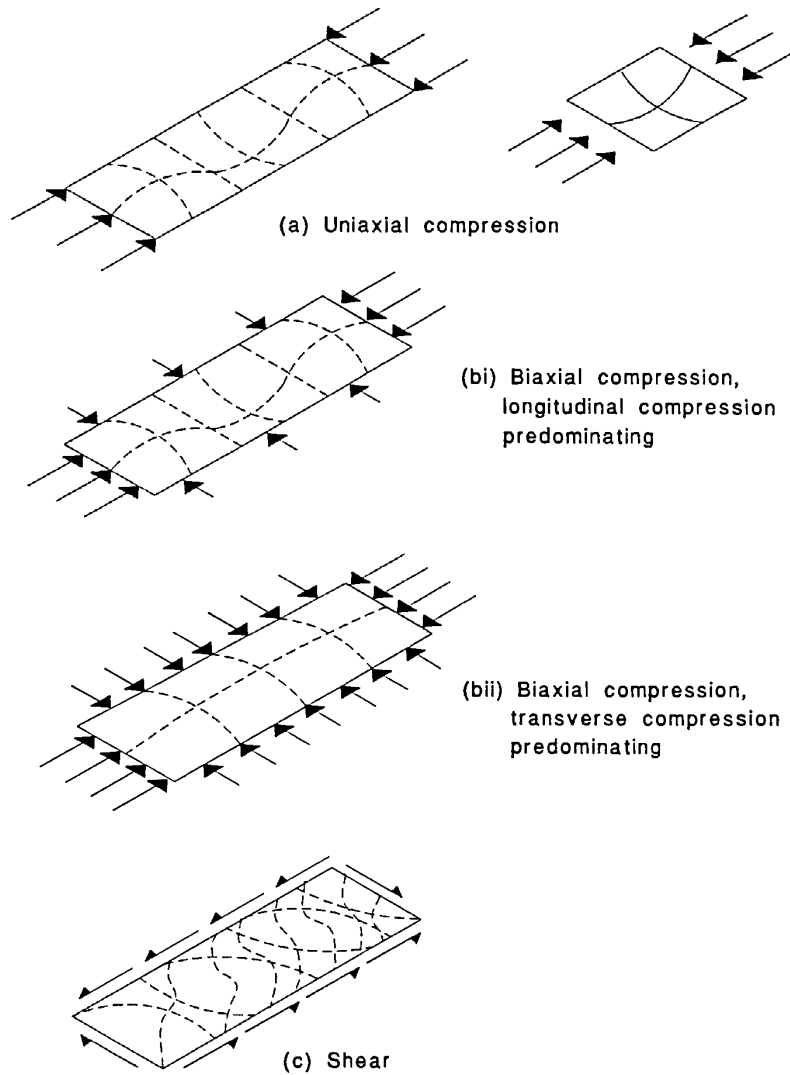
Figure 1.26 Buckling modes for plate panels.
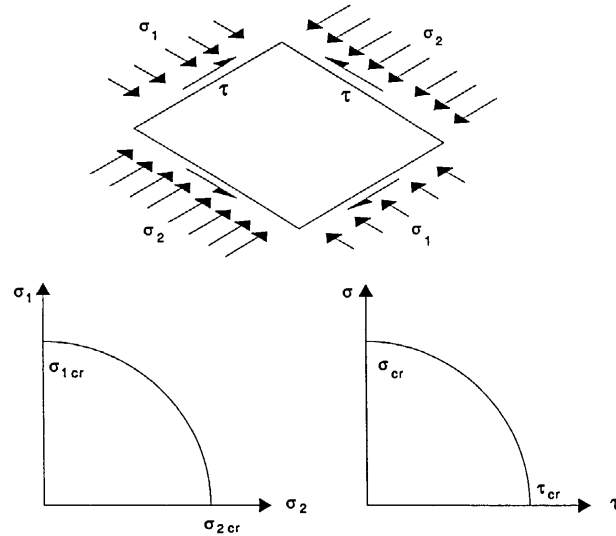
Figure 1.27 Interaction of buckling modes for square plate panel.

1.3.1.4 Post buckling behaviour

Figs. 1.28.a, 1.28.b and 1.28.c describe in more detail the changing distribution of stresses as a plate buckles following the equilibrium path shown in Fig. 1.28.d. As the plate initially buckles the stresses redistribute to the stiffer edges. As the buckling continues this redistribution becomes more extreme (the middle strip of slender plates may go into tension before the plate fails). Also transverse membrane stresses build up. These are self-equilibrating unless the plate has clamped in-plane edges; tension at the mid panel, which restrains the buckling is resisted by compression at the edges, which are restrained from out-of plane movement.

An examination of the non-linear longitudinal stresses in Fig. 1.28.a and 28.c shows that it is possible to replace these stresses by rectangular stress blocks that have the same peak stress and same action effect. This effective width of plate (comprising $b_{eff}/2$ on each side) proves to be a very effective design concept. Fig. l.28.e shows how effective width varies with slenderness (λ_p, is a measure of plate slenderness that is independent of yield stress, $\lambda = 1,0$ corresponds to values of b/t of 57, 53 and 46 for f_y of 235N/mm^2, 275 N/mm^2 and 355 N/mm^2 respectively).

(a) Pre-buckling

(b) Post-buckling
$P \doteq P_{cr}$

(c) Post-buckling
$P > P_{cr}$

(d)
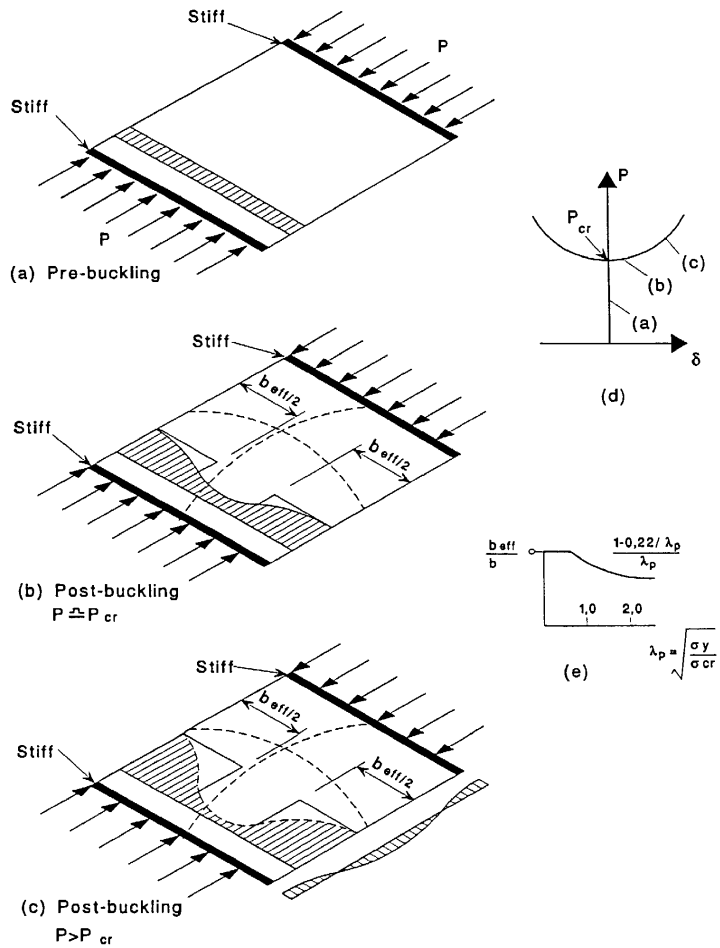
Figure 1.28

Buckling behaviour of
square plate in compression
with simply supported
edges free to pull in but
held straight.

$$\frac{b_{eff}}{b} \quad \frac{1 - 0,22/\lambda_p}{\lambda_p}$$

$$\lambda_p = \sqrt{\frac{\sigma y}{\sigma cr}}$$

(e)

(a) Effective widths

Fig. 1.29 shows how effective widths of plate elements may be combined to give an effective cross-section of a member.

Figure 1.29 (a) Effective section (shaded) for typical members in axial compression.

(b) Effective section (shaded) for typical plate girder under sagging moment.

Figure 1.29 The application of effective widths of plate panels to determine effective cross-sections.

(b) Grillage analogy for plate buckling

One helpful way to consider the buckling behaviour of a plate is as the grillage shown in Fig. 1.30. A series of longitudinal columns carry the longitudinal actions. When they buckle, those nearer the edge have greater restraint than those near the centre from the transverse flexural members. They therefore have greater post buckling stiffness and carry a greater proportion of the action. As the grillage moves more into the post-buckling regime, the transverse buckling restraint is augmented by transverse membrane action.
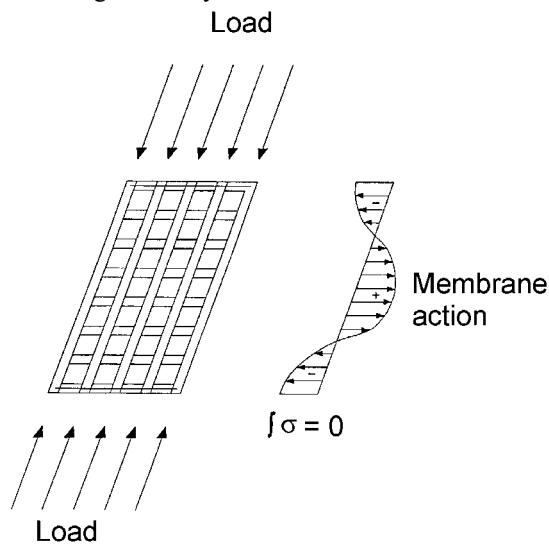
Figure 1.30 Grid model of plate in compression.

1.3.1.5 The influences of imperfections on the behaviour of actual plates

As with all steel structures, plate panels contain residual stresses from manufacture and subsequent welding into plate assemblies, and are not perfectly flat. The previous discussions about plate panel behaviour all relate to an ideal, perfect plate. As shown in Fig. 1.31 these imperfections modify the behaviour of actual plates. For a slender plate the behaviour is asymptotic to that of the perfect plate and there is little reduction in strength. For plates of intermediate slenderness (which frequently occur in practice), an actual imperfect plate will have a considerably lower strength than that predicted for the perfect plate.

20

Fig. 1.32 summarises the strength of actual plates of varying slenderness. It shows the reduction in strength due to imperfections and the post buckling strength of slender plates.
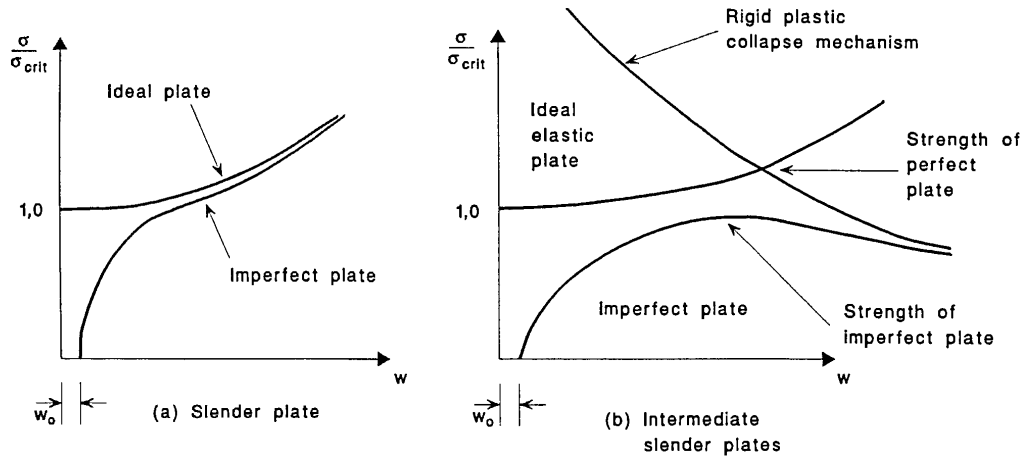
Figure 1.31 The influence of imperfections on the behaviour of plates of different slenderness in compression.
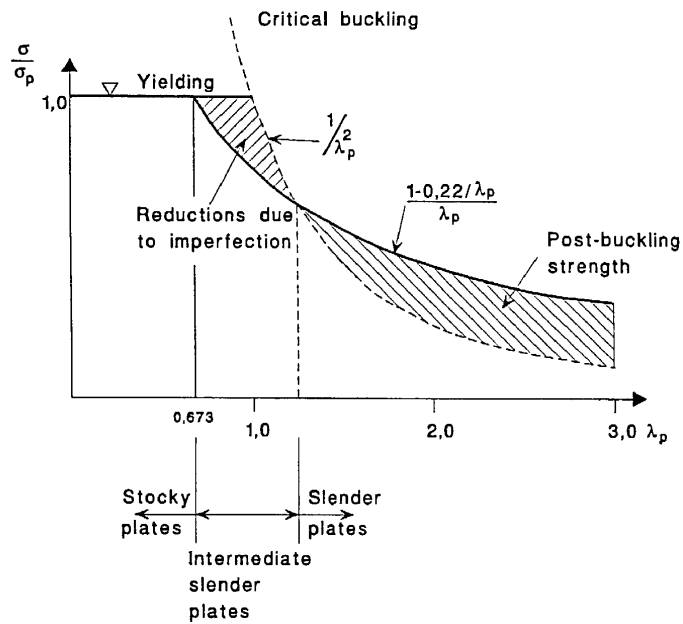
Figure 1.32 Relationship between plate slenderness and strength in compression.

1.3.1.6 Elastic behaviour of plates under lateral actions

The elastic behaviour of laterally loaded plates is considerably influenced by its support conditions. If the plate is resting on simple supports as in Fig. 1.33.b, it will deflect into a shape approximating a saucer and the corner regions will lift off their supports. If it is attached to the supports, as in Fig. 1.33.c, for example by welding, this lift off is prevented and the plate stiffness and action capacity increases. If the edges are encastré as in Fig. 1.33.d, both stiffness and strength are increased by the boundary restraining moments.

Pressure p

(a) Plate under uniform lateral pressure p.

(b) Simply supported edges, corners free to lift.

(c) Simply supported edges, corners held down.

(d) Encastré edges

(e) Simply supported edges, corners held down, large displacements, edges held straught.
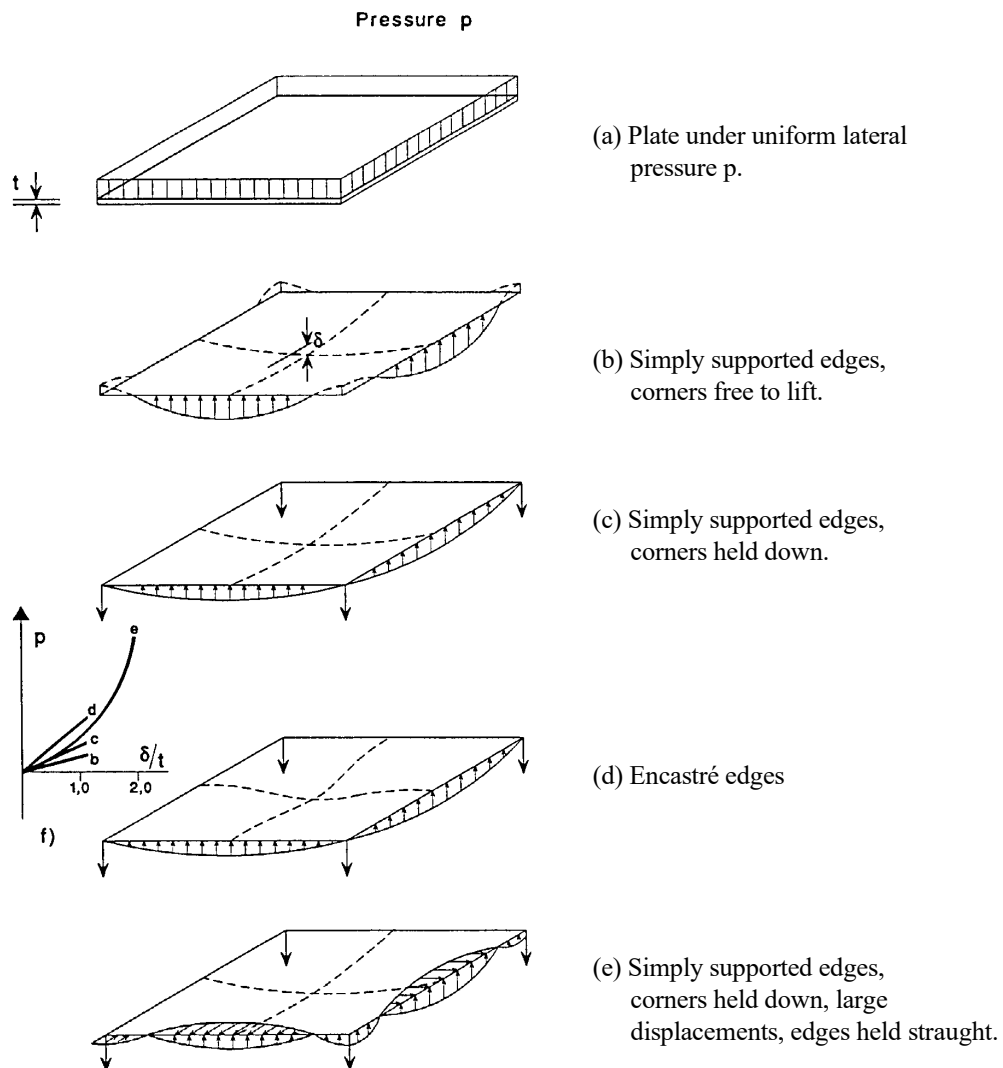
Figure 1.33 Elastic behaviour of square plate under lateral actions with different boundary conditions.

Slender plates may well deflect elastically into a large displacement regime (typically where d > t). In such cases the flexural response is significantly enhanced by the membrane action of the plate. This membrane action is at its most effective if the edges are fully clamped. Even if they are only held partially straight by their own in-plane stiffness, the increase in stiffness and strength is most noticeable at large deflections.

Fig. 1.33 contrasts the behaviour of a similar plate with different boundary conditions.

Fig. 1.34 shows the modes of behaviour that occur if the plates are subject to sufficient load for full yield line patterns to develop. The greater number of yield lines as the boundary conditions improve is a qualitative measure of the increase in resistance.

(a) Plate under uniform lateral pressure p.

(b) Simply supported edges, corners free to lift.

(c) Simply supported edges, corners held down.

(d) Encastré edges
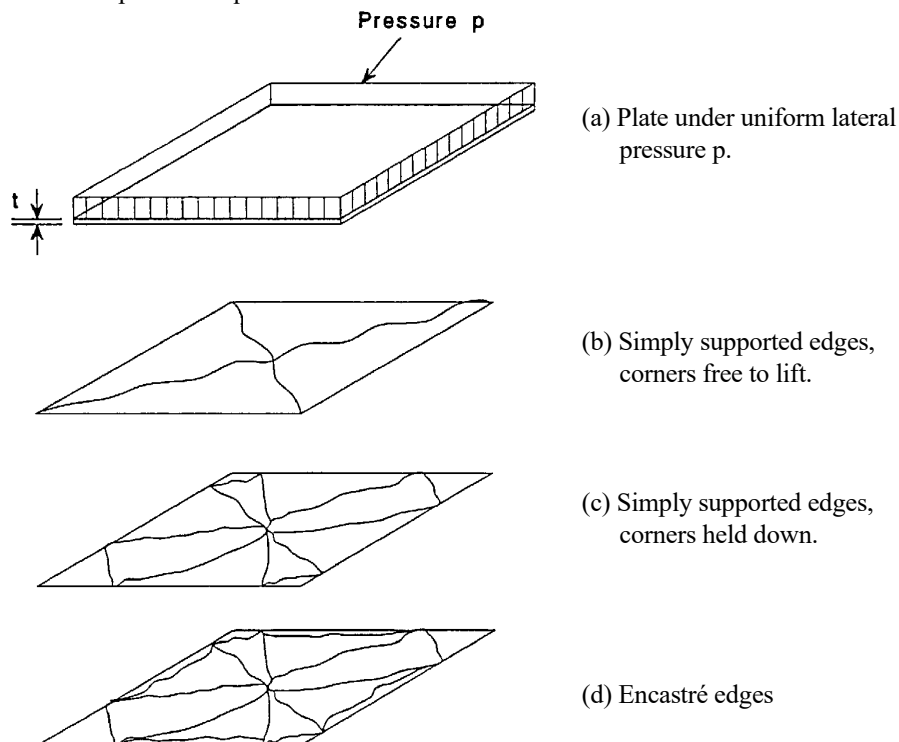
Figure 1.34 Yield line patterns for square plates under lateral loading with various boundary conditions.

1.3.2 Behaviour of stiffened plates

Many aspects of stiffened plate behaviour can be deduced from a simple extension of the basic concepts of behaviour of unstiffened plate panels [ESDEP, 1994]. However, in making these extrapolations it should be recognised that:

- "smearing" the stiffeners over the width of the plate can only model overall behaviour.
- stiffeners are usually eccentric to the plate. Flexural behaviour of the equivalent tee section induces local direct stresses in the plate panels.
- local effects on plate panels and individual stiffeners need to be considered separately.

– the discrete nature of the stiffening introduces the possibility of local modes of buckling. For example, the stiffened flange shown in Fig. 1.35.a shows several modes of buckling. Examples are:

i. plate panel buckling under overall compression plus any local compression arising from the combined action of the plate panel with its attached stiffening, Fig. 1.35.b.

ii. stiffened panel buckling between transverse stiffeners, Fig. 1.35.c. This occurs if the latter have sufficient rigidity to prevent overall buckling. Plate action is not very significant because the only transverse member is the plate itself. This form of buckling is best modelled by considering the stiffened panel as a series of tee sections buckling as columns. It should be noted that this section is monosymmetric and will exhibit different behaviour if the plate or the stiffener tip is in greater compression.

iii. overall or orthotropic bucking, Fig. 1.35.d. This occurs when the cross girders are flexible. It is best modelled by considering the plate assembly as an orthotropic plate.

(a) Stiffened plate

(b) Plate buckling

(c) Stiffened panel buckling

(d) Orthotropic buckling
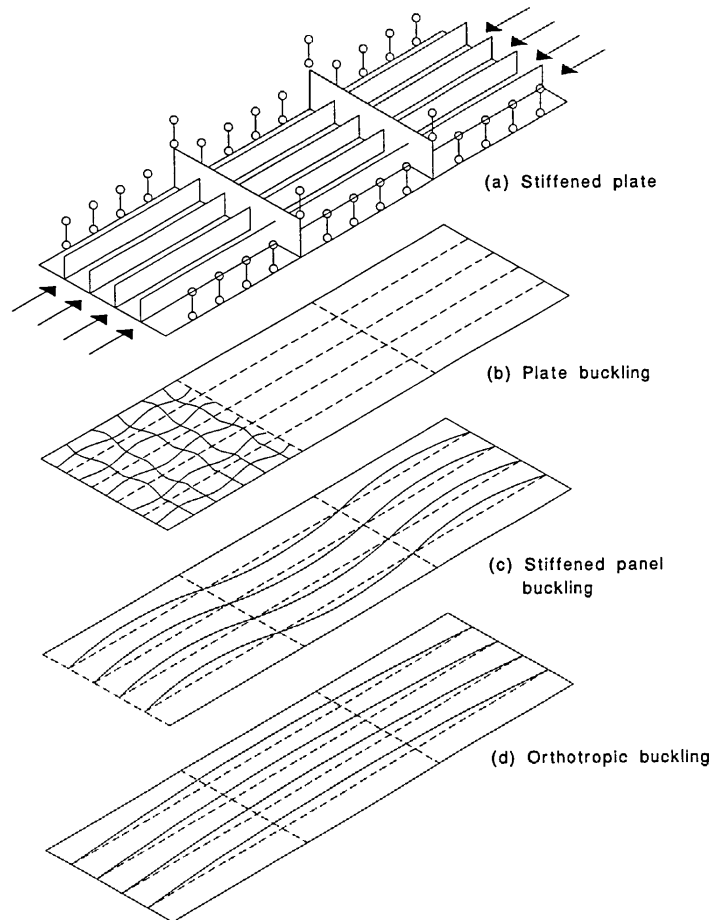
Figure 1.35 Buckling modes for stiffened plates in compression.

1.3.3 Concluding summary

– Plates and plate panels are widely used in steel structures to resist both in-plane and out-of plane actions.
– Plate panels under in-plane compression and/or shear are subject to buckling.
– The elastic buckling stress of a perfect plate panel is influenced by:
  – plate slenderness (b/t).
  – aspect ratio (a/b).
  – boundary conditions.
  – interaction between actions, i.e. biaxial compression and compression and shear.
– The effective width concept is a useful means of defining the post-buckling behaviour of a plate panel in compression.
– The behaviour of actual plates is influenced by both residual stresses and geometric imperfections.
– The response of a plate panel to out-of-plane actions is influenced by its boundary conditions.
– An assembly of plate panels into a stiffened plate structure may exhibit both local and overall modes of instability.

1.4 Modelling of Bridges with Orthotropic Plates

Modern decks consist of concrete slabs or orthotropic steel decks. Despite the different materials, it is possible to identify common themes in their development.

1.4.1 From separation to integration of functions

Partly because of limited understanding of behaviour and methods of analysis, and partly because it suited historical methods of construction, early decks were separated from the remainder of the superstructure. The steel "battledeck" comprised plate panels welded to rolled beams as stiffeners that were supported by and spanned simply between cross-girders which, in turn, spanned between the principal girders. The deck construction was relatively deep but could still fit within the overall depth of the truss. A similar approach can be seen in a concrete deck slab. The slab acts compositely with the stringers but does not contribute to overall bending.

Although this separation reduced the overall efficiency of the design, it is noteworthy that it does assist bridge repairs. For example, the entire deck of the Golden Gate Bridge in San Francisco was replaced during night time possessions, permitting the bridge to continue to be used during the day.

Modern decks in both materials are fully integrated into the overall superstructure. These integrated decks improve the economy of the primary structure considerably. In all - steel construction the cross girders and main girders do not need separate top flanges. With a concrete deck, rolled sections (used for cross girders and main girders for short spans) will be considerably lighter. The top flanges of plate girders will typically be half the cross-section that would have been needed for non-composite construction.

The disadvantage of integrated construction is that repair or replacement of the deck is difficult and usually requires prolonged closure of the bridge.

1.4.2 Greater simplicity

The increasing ratio of labour to material costs has encouraged the development of simpler forms of construction. Simplification has been considerably assisted by the development of modern welding techniques.

For example, early attempts to arrange stringers and cross-girders at the same level required the bolted or riveted connection shown in Fig. 1.36.a. Its modern equivalent in Fig. 1.36.b is readily accomplished with reliable welding.
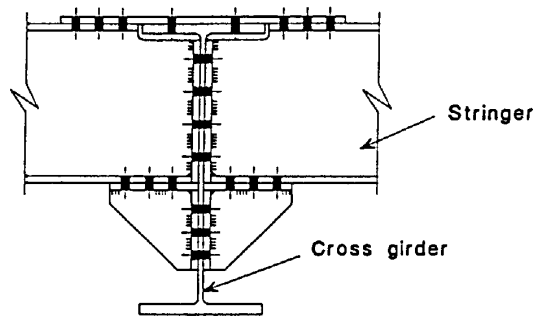
(a) Early bolted or riveted construction
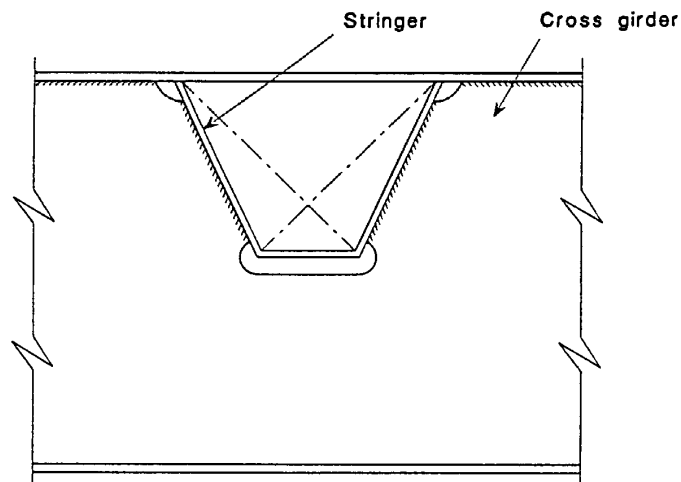
(b) Modern welded construction

**Note:- Different orientation of diagrams
to illustrate connections**

Figure 1.36 Stringer / Cross girder intersections.

1.4.3 Evolution of the stringer in steel plates

A very important aspect of the historical development of steel plates is the evolution in form of longitudinal stiffeners or stringers. Initially, only open stiffeners shown in Fig. 1.37.a were utilised. Flats (i) and (ii) are simple to work with but are relatively inefficient in bending; bulb flats (iii) are more efficient in bending but are prone to lateral instability; tees (iv) and angles (v) offer a good combination of longitudinal bending strength and resistance to lateral buckling. All these open stiffeners have the basic disadvantage that they are flexible in torsion. Their use leads to a panel that is strongly orthotropic with little torsion stiffness ($D_x \gg D_y$ or D_{xy}). Such panels are inefficient as transverse distribution of local loads leading to a narrow effective width in bending and high longitudinal stresses under patch loading.
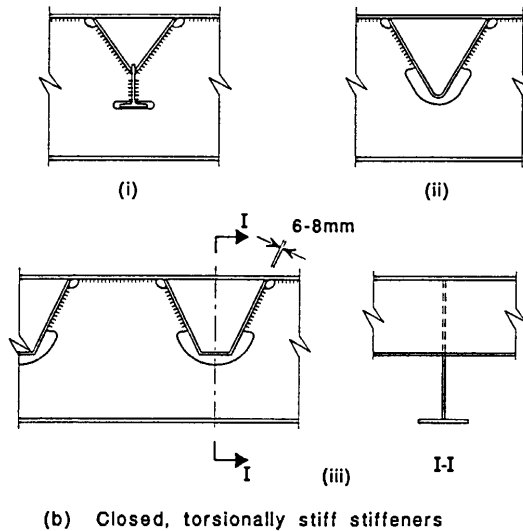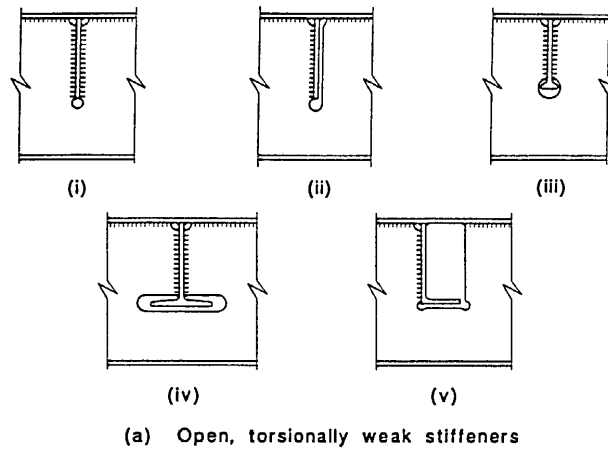
Figure 1.37 Stiffeners (stringers) for orthotropic steel plates.

It would be possible but expensive to introduce local transverse stiffeners to increase D_y, but it is feasible to increase D_{xy}, and thereby improve transverse distribution, by using closed stiffeners. Fig. 1.37.b shows the closed stiffeners that have been developed. Initially, the "wineglass" stiffener (i) was developed for the early post war Rhine bridges in Germany. This stiffener gave a good combination of torsional and bending stiffness but was expensive to fabricate. Subsequently, the Vee and the trapezoidal stiffener were developed. The latter gives better bending resistance than the former, although it loses some torsional stiffness from cross-section distortion.

The earliest welded battledecks were detailed with continuity to the web of the cross girder, for example (a)(i). This created a very poor fatigue detail for the stringers. Subsequently, it became common practice to slot the web and have continuous stringers, for example (a)(iv) + (v) and (b)(ii) and (iii). With suitably rounded openings in the web, no fatigue problem is created in that element. It is noteworthy that the extreme fibres of the stringers are also not welded, thereby improving their fatigue performance.

1.4.4 Modelling of bridges with orthotropic plates

A steel bridge with an orthotropic plate represents an integral structure, where the orthotropic plate serves as a load distributing deck plate as well as a tension or compression flange of the main girders. For modelling purposes the structure is often decomposed into sub-structures to facilitate its analysis [Sedlacek, 1992]. The modelling of the total structure by the finite element method would involve many iterations because of the influence of structural details that have not been settled at the outset and may, therefore, be too expensive to use as a preliminary design tool.

The decomposition in general leads to four subsystems, Fig 1.38, each of which may be analysed separately and finally combined using the principle of linear superposition.

S1   is the deck plate rigidly supported along its connections to the stringers. The composite action of the deckplate with the asphalt layer is disregarded   normally.

S2   is the orthotropic plate composed of the deck plate and the longitudinal stringers with rigid supports along the lines of the webs of the cross girders, longitudinal girders (if there are any) and main girders. The bending stiffnesses of this orthotropic plate are represented by the stringers in the longitudinal direction and the deck plate only in the transverse direction.

S3   represents a grid composed of the cross girders and the longitudinal girders and any other load distributing longitudinal girders, e.g. edge beams. This subsystem is assumed to be rigidly supported along the lines of the webs of the main girders.

S4   is the main girder system with the longitudinal elements of the orthotropic deck being included in the effective breadths of flange acting with the main girders.

The loadings to be taken into account in the analysis of the orthotropic decks are mainly

– the local traffic loads for the subsystems S1, S2 and S3,
– the global traffic loads and all other loading to be combined with the global traffic loads for the subsystem S4.

In Fig. 1.39 [Eurocode 1, 1992] the proposal for the local and global traffic loads (1992) for Eurocode l, Actions on Structures, is given as an example.
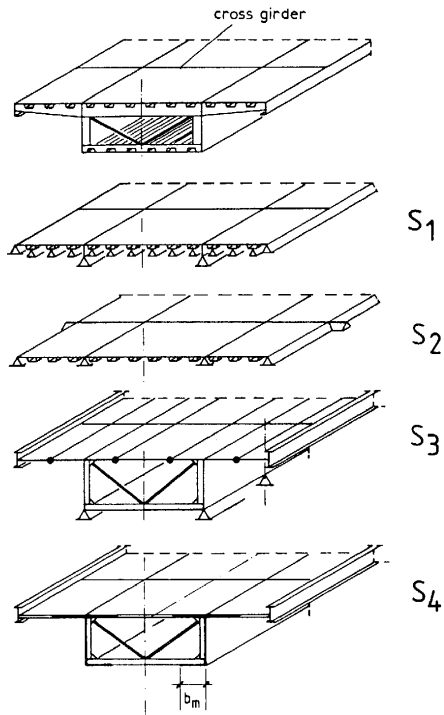
Figure 1.38 Decomposition of a bridge with an orthotropic plate into four subsystems.
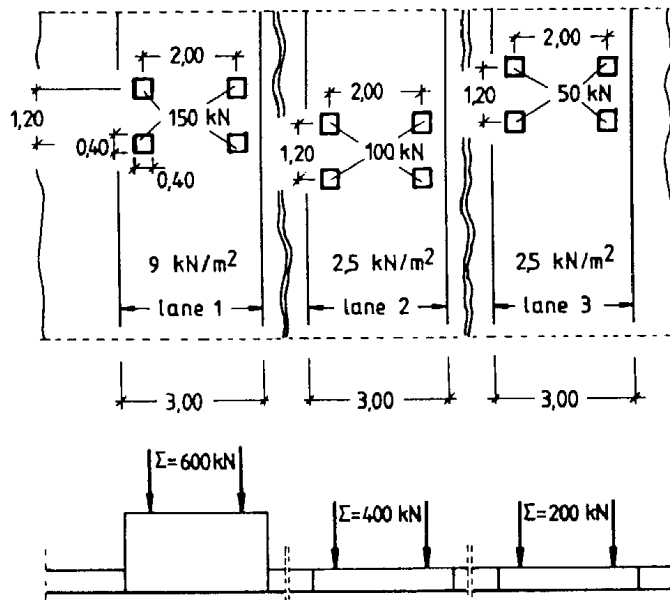
Figure 1.39 Proposed European bridge loading model including impact factors [Eurocode 1, 1992].

2 Theory of the "Orthotropic Plate"

2.1 Small Deflection Theory of Orthotropic Plate

Small deflection theory of orthotropic plate is reviewed on the basis of Pelikan, Esslinger [1957] and Troitsky [1987].

2.1.1 Differential equation of an orthotropic plate

2.1.1.1 Historical study

The fact that the natural solids around us are generally anisotropic or possess different elastic properties in different directions was recalled long ago by the creators of the theory of elasticity. Historically, the first and basic theoretical investigation in this field was conducted by the famous French mathematician Cauchy [1828], who, in his paper published in 1828, gave generalized equations for the elasticity of anisotropic solids.

Gehring [1860] a German physicist published his doctoral dissertation in 1860 on the investigations of a thin anisotropic plate. This work represents the first attempt to apply the theory of anisotropy to a structural element such as a plate. Boussinesq [1879] in his paper considered equilibrium equations for anisotropic plates and bars.

Voigt [1910], in his famous book published in 1910, investigated the elastic properties of anisotropic crystals and found the values of elastic constants.

Geckeler [1928] published his article, "Theory of Elasticity of Anisotropic Bodies," which contained a complete development in this field.

It should be noted that all the above works were purely theoretical and were developed considering those elements possessing properties of natural anisotropy. A comprehensive up-to-date account of the theory of elasticity of anisotropic media was conducted by Lechnitsky [1947] and [1963] in two books, "Anisotropic Plates" and "Theory of Elasticity of Anisotropic Bodies".

2.1.1.2 Concepts and assumptions

The theory of naturally orthotropic plates is based on certain idealizing assumptions and limitations, as follows:
1. Dimensions, deflections, loadings
   In the following analysis, we shall consider a *thin* orthotropic plate with *small* deflections compared to one of uniform thickness. These small deflections should be smaller than one-fifth of the plate thickness.
   The coordinate plane XOY coincides with the middle plane of the plate and we use the positive directions of the Z-axis downward. Thus, the downward deflections are considered positive.
   A vertical loading P is distributed over the upper surface of a plate acting parallel to the Z-axis.
2. Material
   We assume that the plate material is perfectly elastic, continuous, homogeneous, obeys Hooke's law, and possess different elastic properties in two orthogonal directions, X and Y. No body forces exist.

3. The behaviour of the plate under the influence of applied loadings
    a. There is no deformation in the middle plane of the plate. This plane remains neutral during bending.
  According to Kirchoff's theory:
    b. Linear elements perpendicular to the middle plane of the plate before bending remain straight and normal to the deflection surface of the plate after bending.
    c. The normal stress transverse to the plane of the plate can be disregarded.

2.1.1.3 Forces and moments

Let us now consider an orthotropic plate under an external, uniformly distributed load p, acting normally to the surface of a plate.

We assume that the deflections are small in comparison to the thickness of the plate. We consider that, at the boundary, the edges of the plate are free to move in the plane of the plate. Therefore, the reactive forces at the edges are normal to the plate. Since these assumptions permit us to neglect any strain in the middle plane of the plate, there will be no horizontal shearing forces during bending. We take the XOY-plane to coincide it with the middle plane of the plate, and the Z-axis is perpendicular to that plane before deflection.

Our problem is to find the stress conditions at an arbitrary point P of the plate. For this purpose, let us consider an element cut out of the plate by two pairs of planes parallel to the XZ and YZ planes around point P with sides as shown in Fig. 2.1. We assume that during bending of the plate, that the vertical sides of the elements remain plane and rotate about the neutral axes nn, so as to remain normal to the deflected middle surface of the plate. Consequently, the middle plane of the plate does not undergo any extension during this bending, and the middle surface is therefore the neutral surface.
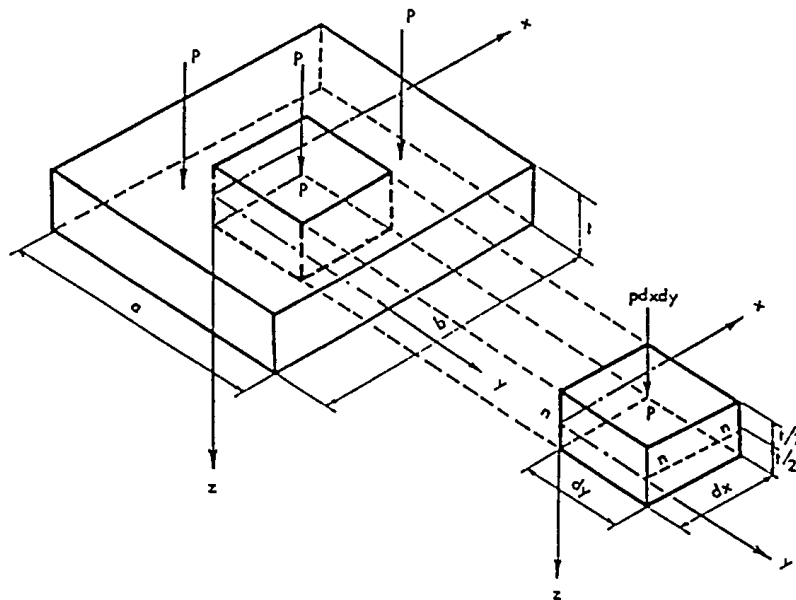
Figure 2.1 Plane and cut.

Due to the bending of the plate, the internal stresses will originate on the vertical sides of the element. The internal stresses diagram of those internal stresses, are shown in Fig. 2.2.
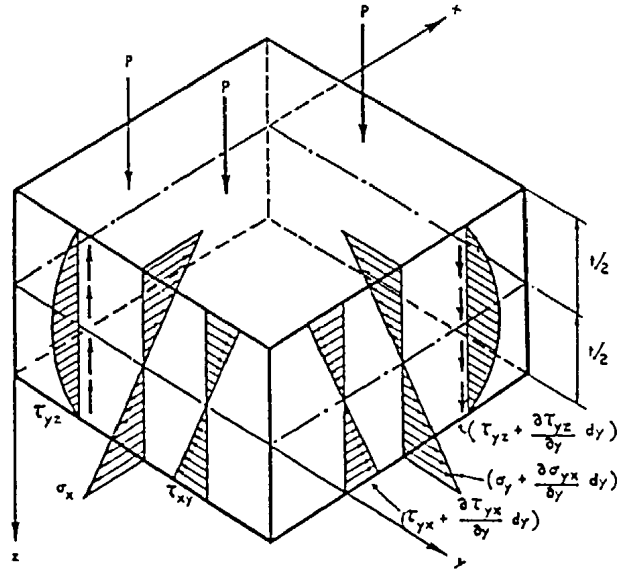
Figure 2.2 Internal stresses diagrams.

We denote the normal unit stresses on the X and Y-directions of an arbitrary plane abcd, at a distance Z from the neutral surface, as σ_x and σ_y. Those corresponding tangential stresses acting m the same planes we denote as τ_{xy}, τ_{yx} and the shear stresses as τ_{xz}, τ_{yz}. The positive directions for those components of internal, normal, tangential and shear stresses are in direction of a positive axis of coordinate system.

In general, internal stresses vary throughout the plate and at any point, a change in the internal stress, for instance, in an X-direction over the length dx is expressed as $\dfrac{\partial \sigma_x}{\partial x}$ dx, where $\dfrac{\partial \sigma_x}{\partial x}$ is the rate of change of the normal stress in an X-direction assumed to be constant over a length dx.

Such changes in the tangential and shear stresses are expressed in a similar manner, as shown in Fig. 2.2. In calculating the resulting forces acting on the element, we consider the sides to be very small. The forces are obtained by multiplying the corresponding stress at the centroid of a side, by the area of this side. In calculating normal bending stresses σ_x, σ_y, as well as tangential stresses τ_{xy}, τ_{yx}, we consider that they are proportional to a distance Z of an elementary strip abcd from the neutral surface.

These normal and tangential stresses, distributed over the vertical sides of the element and resolved to the normal and tangential forces, can be reduced to bending moments M_x and M_y and twisting moments M_{xy}.

In addition, shear stresses τ_{xz}, τ_{yz} distributed over the vertical sides of the element can also be reduced to vertical shearing forces Q_x and Q_y, acting per unit length parallel to Y and X axes on the sides of the element. The resulting diagram is shown in Fig. 2.3, where the directions in which these moments and forces taken as positive are indicated. In general, moments and shearing

forces vary throughout the plate, and at any point, a change in the moment in an X-direction over the length dx is expressed as $\dfrac{\partial M_x}{\partial x}\,dx$, where $\dfrac{\partial M_x}{\partial x}$ is the rate of change of the moment in the X-direction assumed to be constant over the length dx.

The changes in the moments M_{xy} and the shear forces Q_x, Q_y are expressed in a similar manner. The magnitudes of all moments per unit length are:

$$M_x = \int_{-t/2}^{+t/2} \sigma_z\, z\, dz, \qquad M_y = \int_{-t/2}^{+t/2} \sigma_y\, z\, dz, \qquad M_{xy} = \int_{-t/2}^{+t/2} \tau_{xy}\, z\, dz, \qquad \text{/2.1/}$$

And similarly for shear forces:

$$Q_x = \int_{-t/2}^{+t/2} \tau_{xz}\, dz, \qquad Q_y = \int_{-t/2}^{+t/2} \tau_{yz}\, dz, \qquad \text{/2.2/}$$
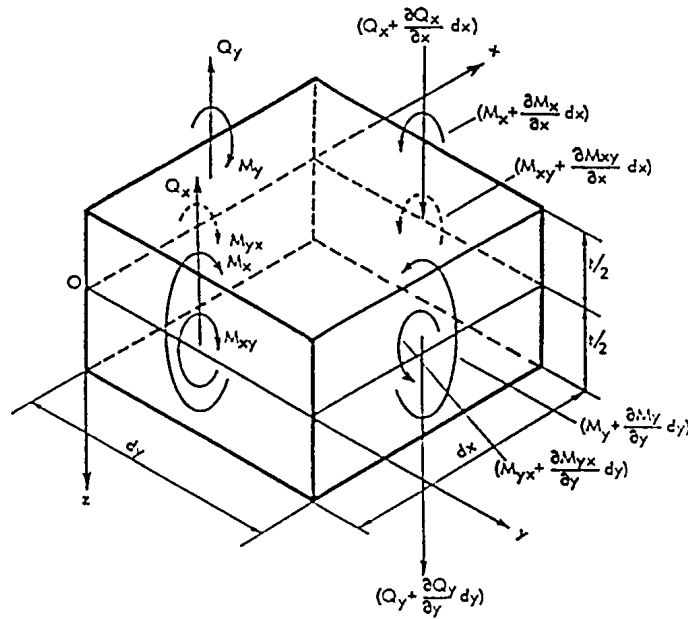
Figure 2.3 The resulting moments diagram.

2.1.1.4 Equilibrium of a plate element

The internal moments and forces acting on an element with an external load p, should be in equilibrium. Since the moments are acting per unit length, their values should be multiplied by their corresponding lengths dx and dy.

We must also consider a load p distributed over the upper surface of the plate. The intensity of this load acting on the element is p·dx·dy.

a) Vertical Forces

The condition of equilibrium is: $\Sigma V = 0$.

Projecting all the forces acting an the element onto the Z-axis, we obtain the equation of equilibrium:

$$\frac{\partial Q_x}{\partial x} + \frac{\partial Q_y}{\partial y} + p = 0 \qquad\qquad /2.3/$$

b) Moments in XOZ Plane

In calculating the moments acting on the elements, we consider the sides to be very small. The resulting moment is obtained by multiplying the moment acting at the centroid of a side along the length of this side.

Taking the moments of all those forces acting on the element with respect to the Y-axis, we obtain the equation of equilibrium:

$$\frac{\partial M_x}{\partial x} + \frac{\partial M_{yx}}{\partial y} - Q_x = 0 \qquad\qquad /2.4/$$

c) Moments in YOZ Plane

In the same manner, by taking those moments with respect to the X-axis, we obtain:

$$\frac{\partial M_{xy}}{\partial x} + \frac{\partial M_y}{\partial y} - Q_y = 0 \qquad\qquad /2.5/$$

d) Equilibrium of the Moments

Let us eliminate the shearing forces Q_x and Q_y from the previous equations by a differentiation of equation /2.4/ by x, equation /2.5/ by y, and substitute in equation /2.3/. Knowing that $M_{yx} = M_{xy}$, by virtue of $\tau_{xy} = \tau_{yx}$, we finally represent the equilibrium of the moments in the following form:

$$\frac{\partial^2 M_x}{\partial x^2} + 2\frac{\partial^2 M_{xy}}{\partial x \partial y} + \frac{\partial^2 M_y}{\partial y^2} = -p(x, y) \qquad\qquad /2.5a/$$

To evaluate the five unknowns, M_x, M_y, M_{xy}, Q_x, Q_y, we have only three equations of equilibrium /2.3/, /2.4/ and /2.5/. The additional conditions we will evaluate by investigating the geometrical problem, considering any deformations of the plate and establishing relationships between the stresses and deformations.

2.1.1.5 Deformation of plate

The relationship between unit elongations and deformations expressed as functions of unit displacements, are given by the theory of elasticity as follows:

$$\varepsilon_x = \frac{\partial u}{\partial x}, \qquad \varepsilon_y = \frac{\partial v}{\partial y}, \qquad \gamma_{xy} = \frac{\partial u}{\partial y} + \frac{\partial v}{\partial x} \qquad\qquad /2.6/$$

To find the values of unit elongations and unit deflections, let us consider one element of the plate dx·dy·t, which deforms under and external vertical unit loading p·dx·dy, Fig. 2.4.

For a smaller deflection at point P, we have:

$$\varphi_x = \frac{\partial w}{\partial x}, \qquad \varphi_y = \frac{\partial w}{\partial y} \qquad\qquad /2.7/$$

The element displacements of the plate at a distance Z from the middle surface in an X- and Y-direction are:

$$u = -z \cdot \sin\varphi_x \approx -z \cdot \varphi_x = -z \cdot \frac{\partial w}{\partial x}$$
$$v = -z \cdot \sin\varphi_y \approx -z \cdot \varphi_y = -z \cdot \frac{\partial w}{\partial y} \qquad\qquad /2.8/$$

By substituting these values in the equation for unit stresses and unit deformations /2.6/, we obtain:

$$\varepsilon_x = -z \cdot \frac{\partial^2 w}{\partial x^2}, \qquad \varepsilon_y = -z \cdot \frac{\partial^2 w}{\partial y^2}, \qquad \gamma_{xy} = -2z \cdot \frac{\partial^2 w}{\partial x \partial y} \qquad\qquad /2.9/$$
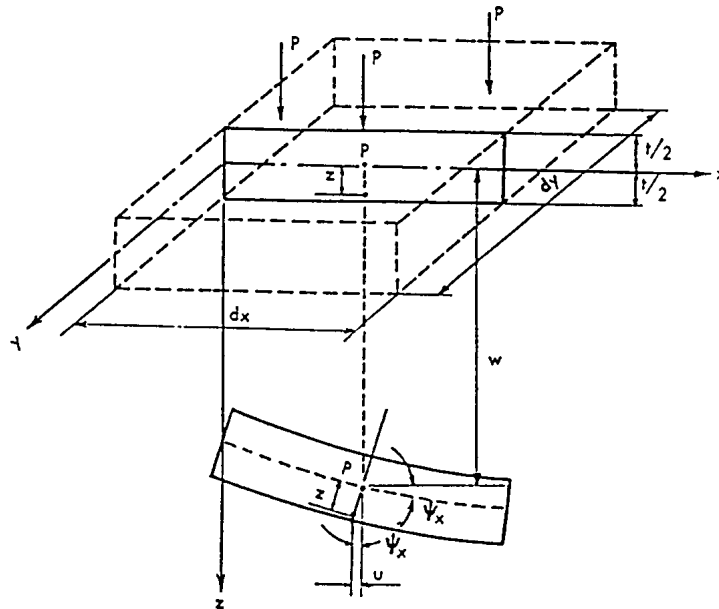
Figure 2.4 Plate deformations.

2.1.1.6 Generalized Hooke's law

The relationship between the components of stress and the components of deformation, known as Hooke's law, have been established experimentally.

Let us consider the element of an orthotropic plate with its sides parallel to the coordinate axes, and subjected to the action of normal stress σ_x, uniformly distributed over two opposite sides, Fig. 2.5.

For an orthotropic plate, those elastic properties expressed by the corresponding moduli of elasticity should be different in the direction of axes X and Y. We denote them as E_x and E_y. The magnitude of the unit elongation of the element in an X-direction and the lateral contraction in the Y-direction is given by the expression, respectively:

$$\varepsilon_x = \frac{\sigma_x}{E_x}, \qquad -v_x \frac{\sigma_x}{E_x} \qquad\qquad /2.10/$$

in which E_x is the modulus of elasticity in tension for an orthotropic plate in an X-direction, v_x is a constant known as Poisson's ratio.
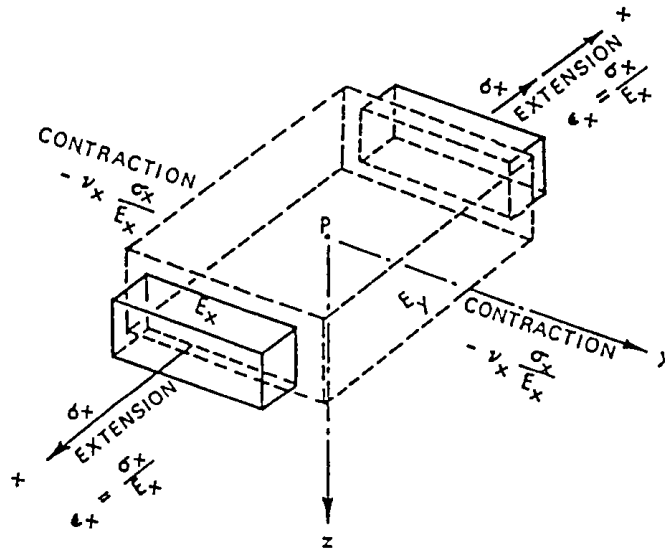
Figure 2.5 Generalized Hooke's law.

Similarly, considering the same element subjected to the action of normal stress σ_y and uniformly distributed over two opposite sides in a Y-direction, we obtain:

$$\varepsilon_y = \frac{\sigma_y}{E_y}, \qquad -v_y \frac{\sigma_y}{E_y} \qquad\qquad /2.11/$$

as the unit of elongation in the Y-direction and as the lateral contraction in an X-direction, consequently.

Further, according to Betti's reciprocal theorem, we obtain the following relationship:

$$\nu_y E_x = \nu_x E_y \qquad\qquad /2.12/$$

If the above element is subjected to the action of normal stresses σ_x and σ_y and uniformly distributed over the sides, the resultant components of deformation can be obtained by a method superposition as follows:

$$\varepsilon_x = \frac{\sigma_x}{E_x} - \nu_y \frac{\sigma_y}{E_y}, \qquad \varepsilon_y = \frac{\sigma_y}{E_y} - \nu_x \frac{\sigma_x}{E_x} \qquad\qquad /2.13/$$

Solving equation /2.13/ for σ_x and σ_y we find:

$$\sigma_x = \frac{E_x}{1 - \nu_x \nu_y}\left(\varepsilon_x + \nu_y \varepsilon_y\right) \qquad \sigma_y = \frac{E_y}{1 - \nu_x \nu_y}\left(\varepsilon_y + \nu_x \varepsilon_x\right) \qquad\qquad /2.14/$$

Let us now consider the state of deformation of a plate element under pure shearing stresses $\tau_{xy} = \tau_{yx}$.

On the basis of theoretical investigation [Klöppel and Yamada, 1960], the value G_{xy} of shear modulus for orthotropic material could be expressed through the values of those known moduli of elasticity E_x, E_y as follows:

$$G_{xy} = \frac{E_x E_y}{E_x + \left(1 + 2\nu_{xy}\right)E_y} \qquad \text{where} \qquad \nu_{xy} = \frac{E_x}{E_y}\nu_{yx}$$

According to Hooke's law for pure sheer, the distortion angle γ_{xy} is proportional to the shearing or tangential stress τ_{xy}, and we can express this relationship as follows:

$$\gamma_{xy} = \frac{\tau_{xy}}{G_{xy}} \qquad\qquad /2.15/$$

where G_{xy} is the shear modulus for orthotropic material.

Further, by introducing the values from the system /2.9/ in equations /2.14/ and /2.15/, we obtain the following expressions of those stresses as a function of deflection w.

$$\sigma_x = -\frac{E_x z}{1 - \nu_x \nu_y}\left(\frac{\partial^2 w}{\partial x^2} + \nu_y \frac{\partial^2 w}{\partial y^2}\right)$$

$$\sigma_y = -\frac{E_y z}{1 - \nu_x \nu_y}\left(\frac{\partial^2 w}{\partial y^2} + \nu_x \frac{\partial^2 w}{\partial x^2}\right) \qquad\qquad /2.16/$$

$$\tau_{xy} = -2G_{xy} z \frac{\partial^2 w}{\partial x \partial y}$$

2.1.1.7 Differential equation of the bent plate

With the assumption of a small deflection w, while neglecting the effect of shearing forces Q_x and Q_y as well as the compressive stress σ_z produced by load p on bending, the deflection w is independent of z. Therefore, by substituting equations /2.1/, the known values for σ_x, σ_y and τ_{xy} from equations /2.16/, and by integration, we obtain the following expressions for the bending moments and torsional moment:

$$M_x = -\frac{E_x t^3}{12\left(1 - v_x v_y\right)}\left(\frac{\partial^2 w}{\partial x^2} + v_y \frac{\partial^2 w}{\partial y^2}\right)$$

$$M_y = -\frac{E_y t^3}{12\left(1 - v_x v_y\right)}\left(\frac{\partial^2 w}{\partial y^2} + v_x \frac{\partial^2 w}{\partial x^2}\right) \qquad \text{/2.17/}$$

$$M_{xy} = -\frac{G_{xy} t^3}{6} \cdot \frac{\partial^2 w}{\partial x \partial y}$$

denoting

$$D_x = \frac{E_x t^3}{12\left(1 - v_x v_y\right)}, \qquad D_y = \frac{E_y t^3}{12\left(1 - v_x v_y\right)}, \qquad D_{xy} = \frac{G_{xy} t^3}{6} \qquad \text{/2.18/}$$

We obtain from equations /2.17/

$$M_x = -D_x\left(\frac{\partial^2 w}{\partial x^2} + v_y \frac{\partial^2 w}{\partial y^2}\right)$$

$$M_y = -D_y\left(\frac{\partial^2 w}{\partial y^2} + v_x \frac{\partial^2 w}{\partial x^2}\right) \qquad \text{/2.19/}$$

$$M_{xy} = -2D_{xy} \cdot \frac{\partial^2 w}{\partial x \partial y}$$

Quantities D_x and D_y we call the *flexural rigidities* of the plate, and the quantity D_{xy}, the *torsional rigidity* of the plate.

By substituting expressions /2.19/ in the moment equation /2.5a/, we obtain:

$$D_x \frac{\partial^4 w}{\partial x^4} + \left(D_x v_y + D_y v_x + 4D_{xy}\right)\frac{\partial^4 w}{\partial x^2 \partial y^2} + D_y \frac{\partial^4 w}{\partial y^4} = p(x, y) \qquad \text{/2.20/}$$

The value of $2D_{xy}$ is defined as the reciprocal value of the angle of twist of a plate element with a side length dx = dy = 1 due to the action of twisting moments $M_{xy} = M_{yx} = 1$.

Introducing the notation,

$$2H = D_x \cdot \nu_y + D_y \cdot \nu_x + 4D_{xy} \qquad \text{/2.21/}$$

we obtain equation /2.20/ in the following form:

$$D_x \frac{\partial^4 w}{\partial x^4} + 2H \frac{\partial^4 w}{\partial x^2 \partial y^2} + D_y \frac{\partial^4 w}{\partial y^4} = p(x, y) \qquad \text{/2.22/}$$

This is the general differential equation of an orthotropic plate deduced by Huber and known in technical literature as "Huber's Equation". We call the value 2H from expression /2.21/ the "*effective torsional rigidity*" of an orthotropic plate.

The general differential equation can be used in the investigation of bending of plates and beams of orthotropic material which have different flexural rigidities in two mutually perpendicular directions.

By substituting in equations /2.4/ and /2.5/ the corresponding values from equations /2.19/, we obtain the following expressions for shear forces:

$$Q_x = -D_x \frac{\partial^3 w}{\partial x^3} - \left(\nu_y D_x + 2D_{xy} \right) \frac{\partial^3 w}{\partial x \partial y^2}$$

$$Q_y = -D_y \frac{\partial^3 w}{\partial y^3} - \left(\nu_x D_y + 2D_{xy} \right) \frac{\partial^3 w}{\partial y \partial x^2} \qquad \text{/2.23/}$$

By substituting in the relationship /2.12/ the values from /2.18/ we obtain:

$$D_x \nu_y = D_y \nu_x \qquad \text{/2.24/}$$

By substituting /2.24/ the values from /2.21/ we obtain:

$$H = D_x \nu_y + 2D_{xy}, \qquad D_x \nu_y = H - 2D_{xy}, \qquad D_y \nu_x = H - 2D_{xy} \qquad \text{/2.25/}$$

By substituting /2.25/ in system /2.23/ we obtain:

$$Q_x = -\frac{\partial}{\partial x} \left(D_x \frac{\partial^2 w}{\partial x^2} + H \frac{\partial^2 w}{\partial y^2} \right), \qquad Q_y = -\frac{\partial}{\partial y} \left(D_y \frac{\partial^2 w}{\partial y^2} + H \frac{\partial^2 w}{\partial x^2} \right) \qquad \text{/2.26/}$$

2.1.1.8 Effective torsional rigidity

Suppose that for a certain plate under a given load distribution and for known boundary conditions, the deflection surface w is determined by the integration of differential equation /2.22/.

By substituting the value of w in equations /2.19/ and /2.20/, we can then derive the values of M_x, M_y, M_{xy}, Q_x, Q_y and, consequently find the stresses at any point in the plate.

The outlined procedure provides a formal mathematical solution of the problem, based on the principles of the theory of elasticity. However, to apply this solution in practical engineering

problems, it is necessary to possess the proper values of the five constants D_x, D_y, D_{xy}, v_x, v_y in the differential equation for the plate. The values of the moduli of elasticity E_x, E_y encountered in expressions for the rigidities D_x, D_y, and Poisson's constants v_x, v_y are usually known for certain orthotropic material. The value of the shear modulus G_{xy} however, encountered in these expressions for the torsional rigidity H, is usually unknown.

The following evaluation of the torsional rigidity D_{xy} based on theoretical analysis should be regarded as a first approximation, and, in cases of practical importance, a direct test is recommended to obtain more reliable values of the modulus G_{xy}.

Let us now consider an orthotropic plate element having its sides of unit length under the influence of twisting moments M_{xy}, M_{yx} acting upon two opposite sides, as shown in Fig. 2.3. Due to the known equilibrium of the tangential stress components $M_{xy}=M_{yx}$.

To determine the value of the torsional rigidity of an orthotropic plate, we will base the following investigation on the analogy between orthotropic and isotropic plates, both under the influence of the twisting moments.

For an isotropic plate, the value of the torsional moment is given by the expression:

$$M_{xy} = -\frac{Gt^3}{6} \cdot \frac{\partial^2 w}{\partial x \partial y} \qquad /2.27/$$

For the isotropic material, the relation between the shear modulus G, the elasticity modulus E and Poisson's constant v is given by the formula $G = \dfrac{E}{2(1+v)}$.

By substituting formula G in /2.27/ and after certain modification, we now obtain the expression of torsional moment of an isotropic plate.

$$M_{xy} = -(1-v) \cdot D \frac{\partial^2 w}{\partial x \partial y} \qquad /2.28/$$

where $D = \dfrac{Et^3}{12(1-v^2)}$, is the torsional rigidity of the isotropic plate.

For an orthotropic plate, however, considering $M_{xy} = M_{yx}$, the torsional moments will depend on the torsional rigidities in both directions. Therefore, to evaluate the twisting moments in the case of an orthotropic plate, a reasonable approximation will be to consider the expression for the twisting moment of an isotropic plate and to substitute the values of D and v by certain middle values of D_x, D_y and v_x, v_y.

Let us use these middle values as:

$$D = \sqrt{D_x D_y}, \qquad\qquad v = \sqrt{v_x v_y} \qquad /2.29/$$

and after substituting in the expression /2.28/, we obtain:

$$M_{xy} = -\left(1 - \sqrt{v_x v_y}\right)\sqrt{D_x D_y}\, \frac{\partial^2 w}{\partial x \partial y} \qquad /2.30/$$

By a comparison of expressions /2.30/ and the final one from the system /2.19/, the value of the torsional rigidity of an orthotropic plate is approximately:

$$2D_{xy} = \left(1 - \sqrt{\nu_x \nu_y}\right)\sqrt{D_x D_y} \qquad\qquad /2.31/$$

By substitution in the expression for the effective torsional rigidity H /2.21/, the value from /2.31/ as obtained:

$$2H = D_x \nu_y + D_y \nu_x + 2\left(1 - \sqrt{\nu_x \nu_y}\right)\sqrt{D_x D_y} \qquad\qquad /2.32/$$

or, after certain transformations,

$$2H = 2D_x D_y + \left(\sqrt{D_x \nu_y} - \sqrt{D_y \nu_x}\right)^2 \qquad\qquad /2.33/$$

By substituting the values from /2.24/ in equation /2.33/, the effective torsional rigidity is then expressed as:

$$H = \sqrt{D_x D_y} \qquad\qquad /2.34/$$

2.1.1.9 Coefficient of torsional rigidity

The theoretical value of the effective torsional stiffness expressed by the formula /2.34/ is valid only if one orthotropic plate generally satisfied the following conditions:

1. the thickness of the plate is constant;
2. deformations are purely elastic;
3. deflections of the plate are relatively very small.

Because these assumptions do not exist in reality, the values of H for practical problems usually should be reduced by multiplying the value $\sqrt{D_x D_y}$ by the coefficient æ, which we may call the "*coefficient of torsional rigidity*" or "*parameter of torsion*".

Therefore:

$$H = \text{æ} \cdot \sqrt{D_x D_y} \qquad\qquad /2.35/$$

It has been found by analysis and confirmed by experimental investigations that for steel decks of an orthotropic type, the value of æ < 1 and varies between 0.3 - 0.5. For example, in the case of the Cologne-Mulheim suspension bridge, it was found experimentally for the steel deck that [Cornelius, 1952]:

$$H = 0.3 \cdot \sqrt{D_x D_y}$$

It should be noted that in this extreme case, the relation between the flexural rigidities was $D_x = 20\, D_y$.

2.1.1.10 Solution of Huber's equation

The solution of Huber's non-homogeneous partial differential equation /2.22/ consists of the superposition of two solutions:

$$w = w_h + w_p \qquad\qquad /2.36/$$

where

w_h represents a general solution of the corresponding homogeneous differential equation,

$$D_x \frac{\partial^4 w}{\partial x^4} + 2H \frac{\partial^4 w}{\partial x^2 \partial y^2} + D_y \frac{\partial^4 w}{\partial y^4} = 0 \qquad\qquad /2.37/$$

and

w_p a particular solution of the non-homogeneous equation /2.22/.

Geometrically, equation /2.36/ represents a superposition of the two deflection surfaces $w_h + w_p$.

w_h represents the deflection of the unloaded portion of the plate or $p(x,y) = 0$.

Under the effects of such deflections, rotations, lineloads or bending moments are applied along the edge where necessary to compensate for the departures of the particular solution w_p from the required shape of the actual plate.

w_p represents the deflection surface of a plate under a given load $p(x,y)$, which possibly satisfies some but not all boundary conditions of the actual plate.

Therefore, by adding two surfaces, $w_h + w_p$, a deflection surface of the actual loaded plate is obtained which satisfies all boundary conditions.

Consider the technically important case of an orthotropic plate simply supported along the edges $x = 0$ and $x = a$ and subject to any boundary conditions along the edges $y = const$.

A solution to the homogeneous equation can be given by a simple series, involving only one summation. This solution, first proposed by Levy [1899] to the analysis of an isotropic plate, may be represented in the general form:

$$w_h = \sum_{m=1}^{\infty} A \cdot e^{\alpha y} \cdot \sin \frac{m\pi x}{a} \qquad\qquad /2.38/$$

where

A and α are constants which should be determined, a is the length of the plate.

By substituting the expression /2.38/ in equation /2.37/, we obtain the following characteristic equation for determination of the function $e^{\alpha y}$.

$$D_x \left(\frac{m\pi}{a}\right)^4 - 2H\alpha^2 \left(\frac{m\pi}{a}\right)^2 + D_y \alpha^4 = 0 \qquad\qquad /2.39/$$

The system /2.39/ defines four values of α. Therefore, in expression /2.38/ for w_h, each term of the series depends on four arbitrary parameters, and a general solution of the differential equation /2.37/ could be expressed as follows:

$$w_h = \sum_{m=1}^{\infty} \left(A_1 \cdot e^{\alpha_1 y} + A_2 \cdot e^{\alpha_2 y} + A_3 \cdot e^{\alpha_3 y} + A_4 \cdot e^{\alpha_4 y} \right) \cdot \sin \frac{m\pi x}{a} \qquad /2.40/$$

where the constants A_1, A_2, A_3 and A_4 could be determined from the boundary conditions.

In order to find a particular solution of the non-homogeneous partial differential equation /2.2/, we make the following two assumptions for deflection and loading:

$$w_p = \sum_{m=1}^{\infty} a_m \cdot \sin \frac{m\pi x}{a} \qquad /2.41/$$

The loading $p(x)$ can then be expressed by a Fourier sine series as follows:

$$p(x) = \sum_{m=1}^{\infty} p_m \cdot \sin \frac{m\pi x}{a} \qquad /2.42/$$

The solution of the non-homogeneous equation is a summary:

$$w = \sum_{m=1}^{\infty} \left[\frac{p_m}{D_x} \left(\frac{a}{m\pi} \right)^4 + A_1 \cdot e^{\alpha_1 y} + A_2 \cdot e^{\alpha_2 y} + A_3 \cdot e^{\alpha_3 y} + A_4 \cdot e^{\alpha_4 y} \right] \cdot \sin \frac{m\pi x}{a} \qquad /2.43/$$

2.1.1.11 Analysis of Huber's equation

Huber's partial differential equation of orthotropic plate /2.22/ has different solutions depending upon the relations between the three rigidities D_x, H and D_y.

Depending upon the relations between the rigidities of the plate, we could consider the following variations of orthotropy.

Case 1. $H^2 > D_x D_y$

This condition of great torsional rigidity is found in the case of an orthotropic deck with box-shaped ribs.

Case 2. $H^2 = D_x D_y$

It is considered that this condition of middle torsional rigidity is found when using reinforced concrete flat slabs.

Case3. $H^2 < D_x D_y$

This condition corresponds to the small torsional rigidity and exists in the case of an orthotropic deck with flexible ribs.

Case 4. $D_x = 0$

This condition of negligible flexural rigidity in a transverse direction, can be considered for an orthotropic deck with box-shaped ribs.

Case 5. H = 0
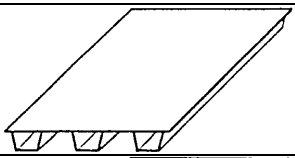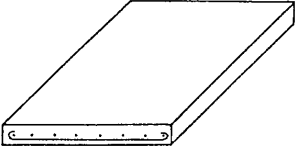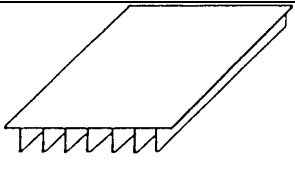
This condition can be considered in the case of an orthotropic deck with flexible ribs having negligible torsional rigidity.

Case6. H = D_x = 0

In this case, torsional and flexural rigidities in the x-direction are disregarded. Under this condition, the plate equation is transferred into a beam equation which is relatively simple and is satisfactory for the analysis of an orthotropic deck with flexible ribs.

A summary of the above analysis is shown in Tabl. 2.1.

Table 2.1 Relations between the rigidities of the orthotropic plates.

Cases		$D_x \dfrac{\partial^4 w}{\partial x^4} + 2H \dfrac{\partial^4 w}{\partial x^2 \partial y^2} + D_y \dfrac{\partial^4 w}{\partial y^4} = p(x,y)$
1	$H^2 > D_x \cdot D_y$	
4	$D_x = 0$	
2	$H^2 = D_x \cdot D_y$	
3	$H^2 < D_x \cdot D_y$	
5	$H = 0$	
6	$D_x = H = 0$	

2.1.2 Application of Huber's theory to orthotropic plate analysis

2.1.2.1. Natural and technical orthotropy

In analyzing the composition of an engineering structure, we should distinguish between two kinds of orthotropic elements. The first shows an orthotropy which is the result of different physical properties, for instance, the crystalline structure of the material itself may be oriented in two mutually perpendicular directions. We may call such elements "*naturally orthotropic*".

The second group includes those elements which are reinforced to ensure strength and stability, arranged in proper geometrical configurations, or composed of two or more different materials. Sometimes, the elements, in spite of being formed of isotropic material, may also be considered to belong to the second group, owing to their geometrical composition.

Typical examples of those structures contained in the second group are: ribbed plates, plate-girders, and reinforced or pre-stressed elements. Such structures generally exhibit different elastic

properties in different directions. The various elastic properties in these cases could be expressed by the different flexural and torsional rigidities of the element in different directions. We may call such elements belonging to the second group and possessing different rigidities in two mutually perpendicular directions "*structurally or technically orthotropic*".

In the elastic domain, this second group may be treated on the basis of the same theory as naturally orthotropic plates are, with some modifications.

Structural or technical orthotropy is of utmost importance in modern engineering. Examples of such structures are: bridge decks, floor panels, bulkheads, ship hulls, aircraft wings and fuselages. In all these structures, the structural orthotropy is the result of geometrical configuration, rather than the physical properties of the materials.

The following examples illustrate the application of structurally orthotropic elements in bridge engineering.

a) Structural elements of different materials

A typical example, shown in Fig. 2.6, is that of a two-way reinforced concrete flat slab of uniform thickness.

In this example, the structural orthotropy is expressed by different amounts of reinforcement and, consequently, by the different static resistance of the cross sections of the slab in each direction.
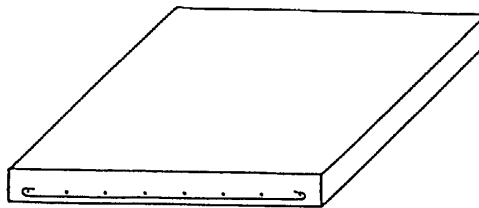
Figure 2.6 Two-way reinforced concrete slab.

b) Geometrical Configuration

The rigidity of a structural element may differ in both directions because of its geometric configuration, as is shown in the example of a concrete slab reinforced by a set of equidistant ribs, Fig. 2.7.

Typical examples of structurally orthotropic elements used for bridge decks are steel plates reinforced with equidistant steel stiffeners in one or two orthogonal directions, as shown in Fig. 2.8 and Fig.2.9.
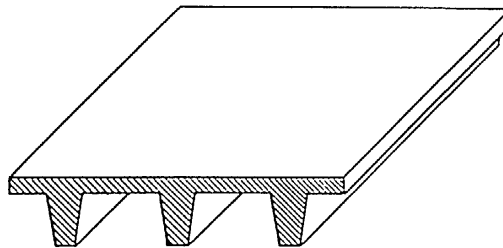
Figure 2.7 Concrete slab reinforced by a set of equidistant ribs.
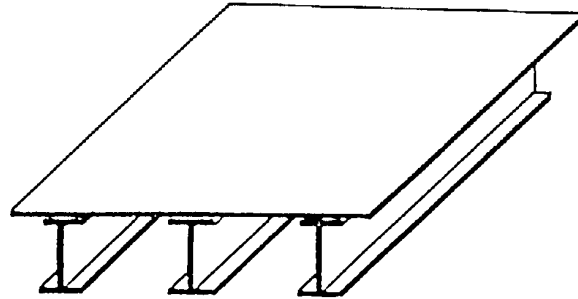
Figure 2.8 A steel plate reinforced by equidistant steel stiffeners.
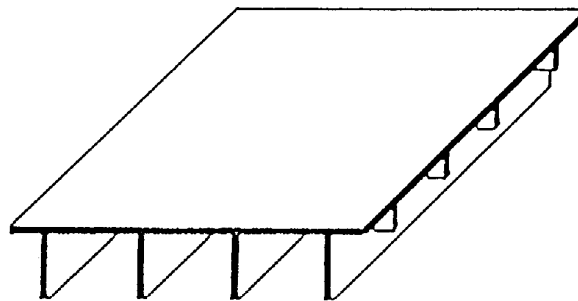
Figure 2.9 A steel plate reinforced by orthogonal stiffeners.

2.1.2.2. Theory of M.T. Huber

Although the general theory of anisotropic bodies was developed in the 19th century and some practical applications shown, the wide use of the theory of orthotropic plates in engineering began in the 20th century, primarily in connection with the development of shipbuilding and the use of steel plates for ship hulls and aircraft structures.

A great contribution was made by Boobnov [1902] in the application of stress analysis to steel plates reinforced by a system of interconnected longitudinal and transversal beams in the period 1902 to 1914. The many applications of stiffened steel plates, concrete slabs reinforced by ribs, plywood plates and similar structural elements give rise to the theory of technical orthotropy.

The idea of the application of the theory of elasticity of orthotropic plates to reinforced concrete flat and ribbed slabs was proposed and developed by Huber. In his first article, published in 1914, he considered the problem of a reinforced concrete slab as a slab with elastic properties differing in two orthogonal directions or as an idealized orthotropic plate [Huber, 1914]. In his works in the period 1923-1929, Huber developed solutions to these problems which allowed their practical applications [Huber, 1922, 1923 and 1929]. Improved and refined methods of stress analysis for technically orthotropic plates were summarized by Huber in books edited in the period 1948-1956 [Huber, 1950, 1956 and 1957].

2.1.2.3. Method of elastic equivalence

The basic assumption proposed by Huber for estimating overall bending deflections and bending stresses in a stiffened slab was to replace such a slab by an equivalent orthotropic slab of constant thickness having the same stiffness characteristics.

Since reinforcing or ribs in actual concrete slabs are usually arranged in an orthogonal pattern, the equivalent slab would have the rigidity characteristics of an orthotropic material. The usual assumptions of "thin plate" theory were made, and the problem was treated in terms of plane stress. On the basis of this assumption, the analysis of bending of stiffened plates may be simplified by replacing the plate stiffener combination by an equivalent homogeneous orthotropic plate.

However, it should be understood that any actual plate stiffener combination obviously cannot be equivalent to an orthotropic plate in every respect. Theoretical investigations and experimental data indicate that orthotropic plate theory is applicable to structurally orthotropic plates under certain provisions as follows:

1. The ratios of stiffener spacing to plate boundary dimensions are small enough to insure approximate homogenity of stiffness.
2. It is assumed that the rigidities are uniformly distributed in both directions.
3. Flexural and twisting rigidities do not depend on the boundary conditions of the plate or on the vertical load distribution.
4. In the case of steel stiffened plates, it is assumed that both the plate and the stiffeners are fabricated of the same isotropic material.
5. A perfect bond exists between the plate and the stiffeners.

The substitution of an orthotropic plate with the same stiffness characteristics as that of a stiffened plate may be called "*method of elastic equivalence*".

By applying the method of elastic equivalence to the analysis of stiffened plates, we thus reduce the actual system of discrete interconnected ribs to that of a statically equivalent system with uniformly distributed stiffnesses in both directions.

For practical application in engineering, an orthotropic plate is defined as a plate with different bending stiffnesses $D = EI$ in two orthogonal directions, x and y, in the plane of a plate.

These may either result from different moduli of elasticity E_x and E_y of the material in two directions, as for a naturally orthotropic plate, or from different moments of inertia I_x and I_y per unit width, as for structurally orthotropic plates.

By applying the principle of elastic equivalence, the discontinuous structure of a technically orthotropic plate is represented by an idealized substitute orthotropic plate, reflecting the characteristic properties of the actual system.
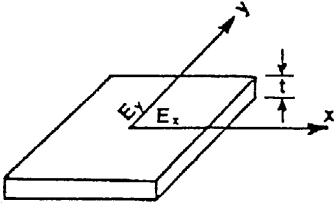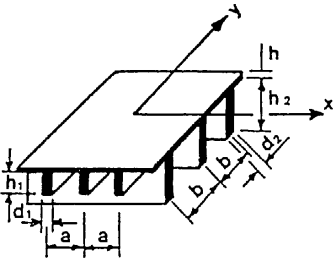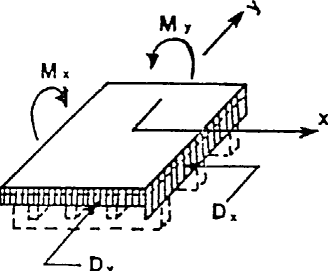
A practical application of the method of elastic equivalence is illustrated in Tab. 2.2.

By this method, we replace structural orthotropy by natural orthotropy.

To find the solution of the orthotropic bent plate problem due to the action of external loadings, it is necessary to determine those internal moments and shear forces acting in the plate. These internal moments and shears are usually expressed by the stress components as the functions of deflection of the plate. This function has to satisfy a linear partial differential equation which, together with the boundary conditions, completely defines W. Consequently, the

solution of the equations gives all the necessary information for the calculation of stresses at any point in the plate.

Table 2.2 Orthotropic deck analysis. Huber's Theory. Principle of static equivalence.

Naturally orthotropic plate	Technically orthotropic plate	Equivalent orthotropic plate
Differential equation of the orthotropic plate		
$$D_x \frac{\partial^4 w}{\partial x^4} + 2H \frac{\partial^4 w}{\partial x^2 \partial y^2} + D_y \frac{\partial^4 w}{\partial y^4} = P$$		

$D_x = \dfrac{E_x t^3}{12\left(1 - \nu_x \nu_y\right)}$ $D_y = \dfrac{E_y t^3}{12\left(1 - \nu_x \nu_y\right)}$ $D_{xy} = \dfrac{G_{xy} t^3}{12}$ $H = \dfrac{1}{2}\left(D_x \nu_y + D_y \nu_x\right) + 2D_{xy}$	$D_x = \dfrac{EI_x}{b}$ $D_y = \dfrac{EI_y}{a}$ $D_{xy} = \dfrac{G}{3}\left(\dfrac{h_1 d_1^3}{a} + \dfrac{h_2 d_2^3}{b}\right)$ $H = \dfrac{Eh^3}{12\left(1 - \nu^2\right)} + D_{xy}$	$M_x = D_x \left(\dfrac{\partial^2 w}{\partial x^2} + \nu_y \dfrac{\partial^2 w}{\partial y^2}\right)$ $M_y = D_y \left(\dfrac{\partial^2 w}{\partial y^2} + \nu_x \dfrac{\partial^2 w}{\partial x^2}\right)$ $M_{xy} = -2D_{xy} \cdot \dfrac{\partial^2 w}{\partial x \partial y}$

Rigorous investigations have shown this method to be correct if the ribs are symmetrically disposed in relation to the middle plane of the plate, but gives approximate values in the case when the ribs are located on only one side.

2.1.2.4. Design methods

With the development of the orthotropic deck system, various design methods to determine the distribution of loads and internal forces were proposed. It should be noted, however, that the use of orthotropic theory has been somewhat limited by certain mathematical difficulties in the analysis.

The current methods used for stress analysis in orthotropic deck systems and based on Huber's theory may be summarized in the following five groups:

a) Ideal gridwork system,
b) Deck as uniform medium orthotropic plate strips,
c) Application of influence surfaces,
d) Semi-empirical method.
e) Methods of deck analysis by computers

All the above methods yield only an approximate solution to the problem.

To show the general nature of those solutions developed, we will briefly review the various analytical methods mentioned above.

a) Ideal gridwork system

This method is based on the application of the orthotropic plate theory, considering the deck statically equivalent to open grids or an ideal gridwork system. This is a simple but approximate method.

Y. Guyon and C. Massonnet

The idea of applying the theory of orthotropic plates to a grid system of a bridge deck by treating it as an idealized plate was proposed by Guyon [1946a]. It is known in technical literature as *the method of distribution coefficients* [Guyon, 1946b]. Guyon, however, analyzed no torsional structures.

In 1950, Massonnet extended the method by introducing into the analysis the effect of torsion [Massonnet, 1950a, 1950b and 1955]. Generally, the problem. which is involved is that of . determining how a concentrated load or system of such loads is distributed among the longitudinal beams of a bridge system for various degrees of transverse stiffness and torsional resistance. Basically, the method consists of replacing the actual bridge deck structure, a system of discrete interconnected longitudinal and transverse members, by an "elastically equivalent" slab system whose structural properties in the two orthogonal directions are uniformly distributed along their length.

b) Deck as an orthotropic plate strip

According to this method, a uniformly distributed medium is substituted in two directions for a stiffened plate.

W. Cornelius Method

A German engineer, W. Cornelius, was the first to use the orthotropic plate theory to analyze a steel deck stiffened by ribs. He developed a practical method for the analysis of orthotropic-type bridge decks and described his method in articles published in the period 1947-1951 [Cornelius, 1952].

c) Application of influence surfaces

Live loading of a highway bridge deck generally consists of the wheel loads, each one in effect distributed over a relatively small area. Due to such load distribution, the analysis of bridge decks is complicated and time consuming. In addition, the first step should be the evaluation of the critical position of the live loading. This problem for beams is solved by the use of influence lines.

By analogy, three-dimensional influence surfaces are used for the plates. The influence surfaces help to find the moments, shear forces and reactions for the given load positions. Evaluating the influence surfaces requires a great amount of work, which, however, need only be done once for a given set of conditions. The influence surfaces may be defined as three-dimensional diagrams which show the variation of a certain structural action as a bending moment.

The advantage of the influence surfaces as a design aid consists in the following: this aid is linked to the practical geometrical range of a particular structural system and is independent of loading. The design loadings are usually related to the particular country. Also, the loading specifications are changeable, being updated. In such cases the influence surfaces are especially useful.

The systematic application of influence surfaces in structural engineering started relatively late with the first work only appearing in 1938. The theory of the influence surface methods is given in the works of Pucher [1938], Bittner [1938], Hawranek and Steinhardt [1958]

d) Semi-empirical method

A deck system is designed by any of the above-mentioned analytical methods. Then a model or full-scale test is made on the designed plating to determine its actual capacity.

For the purposes of superposition of the plating stresses with the overall bridge stresses, the stresses theoretically computed for plating are reduced by a factor derived from tests.

This approach was used in the design of the 856 foot centre span Save River Bridge in Belgrade; Yugoslavia [Pelikan and Esslinger, 1957].

e) Methods of deck analysis by computers

Most of the research published since 1960 involves the theoretical studies of stiffened deck plates and deals with mathematical methods for analyzing such structures. A recent trend has been to develop computer programs based on particular analytical methods, such as finite difference [Adotte, 1967], finite element [Zienkiewicz and Cheung, 1964], finite strip [Cheung, 1968] and other methods.

2.1.3 Pelikan-Esslinger method [1957]

2.1.3.1 Introduction

Of all the methods considered in Chapter 2.1.2.4, experience has shown that the most practical is that of Pelikan and Esslinger [1957]. This method is based on the application of Huber's equation; however, the parameters expressing certain rigidities of the orthotropic deck are disregarded, as they are of little importance in the design.

It is considered that the approach developed by Pelikan and Esslinger provides a practical and relatively simple method for the design of orthotropic-type steel bridges. In this method, the authors assume that the deck system is a continuous orthotropic plate, rigidly supported by its main girders and elastically supported by the floor beams. The design procedure is divided into two stages, Fig. 2.10.

In the first stage, it is assumed that the floor beams, as well as the main girders, are infinitely rigid. In the second stage, a correction is applied, considering the floor beams as elastic supports.

The reactions of the plate on the floor beams are replaced by a load group proportional at each point to the deflection of the floor beam. The total moments are found by superposition, due to the influence of dead and live loads assuming rigid supports and live loads assuming elastic floor beams.

FIRST STAGE-DECK AS
CONTINUOUS PLATE OVER
RIGID FLOOR BEAMS

SECOND STAGE-DECK
OVER ELASTIC FLOOR BEAMS

SUMMARY OF FIRST AND
SECOND STAGE
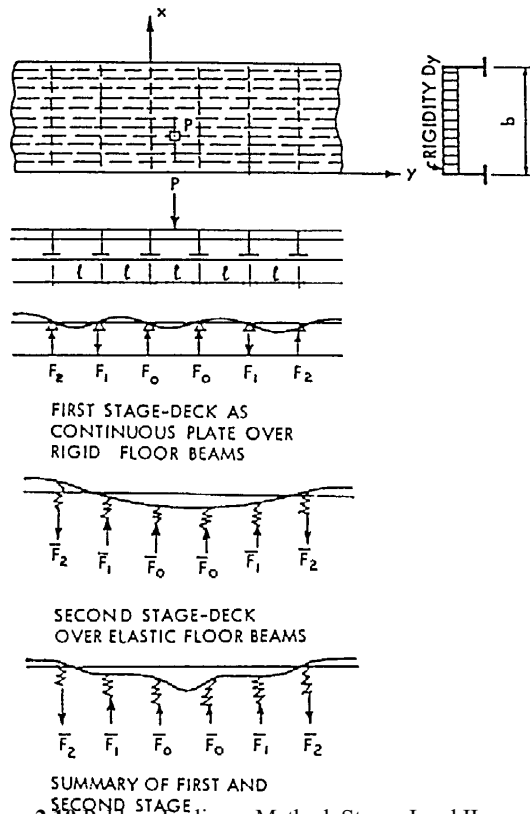
Figure 2.10 Pelikan-Esslinger Method. Stages I and II.

2.1.3.2 Deck with open ribs

For a deck plate stiffened by open or torsionally soft ribs, both the lateral flexural rigidity D_x and the torsional rigidity H are relatively small by comparison to that of the longitudinal flexural rigidity D_y. Therefore, for practical design purposes, they could be disregarded. Using

$$D_x = 0 \text{ and } H = 0 \qquad \qquad /2.44/$$

the general differential equation /2.22/ becomes:

$$D_y \frac{\partial^4 w}{\partial y^4} = p \qquad \qquad /2.45/$$

51

Equation /2.44/, in fact, represents the deflection line of a beam and defines an idealized structural system representing an actual steel plate deck with open ribs. It is assumed that the idealized system consists of a series of infinitely narrow plate strips placed side by side, and running continuously in a y-direction, Fig. 2.11.

Orthotropic Deck Analysis

Pelikan – Esslinger Method
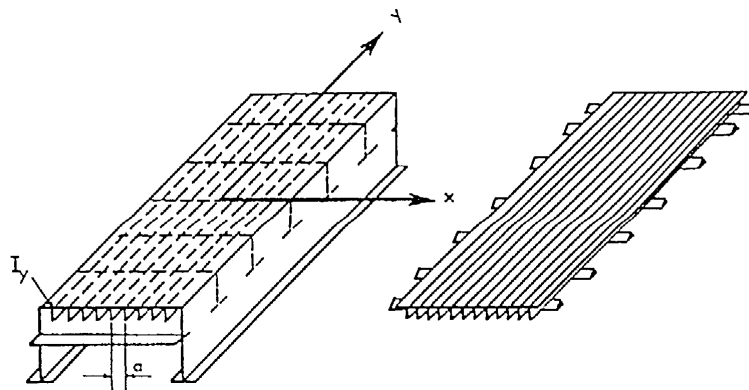
$$D_y = \frac{EI_y}{a}$$

Deck with torsionally soft ribs
$D_x = 0, \qquad H = 0, \qquad D_y \, \dfrac{\partial^4 w}{\partial y^4} = p$

Figure 2.11 Pelikan-Esslinger Method. Open rib deck.

A comparison of the bending moments computed, per unit width, with the full plate and beam /2.45/ formulas indicates a negligible difference for practical design purposes. Therefore, the use of the beam formula for a deck with open ribs is fully justified.

For practical design analysis, it is necessary to separately consider a deck on rigid supports and a deck on flexible floor beams. In both stages, the following data should be evaluated:

First Stage – Deck on Rigid Supports

1. *Bending Moments and Reactions in the Deck in a Longitudinal Direction*

Theoretically, these moments and reactions depend on the following factors:

a. Dead and live loading,

52

b. The relation between the floor beam and the main girder spacing,

c. The influence of the flexural and torsional rigidities of the deck system components.

In modern bridges having an orthotropic deck, the floor beams are closely spaced in relation to the main girder spacing. It is therefore considered that the main girder spacing does not influence that value of bending moments in a longitudinal direction.

2. Bending Moments and Their Reactions in Floor Beams

The evaluation of bending moments and their reactions in floor beams due to the action of dead and live loads depends on the composition of the bridge system. In the case of two main girders only, the floor beam is considered to be a simply supported T-beam. The floor beam is considered as a continuous T-beam if supported by more than two main girders.

3. Section Properties of the T- Ribs and Floor Beams.

For the evaluation of those stresses in the T-ribs and floor beams, it is necessary to determine in their sectional properties their effective span in a longitudinal direction and their effective width in the lateral direction.

Second Stage – Deck on Elastic Floor Beams

In this stage, it is necessary to evaluate the influence of the floor beam flexibility on a load distribution and, consequently, on their bending moments acting in the T-rib.

To achieve this, the following data should be determined:

1. The influence lines for the bending moments acting in T-ribs, considering the T-ribs as continuous beams elastically supported.

2. Additional moments in the T-ribs and relief moments in the floor beams.

3. Sectional properties of the T-ribs, namely the effective span, the effective width and the sectional modulus, considering the influence of flexible floor beams.

4. To evaluate the resulting moments by superposition of both stages and to determine those stresses in the T-ribs.

2.1.3.3 Deck with closed ribs

In the case of a deck plating stiffened by closed torsionally stiff ribs, Fig. 2.12, the transversal rigidity D_x is negligible in comparison to the flexural rigidity in the y-direction D_y and effective torsional rigidity H.

Therefore, the differential equation of the orthotropic plate /2.22/ is reduced to:

$$2H \frac{\partial^4 w}{\partial x^2 \partial y^2} + D_y \frac{\partial^4 w}{\partial y^4} = p \qquad \text{/2.46/}$$

It should be noted that those moments computed with the assumption $D_x = 0$ are generally somewhat greater than those determined from the complete equation; therefore, they are on the safe side.

For the computation of the bending moments in the ribs, the influence surfaces for a continuous orthotropic plate are used, based on those deflections found in the solution of equation /2.46/.

It should be further noted that in both cases for decks with open and closed ribs, although the flexural rigidity D_x of the deck plate does not enter equations /2.45/ and /2.46/ directly, its effect is not entirely disregarded, since this rigidity is a factor in the determination of that effective torsional rigidity expressed by formula.

<div align="center">
Orthotropic Deck Analysis
Pelikan – Esslinger Method
</div>

<div align="center">

Deck with torsionally stiff ribs
$D_x = 0, \qquad 2H \dfrac{\partial^4 w}{\partial x^2 \partial y^2} + D_y \dfrac{\partial^4 w}{\partial y^4} = p$

</div>
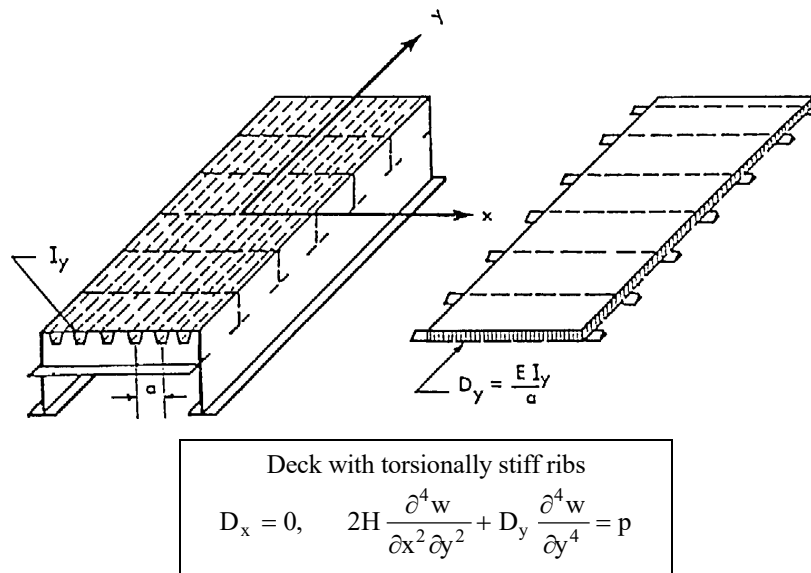
Figure 2.12 Pelikan-Esslinger Method. Closed rib deck.

For practical design purposes, the following data should be determined.

First Stage – Deck on Rigid Supports

1. Expressions for the influence surfaces used in the computations of the bending moments in the ribs, considering different loading conditions.
2. The actual deck loading expressed through the Fourier analysis as a series of sinusoidal component loads.
3. Properties of the sections, such as their effective span, width and section modulus.
4. Flexural and torsional rigidities of the deck.

Second Stage – Deck on Elastic Floor Beams

1. The influence of a flexible floor beam on its load distribution.

54

2. The determination of those additional moments, shear forces and reactions which originate in an orthotropic deck due to the flexibility of the floor beams.
3. Properties of the sections.

2.2 Large Deflection Theory of Orthotropic Plate

Large deflection theory of orthotropic plate is reviewed on the basis of Maquoi and Massonnet [1971] and Troitsky [1976].

2.2.1 General equations for large deflection

2.2.1.1 Introduction

The presently known methods of the analysis of orthotropic plates based on the structural theory of the first order. These methods may be considered as rigorous as long as the basic requirements of the theory are satisfied, namely, that the deflection of the orthotropic plates is small or $w \leq 0.2\ t$ and has no secondary effects on the stresses. By increasing the magnitude of the deflections beyond a certain level when $w \geq 0.3\ t$, we note, however, the lateral deflections are accompanied by stretching of the middle surface, provided that the edges of the plate are restrained against in-plane motion. When the magnitude of the maximum deflection reaches the order of the plate thickness or $w \approx t$, the membrane action becomes comparable to that of bending. Beyond this, when $w > t$, the membrane action predominates.

Although the large-deflection theory of plates assumes that the deflections are equal or larger than the plate thickness, these deflections should remain small relative to the other dimensions of the plate.

The large deflection theory of orthotropic plates presents an extension of the classical large deflection theory of isotropic plates with the necessary modifications. In 1910 Th.von Karman [1910] derived the following two partial differential equations of the large deflection for isotropic plates:

$$\frac{\partial^4 F}{\partial x^4} + 2\frac{\partial^4 F}{\partial x^2 \partial y^2} + \frac{\partial^4 F}{\partial y^4} = E\left[\left(\frac{\partial^2 w}{\partial x \partial y}\right)^2 - \frac{\partial^2 w}{\partial x^2}\frac{\partial^2 w}{\partial y^2}\right]$$

$$\frac{\partial^4 w}{\partial x^4} + 2\frac{\partial^4 w}{\partial x^2 \partial y^2} + \frac{\partial^4 w}{\partial y^4} = \frac{t}{D}\left(\frac{p}{t} + \frac{\partial^2 F}{\partial y^2}\frac{\partial^2 w}{\partial x^2} + \frac{\partial^2 F}{\partial x^2}\frac{\partial^2 w}{\partial y^2} - 2\frac{\partial^2 F}{\partial x \partial y}\frac{\partial^2 w}{\partial x \partial y}\right)$$

/2.47/

where

F = Airy's stress function
w = deflection of the plate
t = thickness of the plate
p = lateral load

$$D = \frac{Et^3}{12\left(1-\nu^2\right)} = \text{flexural rigidity}$$

E = modulus of elasticity of material

ν = Poisson's ratio

Equations in /2.47/ are coupled, nonlinear partial differential equations of the fourth order. The geometric nonlinearities are caused either by higher order terms of derivatives or by their products.

2.2.1.2 General equations for large deflections of orthotropic plates

General differential equations for large deflections of orthotropic plates were derived in 1940 by Rostovtsev [1940], who extended von Karman's equations by introducing the orthotropic stress-strain relationship.

In the following discussion, we will begin with the consideration of the bending of an orthotropic plate under lateral and in-plane forces. If only the first type of force is acting, then the stress distribution is that corresponding to bending. If only the in-plane forces are acting, the state of the generalized plane stress prevails.

In studying the combined action of the bending and in-plane forces in an approximate manner, we assume that the stress components are composed of two parts:

$$\begin{aligned}
\sigma_x &= \sigma_x^b + \sigma_x^m & \tau_{xz} &= \tau_{xz}^m \\
\sigma_y &= \sigma_y^b + \sigma_y^m & \tau_{yz} &= \tau_{yz}^m \\
\tau_{xy} &= \tau_{xy}^b + \tau_{xy}^m
\end{aligned} \qquad /2.48/$$

Here σ_x^b, σ_y^b, τ_{xy}^b are stresses proportional to z due to bending; σ_x^m, σ_y^m, τ_{xy}^m are values of the membrane stress through the thickness, arising from in-plane forces only.

In order to obtain the equation which the deflection w must satisfy, we will introduce the quantities N_x, N_y, N_{xy}, N_{yx} as in-plane forces per unit length.

$$N_x = \int_{-t/2}^{+t/2} \sigma_x dz = t\sigma_x^m, \qquad N_y = \int_{-t/2}^{+t/2} \sigma_y dz = t\sigma_y^m, \qquad N_{xy} = N_{yx} = \int_{-t/2}^{+t/2} \tau_{xy} dz = t\tau_{xy}^m \qquad /2.49/$$

Evidently N_x, N_y, N_{xy} satisfy the equations of equilibrium in the absence of body forces:

$$\frac{\partial N_x}{\partial x} + \frac{\partial N_{xy}}{\partial y} = 0, \qquad \frac{\partial N_{xy}}{\partial x} + \frac{\partial N_y}{\partial y} = 0 \qquad /2.50/$$

In order to determine them, it is necessary to solve the plane problem of the plate.

If we divide the plate into rectangular elements of dimensions dx, dy and t, we can then consider their equilibrium. Besides the forces and moments shown in Fig. 2.13, there will also exist the longitudinal forces shown in Figs. 2.14 and 2.15.
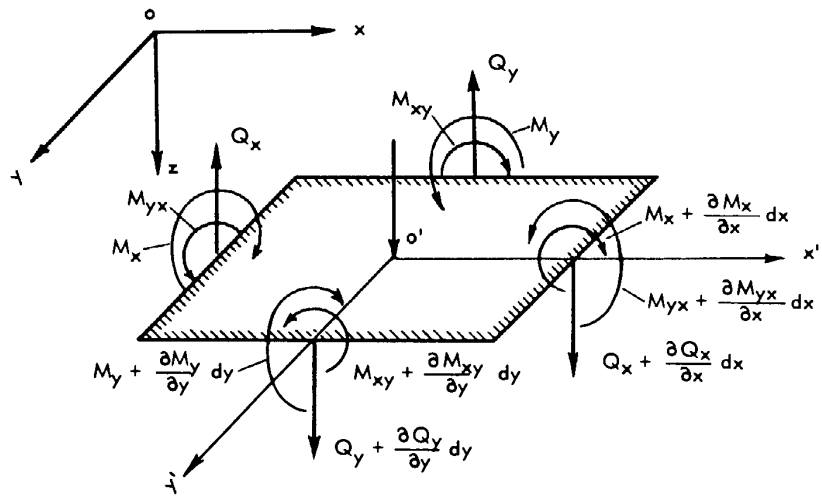
Figure 2.13 Forces and moments.
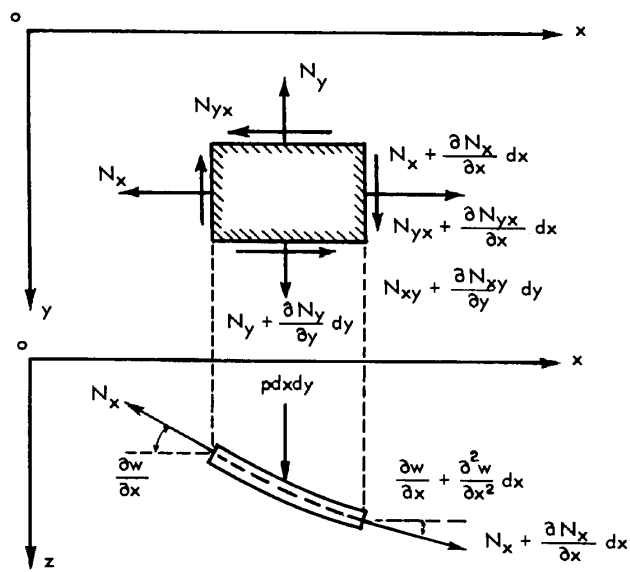
Figure 2.14 Normal and tangential forces in a plane.

57
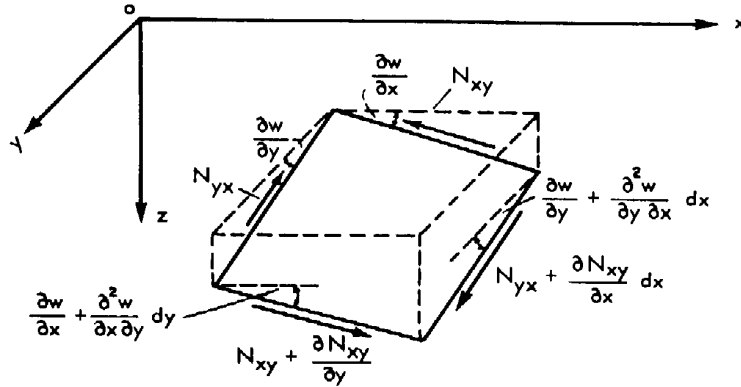
Figure 2.15 Components of normal and tangential forces.

Taking the curvature of the plate into account, the forces N_x, N_y, N_{xy} will not lie in the xy plane in the deformed plate; we obtain for the components of these forces in the z-direction

$$Z = \left(N_x \frac{\partial^2 w}{\partial x^2} + 2N_{xy} \frac{\partial^2 w}{\partial x \partial y} + N_y \frac{\partial^2 w}{\partial y^2} \right) dxdy \qquad /2.51/$$

or, per unit area,

$$\overline{Z} = \left(N_x \frac{\partial^2 w}{\partial x^2} + 2N_{xy} \frac{\partial^2 w}{\partial x \partial y} + N_y \frac{\partial^2 w}{\partial y^2} \right) dxdy \qquad /2.52/$$

This force $\overline{Z}$ must be added to the load p in Huber's Equation /2.22/ and we obtain for the orthotropic plate

$$D_x \frac{\partial^4 w}{\partial x^4} + 2H \frac{\partial^4 w}{\partial x^2 \partial y^2} + D_y \frac{\partial^4 w}{\partial y^4} = p + N_x \frac{\partial^2 w}{\partial x^2} + 2N_{xy} \frac{\partial^2 w}{\partial x \partial y} + N_y \frac{\partial^2 w}{\partial y^2} \qquad /2.53/$$

The problem of orthotropic plate bending with in-plane forces is appreciably more complicated if the deflection is not taken as small as when compared to the thickness. In this case, the deflection and the stress function are determined by a system of two non-linear equations.

Let us assume that the stress components are determined from Eqs. /2.48/ and that the corresponding strains may also be expressed in two parts

$$\varepsilon_x = \varepsilon_x^b + \varepsilon_x^m, \qquad \varepsilon_y = \varepsilon_y^b + \varepsilon_y^m, \qquad \gamma_{xy} = \gamma_{xy}^b + \gamma_{xy}^m \qquad /2.54/$$

The quantities ε_x^b, ε_y^b, γ_{xy}^b are the middle surface strains, depending not only on the displacements u and v, but also on the deflection w. From the general expressions for strain

components, by expansion in series and retaining only the first power of the derivatives of u and v and the second power of the derivatives of w, we get the known expressions

$$\varepsilon_x = \frac{\partial u}{\partial x} + \frac{1}{2}\left(\frac{\partial w}{\partial x}\right)^2, \qquad \varepsilon_y = \frac{\partial v}{\partial y} + \frac{1}{2}\left(\frac{\partial w}{\partial y}\right)^2, \qquad \gamma_{xy} = \frac{\partial u}{\partial y} + \frac{\partial v}{\partial x} + \frac{\partial w}{\partial x}\cdot\frac{\partial w}{\partial y} \qquad /2.55/$$

Elimination of u and v by means of differentiation gives

$$\frac{\partial^2 \varepsilon_x^m}{\partial y^2} + \frac{\partial^2 \varepsilon_y^m}{\partial x^2} - \frac{\partial^2 \gamma_{xy}^m}{\partial x \partial y} = \left(\frac{\partial^2 w}{\partial x \partial y}\right)^2 - \frac{\partial^2 w}{\partial x^2}\frac{\partial^2 w}{\partial y^2} \qquad /2.56/$$

The strains $\varepsilon_x{}^b$, $\varepsilon_y{}^b$, $\gamma_{xy}{}^b$ depend on the bending of the plate and are given by the formulas

$$\varepsilon_x = -z\frac{\partial^2 w}{\partial x^2}, \qquad \varepsilon_y = -z\frac{\partial^2 w}{\partial y^2}, \qquad \gamma_{xy} = -2z\frac{\partial^2 w}{\partial x \partial y} \qquad /2.57/$$

The total stresses σ_x, σ_y, τ_{xy} across the thickness lead to in-plane forces N_x, N_y, N_{xy} expressed by the equations /2.50/, and to the moments M_x, M_y and M_{xy}. The stresses τ_{xz}, τ_{yz} lead to the shear forces Q_x, Q_y. The stresses $\sigma_x{}^m$, $\sigma_y{}^m$, $\tau_{xy}{}^m$ satisfy the equations of equilibrium

$$\frac{\partial \sigma_x^m}{\partial x} + \frac{\partial \tau_{xy}^m}{\partial y} = 0, \qquad \frac{\partial \tau_{xy}^m}{\partial x} + \frac{\partial \sigma_y^m}{\partial y} = 0 \qquad /2.58/$$

from which it follows that they may be expressed in terms of the Airy's stress function F

$$\sigma_x^m = \frac{\partial^2 F}{\partial y^2}, \qquad \sigma_y^m = \frac{\partial^2 F}{\partial x^2}, \qquad \tau_{xy}^m = -\frac{\partial^2 F}{\partial x \partial y} \qquad /2.59/$$

These stresses are connected to the strains by the generalized Hooke's law

$$\varepsilon_x^m = \frac{1}{E_x}\left(\sigma_x^m - \nu_x \sigma_y^m\right), \qquad \varepsilon_y^m = \frac{1}{E_y}\left(\sigma_y^m - \nu_y \sigma_x^m\right), \qquad \gamma_{xy}^m = \frac{1}{G_{xy}}\tau_{xy}^m \qquad /2.60/$$

The transverse shear and in-plane forces satisfy the equation

$$\frac{\partial N_x}{\partial x} + \frac{\partial N_y}{\partial y} + p + N_x\frac{\partial^2 w}{\partial x^2} + 2N_{xy}\frac{\partial^2 w}{\partial x \partial y} + N_y\frac{\partial^2 w}{\partial y^2} = 0 \qquad /2.61/$$

which is obtained by considering the equilibrium of a rectangular plate element of Fig. 2.13, taking into account the force component in the z-direction arising from the longitudinal forces, Figs. 2.14 and 2.15.

After substituting expressions /2.60/ into /2.56/ and replacing the stresses by the corresponding stress function F from /2.59/ we obtain

$$\frac{1}{E_y}\frac{\partial^4 F}{\partial x^4} + \left(\frac{1}{G} - \frac{2\nu_x}{E_x}\right)\frac{\partial^4 F}{\partial x^2 \partial y^2} + \frac{1}{E_x}\frac{\partial^4 F}{\partial y^4} = \left(\frac{\partial^2 w}{\partial x \partial y}\right)^2 - \frac{\partial^2 w}{\partial x^2}\frac{\partial^2 w}{\partial y^2} \qquad \text{/2.62/}$$

The second equation necessary to determine F and w is obtained by substituting expressions for shear forces into /2.61/ and by replacing the longitudinal forces by the corresponding stress function F. Thus we obtain

$$D_x \frac{\partial^4 w}{\partial x^4} + 2H \frac{\partial^4 w}{\partial x^2 \partial y^2} + D_y \frac{\partial^4 w}{\partial y^4} = p + t\left(\frac{\partial^2 F}{\partial y^2}\frac{\partial^2 w}{\partial x^2} - 2\frac{\partial^2 F}{\partial x \partial y}\frac{\partial^2 w}{\partial x \partial y} + \frac{\partial^2 F}{\partial x^2}\frac{\partial^2 w}{\partial y^2}\right) \qquad \text{/2.63/}$$

Equations /2.62/ and /2.63/, together with the boundary conditions, determine the two functions F and w. Taking into account the stress function F, we can then determine the stresses in the middle surface of a plate by applying Eq. /2.59/. From the function w, which defines the deflection surface of the plate, the bending and the shearing stresses can be obtained by using the same formulas as in the case of plates with small deflection.

Thus the investigation of large deflections of plates reduces to the solution of the two non-linear partial differential equations /2.62/ and /2.63/. Integration of these equations is accompanied by great difficulties as a result of the nonlinear terms in the first equation: the solution of these equations in the general case is unknown. Some approximate solutions of the problem are known.

2.2.2 Non-linear theory of the post-critical strength of orthotropic box girders [Massonnet and Maquoi, 1973]

2.2.2.1 Basic considerations

The problem of the evaluation of the collapse strength of a box girder composed of four thin walls in steel and subjected to pure bending is of considerable difficulty, because it is influenced simultaneously by

(a) the geometrical non-linearity (change of geometry effect)
(b) the material non-linearity, due to the yielding of certain portions of the girder
(c) the interaction between the four walls composing . the box girder
(d) the presence of numerous longitudinal stiffeners.

With reference to (a), the Massonnet and Maquoi think that it is sufficiently well established [Maquoi and Massonnet, 1972] [Massonnet, 1968] that the consideration of geometric non-linearities is absolutely compulsory, to omit further comments here.

With reference to (b), taking into account simultaneously large deformations and plastic yielding, though theoretically possible (e.g. by suitable finite elements), complicates the calculations to such a point that, even with a very powerful computer, they become extremely heavy. For this reason, the current theory adopts the viewpoint of Wolmir [1962], Skaloud [1970] and Skalound and Novotny [1962] according to whom collapse of a compressed membrane plate occurs when the mean membrane stress along the lateral unloaded edges reaches the yield stress

σ_y determined by a compression test. This is the first basic hypothesis of the theory of Massonnet and Maquoi.

This hypothesis is compared with the tests of Massonnet and Maquoi and it is shown that it is in reasonable agreement with them. As it is possible to measure the value of the mean membrane strain ε_{mc} at collapse along the unloaded edges of the compressed flange, it should be possible to replace the actual yield stress of the steel used by a fictitious yield stress

$$\overline{\sigma}_y \equiv E\,\varepsilon_{mc} \qquad\qquad /2.64/$$

Finally, this collapse criterion is expressed by the relation

$$\frac{1}{a}\int_{-a/2}^{+a/2}\left(\sigma_x\right)_{y\,=\,\pm b/2}{}^{dx} = \overline{\sigma}_y \qquad\qquad /2.65/$$

in order to improve the degree of agreement of theory of Massonnet and Maquoi with the tests.

With reference to (c), it is obvious that the interaction between the compressed flange and the remainder of the box girder, namely the two webs and the pulled flange, is much smaller than the interaction between the web of a plate girder and its stiffening frame composed of the two flanges and the two adjacent transverse stiffeners [Maquoi and Massonnet, 1972].

More precisely, the flexibility of the webs is such that it is very reasonable to adopt, for the bending boundary conditions of the compressed flange, the simple support condition along the unloaded edges AD, BC; ($w = \partial^2 w/\partial y^2 = 0$) (Fig. 2.16). This relates to the second hypothesis.

With regard to the membrane boundary conditions, a box girder composed of perfectly plane plates and subjected to pure bending would obey Navier's bending theory and along the unloaded edges would be $N_y = N_{xy} = 0$.

If the calculation includes a small unavoidable initial curvature of the compressed flange, the conditions $N_y = N_{xy} = 0$ must remain reasonably correct if the mean collapse stress exceeds only slightly the critical stress (third hypothesis). The discussion of the test results will show that the degree of post-criticality n= does not exceed 1.5 for the box girders used commonly in civil engineering.

Longitudinally, the compressed flange presents a series of buckles alternatively above and below its median plane, separated by transverse straight nodal lines (Fig. 2.16). Investigations will be limited to the rectangular panel of dimensions a, b, corresponding to one of these buckles and bounded transversely by two adjacent nodal lines AB, CD, (Fig. 2.17) along which there is obviously $w = \partial^2 w/\partial y^2 = 0$.

With regard to the second hypothesis (that of simple support along AD and BC), it is obvious that the non-linear buckling deformations of the panel ABCD must affect the deformations of both webs and therefore their collapse stress.

However, it must be emphasized that the main aim is to predict the collapse moment M_{coll} of the whole box girder. The two webs' contribution to the global section modulus of the box girder is less than 15%, so that a large error on the estimation of this contribution would only slightly affect the value of M_{coll}.
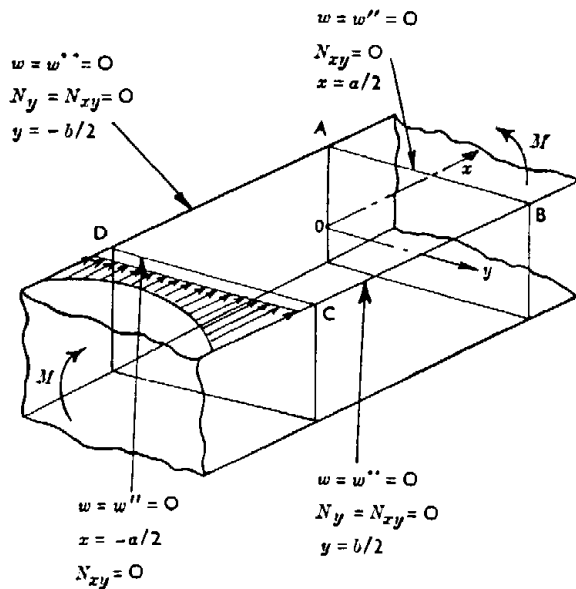
Figure 2.16 Boundary conditions of box girder
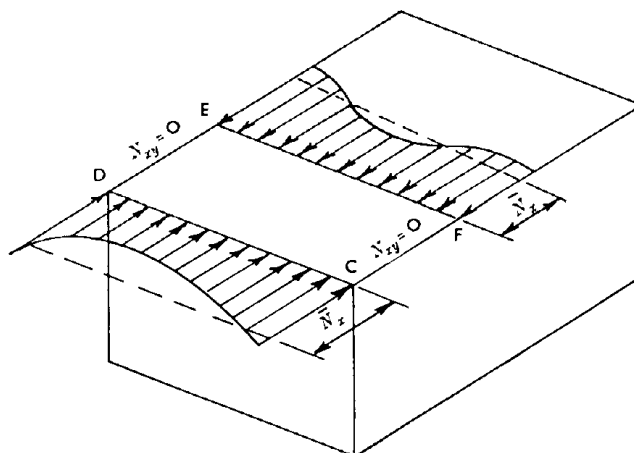
Figure 2.17 Stress distribution of plate

With regard to (d), it should be noted that the large box girders of modern bridges comprise between ten and twenty longitudinal stiffeners. In these conditions, it is not mathematically possible to analyse the individual action of these stiffeners. On the contrary, the bending rigidities of these stiffeners must be spread out continuously, as in the Guyon-Massonnet method for calculating beam grids and orthotropic plates [Bares and Massonnet, 1968]

Combining this consideration with the necessity emphasized in (a), to treat the plate as a non-linear membrane plate, it is necessary to start from the equations of an orthotropic membrane plate. These equations were first developed by Rostovtsev [1968]. However, these equations are valid only if the constitutive material itself is orthotropic. In reality, a structural orthotropy due to one-sided stiffeners must be dealt with. Pflüger [1947] has established the mathematical model of such plates in linear regime and it was indicated therefore to generalize Pflüger's equation by replacing the familiar relations of linear elasticity

$$\varepsilon_x = \frac{\partial u}{\partial x}, \qquad \varepsilon_y = \frac{\partial v}{\partial y}, \qquad \gamma_{xy} = \frac{\partial u}{\partial y} + \frac{\partial v}{\partial x} \qquad /2.66/$$

by the corresponding expressions of non-linear finite elasticity, first proposed by von Karman:

$$\varepsilon_x = \frac{\partial u}{\partial x} + \frac{1}{2}\left(\frac{\partial w}{\partial x}\right)^2, \qquad \varepsilon_y = \frac{\partial v}{\partial y} + \frac{1}{2}\left(\frac{\partial w}{\partial y}\right)^2, \qquad \gamma_{xy} = \frac{\partial u}{\partial y} + \frac{\partial v}{\partial x} + \frac{\partial w}{\partial x}\frac{\partial w}{\partial y} \qquad /2.67/$$

This generalization was presented by Maquoi and Massonnet [1971]. However, the resulting equations are rather complicated and comparative calculations showed that the additional terms due to the eccentricity of the stiffeners introduce corrections of only about 5%.

It was decided, therefore, to adopt the classical formulation of orthotropic membrane plates, but still to use the refined expressions for the bending and torsional rigidities given by the extended Pflüger theory.

2.2.2.2 Fundamental equations and their method of integration

The fundamental equations of an orthotropic membrane plate are two coupled non-linear partial differential equations in terms of

w_0 – the initial deflexion of the median plane of the plate (Fig. 2.17)

w – the additional transverse displacement of this plane

ϕ – the Airy stress function governing the membrane stresses through the relations

$$N_x = \phi^{..}, \qquad N_y = \phi'', \qquad N_{xy} = -\phi^{.'} \qquad /2.68/$$

with the simplifying notations $( )' = \dfrac{\partial}{\partial x}, \ ( )^. = \dfrac{\partial}{\partial y}.$

These equations are:

Compatibility equation

$$\frac{1}{D_x}\phi^{....} + \frac{2}{D}\phi^{..''} + \frac{1}{D_y}\phi'''' - \left(1-(\bar{v})^2\right)\left[(w_0^{..}+w'')^2 - (w_0^{..}+w^{..}) - \right.$$
$$\left. - (w_0''+w'') - w_0^{..2} + w_0^{..}w_0'' \right] = 0 \qquad /2.69/$$

Equilibrium equation

$$\overline{B}_X w'''' + 2\overline{C}\dot{w}\ddot{}''' + \overline{B}_y \dot{w}\cdots - \left[\phi''\left(w_0\ddot{}+\dot{w}\ddot{}\right) + \dot{\phi}\ddot{}\left(w_0''+w''\right) - 2\dot{\phi}\ddot{}'\left(w_0\ddot{}'+w\ddot{}'\right)\right] = 0 \qquad /2.70/$$

The values of the extensional, flexural and torsional rigidities D, D_x, D_y, B, B_x, B_y, B_{xy}, B_{yx}, as well as those of the modified rigidities $\overline{B}_x, \overline{B}_y, \overline{C}, \overline{D}$ are given as follows [Maquoi and Massonnet, 1973]:

Unit extensional rigidities

isotropic plate $D = \dfrac{Et}{1-v^2}$ and

stiffened plate $\quad D_x = \dfrac{1}{b_x}\displaystyle\int_{b_x} E(z)d\Omega_x$,

$\qquad\qquad\qquad D_y = \dfrac{1}{b_y}\displaystyle\int_{b_y} E(z)d\Omega_y$

where the notations $\displaystyle\int_{b_x}$ and $\displaystyle\int_{b_y}$ represent the integrals extended to the cross-sections of the stiffened plate, respectively of width b_x and b_y.
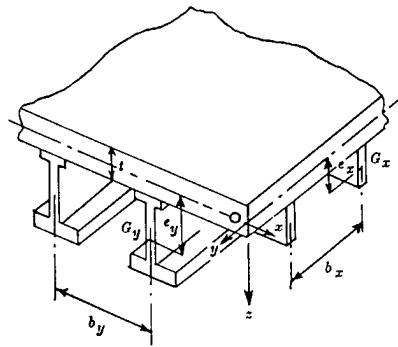
Distances of neutral axes of stiffeners to the middle plane z= 0

$$e_x = \frac{1}{b_x D_x}\int_{b_x} E(z)z\,d\Omega_x \;,\; e_y = \frac{1}{b_y D_y}\int_{b_y} E(z)z\,d\Omega_y$$

Unit flexural rigidities

isotropic plate $B = \dfrac{Et^3}{12\left(1-v^2\right)}$ and

stiffened plate $B_x = \dfrac{b_x}{1}\displaystyle\int_{b_x} E(z)(z-e_x)^2 d\Omega_x \;,\; B_y = \dfrac{b_y}{1}\displaystyle\int_{b_y} E(z)(z-e_y)^2 d\Omega_y$

Unit torsional rigidities

The unit torsional rigidities B_{xy} and B_{yx} are calculated from Saint-Venant's torsion theory. In the particular case of stiffeners with thin-walled open cross-section, $b_x B_{xy}$ and $b_y B_{yx}$ are calculated by formula $G/3\Sigma be^3$ where G is the Coulomb's modulus and b and e are the dimensions of rectangles composing the cross-section of the stiffeners.
The torsional rigidity arising in the fundamental equilibrium equation of linear theory is
$C = B + B_{xy} + B_{yx}$

Modified rigidities according to Pflüger [1947]

It has been demonstrated that the eccentricities of the stiffeners affect the preceding rigidities as follows:

$$\bar{D} = \frac{1-\nu}{1-\nu\dfrac{D^2}{D_x D_y}} D, \qquad \bar{B}_x = B_x - \frac{\bar{\nu}^2}{1-\bar{\nu}^2} e_x^2 D_x, \qquad \bar{B}_y = B_y - \frac{\bar{\nu}^2}{1-\bar{\nu}^2} e_y^2 D_y$$

$$\text{and } \bar{C} = B + \frac{1}{2}\left(B_{xy} + B_{yx}\right) + \frac{\nu}{1-\bar{\nu}^2} e_x e_y D \qquad \text{where} \qquad \bar{\nu} = \frac{D}{\sqrt{D_x D_y}} \nu$$

The boundary conditions (Fig. 2.16) are:
    bending: loaded edges AB and CD ($x = \pm a / 2$):

$$w = 0, M_x = 0, \text{ therefore } w'' = 0 \qquad\qquad /2.71/$$

unloaded edges AC and BD ($y = \pm b / 2$):

$$w = 0, M_y = 0, \text{ therefore } w^{..} = 0 \qquad\qquad /2.72/$$

membrane: loaded edges AB and CD:

$$N_{xy} = 0 \qquad\qquad /2.73/$$

The distance δ_x between these edges remains constant.
Unloaded edges AC and BD ($y = \pm b / 2$):

$$N_y = 0, N_{xy} = 0 \qquad\qquad /2.74/$$

The mathematical problem to be solved is the integration of equations /2.69/ and /2.70/ with the boundary conditions /2.71/ to /2.72/. The well known eigenfunction representing the first buckling mode of a compressed orthotropic plate is

$$w(x, y) = f \cdot \cos\frac{\pi x}{a} \cdot \cos\frac{\pi y}{b} \qquad\qquad /2.75/$$

To simplify the analysis,
(a) the plate presents an initial deflexion

$$w_0(x, y) = f_0 \cdot \cos\frac{\pi x}{a} \cdot \cos\frac{\pi y}{b} \qquad\qquad /2.76/$$

related to the first buckling mode (some idea about the importance of this imperfection may be gathered from reference [Maquoi, 1971]).
(b) in the post-critical range, it takes a supplementary deflexion

$$w(x, y) = f \cdot \cos\frac{\pi x}{a} \cdot \cos\frac{\pi y}{b} \qquad\qquad /2.77/$$

identical to the buckling mode, equation /2.73/.

It has been shown by Wolmir [1962] that this assumption yields rather small errors as long as the degree of post-criticality $n \equiv \overline{\sigma}/\sigma_{cr}$ is less than 1.5, which is the case in our flange plates (fourth hypothesis).

Starting from the expressions /2.75/ and /2.76/ of w and w_0, it is easy to integrate the compatibility equation /2.69/ exactly in closed form. The expression /2.76/ does not, however, satisfy exactly the equilibrium equation /2.68/. It is necessary therefore to resort to an approximate variational procedure, namely to the Bubnov-Galerkin procedure, which gives the value of the amplitude f of the additional transverse deflexion w, by stipulating that the error represented by the left-hand member of /2.70/ must be orthogonal to w. This condition reads

$$\int_{-a/2}^{+a/2} \int_{-b/2}^{+b/2} [\text{left-hand member of equation } /2.70/] \, w \, dx \, dy = 0$$

2.2.2.3 Collapse criterion

After lengthy calculations, and introducing the non-dimensional quantities

$$\frac{f_0}{t} = \varepsilon_0, \qquad \frac{f}{t} = \varepsilon, \qquad \frac{b}{t} = \lambda, \qquad -\frac{\pi^2 D_y \left(1 - \left(\overline{\nu}\right)^2\right)}{16\sigma_{cr}t} = k \, (>0!) \qquad \text{/2.78/}$$

the collapse criterion /2.65/ may be written:

$$\frac{\varepsilon}{\varepsilon + \varepsilon_0}(1 + m\delta) + k\frac{\alpha^2}{\lambda^2}\varepsilon(\varepsilon + 2\varepsilon_0)\left[(1 + 3\xi) + \left(\mu_1\frac{\alpha}{\pi J_1}\text{sh}\frac{\pi J_1}{\alpha} + \mu_2\frac{\alpha}{\pi J_2}\text{sh}\frac{\pi J_2}{\alpha}\right)\right] = \frac{1 + m\delta}{r} \quad \text{/2.79/}$$

where the new notation is defined as follows [Massonnet and Maquoi, 1973]:

$$m = \frac{b}{b'}, \qquad \alpha = \frac{a}{b}, \qquad \delta = \frac{\Omega_r}{bt}, \qquad \xi = \frac{D_x}{\alpha^4 D_y}, \qquad \theta = \frac{\overline{D}}{\sqrt{D_x D_y}},$$

$$J_1 = \sqrt{\frac{D_x}{D}}\sqrt{1 + \sqrt{1 - \theta^2}} \, , \qquad\qquad J_2 = \sqrt{\frac{D_x}{D}}\sqrt{1 - \sqrt{1 - \theta^2}} \, ,$$

$$\mu_1 = \frac{J_2 \text{sh}\dfrac{\pi J_2}{\alpha}}{J_1 \text{sh}\dfrac{\pi J_1}{\alpha}\text{ch}\dfrac{\pi J_2}{\alpha} - J_2 \text{sh}\dfrac{\pi J_2}{\alpha}\text{ch}\dfrac{\pi J_1}{\alpha}}, \qquad \mu_2 = -\frac{J_1 \text{sh}\dfrac{\pi J_1}{\alpha}}{J_1 \text{sh}\dfrac{\pi J_1}{\alpha}\text{ch}\dfrac{\pi J_2}{\alpha} - J_2 \text{sh}\dfrac{\pi J_2}{\alpha}\text{ch}\dfrac{\pi J_1}{\alpha}}, \text{ and}$$

$$\sigma_{cr} = -\frac{\pi^2}{\alpha^2 t(1 + m\delta)}\left(\overline{B}_x + 2\alpha^2\overline{C} + \alpha^4\overline{B}_y\right).$$

2.2.2.4 Limit efficiency of the compressed flange

The limit efficiency ρ_t of the compressed flange is defined to be (Fig. 2.17) the ratio of the mean stress $\overline{\overline{\sigma}}_x$ along the loaded edges $x = \pm a/2$ (Fig. 2.16) to the value of the yield stress in compression $-\overline{\sigma}_y$, at the moment where collapse occurs and collapse criterion /2.65/ [or /2.79/] is satisfied. By definition, then, the following equation is obtained:

$$\rho_t = -\left(\overline{\overline{\sigma}}_x \big/ \overline{\sigma}_y\right) \tag{/2.80/}$$

The calculations give

$$\rho_t = 1 - \frac{2k\alpha^2}{\lambda^2} r \frac{\xi}{1+m\delta} \varepsilon\left(\varepsilon + 2\varepsilon_0\right) \tag{/2.81/}$$

2.2.2.5 Correction to the discontinuous character of the stiffening

The theory discussed so far is based on the assumption of 'smeared' stiffeners. In fact, the plate panels enter rapidly in the post-critical range and present, between two adjacent stiffeners, a series of alternate buckles. The diagram of the longitudinal membrane strains ε_x shows therefore girdles which increase in depth with increased bending of the box girder. It is possible to take account approximately of this effect by introducing a partial efficiency ρ', which is the ratio of the total effort transmitted by the actual stiffened panel by the effort transmitted by the continuous substitution panel considered in present study. According to Fig. 2.18, this partial efficiency is

$$\rho' = \frac{m\, b'_e\left(\overline{\sigma}\right)\overline{\sigma}\, t + m\, A_r\, \overline{\sigma}}{\left(m\, b't + m\, A_r\right)\overline{\sigma}} = \frac{\dfrac{b'_e\left(\overline{\sigma}\right)}{b'} + \dfrac{A_r}{b't}}{1 + \dfrac{A_r}{b't}} \tag{/2.82/}$$

where $b'_e\left(\overline{\sigma}\right)$ specifies that the effective width of the local plate strip of width b' must be calculated for a maximum membrane stress at the edges of this strip, σ'_{max}, equal to $\overline{\sigma}$.

Maquoi and Massonnet [1971] gives a critical review of the various effective width formulae. The result of it is to show that the best formulae are those of Faulkner:

$$\left(\frac{b'_e}{b'}\right)_{Faulkner} = \frac{2}{B}\sqrt{\frac{\sigma_y}{|\overline{\sigma}|}} - \frac{1}{B^2}\frac{\sigma_y}{|\overline{\sigma}|} \tag{/2.83/}$$

with

$$B \equiv \frac{b'}{t}\sqrt{\frac{\sigma_y}{E}} \tag{/2.84/}$$

and Winter:

$$\left(\frac{b'_e}{b'}\right)_{\text{Winter}} = \frac{1.9}{B}\sqrt{\frac{\sigma_y}{|\overline{\sigma}|}} - \frac{0.8}{B^2}\frac{\sigma_y}{|\overline{\sigma}|} \qquad /2.85/$$
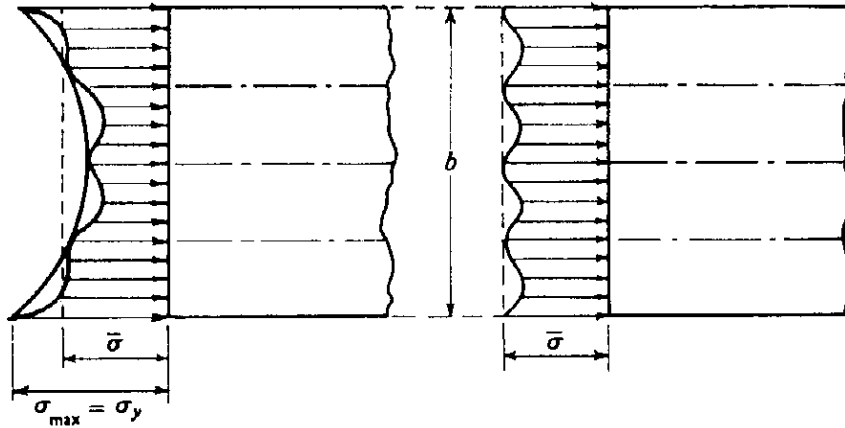
Figure 2.18 Stress distributions with stiffenings

The Winter formula given is not the version used in Maquoi and Massonnet [1971], but the modified, slightly less conservative version introduced in the 1968 edition of the Commentary of the AISI Specifications.

In effect, $\overline{\sigma}$ differs from strip to strip and is minimum at the middle of the stiffened panel (Fig. 2.18). If the stiffening is sufficiently strong, this pocket in the σ_x diagram is not too large and the reduced effective width of all panels may be calculated by Faulkner's formula, equation /2.83/, where $|\overline{\sigma}| = |\overline{\sigma_x}| = \rho_t \sigma_y$, ρ_t being computed by equation /2.81/. The local efficiency ρ' is then immediately furnished by equation /2.82/. For weaker stiffenings, the calculation of ρ' is more involved Maquoi and Massonnet [1971]. The global efficiency of the stiffened plate, ρ_g, is clearly given by the expression

$$\rho_g = \rho_t \rho' \qquad /2.86/$$

where ρ_t is given by equation /2.81/. The mean collapse stress is then

$$\overline{\sigma}_u = \rho_g \sigma_y \qquad /2.87/$$

2.2.2.6 Ultimate strength design of a box girder bridge

Summarizing the preceding theory, Massonnet and Maquoi recommend designing box girder bridges by adopting for the collapse loads determined by the theory described, the same safety

factor as that imposed by the specification regarding the yield stress of the steel for the considered loading case.

The Massonnet and Maquoi believe that the theory summarized here is a reasonable equivalent, for box girder bridges, of the collapse design methods of plate girders, namely the Basler-Thurlimann model and the various improvements made to it at the London IABSE Colloquium of March 1971 [Maquoi and Massonnet, 1972].

The theory described in the preceding sections may be immediately adapted to any kind of load factor or, equivalently, limit state design theory that should be substituted to the conventional factor of safety approach.

2.2.3 Results Comparison and Comments of Tests [Massonnet and Maquoi, 1973]

2.2.3.1 Design of test girders

The behaviour of the test girders must be as similar as possible to that of an actual box girder bridge. Therefore, the following principal parameters must be considered:

(a) the thickness b/t of the compressed stiffened flange
(b) the number (m-1) of longitudinal stiffeners
(c) the relative rigidity γ of longitudinal stiffeners
(d) the side ratio $\alpha = a / b$.

After examining the dimensions of recent large box girder bridges, it appears that it is not possible to make a model exactly to scale, because of the extremely large dimensions compared with the small thickness of the plate. Therefore a minimum thickness of 4 mm for the plate has been adopted to avoid welding problems.

The following requirements have been determined:

(a) the ratios b/t and b'/t are such that $25 < b/t < 70$ and $250 < b'/t < 750$
(b) the height of the webs is about 0.5 times the breadth b of the girder
(c) the side ratio α is often larger than 1 and about 1.2
(d) the neutral axis lies approximately at midheight of the girder.

The test girders are subjected to pure bending and the number of longitudinal stiffeners remains constant in all tests. For convenience, the section of the test box girders is not closed; however, it is sufficiently braced to guarantee the permanence of the rectangular cross-section.

The aim of these tests is to verify the theory of post-critical behaviour presented in the first part of [Massonnet and Maquoi, 1973] and, more precisely, to examine the effect of the rigidity of longitudinal stiffeners. If γ^* is called the 'optimum rigidity' of the linear buckling theory, the actual rigidity of longitudinal stiffeners will vary between 0.4 γ^* and about 4 γ^*.

For all the tests, the following data were selected:

thickness of the compressed plate t = 4 mm
breadth of test girders between axes of webs b = 1600 mm
height of webs   h = 726 - 732 mm
length of stiffened panelsa = 1920 mm
spacing of longitudinal stiffeners b' = 200 mm

length of the test girder   3a = 5760 mm

Thus:

m = 8,   b/t = 400,   b'/t = 50,   α = 1.2.

To avoid early instability of stiffeners, these are made of angles; furthermore, they are so designed to have rigidity ratios γ/γ* equal to 0.4, 1.0, 2.0 and 3.5. The intention is to make two additional tests on stiffened panels with transverse flexible stiffeners.

To emphasize the post-critical range, all the parts of the test box girders, as well as those of the re-usable end girders, are made of high strength steel.

In the fabrication of these test girders, welding sequences have been recommended which minimize the residual stresses. It has also been forbidden to use any artificial treatment intended to reduce the initial deflexions of the plates.

A general view of the cross-section of the test girders is shown in Fig. 2.19.
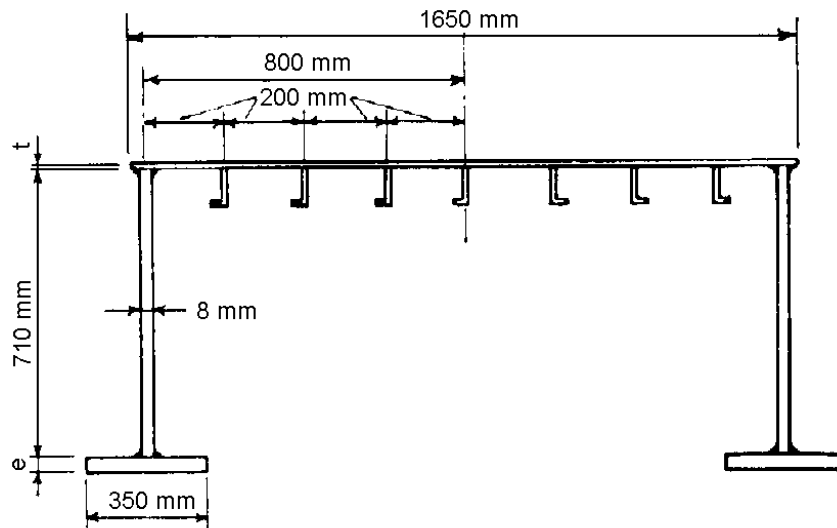
Figure 2.19 Cross-section of test girders.

A preliminary test led [Massonnet and Maquoi, 1973] to modify the stiffening of the test girders for the test panels adjacent to the bolted joints with the re-usable end girders. Indeed, these joints constitute a 'hard spot' and, in the preliminary test, local buckling was experienced in their vicinity. Therefore, an upper stiffening has been added to these panels, whose height decreases linearly from the joint to about 10 cm of the transverse stiffener.

2.2.3.2 Comparison of results and comments

Figures 2.20, 2.21 and 2.22 show, for the global efficiency, a very good agreement between the tests and the theory of the first part of [Massonnet and Maquoi, 1973] since the maximum difference is about ± 5 %. This result must be judged as excellent if the rather simple bases of the theory and the extremely complex character of the post-critical strength of stiffened plates are

considered. Massonnet and Maquoi believe that this difference between experimental and theoretical results could be reduced further if the loading corresponding to the collapse criterion could be determined more precisely. With regard to the centre deflexion, the agreement is still better, as shown in Table 2.3.
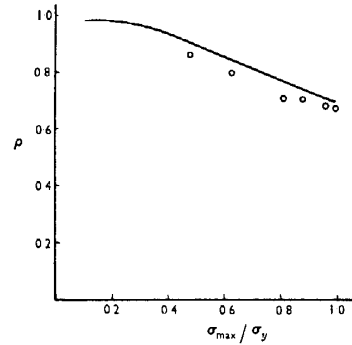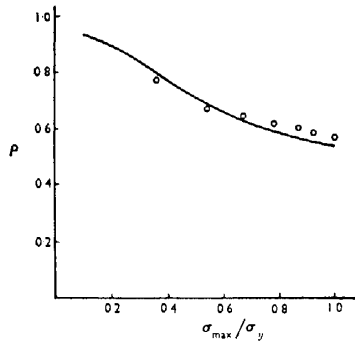
Figure 2.20 Comparison of results, test girder I   **Figure 2.21** Comparison of results, test girder II
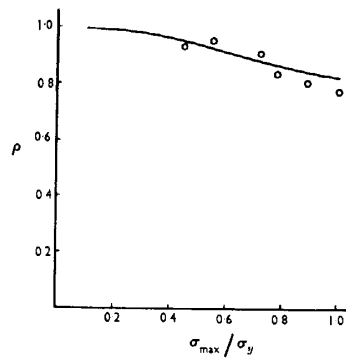
Figure 2.23 Comparison of results, test girder III

Table 2.3 Comparison of results.

Test girder No.	Global efficiency				Centre additional deflexion, *mm*	
	Experimental mid-span section, ρ_m^e	Experimental end section, ρ_e^e	Theoretical ρ^t	$\dfrac{\rho^t - \rho^e}{\rho^t}$	Experimental	Theoretical
I	0.54	0.57	0.53	-4.7 %	38	41.8
II	0.65	0.66	0.69	5.0 %	29	28.0
III	0.77	0.82	0.81	1.9 %	10	12.1

3 Limit States and Modelling of Orthotropic Plate

3.1 Collapses of Plate and Box Girder Bridges

On the turn of sixties and seventies the professional public opinion and the public were deeply shocked by some serious collapse of bridges (Fig. 3.1). In 6 November, 1969. the new Danube-bridge was snapped, which was built on the ring-road, but fortunately the bridge did not collapse. The next bridge was the Cleddau-bridge at Milford Haven (Wales, United Kingdom), where the steel box-girder with slant web-plate collapsed during the cantilever method of erection. In 15 October, 1970. the box-girder of the West Gate bridge at Yara-river collapsed during the cantilever method of erection. 35 people died in the accident, among them the erection manager engineer and his assistant. Just one year after, the steel box-girder of the Rhine-bridge at Koblenz (Germany) collapsed during the cantilever method of erection, 18 people died. Already at first sight, there was common factor in the four accident: all of the four cases the main girders were web-plated box-girders and all of them collapsed during the erection [Cartledge, 1973].

From the beginning of thirties, the web-plated steel structures started widely applied in Europe at building of larger bridges. At this time, the Árpád-bridge in Budapest was started to build, and if it could be finished, the span of the bridge could be a world record. During the bridge reconstruction after the Second World War this structure become more and more popular, and spread rapidly by the "I"-section the so-called box-girders, and the so-called orthotropic steel floor slab is naturalized. All this caused sharp turn against the bar-static, since these were difficult spatial plated-structures. Worked out the theory of gridworks, the calculation method of orthotropic plates, and the theory of the stability of plates (examination of plate buckling) rapidly developed. The way looked soft, the sky looked unclouded, when the four mentioned accident had occurred. Certainly immediate examination started in every case to discover the reasons of the accidents and to find out the responsibility. The national fact-finding committees discovered the causing reasons, pointed out the conditions and factors, which take part in the accident. The international professional public opinion summarized the cases and selected that reasons, which were common in all accidents. It was typical at every accident, that some reasons collective effect caused the collapse. However two reasons were find at every accident, thus general conclusions could be done.

Buckling occurred in all the three accident and at the structure damage in Vienna. The capacity of one of the element of the box-girders (bottom or web-plate) against buckling is used up, the plate deflect from its plain, thus the girder lost the rigidity. That could be occurred, because there were not correspondence between some basic assumptions of the buckling theories, which theories were developed by very big scientific apparatus and invariably do not disputed, and the everyday building practice. The theory basically assume plain plate and straight bracing, and assume the linear behaviour of the steel plate until a certain critical strength. These are idealistic assumptions, which necessary for solving the problems by mathematically. The everyday reality is somewhat different. In practice, there are not perfectly straight and plain plates. Yet a very thick plate deflects a little from its plain in the structure because of the welding stresses. Similarly the bracing, which is welded to the plate, deflect from the theoretical straight. Neither the unloaded ready structure is free from the stresses, because it contains the welding residual stresses. The calculated results therefore necessarily a bit differ from the reality, even if

the manufacturer of the steel structure working with modern technology thus with maximal precision. Together with the increasing production imprecision, the deflections are increasing, too.

The another common problem was the magnitude of the safety against the fracture in the state of erection. Previous to the accidents the common opinion was that, smaller safety reserve is enough during the erection than the safety against the calculated maximal load on the finished structure. Now it is known this opinion is theoretically incorrect. The prescribed moving loads of the finished bridge are such big, that the real occurrence on the bridge is very improbable. On the other hand the construction loads are really effective in every state of erection, and the possible instabilities are bigger during the erection. Therefore it is not justified, that the official regulations ordain bigger risk for the building contractor, than the operator of the finished bridge. The conclusions arisen from the box-girder-catastrophes were reached in every country. During the official orders, the designing and constructional regulations were revised and co-ordinated, the undertaking conditions were rendered more severe.

The bridges at Milford Haven, at Melbourne and at Koblenz were erected, the Danube-bridge at Vienna was repaired, and today they serve the traffic undisturbedly. Gently the confidence restored against the box-girders and nowadays new bridges are erected.

06.10.1969. Wien (Austria)	a)
02.06.1970. Milford-Haven (Great Britain)	b)
15.10.1970. Melburne (Australia)	c)
10.11.1971. Koblenz-Horcheim (Germany)	d)
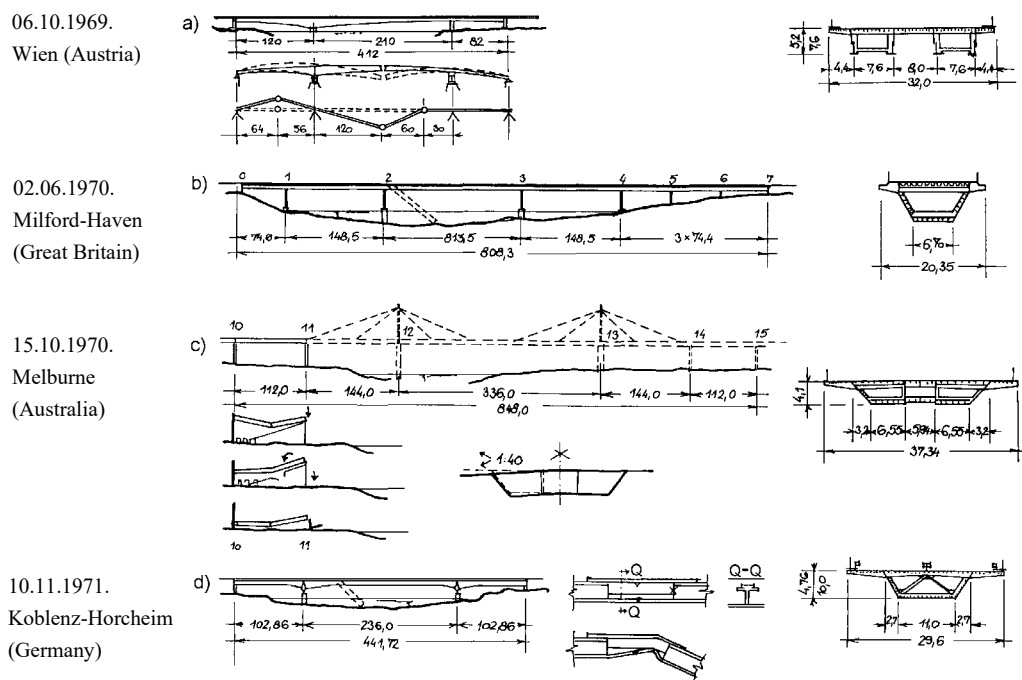
Figure 3.1 Collapse of bridges at the end of Sixties and at the beginning of Seventies.
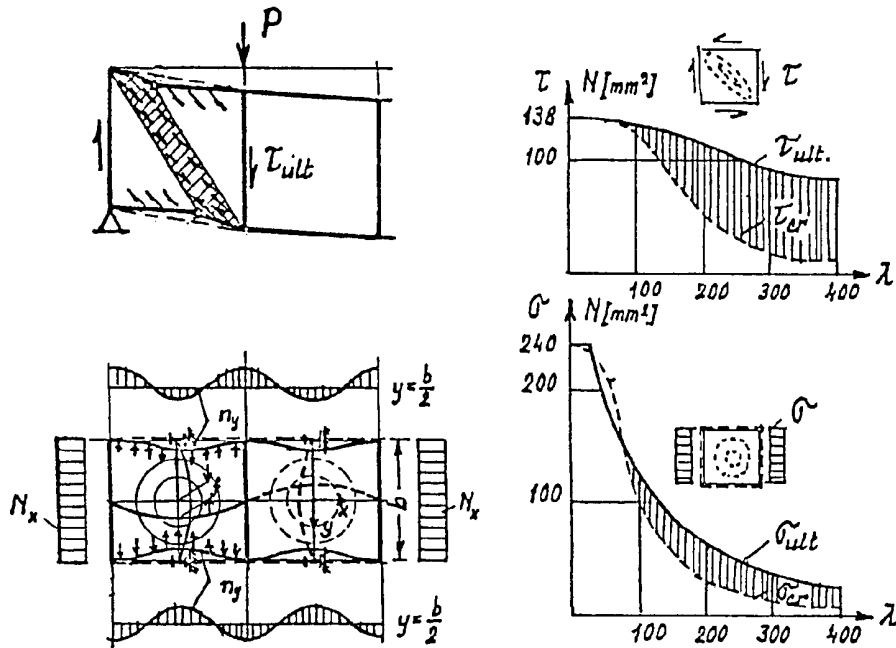
Figure 3.2 Plate buckling curves.

3.2 Design Criteria for the Different Substructures [Sedlacek, 1992]

The post-critical behaviour of sheared plate-panel and compressed plate are similar in several respects, such as the post-buckling state is occurred in the load carrying capacity state, however in other respects they have different behaviour (Fig. 3.2).

All elements of the deck have to be designed for

– the ultimate limit state,
– the serviceability limit state, and
– fatigue

In general the reserve of subsystems S1 and S2 to overloading by static local loads is so great because of their potential membrane strength, that the ultimate limit state does not govern design. This is illustrated by Fig. 3.3 [Pelikan and Esslinger, 1957] which shows the load-deflection curves for two tests conducted with a test deck, made of Fe 235. Tests revealed the results in Table 3.1 for the loads P [kN].

In general the serviceability criteria:

– no excessive local curvature of the deckplate (to prevent cracking of the asphalt surfacing) and
– no accumulated deformations,

together with fatigue criteria are the relevant limit states for the design of the deck plate and the longitudinal stringers. These permit the use of an elastic structural model for the analysis.

Table 3.1 Test results.

Limit State	1st test		2nd test	
	Calculated	Experimental	Calculated	Experimental
First yielding	35.2	41.0	20.01	22.0
First cracks	54.2	480.0	31.0	361.0
Ultimate load		>560.0		372.0
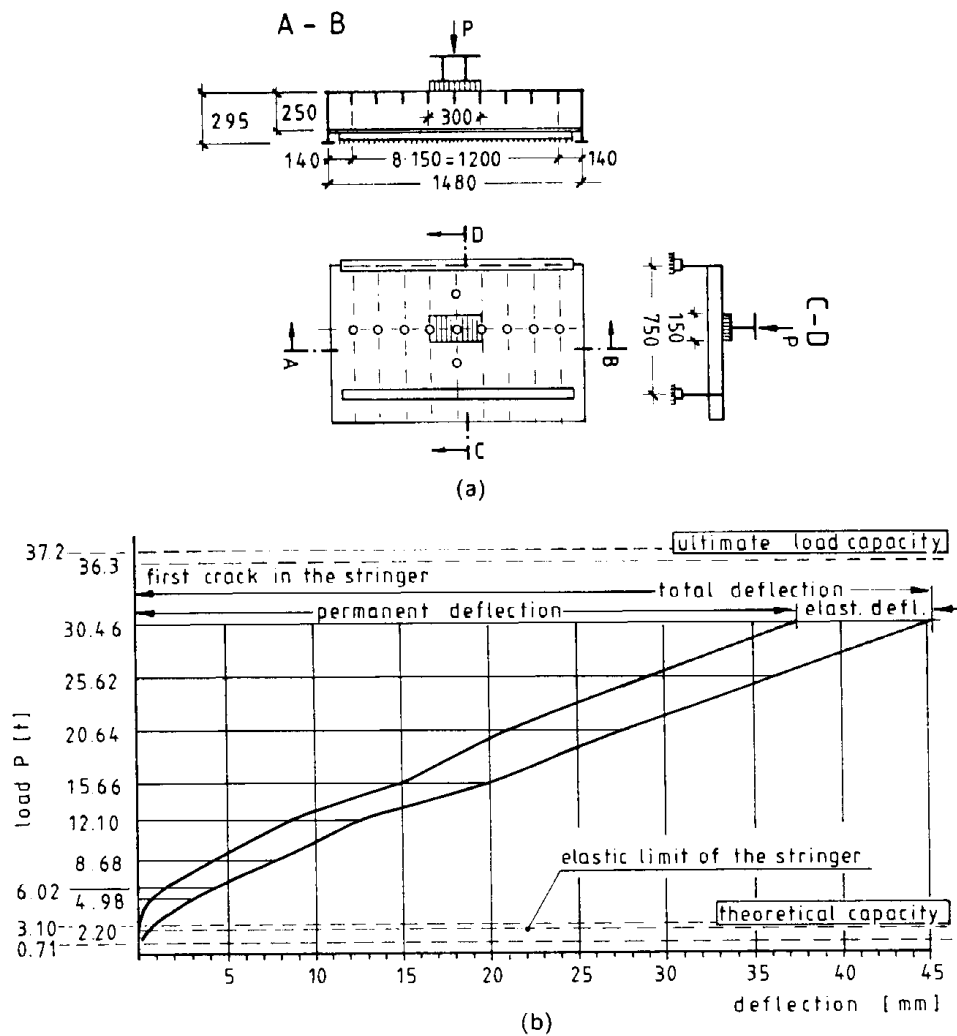
(a)

(b)

Figure 3.3 Results of loading tests. (a) Testpiece A for 1st deck (deck plate and ribs only); (b) testpiece B for 2nd test (deck plate, ribs and cross-beams).

Figure 3.3 Results of loading tests. (a) Testpiece A for 1st deck (deck plate and ribs only); (b) testpiece B for 2nd test (deck plate, ribs and cross-beams).

76
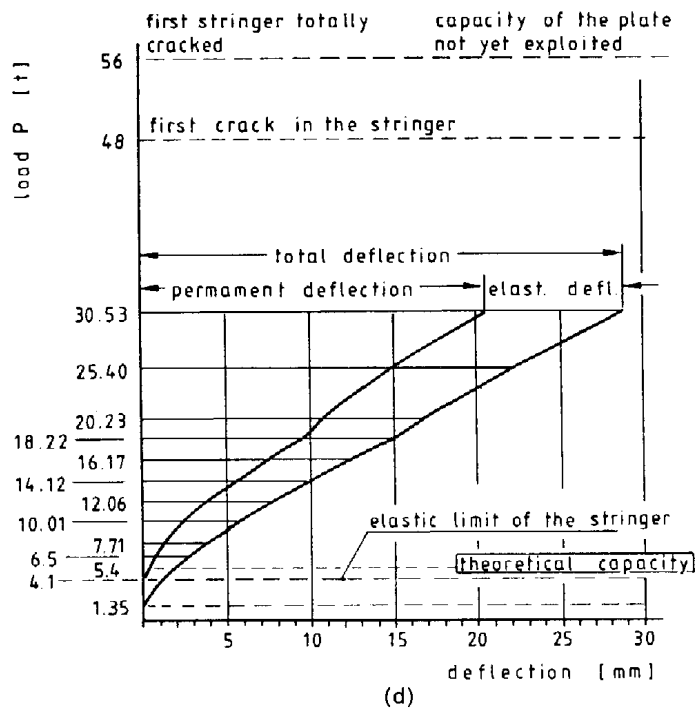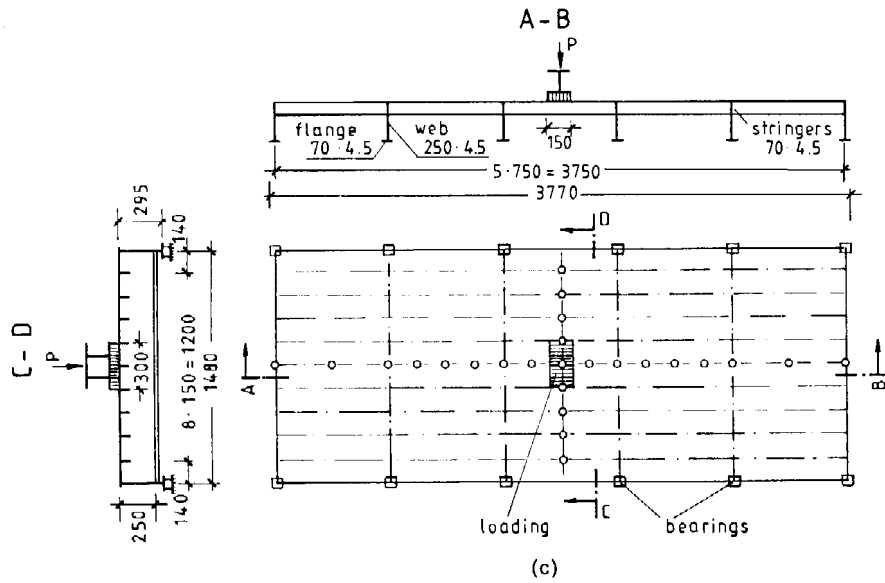
Subsystem S3 is also normally analysed using an elastic model to calculate moments and shears and deflections because the cross girders in general are not compact and so need to be treated elastically. From the analysis of the subsystems S2 and S3 the bending moments and shear forces in the longitudinal stringers and cross girders are derived. To calculate the ultimate limit states of the cross girders with respect to web buckling, e.g. the plate or lateral buckling of the bottom flanges of cantilevering cross girders, Fig. 3.4, full or partial plastic resistance models may be used. For serviceability limit states and for fatigue assessment purposes the models should be elastic. Particular care should be given to the inclusion of the total transverse frame in the assessment of fatigue strength.

The ultimate limit state check of the main girders of the bridge involves the superposition of the local effects from substructures S2 and S3 and the global effects from substructure S4, that take place in the orthotropic plate deck.

As the extreme values of the local traffic loading do not coincide with the extreme values of the global traffic loading, combination factors such as those given in Fig. 3.5 [Sedlacek and Merzenich, 1991] may be used when checking the deck.

When the bottom flanges of the bridge are in compression, the stability checks for the bottom flanges of box-girders or of open bridge sections may be performed taking account of the restraints provided by the integral action of the girders with the deck. For example, in Fig. 3.6 the spring stiffness of the cross frames influences the buckling wavelength of the bottom flanges of the open girders.
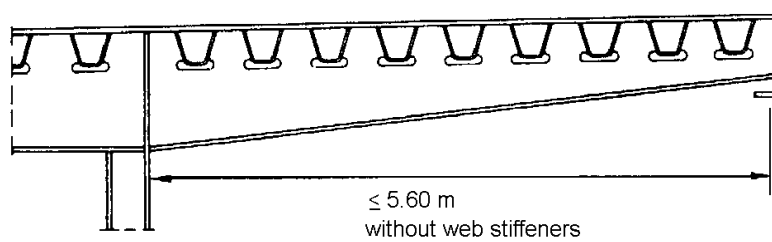
Figure 3.4 Cantilevering plates.
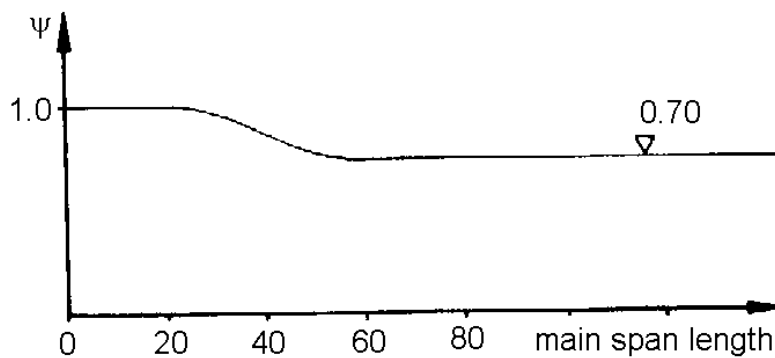
Figure 3.5 Combination factor for global loads for local plate verifications.
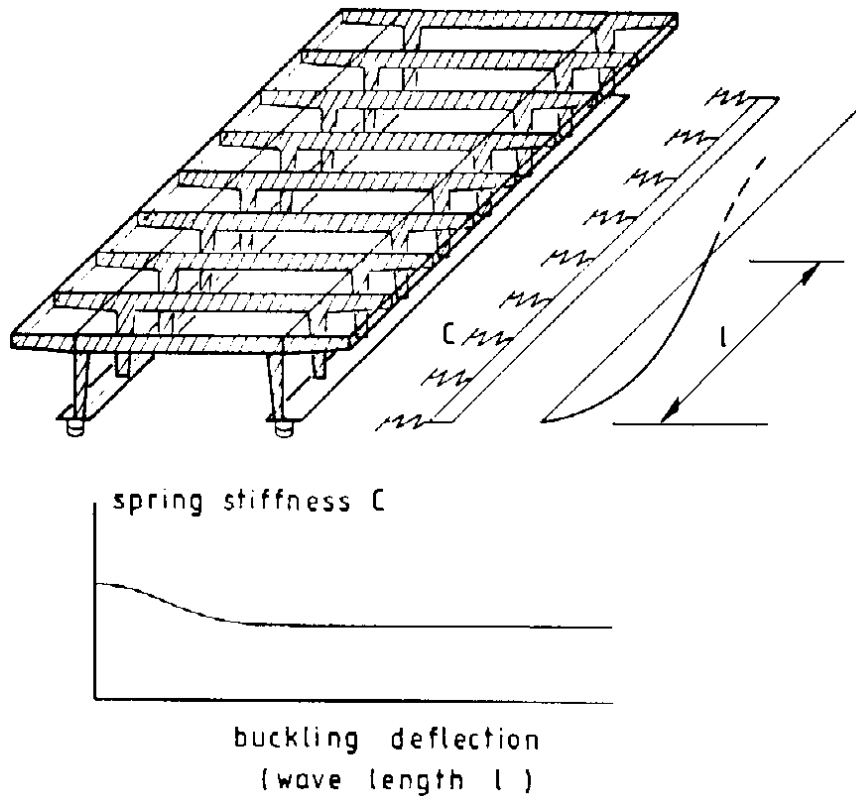
Figure 3.6 Spring stiffness of the frame depending on the buckling wave length *l*.

3.2.1 Analytical model for substructures S1

It is not normally necessary to model the deck plate in substructure S1 to check the ultimate limit state, as tests and background studies have shown that the stresses in the plate due to local bending may be neglected in design provided the minimum stiffness criteria for the durability of the asphalt layer given previously are satisfied. The ultimate local load capacity of the plate is so high, that the ultimate limit state is never relevant.

Tests also suggest that compliance with the minimum stiffness criteria and with the recommended welded details given for full penetration welds in Fig. 3.7 negates the need to carry out more elaborate fatigue calculations for the stringer-to-deck plate welds. Such welds may be laid without bevelling by automatic welding, when evidence of sufficient penetration is provided by proof tests.

It should be noted that the minimum stiffness criteria are only valid for stringers running in the longitudinal direction. When stringers run in the transverse direction, the situation for the durability of the asphalt surfacing worsens due to the 'wash-board-effect' of the traffic loading.

78

When no suitable minimum stiffness criteria are available serviceability and durability criteria should be established to limit the stresses, deflections or curvatures of the steel plate as calculated by superimposing the effects from substructures S1 and S2 [Günther et. al, 1987].
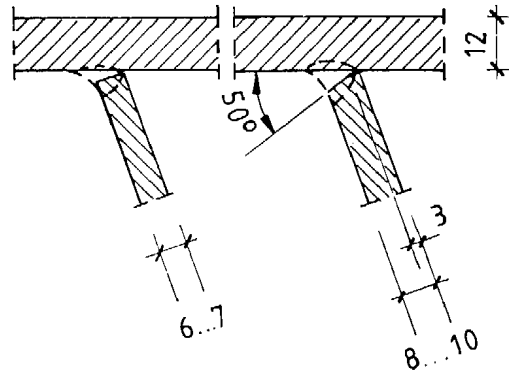
Figure 3.7 Weld preparation for the connection of the stringers to the deck plate [Kahmann, 1973].

3.2.2 Analytical model for substructures S2

3.2.2.1 Transverse stiffness of the orthotropic plate (Dₓ)

The transverse stiffness of the plate supported by rigid beams and elastic crossbeams is identical to the plate itself, besides the small stiffening effect of the longitudinal and transverse beams is neglected even in case of exact calculation. According to this:

$$D_x = \frac{E \cdot t^3}{12(1 - v^2)} = \frac{E \cdot t^3}{10,92} \,,$$

/3.1/

where E is the Young's modulus, t is the thickness of the plate, and v is the *Poisson's* ratio (v = 0,3 for steel).

As it was mentioned earlier further on $D_x=0$ approximation is used.

3.2.2.2 Longitudinal stiffness of the orthotropic plate (D_y)

The longitudinal beams stiffen the plate. When consider the plate as a continuum, the longitudinal stiffness of the orthotropic plate is the unit stiffness of the longitudinal beams, so:

$$D_y = \frac{EI_y}{a} \,,$$

/3.2/

where EI_y is the bending stiffness of a longitudinal beam where the effective width of the composite plate, as the flange is taken into account, a is the distance between the beams.

The only problem here is the consideration of the effective width of the plate. *Pelikan* and *Esslinger* provide an approximate calculation. Fig. 3.8 shows the cross section of the floor structure, where a, real width belongs to a longitudinal beam. a_0 effective width results from the condition, that if the a_0 width plate strip is compressed with the sliding force acting at the connection of the beam and the plate, the elongation of the plate strip will be identical to the elongation of the plate at the connection of the beam. According to this condition the effective

width depends on the a/k_l ratio and on the loading of the longitudinal beams. Here k_l- since the longitudinal beams are multi-span beams – is a smaller value than k, the span of the longitudinal beams. k_l is the distance of the points of zero moment, approximately $k_l=0.7k$. If only one longitudinal beam is loaded the effective width will be $a_0=0{,}3627k_1$. If each longitudinal beam has the same loading the a_0/a ratio can be taken from the graph of Fig. 3.9 in the function of $\beta=\pi{\cdot}a/k_l$.
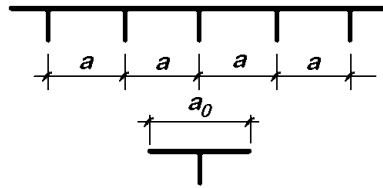
Figure 3.8 Effective width.
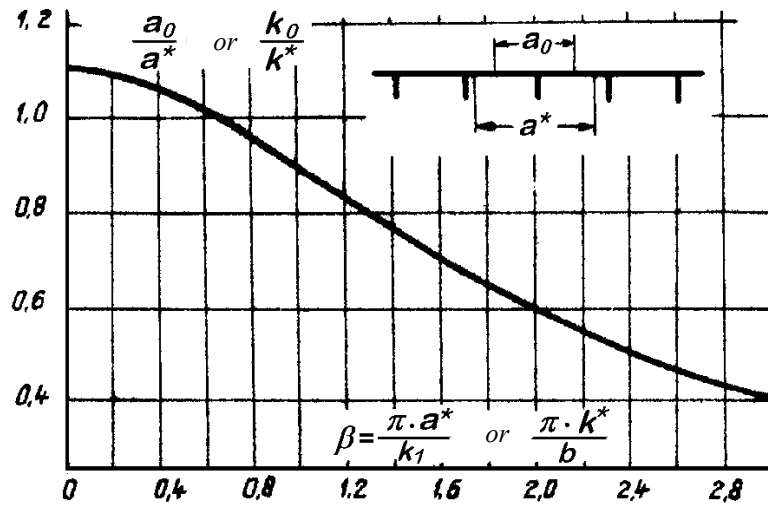
Figure 3.9 The determination of effective width [Halász, Hunyadi, 1959].

If the loading of the longitudinal beams is not the same on each, we will be allowed to count with a^* instead of a (Fig. 3.10). a^* is:

$$a^* = \frac{2A_0}{A_0 + A_1}\cdot a,\qquad\qquad /3.3/$$

where A_0 is the load of the beam No "0" and A is the load of the beam No "1". In this case at the graph of Fig. 3.9 a^* is used instead of a. The ratio of a^*/a can be taken from Fig. 3.14.b in the function of b_l/a. The determination of the loading of the longitudinal beam is discussed in chapter 3.2.3.1.
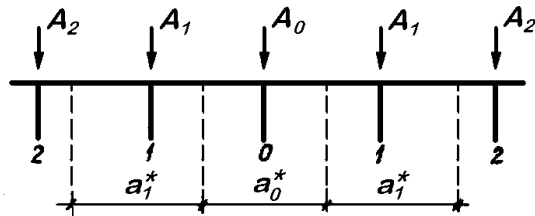
Figure 3.10 Effective width of differently loaded longitudinal beams.

3.2.2.3 The torsion stiffness of the orthotropic plate (H)

Torsion stiffness of longitudinal beams with open section

The torsion stiffness of the open section beams comes from the stiffness of the plate and the beams (Fig 3.11):
  - plate:

$$H_1 = D = \frac{E \cdot t^3}{10{,}92} ,$$
/3.4/

  - beam:

$$2H_b = \frac{GI_T}{a} = \frac{G \cdot d^3 \cdot h}{3a} ,$$
/3.5/

Here G is the shear modulus, I_T is the torsion inertia of the beam.
The complete torsion stiffness is:

$$H = H_1 + H_b = \frac{E \cdot t^3}{10{,}92} + \frac{G \cdot d^3 \cdot h}{6a} ,$$
/3.6/

In the further calculations the torsion stiffness of the beams will be neglected and we consider that $D_x = H = 0$.
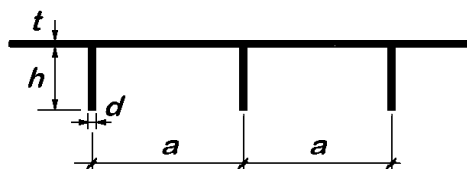
Figure 3.11 Longitudinal beam with open section.

Torsion stiffness of longitudinal beams with closed sections

The determination of the torsion stiffness of beams with closed section is rather difficult. *Pelikan* and *Esslinger* determines the torsion stiffness of semicircle, and trapezoid sections. The torsion inertia for closed sections

$$I_T = \frac{4A^2}{\Sigma \frac{\lambda}{s}},$$

/3.7/

is adequate only in case of pure torsion (here *A* means the area of the closed section). The effect of the section-distortion is taken into account by λ reduction factor. An assumption based on energy-principle is used, that the deformation work from the torsion in the real longitudinal beam is identical to deformation work of an idealized beam (with reduced torsion stiffness) from pure torsion. According to this, the torsion stiffness of the longitudinal beams in Fig. 3.12:

$$H = \lambda \cdot \frac{GI_T}{2(a+e)},$$

/3.8/
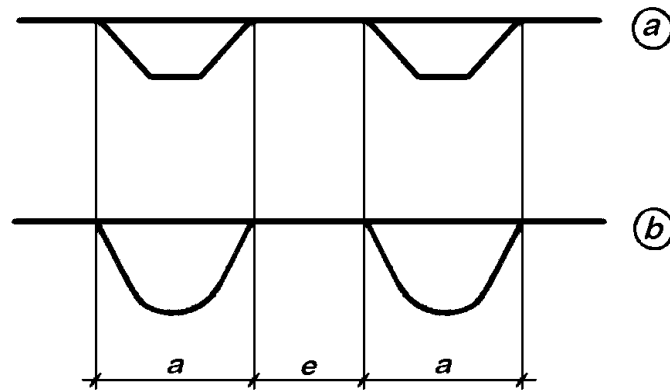
Figure 3.12 Longitudinal beam with closed section.

The value of λ reduction factor depends on the cross-section geometry. The formulas for trapezoid and semicircle section are available in the above-mentioned reference.

3.2.3 Analytical model for substructures S3

As it was already mentioned earlier, in case of plates stiffened by simply longitudinal beams the approximation of $D_x = H = 0$ can be used and through this the differential equation of the orthotropic plate is:

$$D_y \cdot \frac{d^4 w}{dy^4} = p(y),$$

/3.9/

The plate with D_y longitudinal bending-stiffness can be calculated as many endless continuous beams close to each other with the same spans, which are supported by the elastic crossbeams. The calculation is carried out in two steps. In the first step the crossbeams are considered as rigid, so the stresses are calculated on continuous beams with fixed supports. In the second step the deformation of the crossbeams is taken into account, and correcting elements are determined (Fig. 3.13).

First step

Second step

The sum of the first and second steps
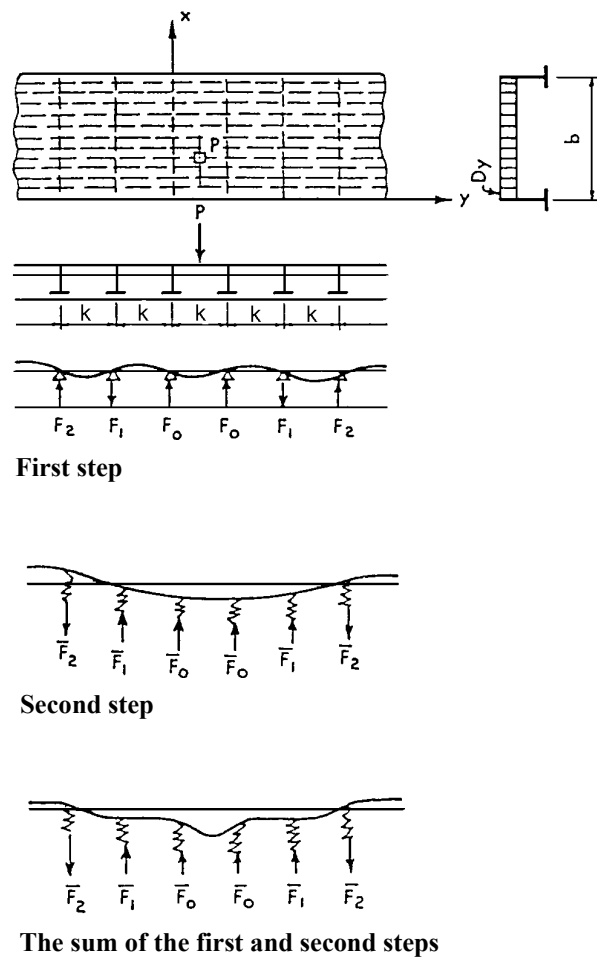
Figure 3.13 The *Pelikan-Esslinger* method [1957].

83

3.2.3.1 The determination of the loading of the longitudinal beams

The plate transmits the load between the beams. When determining the load-transmitting role of the plate, this can be handled as many continuous crossbeams close to each other, which are rigidly supported by the longitudinal beams. The loading of each longitudinal beam is the reaction force of these beams. It depends on the arrangement of the loading, the width of the loaded strip and on the distance between the longitudinal beams. For a general longitudinal beam the loading can be obtained from the graph of fig. 3.14.a.
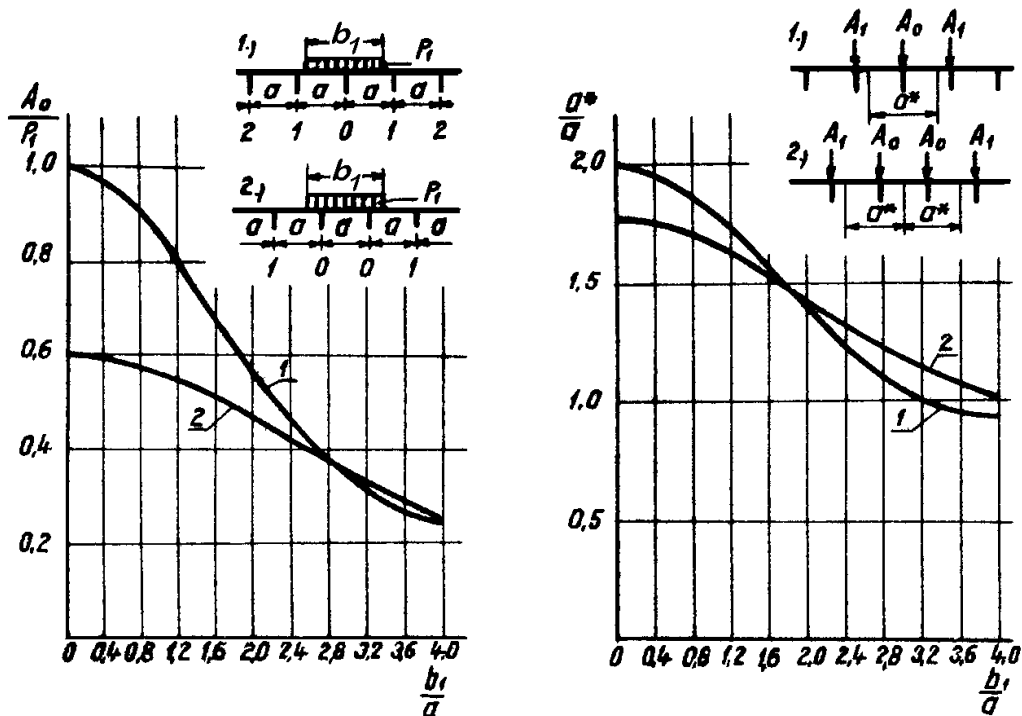
Figure 3.14 The loadings and the effective width of the longitudinal beam [Halász, Hunyadi, 1959].

3.2.3.2 Determination of bearing forces, considering rigid crossbeams

Moments on the longitudinal beams

The bending moment depend on the loading, the distance of the longitudinal and crossbeams, but independent on the sizes of the beams, so they are calculated for a structure only once. The moments can be calculated when knowing the loads, with the help of the influence diagram for continuous beams. *Pelikan* and *Esslinger* provide formulas for different loadings. These can be used because of their easy use [Pelikan, Esslinger, 1957] [Visontai, 1965]:

1) Moments of span

In cases of shown in Fig. 3.15 the formulas are the following:
a) load-case, *A* concentrated force in the middle of the span distributed on a strip with *2c* width (A=2cq):

$$M_{00} = A \cdot k \cdot \left[0{,}1708 + 0{,}1057 \left(\frac{c}{k} \right)^2 - 0{,}2500 \frac{c}{k} \right], \qquad /3.10/$$

b) load case, concentrated load in the midspan:

$$M_{00} = A \cdot k \cdot \left[0{,}1708 + 0{,}3170 \left(\frac{d}{k} \right)^2 - 0{,}5000 \frac{d}{k} \right], \qquad /3.11/$$

c) load case, concentrated load in an optional span:

$$M_{00} = A \cdot k \cdot \left[0{,}3170 \left(\frac{d}{k} \right)^2 - 0{,}1370 \left(\frac{d}{k} \right)^3 - 0{,}1830 \frac{d}{k} \right] (-0{,}2679)^m, \qquad /3.12/$$

where *m* is the smaller value from the numbers of the loaded span
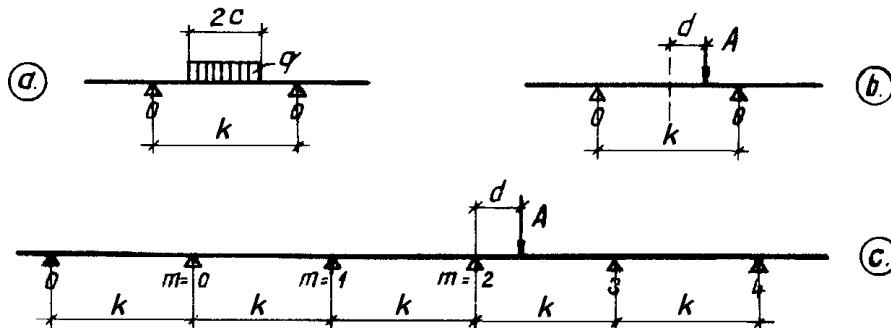
Figure 3.15 Load cases for moments of span.

2) Moments at the supports

The moment at the support "0" for the load cases shown in Fig. 3.16 is given by the following formulas:
a) load case, *A* concentrated force in the middle of the span distributed on a strip with *2c* width (*A=2cq*):

$$M_0 = A \cdot k \cdot \left[0,8661 \left(\frac{d}{k} \right)^2 - 0,3661 \left(\frac{d}{k} \right)^3 - 0,5 \frac{d}{k} + \right.$$
$$\left. + \left(\frac{c}{k} \right)^2 \cdot \left(0,2887 - 0,3661 \frac{d}{k} \right) \right] (-0,2679)^m .$$

/3.13/

The authoritative location of the load:

$$\frac{d}{k} = 0,3800 ,$$

/3.14/

and the moment at the support for this

$$M_0 = A \cdot k \cdot \left[-0,0850 + 0,1496 \left(\frac{c}{k} \right)^2 \right] ,$$

/3.15/

b) load case, concentrated load in an optional span:

$$M_0 = A \cdot k \cdot \left[0,8661 \left(\frac{d}{k} \right)^2 - 0,3661 \left(\frac{d}{k} \right)^3 - 0,5 \frac{d}{k} \right] (-0,2679)^m ,$$

/3.16/

where *m* is to be understood as previously.
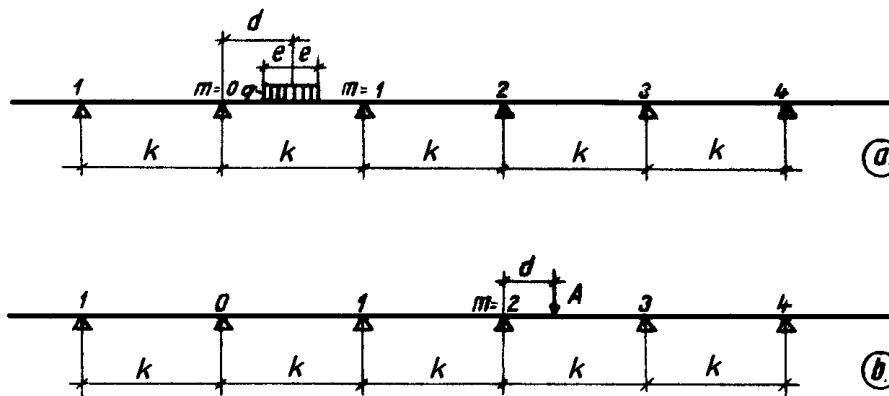
Figure 3.16 Load cases for moments at the supports.

Bearing forces of the crossbeams

The load from the longitudinal beams to the crossbeams is calculated as the reaction force of the fix supported continuous longitudinal beams. According to the reaction force influence diagrams the formulas can be used for the load cases shown in Fig. 3.17.

a) load case, a concentrated force in the 0-1 span:

$$B_0 = A \cdot \left[1 - 2{,}1961 \left(\frac{y}{k} \right)^2 + 1{,}1961 \left(\frac{y}{k} \right)^3 \right], \qquad /3.17/$$

b) load case, a concentrated force in an optional span

$$B_0 = A \cdot \left[1{,}3923 \left(\frac{y}{k} \right)^2 - 0{,}5884 \left(\frac{y}{k} \right)^3 - 0{,}8039 \frac{y}{k} \right] (-0{,}2679)^{m-1}, \qquad /3.18/$$

where *m* is the smaller value from the numbers of the loaded span
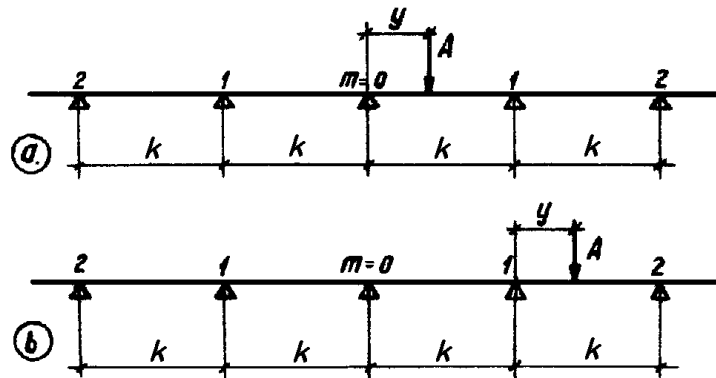
Figure 3.17 Load cases of fix supported continuous beam.

When calculating the reaction forces, the distributed loads can always be substituted by their resultant, so only concentrated forces are used.

The bearing forces from the transmitted loads can be determined on the crossbeam as a simply supported beam.

3.2.3.3 The effect of the elasticity of the crossbeam

After the loads of the crossbeam are determined, assuming continuous longitudinal beams with fix supports, we remove the fix supports and the external load at the joints, then we load the crossbeams with the reciprocal value of the determined reaction forces. Since according to our

assumption, the system contains infinite number of longitudinal beams, this load will be distributed. Although the torsion stiffness of the orthotropic plate is neglected, the load cycles of each longitudinal beam will not be independent on each other and due to the elastic deformation of the crossbeam – as the support of the longitudinal beams – some longitudinal beam will be loaded which normally would be unloaded. If the longitudinal beams are handled as continuous beams with sinking supports it will be necessary for the sinking of the supports to be proportional to the loading. Mathematically this means:

$$\frac{\text{deflection}}{\text{load}} = \frac{w(x)}{p(x)} = \frac{w(x)}{EI_{cb} \cdot w''''(x)} = \rho = \text{const.} \tag{/3.19/}$$

For the length of the whole crossbeam. From this:

$$w = \rho \cdot EI_{cb} \cdot w'''' \tag{/3.20/}$$

where ρ is the proportionality factor is the Young's modulus, EI_{cb} is the inertia of the crossbeam.

If the deflection curve is taken as a sine function variable (or function series) the load function will be a sine function too, since its fourth derivative is also a sine function. So the loading of the crossbeam has to be expanded in *Fourier* series and for the effect of the partial loads the calculation has to be carried out on the longitudinal beam as a continuous beam with elastic supports. The research of *Pelikan* and *Esslinger* resulted that the in often appearing cases when there are only two beams, it is enough to take into account only the firs member of the series (a system with half wave) (Fig. 3.18).
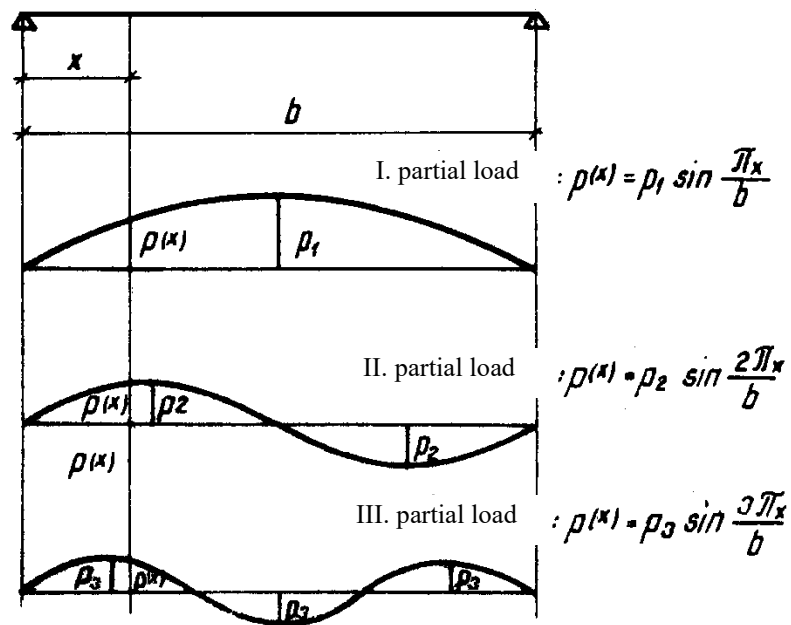
Figure 3.18 Partial loads of crossbeam [Halász, Hunyadi, 1959]

The spring constant from /3.19/ after four integrations:

$$EI_{cb} \cdot w'''' = p(x) = p_1 \cdot \sin\frac{\pi}{b}x, \qquad w(x) = \frac{1}{EI_{cb}} \cdot \frac{b^4}{\pi^4} \cdot p(x) = \frac{1}{EI_{cb}} \cdot \frac{b^4}{\pi^4} \cdot p_1 \cdot \sin\frac{\pi}{b}x$$

but the $w(x) = \rho \cdot p(x)$, therefore

$$\rho = \frac{1}{EI_{cb}} \cdot \frac{b^4}{\pi^4}, \qquad\qquad /3.21/$$

The Fourier series for the most often appearing load cases are shown in Fig. 3.19.

$$p_n = \frac{4p}{n\pi}\sin^2\frac{n\pi}{2}$$

$$p_n = \frac{2P}{b}\sin\frac{n\pi d}{b}$$

$$p_n = \frac{8p}{n\pi}\sin\frac{n\pi d}{b}\cdot\cos\frac{n\pi e}{b}\sin\frac{n\pi c}{b}$$
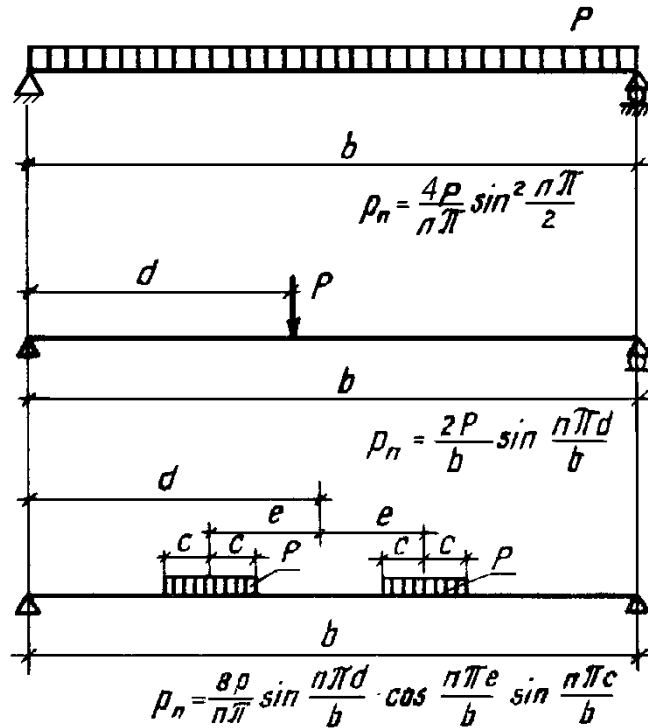
Figure 3.19 The most often appearing load cases [Halász, Hunyadi, 1959]

The bearing forces of the longitudinal beam from the elastic deformation of the crossbeam can be obtained in a way, that we determine the influence line of the continuous longitudinal beam with elastic support with the above-determined spring constant, and we load these curves with the partial loads. *Pelikan* and *Esslinger* provided some influence lines. The tables of these is a function of γ:

$$\gamma = \frac{I_b \cdot b^4}{I_{cb} \cdot k^3 \cdot a \cdot \pi^4}, \qquad\qquad /3.22/$$

where

    I_b is the inertia of the longitudinal beam

    I_{cb} is the inertia of the crossbeam,

    b   is the span width of the crossbeam,

    k   is the span width of the longitudinal beams (the distance between the crossbeams)

    a   is the distance between the longitudinal beams

The spring constant ρ is included in γ.

3.2.3.4 Calculation of orthotropic plates in case of longitudinal beams with torsion stiffness

In case of longitudinal beams with closed sections, the torsion stiffness of the plate H cannot be neglected; D_x bending stiffness can be neglected. The differential equation will be the following:

$$2H \cdot \frac{\partial^4 w}{\partial x^2 \partial y^2} + D_y \cdot \frac{\partial^4 w}{\partial y^4} = p(x, y),$$ /3.23/

so the calculation has to be carried out according to the plate- phenomenon. The general solution of the equation:

$$w = \sum (C_1 \cdot sh\alpha y + C_2 \cdot ch\alpha y + C_3 \cdot \alpha y + C_4) \cdot \sin\frac{n\pi x}{b},$$ /3.24/

The integral constants are determined according to the supports. The solution is an infinite series, so the loads have to be expanded into *Fourier* series.

The calculation is carried out in two steps. First the bearing forces at the place of the crossbeams are calculated as continuous plate, than the elasticity of the crossbeam will be taken into account. This last process is the same as written in the previous chapter.

So the problem is the determination of the bearing forces of an infinite length – continuous plate fix supported at the places of the crossbeam. The calculation process is similar to the process with the continuous beams. First the influence surfaces for the moments at the supports and the mid-spans and the reaction forces are determined, then these are loaded with the given load. The determination of the influence surfaces is a cinematic method; the surfaces are determined so that in case of moment surfaces $\vartheta = 1 \cdot \sin\frac{n\pi x}{b}$ relative rotation is applied at the

midspan (its distribution is a sine function) and in case of reaction force surfaces $w = 1 \cdot \sin\frac{n\pi x}{b}$

deflection is applied at the supports (its distribution is a sine function too), and from the deflection surface the solution is given. There are formulas for the moment- and reaction force values of these surfaces. Of course the influence surfaces and the loading were expanded in *Fourier* series in these calculations and the result is given as series too. The accuracy of the calculation depends on the number of the elements taken into account.

The general formula for the moments:

$$M = q \cdot k \cdot \sum \frac{q_x}{q} \cdot \frac{M}{Q \cdot k}, \qquad\qquad /3.25/$$

Here q is the intensity of the loading of Fig. 3.16, q_x/q is the load's *Fourier* coefficient and $Q = q \times 2c$.

The unit moment of M/(Q×k) is:

a) in case of moment in the span

$$\frac{M}{Q \cdot k} = \frac{1}{2\alpha k \cdot \alpha c} \cdot \left[1 - \frac{ch\alpha\left(\frac{k}{2} - c\right)}{ch\alpha\frac{k}{2}} \right] + \frac{M_0^*}{k} \cdot \left(1 - \frac{sh\alpha c}{\alpha c} \cdot \frac{1}{ch\alpha\frac{k}{2}} \right), \qquad /3.26/$$

where:

$$\alpha = \frac{n\pi}{b} \cdot \sqrt{\frac{2H}{D_y}}, \qquad\qquad /3.27/$$

$$\frac{M_0^*}{k} = \frac{\kappa}{a^* \cdot (1 - \kappa)} \cdot \frac{1}{2ch\alpha\frac{k}{2}}, \qquad\qquad /3.28/$$

$$\kappa = -c + \sqrt{c^2 - 1}, \qquad\qquad /3.29/$$

$$c = \frac{\alpha k \cdot cth\alpha k - 1}{1 - \frac{\alpha k}{sh\alpha k}}, \qquad\qquad /3.30/$$

$$a^* = 1 - \frac{\alpha k}{sh\alpha k}, \qquad\qquad /3.31/$$

b) in case of moment at the support, formula /3.26/ is used, but instead of /3.28/ the following member comes in:

$$\frac{M_0^*}{k} = \frac{\kappa}{a^* \cdot (1 - \kappa^2)}, \qquad\qquad /3.32/$$

of course these formulas have to be generated as a sum of n member, by taking into account that in α *n=1,3..n*.

For the determination of the *Fourier* coefficients for the two load cases of Fig. 3.20 we have the following formulas:

a) case

$$\frac{q_x}{q} = \sum \frac{4}{n\pi} \cdot \sin\frac{n\pi g}{b}, \quad n = 1,3,5\ldots,$$

b) case

$$\frac{q_x}{q} = \sum \frac{8}{n\pi} \cdot \cos^2 \frac{n\pi e}{b} \cdot \sin \frac{n\pi c}{b}, \quad n = 1,3,5\dots,$$
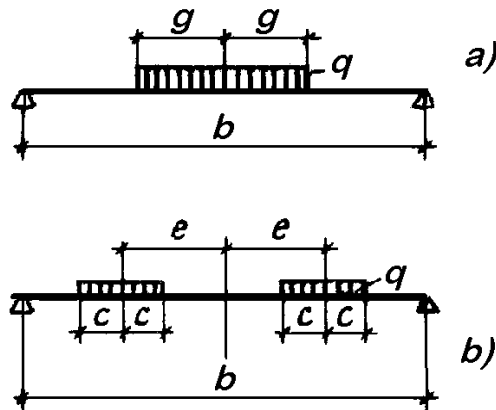
Figure 3.20 Load cases of crossbeam.

For the determination of the crossbeams, the determination of the reaction forces is necessary. This can be done according to the beginning of this chapter. The calculation of the crossbeams, and the correction from the elasticity of the crossbeams can be carried out according to the beginning of this chapter.

3.2.3.5 Stresses in the floor slab from direct loading (tertiary stresses)

The floor slab is a fix supported continuous isothropic plate, with infinite number of spans, supported by the longitudinal beams. The load is divided between the beams through the floor slap, while there are bending stresses it it as well. These stresses are called tertiary stresses. Load-transmitting and dividing role of the plate has already been discussed in 3.2.3.1, and we concluded that from the load transmitting point of view the plat can be modelled as plenty of beams with infinite length close to each other. But the stresses in the plate cannot be determined like this. Since the orthotropic plate itself is a statically indeterminate structure it has huge load bearing reserves, so the use of the plate phenomenon is not necessary either. *Pelikan* and *Esslinger* provides an approximate process, which is simply and enough accurate [Pelikan, Esslinger, 1957]. The essence of this process is that the bending moment in the plate is a product of K plate coefficient and the moments of the structure modelled by beams.

$$m_l = K \cdot m_g, \qquad\qquad /3.33/$$

Where m_l is the unit moment (mMp/m) in the plate, K is the plate coefficient and m_g is the moment of a 1 m wide plate-strip as a beam.

92

Case	Moment in the span	Moment at the support
1.		
2.		
3.		

Figure 3.21 Load cases of floor slab.

The value of K is given for three load cases (Fig. 3.22)

During the calculation process first the moments of the plate as beams according to /3.10/-/3.13/ are determined, than from the graphs of Fig. 3.22 we obtain *K*. the real moments of the plate are obtained from /3.33/.
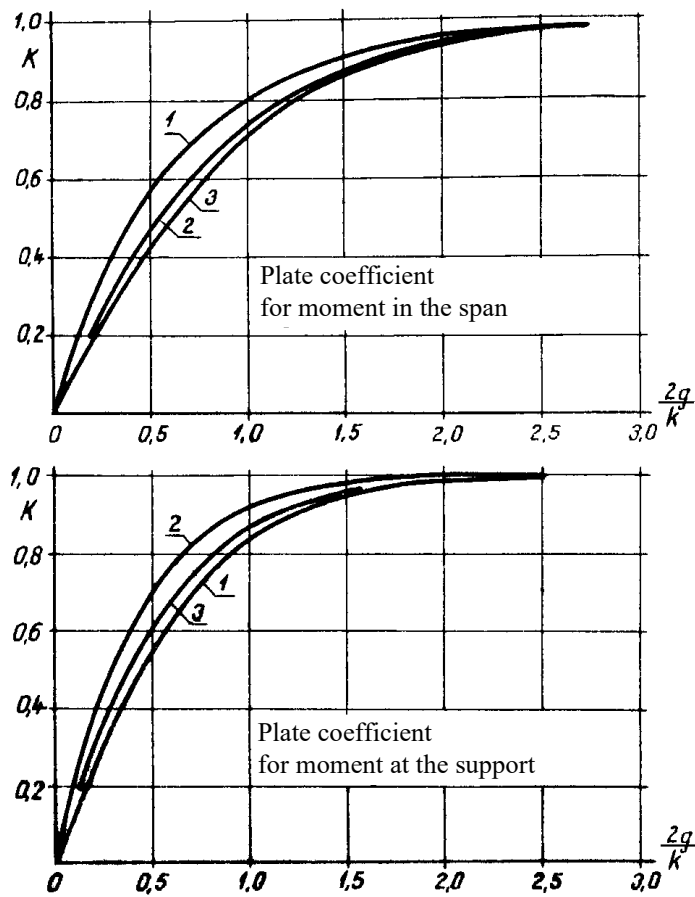
Figure 3.22 Plate coefficients [HALÁSZ, HUNYADI, 1959].

93

3.2.3.6 Calculation of gridworks

3.2.3.6.1 Introduction

Gridwork is a spatial structure, which consists of beams in two directions, which are connected to eachother in some way (Fig. 3.23).

The layout of the beams can be totally random. Here we discuss only the calculation process of such gridworks, where two spreads of beam (consists of parallel beams) are connected to eachother in a way that some relative deformations are allowed. Mostly the beams are perpendicular. The longitudinal directional beams are called main girder, the transversal directional beams – supported by the main girder – are called cross-girder. The connection of the main and the cross girder is usually rigid, which is able to carry torsion moments as well, but in some cases e.g. steel structures, where the torsion stiffness of the main girders are small, this can be neglected [Szabó, Visontai, 1962].

Further on we discuss special gridworks, where the main girders are parallel, simply-supported with identical spans, and the cross girders are perpendicular to the main ones.
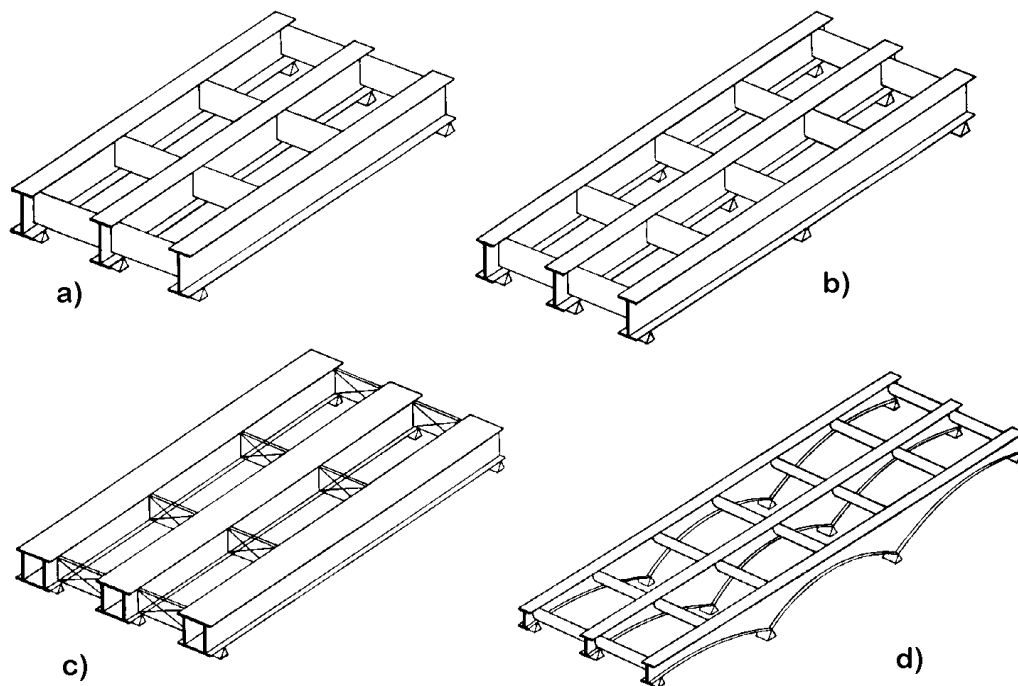
Figure 3.23 Gridworks *a), b)* simple and multi-span open main girder *c)* simple span box girder, *d)* multi-span variable web-plated main girder.

The basic models of the calculations can be divided into two classes:

a) the torsion is neglected, so the connection is able to transmit only vertical forces

b) the connection has torsional stiffness

In both classes assumptions are made, in order to make the calculation easier, but of course they provide approximate results.

In case a), the most often applied assumption is to use one ideal main girder. This comes from *Faltus*, but it has been is known from *Leonhardt* [Faltus, 1927] [Leonhardt, 1938].

It is worth to mention the process from class b), where the gridwork is substituted by a plate. Since the bending stiffness of the full gridworks is different in the directions of the main and the cross girders, the gridwork has to be substituted by an anisotropic plate where the elastic parameters are different in the two directions. If these directions are perpendicular, the plate is orthotropic plate. *Guyon* and *Massonnet* investigated this topic in details [Guyon, 1946a] [Massonnet, 1950c]. *Huber* and *Cornelius* made investigations on the exact calculation of gridworks with torsional stiffness.

Further on we show the approximation method of *Leonhardt* and the one from *Guyon* and *Massonnet*.

3.2.3.6.2 Analysis of a straight gridwork with one cross-girder with compatibility method [Szabó, Visontai, 1962]

The assumption of the primary structure

The basic model of the analysis is shown in Fig. 3.24. The connection of the girders is able to transmit only vertical forces, so the cross girders works as an elastically supported continuous beam. The primary structure of gridwork can be taken in a way that we cancel the connections between the main and the cross girders. The grade of the indeterminateness of the gridwork is identical to the cross girder's (as an elastically supported continuous beam) indeterminateness. In case of r pieces of main girder the indeterminateness is *r*-2. The cancelled connection forces are substituted by *r*-2 pieces of (now unknown) X_i force, which are vertical in case of vertical loads. So these forces are the intermediate reaction forces of the elastically supported continuous cross girder. With the determination of these forces the gridwork is solved, since we know all the forces acting on every member.
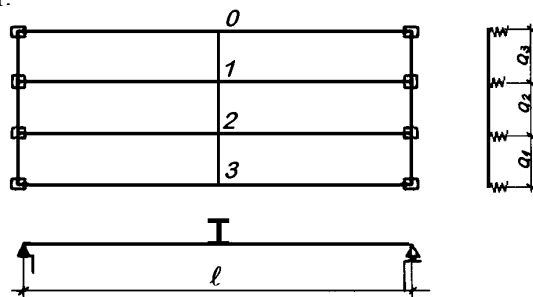
Figure 3.24 Straight gridwork with one cross-girder.

The easiest way for the termination of these X_i forces uses the so-called *cross-distribution factors*. The cross-distribution factors are the joint forces, which arise when a unit load acts at a joint. The sign of these factors is q_{ik}, where the first index denotes the location of the joint, the second one denotes the location of the $P_0 = 1$ kN unit load. So q_{ik} means the joint force at joint i, which arise from the effect of P_0 unit load at joint k. The cross-distribution factors are unit factor-like, but their components mean forces.

Determination of cross-distribution factors

According to the previous interpretation, the cross distribution factors are the reaction forces of the elastically supported continuous cross girder when the unit load is on a joint. So the reaction force influence lines of the elastically supported continuous cross girder have to be determined. The ordinates of these lines at the supports give the cross distribution factors.

The spring constant of the supports of the cross girder can be obtained from the deflection of the main girder under unit load. So in case of simply supported main girders with constant stiffness, when the cross girder is in the middle:

$$\rho_i = \frac{\ell_i^3}{48EI_i},$$

The reaction force influence lines from the already known formula:

$$\eta(B_i) = \eta(B_i)^0 + \sum_{i=0}^{n} B_{ik} \eta(X_k),$$

where B_i is the reaction force influence line of the support "i" of the body structure of the cross girder B_{ik} means the reaction force when the unit moment acts at k. $\eta(X_k)$ is the moment influence line of point k.

For instance in case of a gridwork with 5 main girders, the reaction force influence line of the cross girder at point 2 (Fig. 3.25)

$$\eta(B_2) = \eta(B_2)^0 + B_{21} \cdot \eta(X_1) + B_{22} \cdot \eta(X_2) + B_{23} \cdot \eta(X_3),$$

where

$$B_{21} = \frac{1}{a_2}, \quad B_{22} = -\frac{1}{a_2} - \frac{1}{a_3}, \quad B_{23} = \frac{1}{a_3} .,$$

The ordinates of the reaction force influence line at the supports give the cross distribution factors q_{20}, q_{21}, q_{22}, q_{23} and q_{24}.

When determining all the influence lines of the reaction forces, we get all the cross distribution factors (Fig. 3.26).
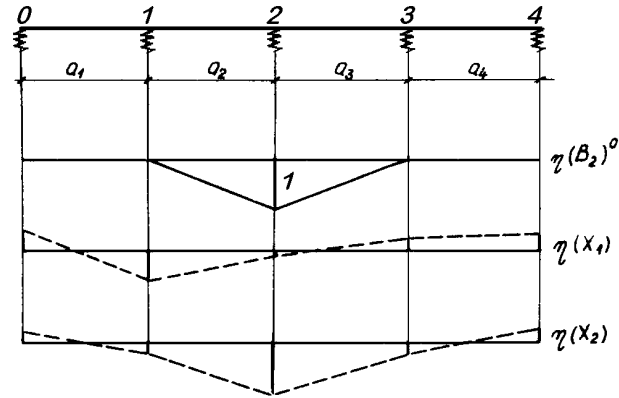
Figure 3.25 The reaction force influence lines of the cross girder.
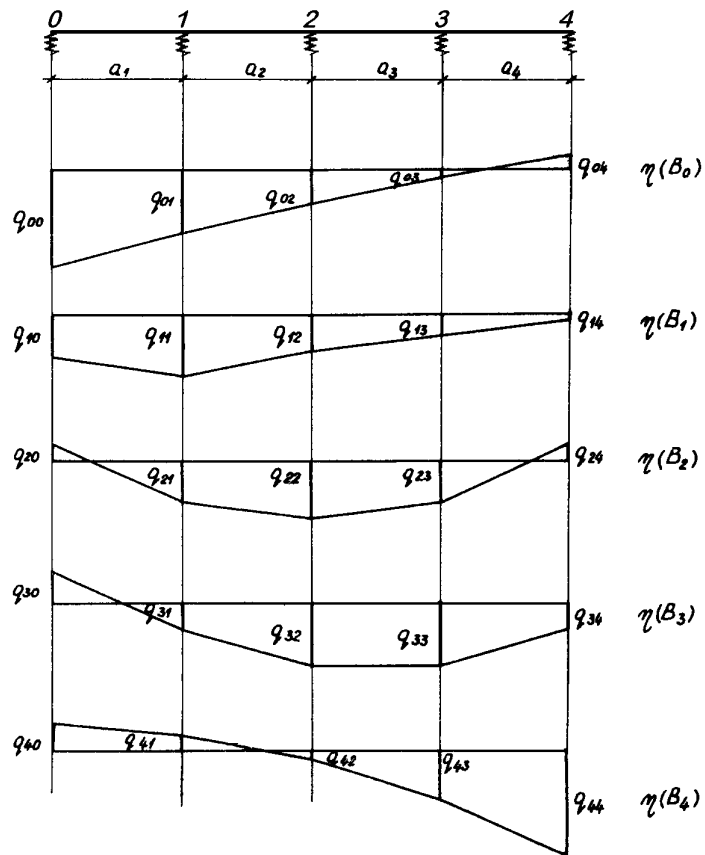
Figure 3.26 Determination of the cross distribution factors.

97

There are some relations between the cross distribution factors. On the one part because of the equilibrium of the structure, the sum of the reaction forces of a loading is unit, so.

$$\sum_{i=0}^{n} q_{ik} = 1 = +q_{02} + q_{12} + q_{22} + q_{32} + q_{42} = 1$$

On the other part according to *Maxwell*'s reciprocal theorem:

$$e_{ki} = e_{ik},$$

so:

$$\rho_k \cdot q_{ki} = \rho_i \cdot q_{ik},$$

from when:

$$q_{ik} = \frac{\rho_k}{\rho_i} \cdot q_{ki},$$

When the main girders are of constant stiffness and the main girder is in the middle:

$$q_{ik} = \frac{I_i}{I_k} \cdot q_{ki},$$

These formulas are either for checking, or for make the calculation process easier.

Determination of influence lines

The vertical loads of the grid can act within region T. We can analyse the value of effect $C_{x,y}$ at point (ξ, η) for the force $P(\xi, \eta)$ respectively the effect C as a function of $1/2C_{x,y}(\xi, \eta)$. This function under region T can be demonstrated by a surface, which is called *influence surface*. When determining the influence surface of a cross section the basic assumption is that the forces acting between the main girders are transmitted by virtual simply supported beams, parallel to the cross girders. From this comes, that its vertical sections, belonging to the plane of the main girders, can obtain the influence surface of a cross section. So the same number of sections can determine an influence surface as the number of the main girders.

A section in the plan of a main girder – which is an influence line – provides the chosen bearing force as a function of the location of the unit load. Two cases are distinguish:

1. P_0 force acts on the same main girder where the chosen cross-section is
2. P_0 force acts on an other girder

These two cases are demonstrated on the example of the previous gridwork with 5 main girders. Let section k on the main girder No. 2 be the one where the bearing forces are analysed (Fig. 3.27).
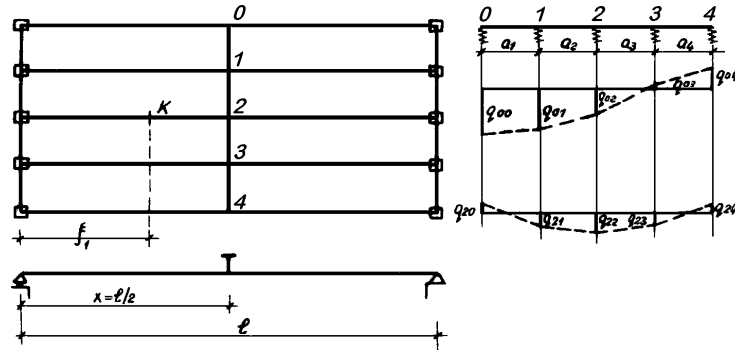
Figure 3.27 The layout of the examined gridwork.
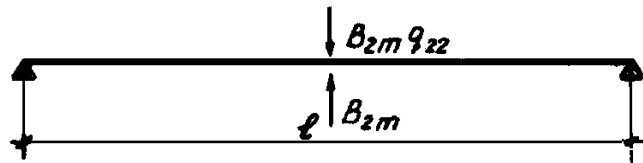
Figure 3.28 The model of main girder No. 2.

1. P_0 acts through the main girder No.2, so the section of the influence surface *C* of cross section *k* is to be determined at the main girder No.2. Main girder No.2 is directly loaded besides P_0 by joint force X_2 as well. The question is the value of X_2. According to *Leonhardt*, we make the following assumption. If main girder No. 2. were rigidly supported by the cross girder, the structure would be a two span continuous beam. Let the reaction force of the intermediate support be B_{2m} (the second index denotes the location of P_0, see Fig. 28). let us ignore the assumed fix support; this means that we put a force on the girder, which has the same value as B_{2m}, but its direction is opposite. However this force is distributed among the main girders through the cross girder. From this the force on girder No. 2 is $B_{2m} \times q_{22}$, acts down. So altogether:

$$X_2 = -(B_{2m} - B_{2m} \cdot q_{22}) = -B_{2m}(1 - q_{22}),$$

force (acts upwards that's why it is negative) acts on main girder No. 2. So B_{2m} means the reaction force influence line of the main girder fix supported in the middle. In case of a girder with constant inertia, when the analysed cross section is in the middle of the cross girder, the reaction force influence line can be determined analytically. According to the kinematic way of solution:

$$B_{2m} = \frac{e_{m2}}{e_{22}},$$

where e_{m2} denotes the deflection influence line of the simply supported beam, and e_{22} denotes the deflection of the mid-section under unit force (Fig. 3.29). The value of the deflection of a point with abscissa x:

$$e_{m2} = \frac{1}{EI}\left(\frac{1}{2}\frac{\ell}{4}\cdot\frac{\ell}{2}\cdot x - \frac{x^2}{4}\cdot\frac{x}{3}\right) = \frac{1}{EI}\left(\frac{\ell^2}{16}x - \frac{x^3}{12}\right) =$$

$$= \frac{\ell^3}{48EI}\left[3\frac{x}{\ell} - 4\left(\frac{x}{\ell}\right)^3\right]$$

and

$$e_{22} = \frac{\ell^3}{48EI},$$

thus

$$B_{2m} = 3\left(\frac{x}{\ell}\right) - 4\left(\frac{x}{\ell}\right)^3 = \xi,$$
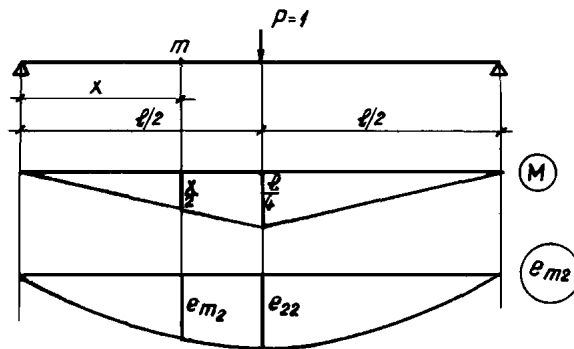
Figure 3.29 Bending moment and deflection curves of simple span beam.

With this we obtain the value of the joint force, which is:

$$X_2 = -\xi(1 - q_{22}),$$

The bearing of the cross section is a result of the bearing forces from P_0 and X_2:

$$C = C_0 + X_2 C_2,$$

where C_2 denotes the bearing force under the unit load at joint 2.
In case of influence line:

$$\eta(C) = \eta(C_0) + C_2\eta(X_2) = \eta(C_0) - C_2\xi(1 - q_{22}),$$

The value of C_2 is the ordinate of $\eta(C_0)$ at the joint (at $\ell/2$ distance); let us denote it with $\eta_{0,\frac{\ell}{2}}$

so

$$\eta(C) = \eta(C_0) - \xi \cdot \eta_{0,\frac{\ell}{2}} \cdot (1 - q_{22}),$$

and in general, when main girder i is analysed:

$$\eta(C) = \eta(C_0) - \xi \cdot \eta_{0,\frac{\ell}{2}} \cdot (1 - q_{ii}),$$

Let us determine the bending moment influence line of cross section k (Fig. 3.30):

$$\eta(M_k) = \eta(M_{k0}) - \xi \cdot \frac{\xi_1}{2} \cdot (1 - q_{ii}),$$
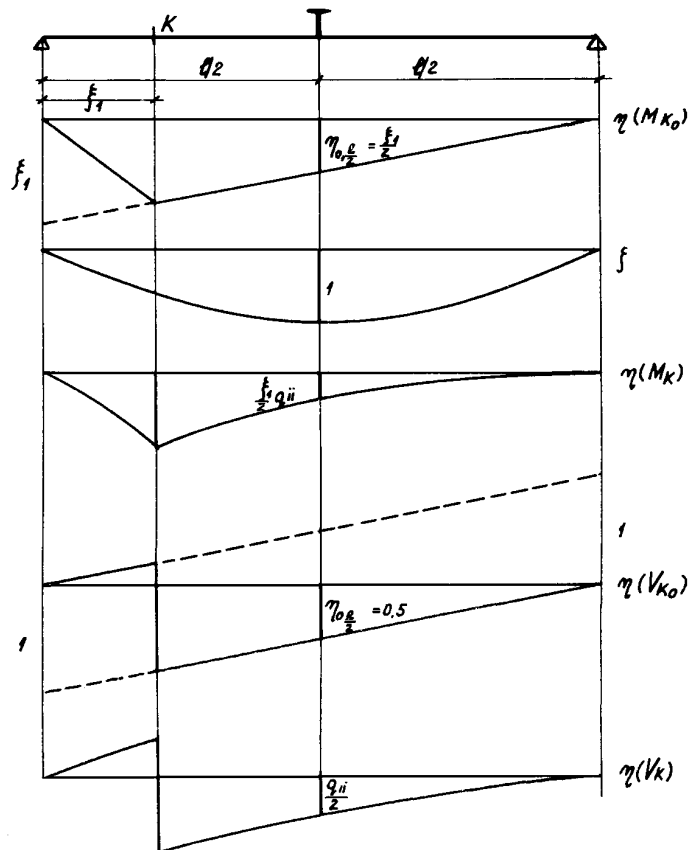
Figure 3.30 Preparation of the bending moment influence line and the shear force influence line of k section.

Or the shear force influence line (Fig. 3.30)

$$\eta(T_k) = \eta(T_{k0}) - \xi \cdot \frac{1}{2} \cdot (1 - q_{ii}),$$

2. P_0 acts through main girder No.4. The girder is not loaded directly, the value of the force transmitted at the joint:

$$X_4 = q_{42} \cdot B_{2m},$$

The value of a bearing force:

$$C = \eta_{0,\frac{\ell}{2}} \cdot q_{42} \cdot B_{2m} = \eta_{0,\frac{\ell}{2}} \cdot q_{42} \cdot \xi,$$

For example, the section of the influence surface of k at girder 4:

$$\eta(M_k) = \eta_{0,\frac{\ell}{2}} \cdot q_{42} \cdot \xi = \frac{\xi_1}{2} \cdot q_{42} \cdot \xi,$$

Or in general, the section at girder j:

$$\eta(M_k) = \frac{\xi_1}{2} \cdot q_{ji} \cdot \xi,$$

so any section at any other girder is proportional to diagram ξ.

The sections at the girders determine the influence surface. In case of forces acting between two girders, the loading of the main girder is calculated by assuming simply supported beams. So linear ranging of the influence surface sections is assumed. For instance a moment influence surface is according to Fig. 3.31.
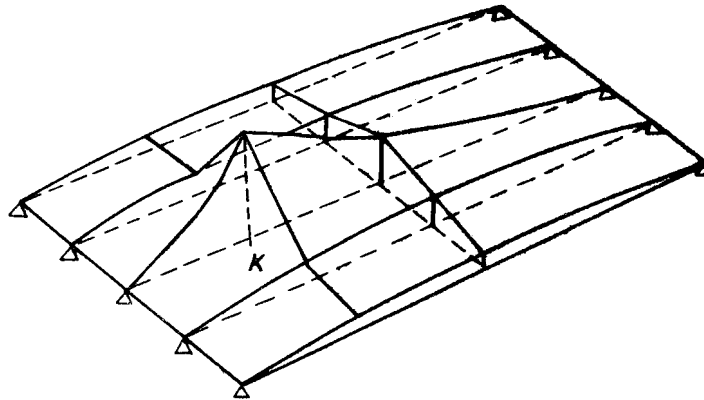
Figure 3.31 The bending moment influence surface of k section.

According to the influence surface, the effect of an external load is obtained in a way that the intensity of the load, distributed on area F, is multiplied by the volume of the influence surface under the loaded area, so:

$$C_k = p \cdot V_\eta,$$

In case of concentrated load, the volume turns into an ordinate:

$$C_k = P \cdot \eta,$$

Let us analyse the behaviour of the grid of fig. 3.32 parametrical according to Lindner and Bamm [1982], by changing the characteristics of the cross girder. The load is located at girder 1.

girder 1
girder 2
girder 3

examined girder
loaded girder

Figure 3.32 Behaviour of gridwork with one cross-girder.

It is observable, that a detectable rearrangement of the bearing forces occurs at the values of $z \geq 2$. Fig. 3.33 shows the effect of the change of z.

Fig. 3.33.a shows the cross distribution diagram. According to this in case of small values of z, only main girder 1 will be loaded, while in cases of high values of z the other girders will be loaded as well.

Fig. 3.33.b illustrates the behaviour of gird 2.

Fig. 3.34 shows the behaviour of the grid with more cross girders. The value of z was taken to 4,3.

Fig 3.34.a shows the cross distribution diagram of girder 1, in case of more cross girders, Fig. 3.34.b illustrates the behaviour of girder 2.

Figure 3.33 part a) and b):

cross distribution

girder 1

Z=0,16 4,3 34,3 4300 cross girder

I_H girder 1
I_H girder 2
I_H I_Q girder 3

ℓ

cross girder

P

1. B 2. B 3.

b)

girder 2

Z=4300

34,3

4,3

0,16

$$Z = \frac{I_Q \cdot \ell^3}{I_H \cdot B^3}$$
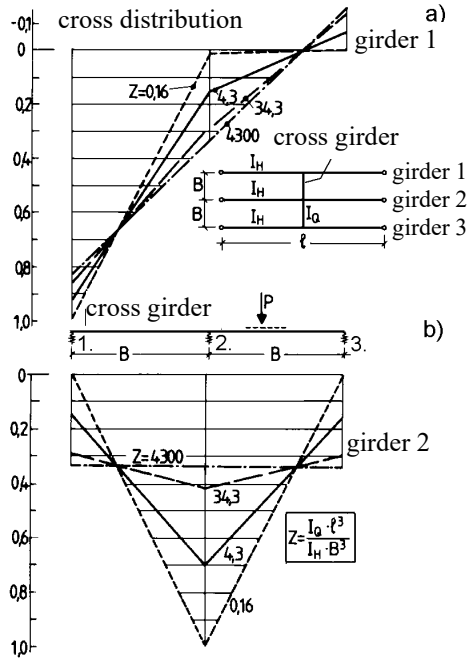
Figure 3.33 The effect of varying the z factor.

cross distribution a)

girder 1

n=1
n=3
n=5

I_H girder 1
I_H I_Q girder 2
I_H I_Q girder 3

ℓ

n cross girder

cross girder

1. B 2. B 3.

b)

girder 2

n=1
n=3
n=5

z = 4,3
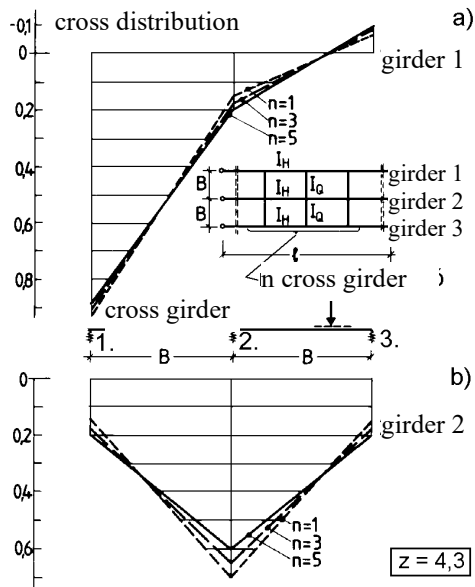
Figure 3.34 Behaviour of gridwork with more cross-girders.

3.2.3.6.3 Approximate calculation of gridworks by substituting them with orthotropic plate

The Guyon–Massonnet method

Calculation of orthotropic plates and grids is a quite often appearing problem, and the only difficulty of these, that the known calculation methods provide the result after long calculation. [Bölcskei, 1968].

The *Guyon-Massonnet* method provides the load distribution by easy-to handle and fast graphs. It takes into account also the *torsion stiffness* of the grid members. It is applicable for every grid and orthotropic plate, where the value of the bending and the torsion stiffness (related to unit length) of the main and cross girders can be assumed as constant. The simplest case according to this for example the regular grid, where, the distance between the main and cross girders is constant, both, in longitudinal and transversal direction, and the stiffness of every member is identical as well..

The solution of the differential equation

The form of the general solution of the homogeneous equation

$$w(x, y) = \sum_{m=1}^{n} Y_m(y) \cdot \sin \frac{m\pi x}{\ell},$$

In case of one line-load, the above given solution is valid for every point of the grid outside the loaded line. The loading is a sine function, and the general equation is [Szabó, Visontai, 1962]:

$$p(\xi) = \sum_{m=1}^{\infty} p_m \cdot \sin \frac{m\pi\xi}{\ell},$$

By substituting the above formula of *w* deflection into the homogeneous equation, we get:

$$AY_m \frac{m^4\pi^4}{\ell^4} - 2HY_m'' \frac{m^2\pi^2}{\ell^2} + BY_m'''' = 0,$$

Guyon offers in order to make the calculation process easier, the assumption, that the transversal load distribution is independent on the collinear load's character. So the calculated values of the cross distribution factors for a loading are valid for every other loading as well. Let the collinear load be according to one sine wave (m=1):

$$p(\xi) = p_1 \cdot \sin \frac{\pi\xi}{\ell},$$

and the differentia equation:

$$AY_1(y)\frac{\pi^4}{\ell^4} - 2HY_1''(y)\frac{\pi^2}{\ell^2} + BY_1''''(y) = 0\,,$$

With the substitution of $H = \alpha\sqrt{AB}$ and the dividing of the equation by B, we get:

$$Y_1''''(y) - 2\sqrt{\frac{A}{B}} \cdot \frac{\pi^2}{\ell^2}Y_1''(y) + \frac{A}{B}Y_1(y)\frac{\pi^4}{\ell^4} = 0\,,$$

by inserting

$$\lambda^2 = \frac{\pi^2}{\ell^2}\sqrt{\frac{A}{B}}\,,$$

we can write:

$$Y_1''''(y) - 2\alpha \cdot \lambda^2 \cdot Y_1''(y) + \lambda^4 \cdot Y_1(y) = 0\,,$$

This differential equation was solved by *Massonnet* for $\alpha = 1$, and by *Guyon* for $\alpha = 0$, so:

$$Y_1'''' - 2\lambda^2 \cdot Y_1'' + \lambda^4 \cdot Y_1 = 0\,, \qquad\qquad \textit{(Massonnet)}$$

$$Y_1'''' + \lambda^4 \cdot Y_1 = 0\,, \qquad\qquad \textit{(Guyon)}$$

The solution is:

$$Y_1 = A_1 \cdot e^{\lambda y} + B_1 \cdot \lambda ye^{\lambda y} + C_1 \cdot e^{-\lambda y} + D_1 \cdot \lambda ye^{-\lambda y}\,,$$

and the integral constants are determined from the adequate boundary conditions. Namely the line of the collinear load divides the plate into two half, and for each of these parts the general solution can be written. Let the solution for the one half plate be Y_1^I, and for the other Y_1^{II}. The 8 unknown coefficients of these functions comes from the following conditional equation:

- - at the edges the moments and the shear forces are zero:

$$(Y_1^I)'' = (Y_1^{II})'' = 0\,, \text{ and } (Y_1^I)''' = (Y_1^{II})''' = 0\,,$$

- - at the connection at the two parts, the deflections the rotations and the moments are equal, so:

$$Y_1^I = Y_1^{II}\,, (Y_1^I)' = (Y_1^{II})'\,, (Y_1^I)'' = (Y_1^{II})''\,,$$

- - the difference between the shear forces is equal to the line-load:

$$(Y_1^I)''' + \frac{P}{EI} = (Y_1^{II})''',$$

Let the width of the plate be 2b, the span ℓ, the coordinate of the location of the line-load η and the coordinates of the unknown w deflection x and y (Fig. 3.35). Then with the substitution of

$$\vartheta = \frac{b}{\pi}\lambda = \frac{b}{\pi}\frac{\pi}{\ell}\sqrt[4]{\frac{A}{B}} = \frac{b}{\ell}\sqrt[4]{\frac{A}{B}},$$

the w deflection of every point with x and y coordinates is computable in a function of ϑ. The $w_0(x, \eta)$ deflection of the simply supported beam at the line of the collinear load is computable as well. The quotient of the two results is the cross distribution factor:

$$K(y, \eta) = \frac{w}{w_0},$$

The cross distribution factors also give that how many of a load at η location acts at a strip of y width.

These cross distribution factors were determined in the function of the parameter ϑ, by *Massonnet* for $\alpha = 1$ and *Guyon* for $\alpha = 0$ for different load cases. The results were summarized in graphs and tables.
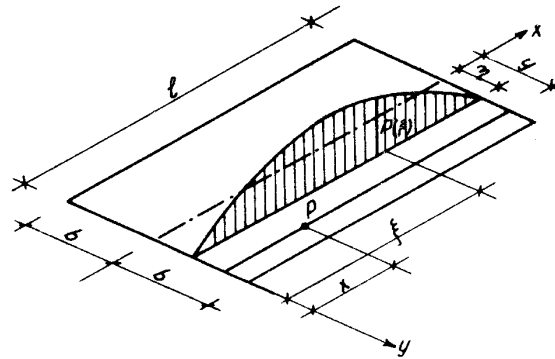
Figure 3.35 The position of the line-load.

The introduction of the calculation process

The process is based on the differential equation of the orthotropic plate [Bölcskei, 1968]:

$$D_x \frac{\partial^4 w}{\partial x^4} + 2H \frac{\partial^4 w}{\partial x^2 \partial y^2} + D_y \frac{\partial^4 w}{\partial y^4} = p(x, y),$$

We insert the following notations (Fig. 3.36):

EI_m bending stiffness of one main girder

EI$_c$ bending stiffness of one cross girder
GI$_{mt}$ torsion stiffness of one main girder
GI$_{ct}$ torsion stiffness of one cross girder
h   distance between the main girder
k   distance between the cross girders
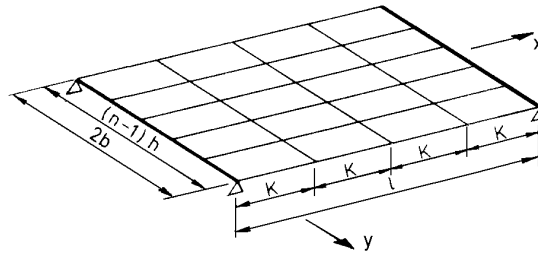
Figure 3.36 The geometry of gridwork.

Neglecting the effect of the contraction, the constants of the differential equation will be:

$$D_x = \frac{EI_m}{h}, \quad D_y = \frac{EI_c}{k}, \quad H = \frac{G}{2} \cdot \left(\frac{I_{mt}}{h} + \frac{I_{ct}}{k} \right),$$

Writing H in the following form: $H = \alpha \sqrt{D_x \cdot D_y}$, the characteristic value for the torsion stiffness of the gridwork:

$$\alpha = \frac{G \left(\dfrac{I_{mts}}{h} + \dfrac{I_{ct}}{k} \right)}{2E \sqrt{\dfrac{I_m}{h} + \dfrac{I_c}{k}}}, \qquad /3.34/$$

while the characteristic parameter for the bending stiffness of the gridwork:

$$\vartheta = \frac{b}{l} \sqrt[4]{\frac{I_m / h}{I_c / k}}, \qquad /3.35/$$

At the members of the gridwork $\alpha = 0$ and $H = 0$ lower limit shows the neglection of the torsion stiffness, the upper limit is $\alpha = 1$ value for the isotropic plate's two directional torsion stiffness.

The calculation is based on that, anywhere the load is on the main girder, the distribution of the loading is always identical in an optional cross section (in the direction of the cross girder).

From practical point of view the determination of the *cross distribution factors* is essential [Bölcskei, 1968]. These two factors are seen in the graphs of Fig 3.37 – 47 in the function of α and ϑ.

K_0 is the cross distribution factor for the limit state $\alpha = 0$

K_1 is the cross distribution factor for the limit state $\alpha = 1$

These values are theoretically valid for orthotropic plate, but they can be used for gridworks with one cross girder too.

In case of when the characteristic value for the torsion stiffness is between $\alpha = 0$ and $\alpha = 1$, the cross distribution factor has to be inter interpolated in the following way:

$$K_\alpha = K_0 + (K_1 - K_0)\sqrt{\alpha} \,, \qquad\qquad /3.36/$$
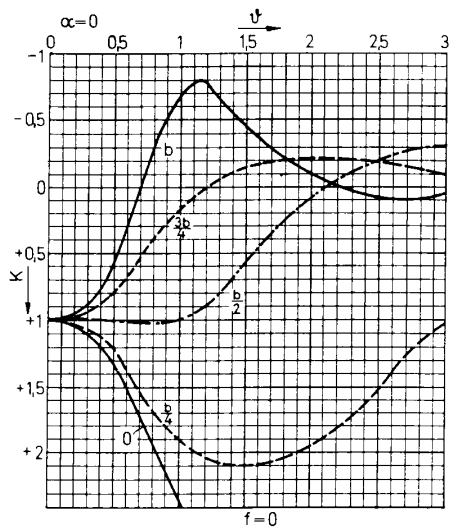
Figure 3.37 Cross distribution factors.
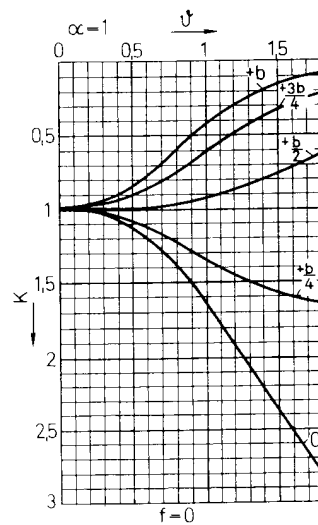
Figure 3.38
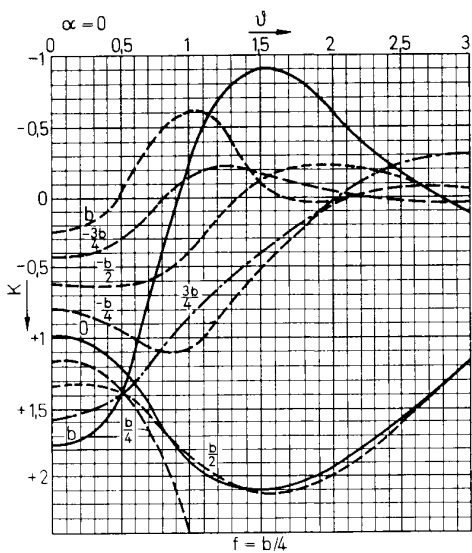
Figure 3.39

Figure 3.40

109
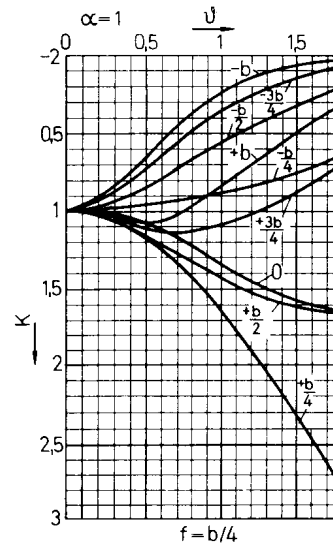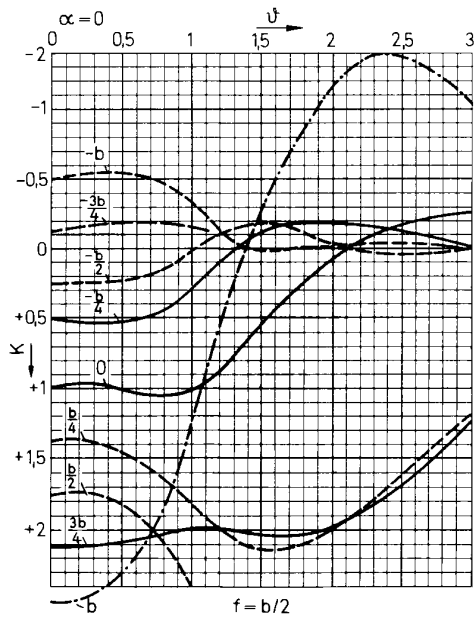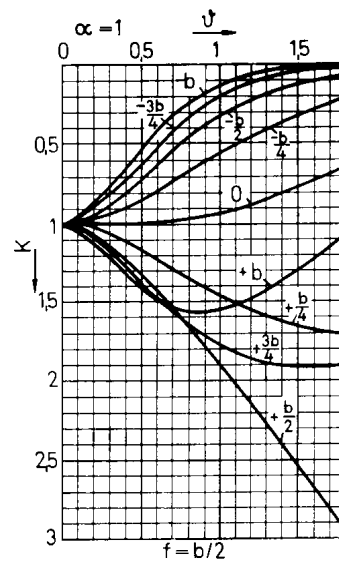
Figure 3.41

Figure 3.42
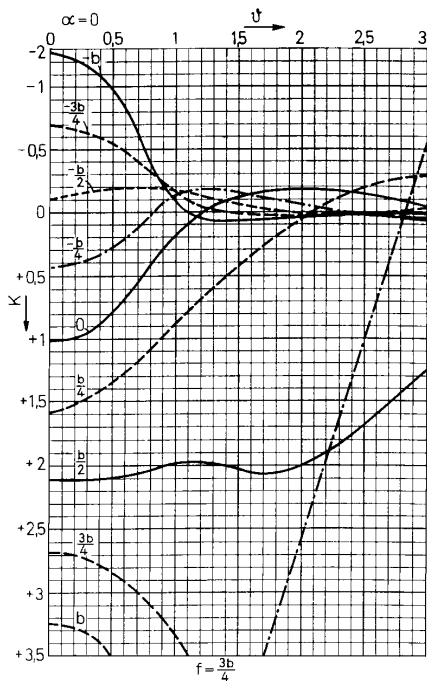
Figure 3.43

Figure 3.44

110
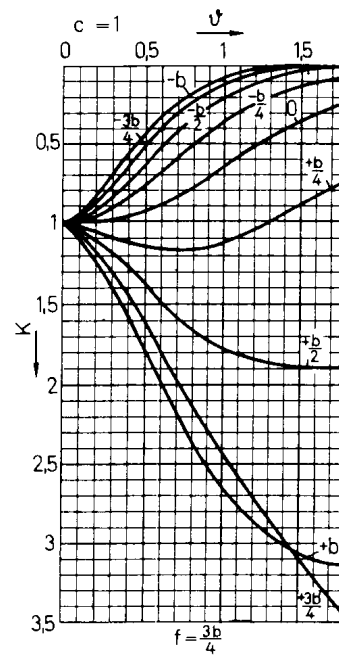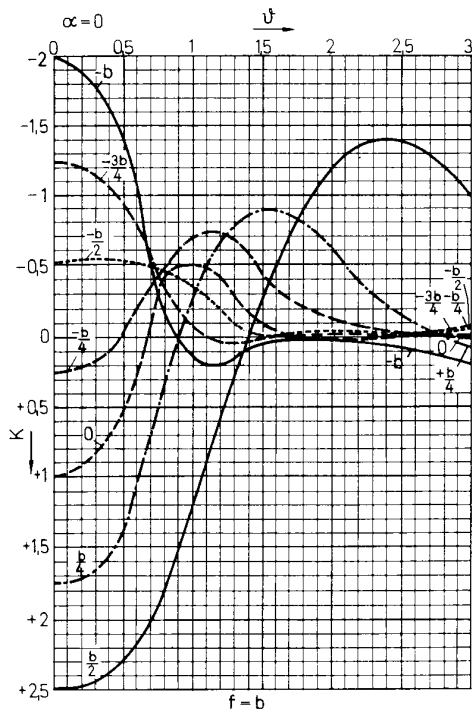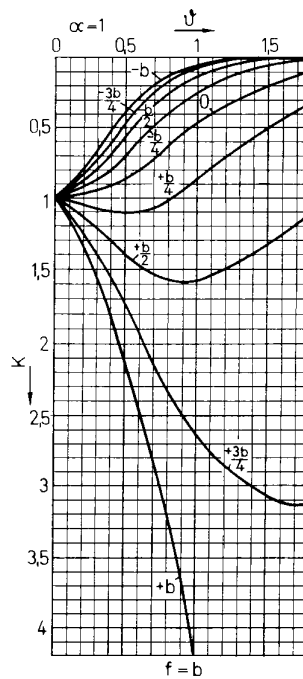
Figure 3.45

Figure 3.46

Figure 3.47.

111
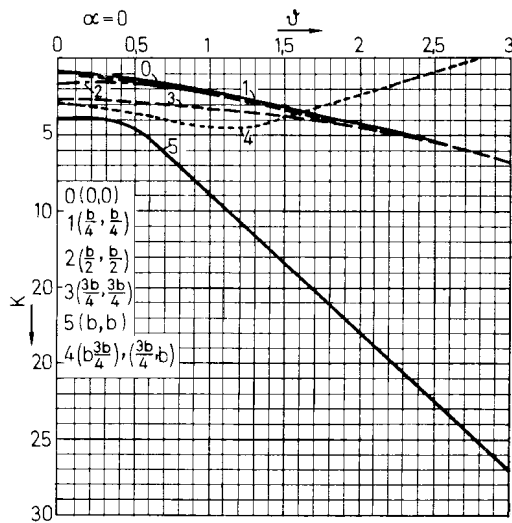
Now the bending moment of the main girders is computable.

Let us assume first that simple case that the loading is one force system, acting at distance η from the axis of the bridge according to Fig. 3.48. Let us determine the moment of the main girder's x cross section, which is in f distance from the bridge axis.
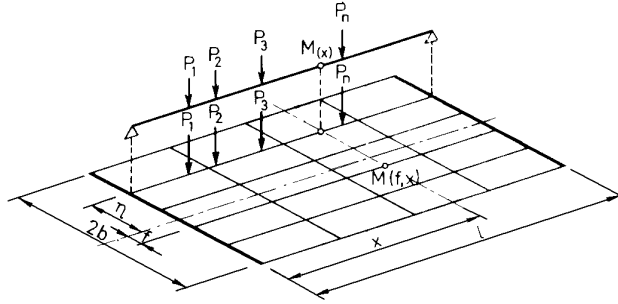
Figure 3.48 The position of loading.

Firstly we determine the $M_0(x)$ bending moment from the whole loading on the virtual simply supported beam at the line of the loading in the usual way, then we multiply this with $K_\alpha(\eta, f)$ from the diagrams. K_0, K_1 (from the diagrams) and K (from formula /3.36/) give the ordinates of the cross distribution diagrams of the main girders at the eighths of bridge cross-section. In case of orthotropic plate they relate to the points at the eighths of the cross section the area of the cross distribution diagram is $2b$. Therefore in case of orthotropic plate the unit value of the longitudinal moment at a point of the cross section:

$$m_h(f, x) = \frac{M_0(\eta, x)}{2b} \cdot K_\alpha(\eta, f), \qquad /3.37a/$$

In case of gridwork the longitudinal moment for one main girder comes from the product of distance h and the moment of formula (4a):

$$M_h(f, x) = m_h(f, x) \cdot h = \frac{h}{2b} \cdot M_0(\eta, x) \cdot K_\alpha(\eta, f), \qquad /3.37b/$$

If the load acts along more lines the moment at an optional place is the sum of the moments calculated according to the above-described way.

3.2.4 Analytical model for substructures S4

The influence of the deformation of the cross section on stresses has been analyzed by the Advanced Theory of Bending, Torsion and Distortion [Tesar, 1977] [Iványi et al., 1990] which is a simple method of analysis but precise enough to study the three-dimensional behaviour of the bridge.

Besides the axial deformation v_1, the two displacements v_2 and v_3 and the rotation of cross section v_4 displacement elements further sectional deformations develop in accord with the cross-

section's transverse stiffness. These are equivalent to the relative position change of prismatic plates.

In case of open sections the number of displacement degree of freedom (v) equals to the number of joint-hinges (n). With the formation of the joint-hinges the cross sections' frame-stiffness ceases. To secure the kinematical stability of this "released" section n additional bars are needed. (Fig.3.49.)
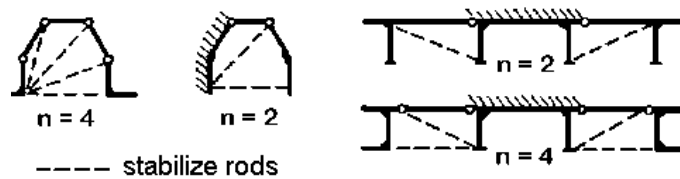
Figure 3.49 Displacement degree of freedom in case of open sections
(n is the number of the hinges that breaks up the frame-stiffness of the section,
v is the number of stabilizer bars)

In case of closed cross section (Fig.3.50.) the further number of displacement degree of freedom (v) are to be calculated according to the following formula:

$$2n - (s + 3) = v \qquad\qquad /3.38/$$

where n is the number of the hinges that breaks up the frame-stiffness of the section, and s is the number of the section's prism-components (elements).
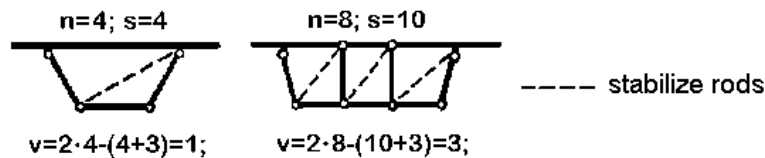
Figure 3.50 Displacement degree of freedom in case of closed cross sections
(n is the number of the hinges that breaks up the frame-stiffness of the section,
s is the number of the section's prism-components (elements),
v is the number of stabilizer bars)

The complete deformation of the cross section can be determinated, as the linear combination of the independent elements of the displacement of distortion of cross-section v_p (p>4). We will get these components (elements) if we progressively operate suitable chosen unitary $\vartheta=1$ deflections on the section that is released by hinges, while there is always a stabilizer bar released (see Fig.3.51).
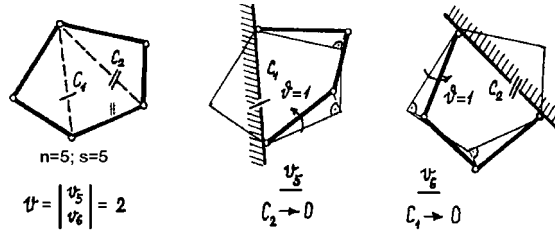
Figure 3.51 Kinematics of cross-sectional degrees of freedom

So the $\tilde{v}$ displacement vector:

$$
\tilde{v} = \begin{bmatrix} \tilde{v}_t \\ \hdots \\ \tilde{v}_p \end{bmatrix} = \begin{bmatrix} \tilde{v}_1 \\ \tilde{v}_2 \\ \tilde{v}_3 \\ \tilde{v}_4 \\ \hdots \\ \tilde{v}_5 \\ \tilde{v}_6 \\ \vdots \\ \tilde{v}_n \end{bmatrix} = \begin{bmatrix} \xi \\ \eta \\ \zeta \\ \vartheta \\ \hdots \\ \tilde{v}_5 \\ \tilde{v}_6 \\ \vdots \\ \tilde{v}_n \end{bmatrix} \qquad /3.39/
$$

of which has $\tilde{v}_t$ rigid body modes and $\tilde{v}_p$ distortional modes (p subscript refers to the displacement of the distortional cross-section).

Moreover we assert the basic principle of bending-torsion, which says that all the section's prism-components keep their shapes. So the Bernoulli-Navier hypothesis is valid for each prism (plate element).

According to the previous conception, the formula /3.39/ can be extended, which gives the tangential component of the strain:

$$
\frac{df}{dx} = f' = f_t' + f_p' = \eta' \cdot \cos\alpha + \zeta' \cdot \sin\alpha + \vartheta' \cdot r_M +
$$
$$
+ \tilde{v}_5' \cdot \tilde{r}_5 + \tilde{v}_6' \cdot \tilde{r}_6 + \ldots + \tilde{v}_n' \cdot \tilde{r}_n \, ,
$$

So

$$
f' = (\tilde{v}')^{\mathrm{T}} \cdot \tilde{r} \qquad /3.40/
$$

Where

$$
\tilde{r} = \begin{bmatrix} r_t \\ \hdots \\ \tilde{r}_p \end{bmatrix} = \begin{bmatrix} 0 \\ \cos\alpha \\ \sin\alpha \\ r_M \\ \hdots \\ \tilde{r}_5 \\ \tilde{r}_6 \\ \vdots \\ \tilde{r}_n \end{bmatrix}
\qquad
\tilde{v}' = \begin{bmatrix} v_t' \\ \hdots \\ \tilde{v}_p' \end{bmatrix} = \begin{bmatrix} \xi' \\ \eta' \\ \zeta' \\ \vartheta' \\ \hdots \\ \tilde{v}_5' \\ \tilde{v}_6' \\ \vdots \\ \tilde{v}_n' \end{bmatrix}
$$

114

,   ;

and $\tilde{r_5}, \tilde{r_6}, \ldots, \tilde{r_n}$ are the referring sectional prism's force arms to the rotation-centres.
The axial component of the displacement of thin-walled section centre-line:

$$\tilde{u} = -\int (\tilde{v}')^T \cdot \tilde{r} \, ds = -(\tilde{v}')^T \cdot \int \tilde{r} \, ds = -(\tilde{v}')^T \cdot \tilde{w} \qquad\qquad /3.41/$$

Where $\tilde{w}$ is the warping vector.
Values of $\tilde{w}$ for open sections (Fig.3.52)

$$\tilde{w} = \begin{bmatrix} w_t \\ \hdotsfor{1} \\ \tilde{w}_p \end{bmatrix} = \int \tilde{r} \, ds = \begin{bmatrix} 1 \\ y \\ z \\ \omega_M \\ \hdotsfor{1} \\ \tilde{w}_5 \\ \tilde{w}_6 \\ \vdots \\ \tilde{w}_n \end{bmatrix} \qquad\qquad /3.42/$$
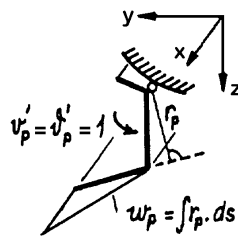
Figure 3.52 The axial component of displacement of the thin-walled section centre-line

In case of closed cross sections we extract the open "statically determinate" basic system first, with suitable chosen sections.

We can take into account the condition for continuity for the hollow section through the extension of $\dfrac{\widetilde{\underline{\psi}}}{t} = \dfrac{\widetilde{\underline{\psi}}_p}{t}$ vector.

We get an analogue equation system with /3.42/ for the vector components:

$$
-\int\limits_{j-1}^{j} \frac{\widetilde{\psi}_{p,j-1}}{t}\, ds + \oint\limits_{j} \frac{\widetilde{\psi}_{p,j}}{t}\, ds - \int\limits_{j}^{j+1} \frac{\widetilde{\psi}_{p,j+1}}{t}\, ds = \int\limits_{j} \widetilde{r}_p\, ds
$$

The warping vector is:

$$
\widetilde{w} = \begin{bmatrix} w_t \\ \cdots \\ \widetilde{w}_p \end{bmatrix} = \int \left(\widetilde{r} - \frac{\widetilde{\underline{\psi}}_p}{t} \right) ds =
$$

$$
= \int \left(\begin{bmatrix} 0 \\ \cos\alpha \\ \sin\alpha \\ r_M \\ \cdots \\ \widetilde{r}_5 \\ \widetilde{r}_6 \\ \vdots \\ \widetilde{r}_n \end{bmatrix} - \begin{bmatrix} 0 \\ 0 \\ 0 \\ \psi_4/t \\ \cdots \\ \widetilde{\psi}_5/t \\ \widetilde{\psi}_6/t \\ \vdots \\ \widetilde{\psi}_n/t \end{bmatrix} \right) ds = \begin{bmatrix} 1 \\ y \\ z \\ \omega_M \\ \cdots \\ \widetilde{w}_5 \\ \widetilde{w}_6 \\ \vdots \\ \widetilde{w}_n \end{bmatrix} \qquad \text{/3.43/}
$$

The normal stress of cross section centre line:

$$
\widetilde{\sigma} = -E \cdot (\widetilde{v}'')^T \cdot \widetilde{w} \qquad\qquad \text{/3.44/}
$$

The primary shear stress is:

$$
\widetilde{\tau}_I = G \cdot (\widetilde{v}')^T \cdot \frac{\widetilde{\underline{\psi}}_p}{t} \qquad\qquad \text{/3.45/}
$$

Where $\widetilde{v}$ is the section's global deflection vector according to /3.39/. The relation between the rotation vector of the section's prisms $\widetilde{\underline{\vartheta}}_p = \left\{ \vartheta_{p,m} \right\}$ and the section's $\widetilde{v}_p$ formal-change vector is the following:

$$
\widetilde{\underline{\vartheta}}'_p = \widetilde{F}_p \cdot \widetilde{v}'_p
$$

When $\widetilde{F}_p$ matrix has to be compiled by taking into account the chosen $\widetilde{v}_p$ basic formal-changes (Fig. 3.51).

So the torsion moment vector referring to the sectional prisms' free torsion is the following:

$$T = G \cdot K \cdot \widetilde{F} \cdot \widetilde{v}' = G \cdot \widetilde{F}^* \cdot \widetilde{v}'$$

Where

$$\widetilde{v}' = \begin{bmatrix} v'_t \\ \widetilde{v}'_p \end{bmatrix} \quad \text{and} \quad \widetilde{F}^* = \begin{bmatrix} \widetilde{F}_t^* \\ \widetilde{F}_p \end{bmatrix}, \text{ where } \quad \widetilde{F}^* = K \cdot \widetilde{F} \quad . \qquad /3.46/$$

We have to determine the relation between the transverse moments in the section's prismatic element and the section's $\widetilde{v}_p$ formal-change vector. So we compile the prism's common relative rotations at the hinges ε_{im}, in the common deflection vector of the section-walls $\widetilde{e}$ (Fig. 3.53):

$$\widetilde{e} = \{\widetilde{\varepsilon}_i\} = \{\Delta\widetilde{\vartheta}_i\} = \Delta\widetilde{F} \cdot \widetilde{v} \qquad /3.47/$$

Where

$$\widetilde{\varepsilon}_i = \widetilde{\vartheta}_{m+1} - \widetilde{\vartheta}_m = \Delta\widetilde{\vartheta}_i$$
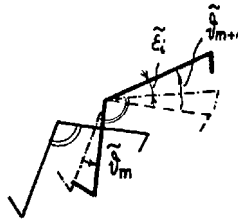
Figure 3.53 Relative rotations of walls of cross-section: $\varepsilon_i = \Delta\vartheta_i$

The rows of matrix $\Delta\widetilde{F}$ come from matrix $\widetilde{F}$ matching rows' difference. Further on we can suppose that the plate-stiffness of the wall can be substituted by the bending stiffness of infinitely many and infinitely broad frames that are close to each other. So the plates' torsion moments, and longitudinal moments in the section-wall are neglected.

If EI_r the bending stiffness of the unitary wide sectional frame, than M_{ri}, transversal moment at hinge i and which is a function of $\widetilde{\varepsilon}_j$, the common rotations of the section-walls at j places, comes from this formula:

$$\widetilde{M}_{ri} = \sum \beta_{ij} \cdot \widetilde{\varepsilon}_j \qquad \text{and} \qquad \widetilde{M}_r = \{\widetilde{M}_{ri}\} = B \cdot \widetilde{e}$$

In case of a simply open section of which centre line is developable to a continuous line, the coefficients in matrix $B = \{\beta_{ij}\}$ come from the inverse of matrix $D = \{\delta_{ij}\}$, where δ_{ij} elements are unit factors of a statically determinated basic system according to the compatibility method (Fig. 3.54).
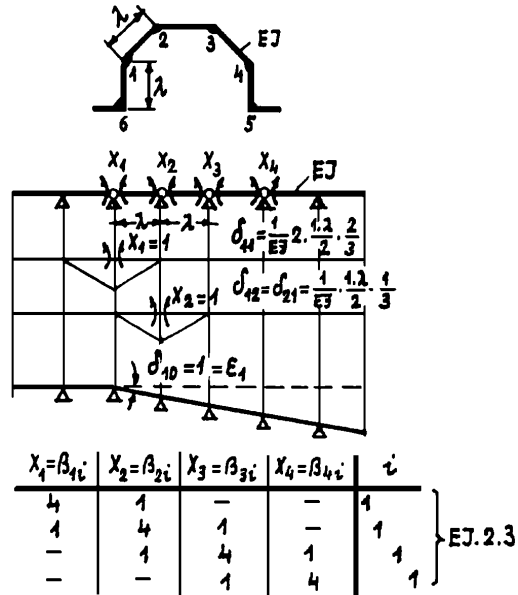
Figure 3.54 Determination of the β elements as the elements of inverse of matrix $D = \left\{\delta_{ij}\right\}$ of continuous beam

If we express the rotation vectors of the section-walls, according to /3.47/ we'll get:

$$\widetilde{M}_r = B \cdot \Delta\widetilde{F} \cdot \widetilde{v} = \Delta\widetilde{F}^* \cdot \widetilde{v} \qquad \qquad /3.48/$$

Where $\Delta\widetilde{F}^* = B \cdot \Delta\widetilde{F}$.

We depart from the principle of virtual work. The work of the internal forces comes from the extended formula bellow:

$$\delta\Pi_{internal} = \int\limits_0^L \left[\int\limits_A (\sigma \cdot \delta\varepsilon + \tau_I \cdot \delta\gamma_I) \cdot dA + T^T \cdot \delta\underline{\vartheta}' + M_r^T \cdot \delta\widetilde{e} \right] \cdot dx,$$

$$\delta\Pi_{internal} = \int\limits_0^L \left[E(\widetilde{v}'')^T \int\limits_A \widetilde{w} \cdot \widetilde{w}^T dA \cdot \delta\widetilde{v}'' + G(\widetilde{v}')^T (\int\limits_A \frac{\widetilde{\psi}_p}{t} \cdot \frac{\widetilde{\psi}_p^T}{t} dA + \right.$$
$$\left. + (\widetilde{F}^*)^T \cdot F) \cdot \delta\widetilde{v}' + \widetilde{v}^T (\Delta\widetilde{F}^*)^T \cdot \Delta\widetilde{F}) \cdot \delta\widetilde{v} \right] dx \qquad /3.49/$$

If we do the examination of the energy balance, that means we use

$$\delta\Pi = \delta\Pi_{internal} - \delta\Pi_{external} = 0$$

condition, and do the partial integration, by taking into account the following extended stiffness matrixes:

$$\widetilde{I} = \left\{\widetilde{I}_{w_i w_k}\right\} = \int_A \widetilde{w} \cdot \widetilde{w}^T \, dA \qquad /3.50/$$

as the complex warping stiffness matrix,

$$\widetilde{K} = \left\{\widetilde{K}_{ik}\right\} = \int_A \frac{\widetilde{\underline{\Psi}}}{t} \cdot \frac{\widetilde{\underline{\Psi}}^T}{t} \, dA + (\widetilde{F}^*)^T \cdot \widetilde{F} \qquad /3.51/$$

as the simple torsional stiffness matrix

$$\widetilde{R} = \left\{\widetilde{R}_{ik}\right\} = (\Delta\widetilde{F}^*)^T \cdot \Delta\widetilde{F} \qquad /3.52/$$

and as the transverse bending stiffness matrix, then we get the extended simultaneous equilibrium system of differential equations:

$$\boxed{\begin{aligned}
& E\widetilde{I} \cdot \widetilde{v}'''' - G\widetilde{K} \cdot \widetilde{v}'' + \widetilde{R} \cdot \widetilde{v} - p \cdot \widetilde{r} - \int_A n' \cdot \widetilde{w} \cdot dA = 0 \\
& \left[-E\widetilde{I} \cdot \widetilde{v}''' + G\widetilde{K} \cdot \widetilde{v}' + \int_A n \cdot \widetilde{w} \cdot dA - P \cdot \widetilde{r} \right]_0^L = 0 \\
& \left[E\widetilde{I} \cdot \widetilde{v}'' + N \cdot \widetilde{w} \right]_0^L = 0
\end{aligned}} \qquad /3.53/$$

These equations give besides $\widetilde{v}$ global deflection vector, the effect of the section centre-line change as well.

When solving open sections (Fig. 3.55) in case of ordinary plate slenderness of bridge systems, the torsional stiffness of the walls (prisms) can be neglected.
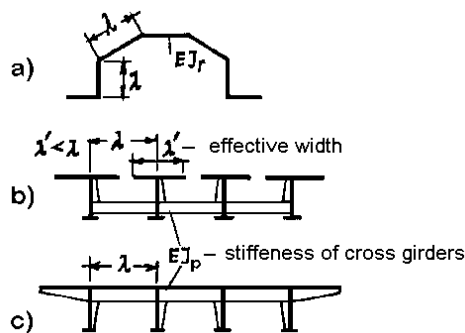
Figure 3.55 Different shapes of open sections

In case of <u>open sections</u> if we diagonalize matrix $\bar{I}$ and $\bar{R}$, it is obvious, that we can separate all the four deflection components of the shape-keeping section (ξ, η, ζ and ϑ).

After the normalization we get the independent difference equation system with **I** and **R** diagonal stiffness matrixes, where every element of **v** global deflection vector are equivalent to a model of a continuously elastic supported bar with R_i and with EI_i bending stiffness, and which is loaded by $p \cdot r_i$ load intensity in cross direction (see Fig. 3.56).

Figure 3.56 The normal function in case of open sections
a) The partially normalised simultaneous differential equations from the first phase to determine the eigenvectors in case of open section
b) Totally normalized independent differential equations in case of open section –analogue of the continuously supported transversally loaded bar

In case of <u>closed cross-sections</u> (Fig. 3.57) a relevant torsional stiffness comes because of the $\underline{\Psi}_p / t$ vector. So it is suitable to neglect the cross directional stiffness of the section, which means that we assume that the section is a closed hinged mechanism (Fig.3.58). The fault of this assumption, that the fourth component of the deflection (ϑ) is not independent.
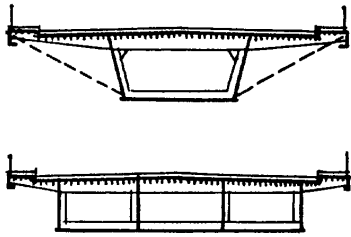
Figure 3.57 Shapes of closed sections

120
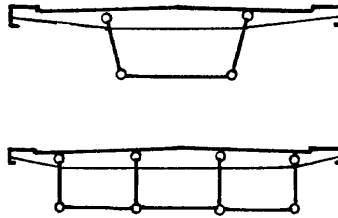
Figure 3.58 Kinematically determinated closed hinged mechanisms

Figure 3.59 The normal function in case of open sections
a) The partially normalised simultaneous differential equations from the first phase to determine the eigenvectors
in case of closed section
b) Totally normalized independent differential equations
in case of open section –analogue of the transversally loaded and tensioned bar

After the normalisation we get an independent system of differential equations with **I** and **K** diagonal stiffness matrixes, where each component of **v** global deflection vector equals to a bar with EI_i bending stiffness, with a transverse load of $p \cdot r_i$, and with GK_i fictive axial load at the ends (see Fig. 3.59).

For further details see Iványi [2002].

3.3 Shear Lag Phenomenon and Effective Width

Shear lag phenomenon and effective width is reviewed on the basis of Nakai and Yoo [1988] and Sedlacek and Bild [1984].

3.3.1 Shear lag phenomenon

The normal stress distribution $\sigma_z(x)$ in the flange plate of a π beam made of thin plates does not have a constant value, as is obtained by the elementary beam theory, but varies in the direction of coordinate x axis, as illustrated in Fig. 3.60. Then the maximum flexural normal stress $\sigma_{z,max}$ occurs at the junction point of flange and web plates, and this result is significantly different from σ_z = constant, which is calculated by elementary beam theory. This phenomenon is caused by the lag of shear strain in the flange plate between the web plates and is referred to as the *shear lag phenomenon*.
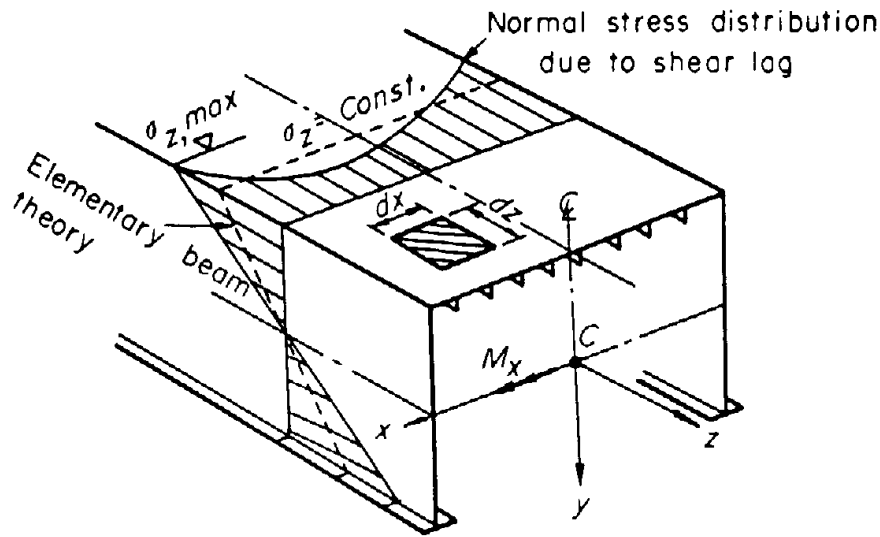
Figure 3.60 Actual bending normal stress distribution in a thin-walled beam.

The shear lag phenomenon can be analyzed on the basis of the theory of elasticity by assuming that the flange plate can be analyzed as a plane-stress problem. Figure 3.61 shows the stresses σ_z, σ_x, τ_{xy}, τ_{zx} in a small element $dx \cdot dz$, removed from the flange plate of a beam shown in Fig. 3.60, so that the equilibrium condition of stresses in the direction of the z axis can be written

$$\frac{\partial \sigma_z}{\partial z} + \frac{\partial \tau_{xz}}{\partial x} = 0$$

$$\frac{\partial \sigma_y}{\partial x} + \frac{\partial \tau_{zx}}{\partial z} = 0$$

/3.54/

The relationships between displacements u and v in the direction of coordinate axes (z, x) and strains ε_z, ε_x, and γ_{zx} can be written as

$$\varepsilon_z = \frac{\partial u}{\partial z}, \qquad \varepsilon_x = \frac{\partial u}{\partial x}, \qquad \gamma_{zx} = \frac{\partial u}{\partial x} + \frac{\partial v}{\partial z}$$

/3.55a-c/

In addition, the compatibility equation for plane stress elasticity is given by

$$\frac{\partial^2 \varepsilon_z}{\partial x^2} + \frac{\partial^2 \varepsilon_x}{\partial z^2} = \frac{\partial^2 \gamma_{zx}}{\partial z \partial x} \qquad \text{/3.55d/}$$
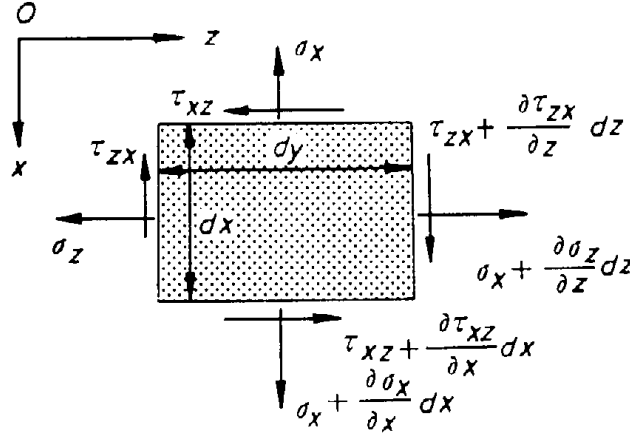
Figure 3.61 Actual bending normal stress distribution in a thin-walled beam.

Stress-strain relationships for two-dimensional elasticity are

$$\varepsilon_z = \frac{1}{E}(\sigma_z - \mu\sigma_x), \qquad \varepsilon_x = \frac{1}{E}(\sigma_x - \mu\sigma_z), \qquad \gamma_{zx} = \frac{\tau_{zx}}{G} \qquad \text{/3.55e-g/}$$

where μ is Poission's ratio and $G = E/[2(1 + \mu)]$. Substituting the stress-strain relationships in Eqs. (3.55e) to (3.55g) and the equilibrium condition in Eq. (3.54) into the compatibility equation, Eq. (3.55d), we can derive a general compatibility condition in terms of stress:

$$\left(\frac{\partial^2}{\partial z^2} + \frac{\partial^2}{\partial x^2}\right)(\sigma_z + \sigma_x) = 0 \qquad \text{/3.55h/}$$

Thus, the shear lag problem is reduced to solving for the stresses σ_z, σ_x and τ_{zx}, such that equilibrium and compatibility conditions are met.

These procedures can be much simplified by introducing Airy's stress function $\Phi(z, x)$:

$$\sigma_z = \frac{\partial^2 \Phi}{\partial x^2}, \qquad \sigma_x = \frac{\partial^2 \Phi}{\partial z^2}, \qquad \tau_{zx} = -\frac{\partial^2 \Phi}{\partial z \partial x} \qquad \text{/3.56a-c/}$$

Then Eq. (3.55h) can readily be rewritten as

$$\frac{\partial^4 \Phi}{\partial z^4} + 2\frac{\partial^4 \Phi}{\partial z^2 \partial x^2} + \frac{\partial^4 \Phi}{\partial x^4} = 0 \qquad \text{/3.56d/}$$

3.3.2 Definition of effective width

If the normal stress distribution $\sigma_z(x)$ in the flange plate is determined by the preceding procedure, it is convenient to define the effective width of the flange plate for practical design use. Fig. 3.62 illustrates a normal stress distribution in the deck plate of a π beam. In this figure, the most important stress in our design calculations is the maximum stress $\sigma_{z,max}$ at the junction point of the web and flange plates, so we try to obtain the same stress on the basis of elementary beam theory. For this purpose, it is assumed that a middle part of the flange plate does not cooperate with the cross section of π beam but that the flange plates in a region b_m are only effective as shown in Fig. 3.62b.
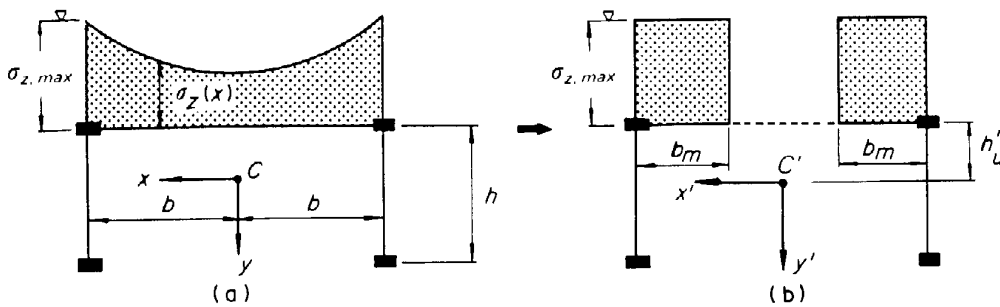
Figure 3.62 Definition of effective width: (a) original stress distributions, (b) idealized stress distribution and effective width b_m.

However, since the normal forces acting on the flange plate of Fig. 3.62a and 3.62b must have an identical value, the following equilibrium conditions should be satisfied:

$$\int_0^b \sigma_z(x)dx = b_m \sigma_{z,max} \qquad \text{/3.57a/}$$

Accordingly, the effective width b_m, can be estimated by

$$b_m = \frac{\int_0^b \sigma_z(x)dx}{\sigma_{z,max}} \qquad \text{/3.57b/}$$

When a new centroidal point C' and the corresponding geometric moment of inertia I'_x and I'_y and product of inertia I'_{xy} are calculated by taking into account the effective width b_m, as illustrated in Fig. 3.62b, the flexural normal stress $\sigma_{z,max}$ including the shear lag phenomenon can be estimated on the basis of the elementary beam theory. From this, we see that a conservative and rational stress analysis can be conducted by introducing the concept of the effective width of the flange plate.

3.3.3 Simplified rules for the determination of the effective width of bridge decks caused by shear lag

(a) General

Now it presents an approximative method to allow for the effects of shear lag in the elastic range when calculating the stress distribution over the cross-sections of two bay bridges due to bending and torsion (Fig. 3.63).
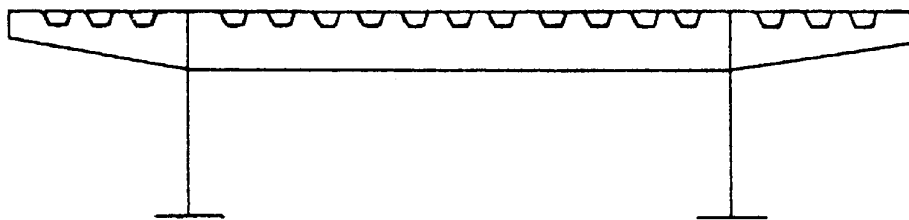
Figure 3.63 Cross-section of a two bay highway bridge with orthotropic deck.

(b) Approximate calculation method for the effects of shear lag in two bay bridges with an orthotropic deck [Roik and Sedlacek, 1971] [Sedlacek, 1982]

The stress distribution in a cross-section without shear lag is generally considered as a linear combination of four orthogonal elementary warping distributions caused by tension, bending about the strong axis, bending about the weak axis and torsion (Fig. 3.64).
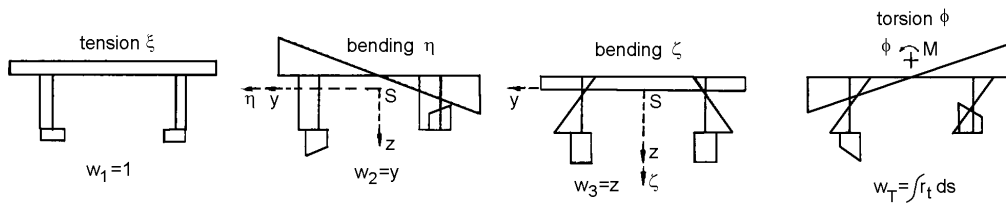
Figure 3.64 Elementary stress distributions "1" due to tension, "y" and "z" due to bending about the strong and weak axis respectively and "w$_T$" due to torsion.

The cross-sectional stiffnesses for the corresponding deformations ξ, η, ζ and ϕ can be derived from these elementary distributions as follows:

area:
$$A = \int 1 \cdot 1 \, dA \qquad \text{/3.58a/}$$

moment of inertia:
$$A_{yy} = \int y \cdot y \, dA \qquad \text{/3.58b/}$$

moment of inertia:
$$A_{zz} = \int z \cdot z \, dA \qquad \text{/3.58c/}$$

torsional warping stiffness:
$$A_{ww} = \int w \cdot w \, dA \qquad /3.58d/$$

The torsional effects are normally calculated with the solution of the differential equation for torsion

$$-E \cdot A_{ww} \cdot \phi'' + G \cdot I_D \cdot \phi = M_{T,0} \qquad /3.59/$$

where I_D represents the Saint-Venant stiffness:

$$I_D = \sum_j \frac{a_j \cdot t_j^3}{3} + \sum_k I_{Dok} \qquad /3.60/$$

with I_{Dok} = torsional stiffness of the longitudinal hollow stringers and $M_{T,0}$ o is the bimoment due to torsion without Saint-Venant stiffness.

For taking account of the effects of shear lag the number of elementary distributions can be extended to more than four by allowing for additional non straight lined distributions w_{si}, e.g. parabolic distributions according to Fig. 3.65.
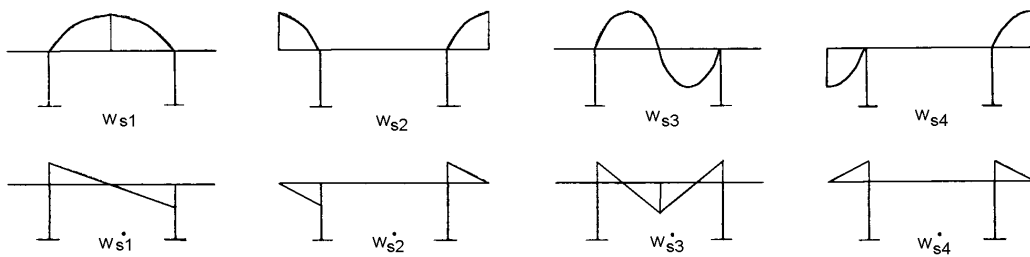
Figure 3.65 Additional elementary warping distributions w_{si} for taking account of shear lag.

Each of these assumed basic distributions w_s allows for an additional deformation v_s, which is defined by the equations

$$\begin{aligned} \varepsilon &= -w_s \cdot v''_s \\ \sigma &= -E \cdot w_s \cdot v''_s \end{aligned} \qquad /3.61/$$

From the curvature of an additional basic distribution w_s a new shear distribution results, which can be defined by

$$\begin{aligned} \gamma &= -w^{\cdot}_s \cdot v'_s \\ \tau &= -G \cdot w^{\cdot}_s \cdot v'_s \end{aligned} \qquad /3.62/$$

$$\text{where} \quad w^{\cdot}_s = \frac{\partial w_s}{\partial s}$$

126

This definition corresponds to the assumption that the transverse deformations of the fibres of a cross-section are infinitely small and that only longitudinal deformations are allowed:

$$\dot{\varepsilon} = \gamma'$$
/3.63/

From the additional elementary distributions one can derive additional warping stiffnesses A_{jk} and shear stiffnesses S_{jk}

$$A_{jk} = \int w_j \cdot w_k \cdot dA$$
$$S_{jk} = \int \dot{w}_j \cdot \dot{w}_k \cdot dA$$
/3.64/

In order to get independent equations for v_{si} (only diagonal values) the additional elementary distributions w_{si} must be orthogonalized by firstly eliminating all components of the base distributions 1, y, z, w_T and secondly combining them linearly. From this procedure a set of additional warping distributions follows (Fig. 3.66).
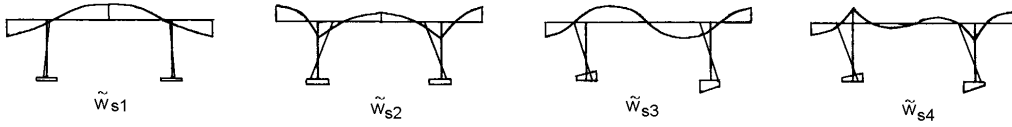
Figure 3.66 Orthogonal additional elementary warping distributions with the stiffnesses.

$$\widetilde{A}_{ss,i} = \int \widetilde{w}_{si} \cdot \widetilde{w}_{si} \cdot dA$$
$$\widetilde{S}_i = \int \dot{\widetilde{w}}_{si} \cdot \dot{\widetilde{w}}_{si} \cdot dA$$
/3.65/

This leads to a set of independent differential equations

$$-E \cdot \widetilde{A}_{ss,i} \cdot \widetilde{w}''_{si} + G \cdot \widetilde{S}_i \cdot \widetilde{w}_{si} = M_{si,0}$$
/3.66/

which are fully analogous to the differential equation /3.59/ for torsion.

By using the well known solutions of these differential equations, the additional stress distributions due to shear lag can be determined by

$$\sigma_s = \sum \sigma_{si} = \sum -E \cdot \widetilde{w}_{si} \cdot \widetilde{w}''_{si} = \sum \frac{M_{si,0}}{\widetilde{A}_{ss,i}} \cdot \widetilde{w}_{si}$$
/3.67/

and added to the stresses

$$\sigma = \frac{N}{A} \cdot 1 + \frac{M_y}{A_{yy}} \cdot y + \frac{M_z}{A_{zz}} \cdot z + \frac{M_w}{A_{ww}} \cdot w_T$$
/3.68/

127

which are calculated without regard to shear lag. An example for the resulting distribution for symmetrical and asymmetrical loading is given in Fig. 3.67.

stress distribution for
symmetrical loading

stress distribution for
asymmetrical loading
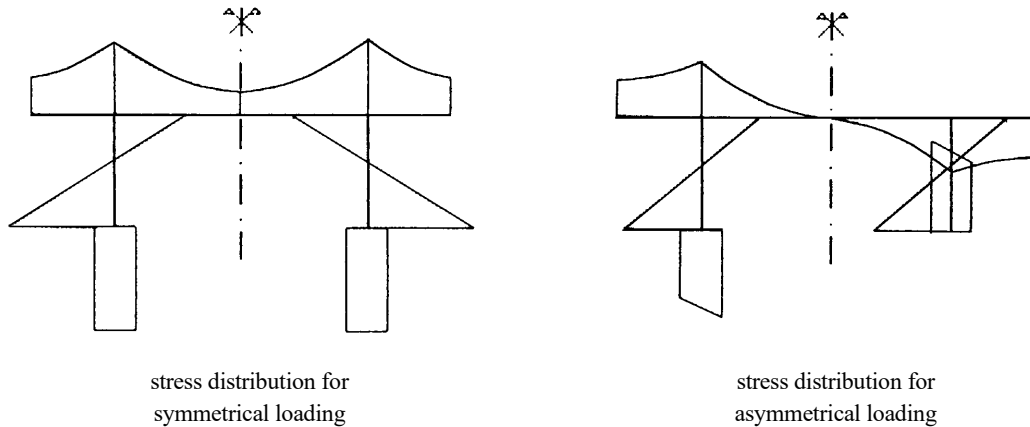
Figure 3.67 Resulting stress distributions with shear lag considered.

(c) Parametric study to determine the effects of symmetrical and unsymmetrical loading

The calculation method described in section (b) is applied for a double span continuous girder bridge under, uniformly distributed loading on the webs (Fig. 3.68).
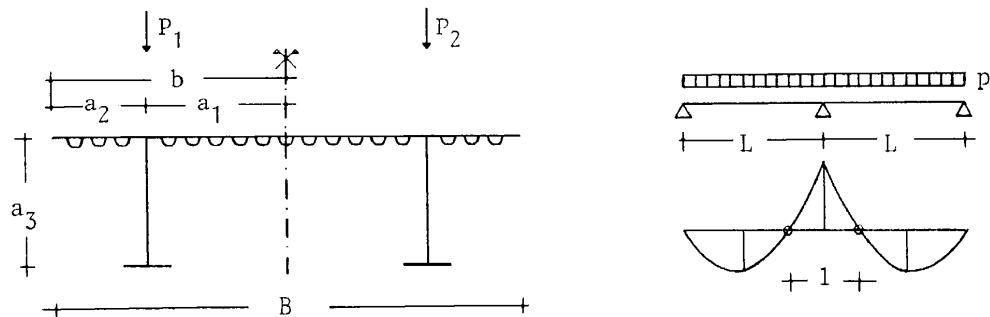
Figure 3.68 Cross-section and longitudinal system of a highway bridge.

The geometrical parameters which are modified are a

$$1 \leq \frac{1}{b} \leq 100 \qquad\qquad 0 \leq \frac{a_2}{b} \leq 1$$

The purpose of the parametric study is to compare the values of the effective width of the deckplate at the inner support as calculated for the indicated unsymmetric loadings with the ones

128

calculated for only the symmetrical part of the loadings. The differences will demonstrate, whether the asymmetrical effect on the effective width may be neglected as it is common practice or not.

The stress distributions including the effects of shear lag are calculated with the bending moment, the bimoment due to torsion and the stress resultants due to the additional deformations at the inner support, which can be calculated by

$$M_{v_s} = -\frac{p_{v_s} \cdot L^2}{8} \cdot f(\gamma)$$

/3.69/

with p_{v_s} = load causing the additional deformation v_s

$$\gamma = \sqrt{\frac{G \cdot S}{E \cdot A_{ss}}} \cdot L$$

/3.70/

$$f(\gamma) = \frac{4}{\gamma} \cdot \frac{\gamma \cdot \sinh\gamma + 2 \cdot (\cosh\gamma - 1)}{\gamma \cdot \cosh\gamma - \sinh\gamma}$$

/3.71/

The effective width b_m is determined by

$$b_m = \lambda \cdot b$$

/3.72/

with
$$\lambda = \frac{\int \sigma ds}{\sigma_{max} \cdot b}$$

/3.73/

for the symmetrical and unsymmetrical case (Fig. 3.69).

symmetrical loading   asymmetrical loading
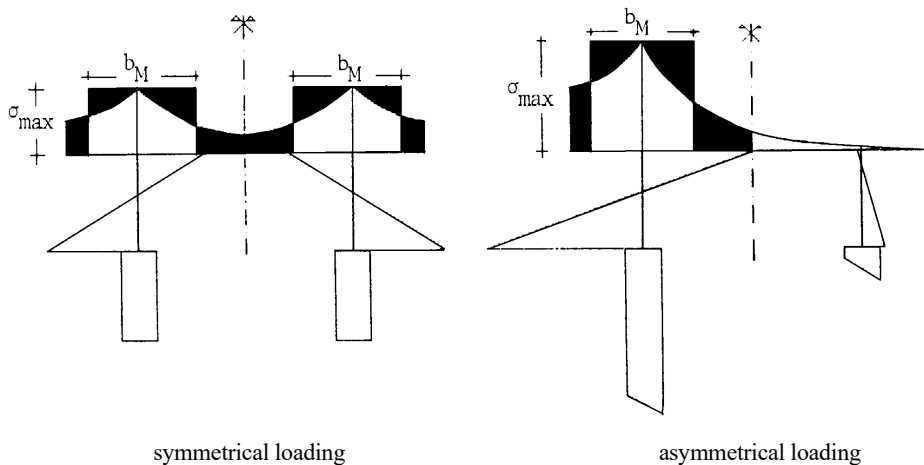
Figure 3.69 Definition of the effective width.

For the loading situation 1 the resulting λ_s and λ_{s+a} - values are shown in a three dimensional graph in Fig. 3.70.
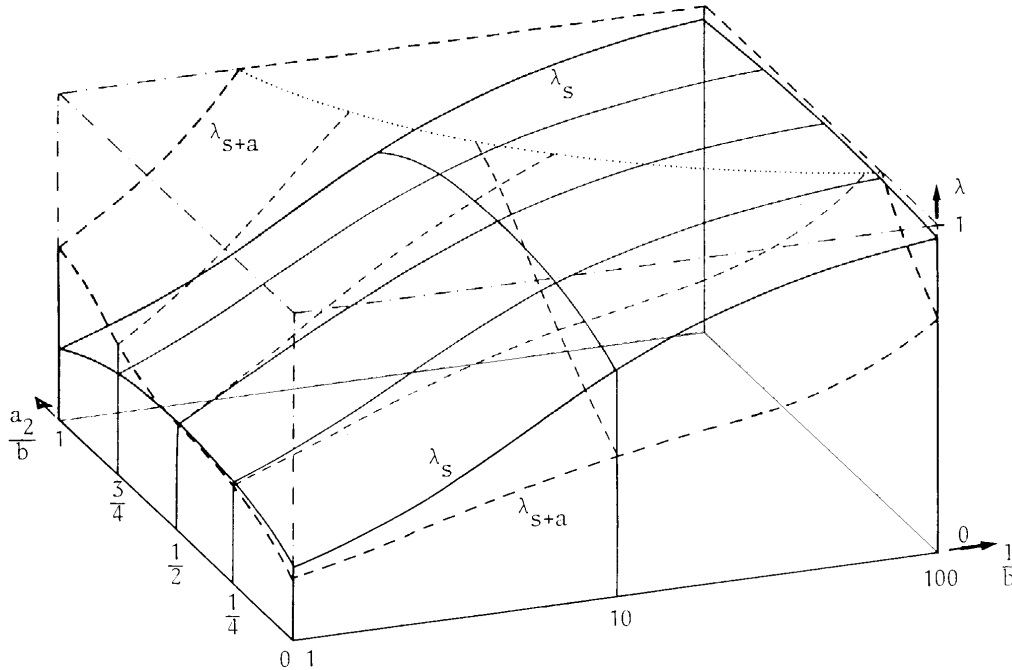
Figure 3.70 Three dimensional graph.

The results show that λ_s and λ_{s+a} are almost equal for small l/b-values. For large l/b-values the λ_s values are approaching $\lambda_s = 1$ whereas the λ_{s+a}-values approach values, which result from the effects of bending and torsion only without any influence of shear lag. The position of the web under the bridge deck has no significant effect on the λ_s-values, however the λ_{s+a}-values depend sensitively on the a_2/b-values for large l/b-ratios.

The maximum differences can be found for cross-sections with edge webs and medium l/b-values. They are observed for extreme conditions of the cross-sectional shape and of the loading simultaneously.

The small differences between the λ_s and λ_{s+a}-values for bridge loadings justify the common practice to apply the λ_s values only and to allow for asymmetrical loading merely by determining the load part on one girder by level distribution.

(d) Derivation of a practical formula for the determination of the effective width

As demonstrated in section (c), the effective width may be derived from a symmetrical cross-section defined by

130

$$\alpha = \frac{A_F}{A_w} \qquad\qquad /3.74/$$

as indicated in Fig. 3.71.

$A_F = 2\,bt$	z distribution	w_s distribution
$A_w = h \cdot s$		$A_{ss} = \dfrac{16}{15} \cdot A_F \cdot \dfrac{\alpha+1}{6\alpha+1}$
$\alpha = \dfrac{A_F}{A_w}$	$A_{zz} = \dfrac{1}{12}h^2 \cdot A_F \cdot \dfrac{6\alpha+1}{\alpha}$	$S = \dfrac{16}{3}\dfrac{t}{b}$
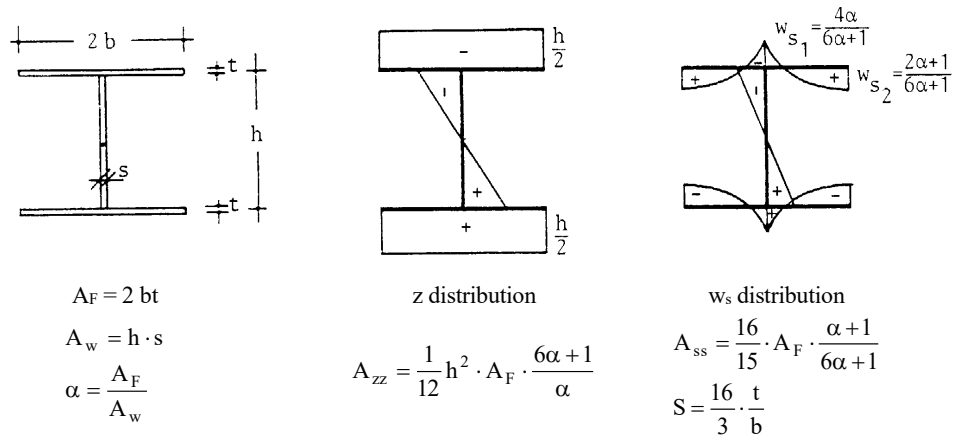
Figure 3.71 Cross-section and cross-sectional values.

In order to consider different support- and loading conditions in a simple way, it is advantageous to subdivide a continuous girder according to the existing bending moment distribution into independent parts, which are separated at the counter-flexure points as shown in Fig. 3.72 [BS 5400, 1982] [Eibl, 1983].
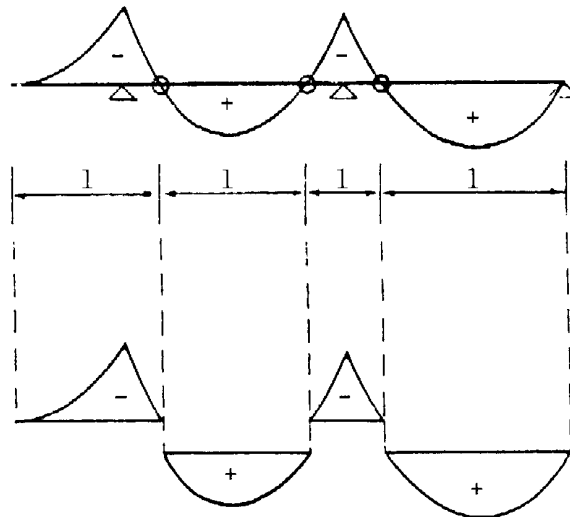
Figure 3.72 Subdivision of a continuous girder in independent parts.

131

By this subdivision the problem of determining λ -values for different kinds of supporting conditions of a girder and different loading may be reduced to the problem of developing a λ-formula for the midspan of a simply supported beam loaded by both a uniformly distributed and a single load (Fig. 3.73).

$$\eta = \frac{p \cdot 1}{P}$$

shape parameter:

$$\psi = \frac{4 \cdot \Delta M}{M_{max}} = \frac{1}{\dfrac{2}{\eta} - 1}$$
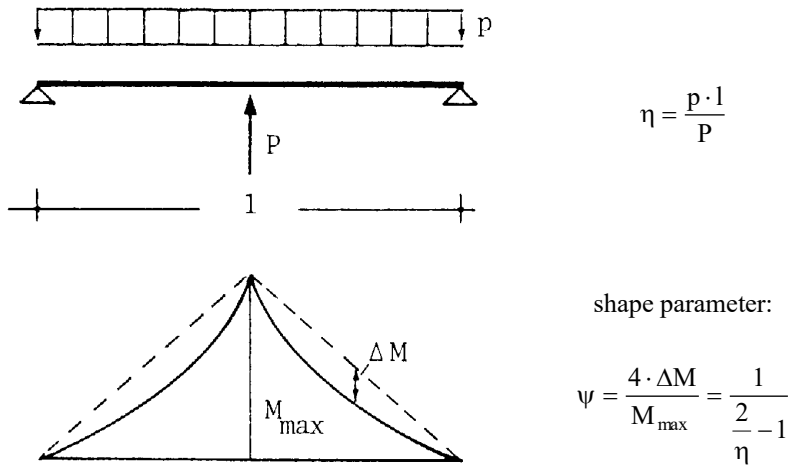
Figure 3.73 Explanation of the shape parameter ψ.

The shape of the bending moment distribution is thus governed by the factor

$$\psi = \frac{4 \cdot \Delta M}{M_{max}}$$

/3.75/

Special cases for this shape parameter are indicated in Fig. 3.74.
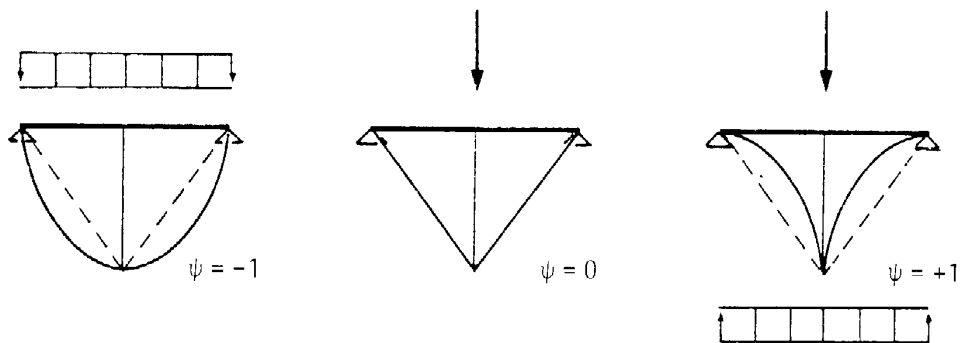
Figure 3.74 Special cases for the shape parameter ψ.

132

The stress resultants for the bending deformation ζ and the additional deformation v_s due to shear lag are indicated in Fig. 3.75. The resulting stress distribution is given in Fig. 16.

$$M_z = \frac{1}{4} \cdot P\, l \cdot \frac{1}{1+\psi}$$

$$M_s = \frac{1}{4} \cdot P\, l \cdot \frac{1}{1+\psi} \cdot k_{zs} \cdot f(\psi,\gamma)$$
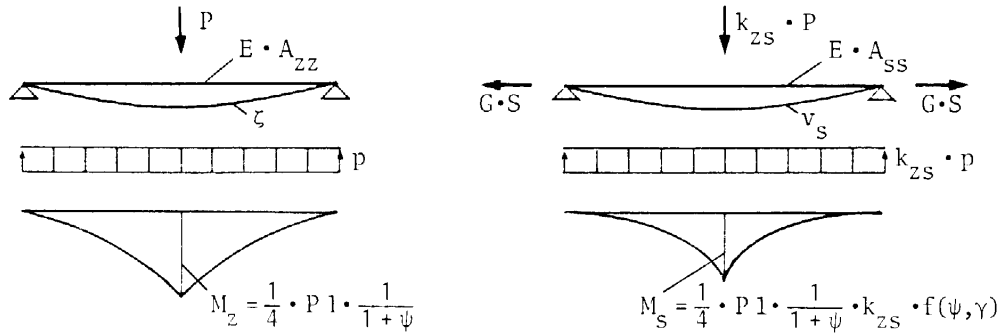
with
$$k_{zs} = \frac{8}{h} \cdot \frac{\alpha}{6\alpha+1}$$

$$\gamma = \sqrt{\frac{5}{2k} \cdot \frac{6\alpha+1}{\alpha+1} \cdot \frac{1}{b}}$$

$$k = \frac{E}{G} \cdot (1-\alpha_{orth})$$

$$\alpha_{orth} = \frac{\sum a_\sigma}{2b \cdot t}$$

$$\sum a_\sigma = \text{total area of additional stiffeners}$$
$$\text{connected with the deck plate}$$

$$f(\psi,\gamma) = (1+\psi) \cdot \frac{2}{\gamma} \cdot \tanh\frac{\gamma}{2} - \psi \cdot \frac{8}{\gamma^2} \cdot \left(1 - \frac{1}{\cosh\frac{\gamma}{2}}\right)$$

Figure 3.75 Stress resultants and total stress distribution.
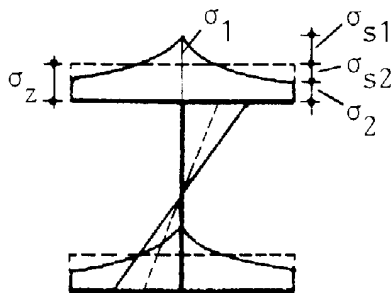
$$\sigma_z = -\frac{1}{4} P \cdot l \cdot \frac{1}{1+\psi} \cdot \frac{1}{A_G \cdot h} \cdot \frac{6\alpha}{6\alpha+1}$$

$$\sigma_{s1} = -\frac{1}{4} P \cdot l \cdot \frac{1}{1+\psi} \cdot \frac{1}{A_G \cdot h} \cdot \frac{6\alpha}{6\alpha+1} \cdot f(\psi,\gamma) \cdot \frac{5\alpha}{\alpha+1}$$

$$\sigma_{s2} = -\frac{1}{4} P \cdot l \cdot \frac{1}{1+\psi} \cdot \frac{1}{A_G \cdot h} \cdot \frac{6\alpha}{6\alpha+1} \cdot f(\psi,\gamma) \cdot \frac{5}{4} \cdot \frac{2\alpha+1}{\alpha+1}$$

Figure 3.76 Resulting stress distribution.

Equation /3.73/ gives then:

$$\lambda = \frac{1}{3} + \frac{2}{3} \cdot \frac{\sigma_2}{\sigma_1}$$

/3.76/

or, according to Fig. (3.76)

$$\lambda = \frac{1}{1 + \dfrac{5}{6} \cdot \dfrac{6\alpha + 1}{6\alpha} \cdot f(\psi, \gamma) \cdot \dfrac{1}{1 - \dfrac{5}{6} \cdot \dfrac{1}{\alpha + 1} \cdot f(\psi, \gamma)}}$$

/3.77/

This formula ought to be simplified for practical use.

The first step of simplification will be achieved by eliminating the effect of the cross-section. A parametric study with $\alpha = 0$, $\alpha = 1$ and $\alpha = \infty$ shows that $\alpha = \infty$ gives the lowest values for λ (Fig. 3.77).
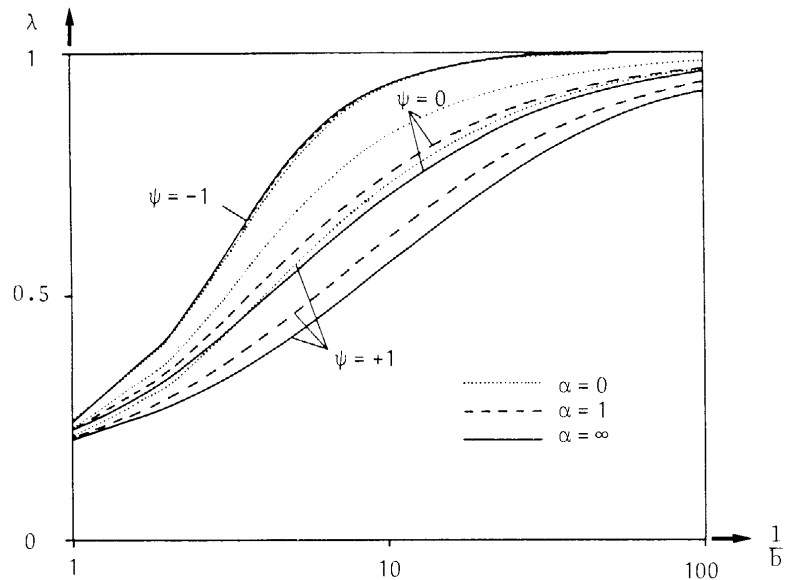
Figure 3.77 λ- values according to equation (20) for $\alpha = 0$, $\alpha = 1$ and $\alpha = \infty$.

By putting $\alpha \to \infty$ equation (20) becomes

$$\lambda = \frac{1}{1 + 5 \cdot f(\psi, \gamma)}$$

/3.78/

The next step of simplification will be to replace f (ψ, γ) as given in Fig. 3.75 by a more suitable expression f* (ψ, γ) that approximates f (ψ, γ) with a sufficient accuracy in the range $\gamma > 2$ and deviates from f (ψ, γ) for $\gamma < 2$ in such a way that the approach to λ-values determined by more accurate methods [Maquoi and Massonnet, 1982] is improved.

134

This condition is satisfied by adopting

$$f^*(\psi,\gamma) = (1+\psi)\cdot\frac{2}{\gamma} + (1-\psi)\cdot\frac{4}{\gamma^2}$$

/3.79/

which is compared with $f(\psi,\gamma)$ in Fig. 3.78.
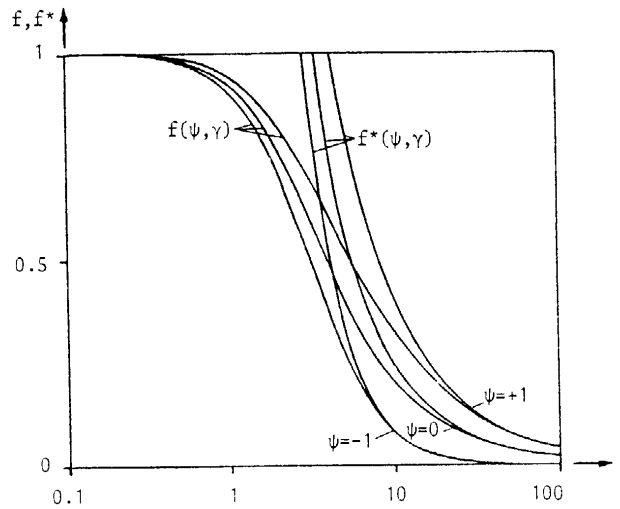
Figure 3.78 Comparison of $f(\psi,\gamma)$ with $f^*(\psi,\gamma)$.

Inserting equation /3.78/ into equation /3.78/ gives

$$\lambda = \frac{1}{1 + (1+\psi)\cdot\dfrac{10}{\gamma} + (1-\psi)\cdot\dfrac{20}{\gamma^2}}$$

with

$$\gamma = \sqrt{\frac{15}{k}}\cdot\frac{1}{b}$$

and finally

$$\lambda = \frac{1}{1 + (1+\psi)\cdot\sqrt{\dfrac{k}{0.15}}\cdot\dfrac{1}{b} + (1-\psi)\cdot\dfrac{k}{0,75}\cdot\left(\dfrac{b}{1}\right)^2}$$

/3.80/

This formula is identical with that developed in [Maquoi and Massonnet, 1982] for $\psi = -1$. Some λ-values calculated with equation /3.80/ are shown in Fig. 3.79.
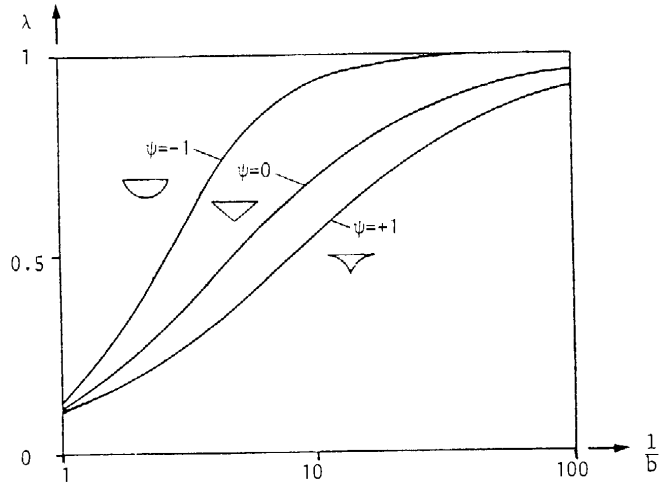
Figure 3.79 λ - values for the effective widths $b_m = \lambda \cdot b$ calculated with formula /3.80/.

(e) Comparison of the effective width formula /3.80/ with code-specifications

For the practical application of formula /3.80/ for bridges the assumption as given in Fig. (3.80) may be made [Eibl, 1983]:

$$l_1 = 0.8 \cdot L_1$$
$$l_2 = 0.25 \cdot (L_1 + L_2)$$
$$l_3 = 0.6 \cdot L_2$$
$$l_4 = 0.25 \cdot (L_2 + L_3)$$
$$l_5 = 0.8 \cdot L_3$$
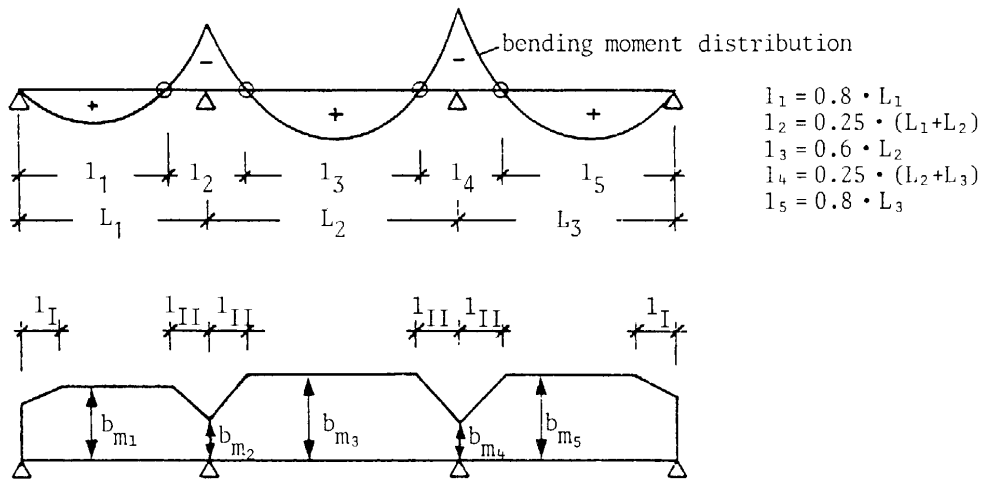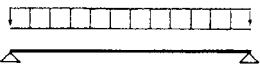
Figure 3.80 Geometrical assumption for the determination of the effective width.

A comparison with code-specifications, e.g. BS 5400 is given in Table 3.2.

136

Table 3.2 Comparison of formula /3.80/ with BS 5400 [1982].

λ – values	b/l	$\alpha_{orth} = 0$		$\alpha_{orth} = 1$	
		BS 5400	/3.80/	BS 5400	/3.80/
ψ = -1	0	1	1	1	1
	0.05	0.98	0.98	0.97	0.97
	0.1	0.95	0.94	0.89	0.88
	0.2	0.81	0.78	0.67	0.64
	0.3	0.66	0.62	0.47	0.44
	0.4	0.50	0.47	0.35	0.31
	0.5	0.38	0.37	0.28	0.22
	0.6	0.32	0.29	0.24	0.17
	0.8	0.21	0.18	0.16	0.10
	1	0.16	0.13	0.12	0.07
ψ = 0	0	1	1	1	1
	0.05	0.80	0.82	0.75	0.76
	0.1	0.67	0.69	0.59	0.60
	0.2	0.49	0.51	0.40	0.41
	0.3	0.38	0.39	0.30	0.30
	0.4	0.30	0.31	0.23	0.22
	0.5	0.24	0.25	0.17	0.18
	0.6	0.20	0.21	0.15	0.14
	0.8	0.14	0.15	0.10	0.08
	1	0.12	0.12	0.08	0.07
ψ = 1	0	1	1	1	1
	0.05	0.68	0.71	0.61	0.63
	0.1	0.52	0.55	0.44	0.46
	0.2	0.35	0.38	0.28	0.30
	0.3	0.27	0.29	0.22	0.22
	0.4	0.21	0.23	0.17	0.18
	0.5	0.18	0.19	0.14	0.15
	0.6	-	0.17	-	0.12
	0.8	-	0.13	-	0.10
	1	-	0.11	-	0.08

137

4 Construction of Orthotropic Steel Bridges

4.1 Structural Systems and Erections of Collapses of Orthotropic Steel Bridges

Two periods could be distinguished in the construction of steel structures: the period of *riveted* structures were built from the last decades of eighties until the forties of the last century, and the period of *welded* or modern structures. The method of joining has basic effect for all structure: determines the construction, the grade of the basic material, the technology of manufacturing and erecting, the methods of controlling, and eventually the aesthetic aspects of the establishment.

The significant differences are the following between the two system:

– in the riveted structures the elements join each other by bracers and angles made applying simply tools, while in the welded structures the elements join directly each other by difficult cohesive holds;
– the implementation, the sufficient quality and the controlling of riveted connections are simple manual work, while the welding requires big apparatus and qualification;
– the manufacturing and erecting units of riveted structures are planar, relatively small elements join at in-situ joints; while the welded units are three-dimensional, and in an erecting unit often big numbered (30 – 60) elements join to each other;
– the riveting is not sensitive for the position of the joint and the erection conditions, thus – contrary to the welding – practically it is indifferent, that the joint is made in the factory or in-situ;
– the welding – contrary to the riveting – changes the property of basic material, and generates stresses, shrinking, deformations, cracking and rigid-fraction.

The building procedures of the traditional structures are simple, most of them could be done by semiskilled workers.

The manufacturing and erection of welded structures – mainly the difficulties of the producing and controlling of welding, the difficulties of keeping the shape and size according to the plan, and the difficulties of making of the in-situ connections – is a extremely demanding work, which requires highly qualified professionals.

Due to the above mentioned differences the changeover to the welded structures was a multi-stages, long procedure.

In the beginning, the designers had to convert the rules of the construction details of riveted structures according to the requirements of the new joining method, the welding.

The main object of the construction was to produce and apply the sufficient basic material, the welding methods, the welding materials, the welding technology, and controlling methods.

The material saving characterized the second phase of the development – in the years after the world war. Today, in the third phase, the main object is to increase the effectiveness of the erection and to improve the working conditions. This could be reached by simplification of the construction and by mechanization of the manufacturing and erection [Domanovszky, 1984].

The manufacturing and erecting of the modern steel bridges are close-knit with the structural system. The floor slabs of modern bridge structures consist of orthotropic plates, which draw up special conditions against the erection, too [Weitz, 1966, 1974, 1975].

Existing structures	Opened to traffic in	Shape of longitudinal ribs	Rib spacing "a" (mm)	Cross girder spacing "b" (mm)
Rhine bridge Düsseldorf-Neuß	1951		440	1910
Rhine bridge Cologne-Mülheim	1951		305	1770-1810
Bürgermeister bridge Bremen	1952		300	1750-1960
Rhine bridge Speyer	1956		350	1750
Northern bridge Düsseldorf	1957		400	1800
St Alban bridge Basel	1955		300	1670
Sava bridge Belgrade	1956		300,2	1562
Severins bridge Cologne	1959		293-384	2000
Rhine bridge Kehl-Straßburg	1960		300	2560
Europe bridge Innsbruck	1963		370	1500
Northern Elba bridge Hamburg	1957		340-380	2670
Rhine bridge Mainz-Weisenau	1961		300	1540
Kaiserlei bridge Frankfurt	1962		300	1425
Jülicherstraße bridge Düsseldorf	1963		300	2000
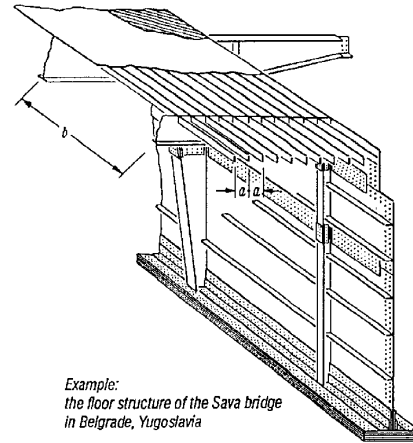
Example:
the floor structure of the Sava bridge in Belgrade, Yugoslavia

Figure 4.1 Variants of orthotropic plate with open longitudinal ribs.

Existing structures	Opened to traffic in	Shape of longitudinal ribs	Rib spacing "a" (mm)	Cross girder spacing "b" (mm)
Weser bridge Porta	1954		316	2360
Rhine bridge Duisburg-Homberg	1954		300	2014-2089
Rhine bridge Mannheim-Ludwigshafen	1958		300	2030
city highway Duisburg	1963		270-330	2000-2200
Haseltal bridge	1961		310	2310
Rhine bridge Schierstein	1962		300	3000
Fulda bridge Berghausen	1962		300	2650-2750
Rhine bridge Leverkusen	1964		300	2530
Rhine bridge Emmerich	1964		296	2525
Rhine bridge Bonn-Nord	under construction		300	2243
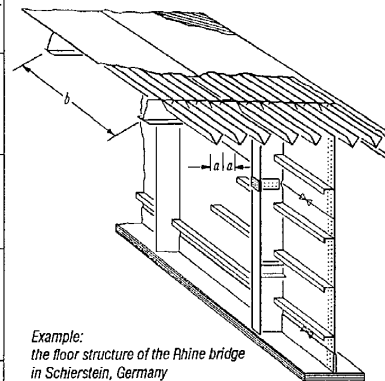
Example:
the floor structure of the Rhine bridge in Schierstein, Germany

Figure 4.2 Variants of orthotropic plate with closed longitudinal ribs.
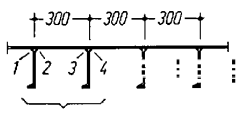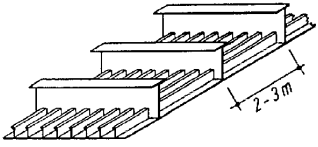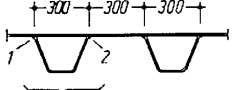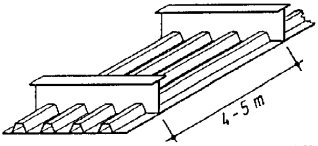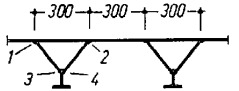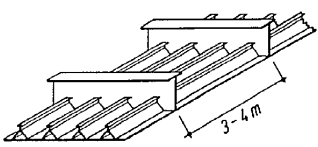
1. Orthotropic plate with open longitudinal ribs	0.3 cross girders per metres of the plate 0.6 intersection points per units of longitudinal ribs and metres of plate
┌─300─┬─300─┬─300─┐ ┌1┐┌2┐┌3┐┌4┐ ┆ ┆ ┆ ┆ 4 longitudinal welds per units of longitudinal ribs	
2. Orthotropic plate with hollow longitudinal ribs	0.2 cross girders per metres of the plate 0.2 intersection points per units of longitudinal ribs and metres of plate
┌─300─┬─300─┬─300─┐ 1 _/ 2 _/ 2 longitudinal welds per units of longitudinal ribs	
3. Orthotropic plate with built-up longitudinal ribs	0.25 cross girders per metres of the plate 0.25 intersection points per units of longitudinal ribs and metres of plate
┌─300─┬─300─┬─300─┐ 1 \Y/ 2 3 ⊥ 4 4 longitudinal welds per units of longitudinal ribs	

Figure 4.3 Longitudinal rib shapes for floor slabs of light steel bridges.

floor slab with longitudinal ribs interrupted
and continuous cross girders

floor slab with longitudinal ribs continuous
and cross girders cut into comb-like shape
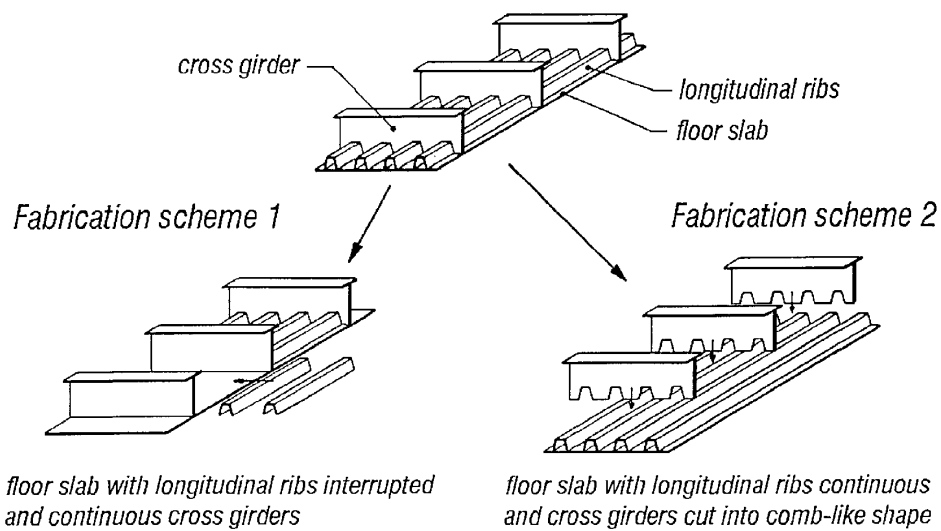
Figure 4.4 Fabrication of the floor slabs of light steel bridges with hollow longitudinal ribs.
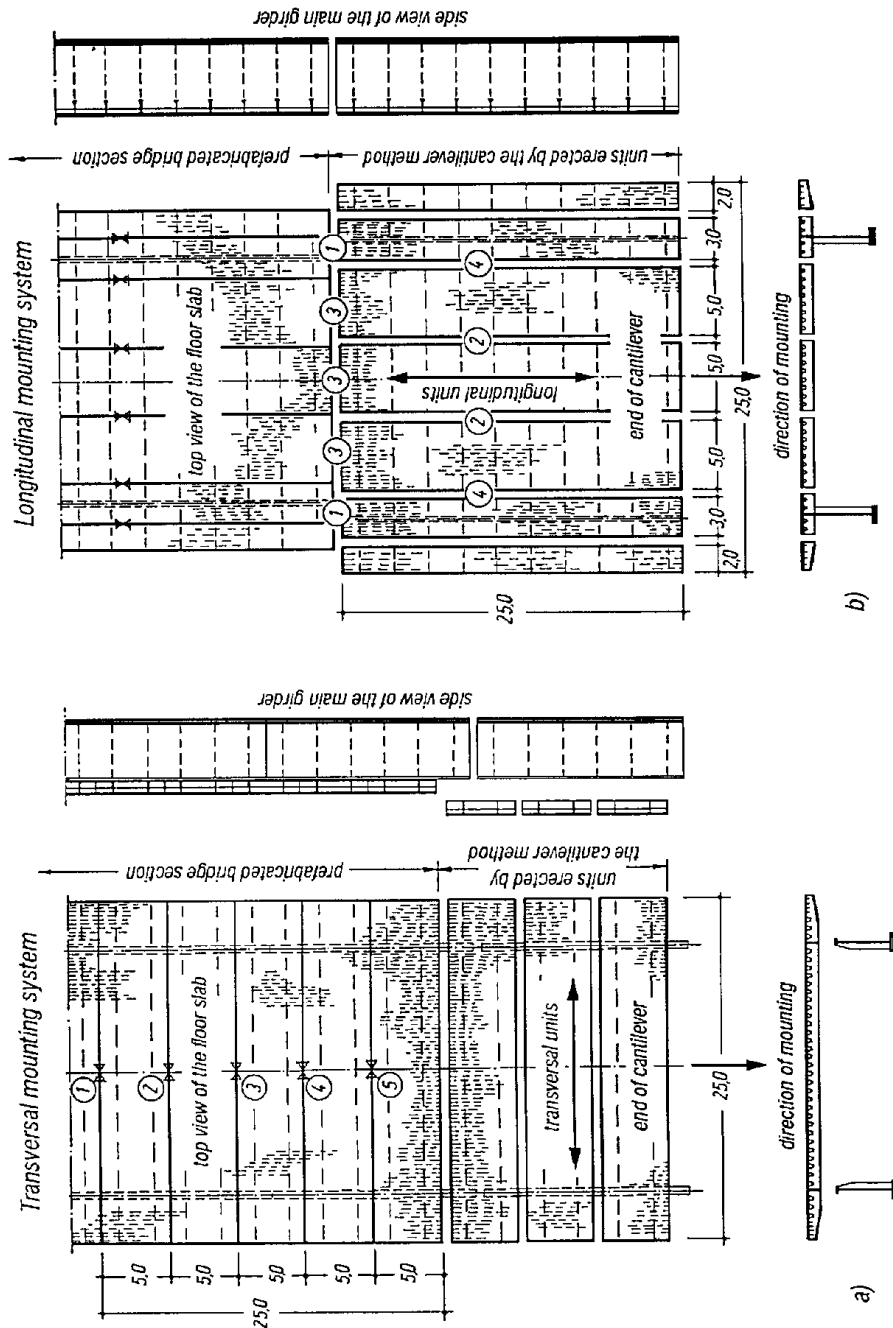
Figure 4.5 Division of an orthotropic steel bridge floor structure, using welded joints, in the context of the cantilever method of erection. a) transversal mounting system; b) longitudinal mounting system.
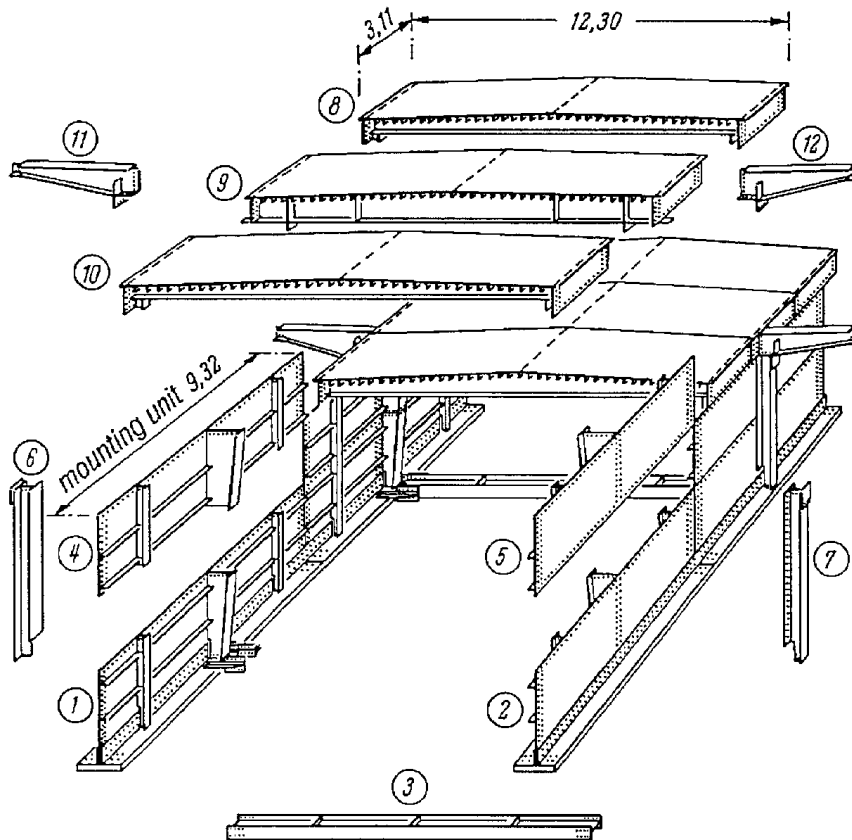
Figure 4.6 Sava bridge at Belgrade, Yugoslavia

The division of the structure into fabrication units, and formation of mounting joints. Example for the transversal division. Numbers relate to the building sequence.

- longitudinal joints of the main girder:	riveted webs, riveted cross bracings
- transversal joints of the floor slab:	butt welded
- longitudinal joints of the floor slab:	no joint, no joints in the lower flanges
- joints of the cross girder in the floor structure:	no joints in the webs
- joints of the longitudinal ribs in the floor structure:	butt welded
- transversal joints of the main girder:	riveted webs
- joints in the bottom flange of the main girder:	riveted
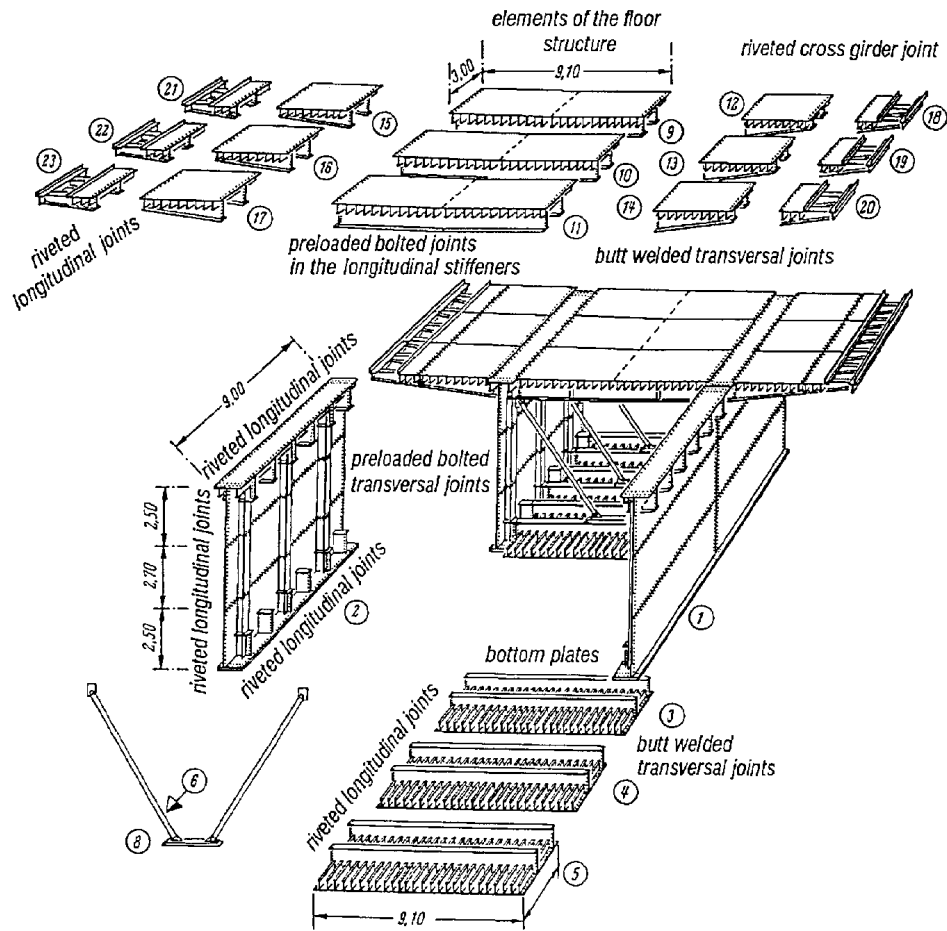
Figure 4.7 Europe Bridge in Innsbruck, Austria

The division of the structure into fabrication units, and formation of mounting joints.

Example for the transversal and longitudinal division. Numbers relate to the building sequence.

- transversal joints of the floor slab: butt welded
- longitudinal joints of the floor slab: riveted
- joints of the longitudinal floor stiffener: preloaded bolted
- joints of the floor cross girder: riveted
- transversal joints of the main girder (web and flanges):preloaded bolted
- longitudinal joints of the main girder: riveted
- transversal joints of the bottom plate: butt welded
- longitudinal joints of the bottom plate: riveted

143
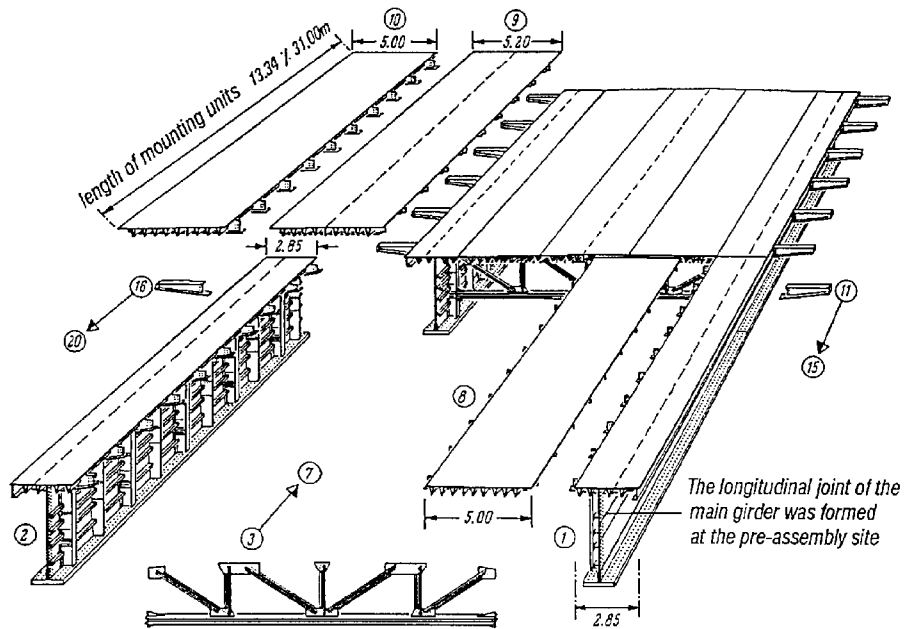
Figure 4.8 Rhine bridge at Wiesbaden-Schierstein, Germany

The division of the structure into fabrication units, and formation of mounting joints.
Example for the longitudinal division of elements. Numbers relate to the building sequence.

- longitudinal joints of the main girder:	butt welded webs, riveted web and flanges in the cross brace – at the pre-assembly site
- transversal joints of the floor slab:	butt welded (Fusare process)
- longitudinal joints of the floor slab:	butt welded (Fusare process)
- joints of the floor cross girder:	bottom flanges butt welded, webs with preloaded bolts
- joints of the longitudinal floor stiffener:	butt welded (with backing plate)
- transversal joints of the main girder:	riveted (bolts used near the floor structure)
- joints in the lower chords of the main girder:	riveted

144

Rhine bridge   *Speyer*   1956

1625 t

—52—|———163————|————107————|

———322———

Field joints on the sections
assembled from scaffolding

Field joints on the sections
assembled using floating crane

Rhine bridge   *Wiesbaden-Schierstein*   1962

3700 t

|—85—|————205————|—85—|

———375———

Spacing of field joints

1. Space for pre-assembly is needed

2. Two different mounting processes with
   three different initial positions

3. Three apparatus of different kinds,
   applied at three different locations

4. There is no definitely permanent mounting direction

5. The division of cross-sections is changing in
   accordance with the different mounting processes

6. A mounting bent is needed in the river bed

1. No pre-assembly space is needed

2. One single uniform mounting procedure

3. Two identical compositions of machines in two application
   places, organized according to the same principles

4. The mounting direction is definitely permanent

5. The dismembering of cross-section (along the length of the bridge)
   is not changing, a rhythmical mounting sequence can be applied

6. Erection by the cantilever method in the river bed,
   without mounting bent

Figure 4.9 Comparison of the mounting processes of the slab-and-beam bridges (long span river bridges)
at Speyer and Wiesbaden-Schierstein, Germany
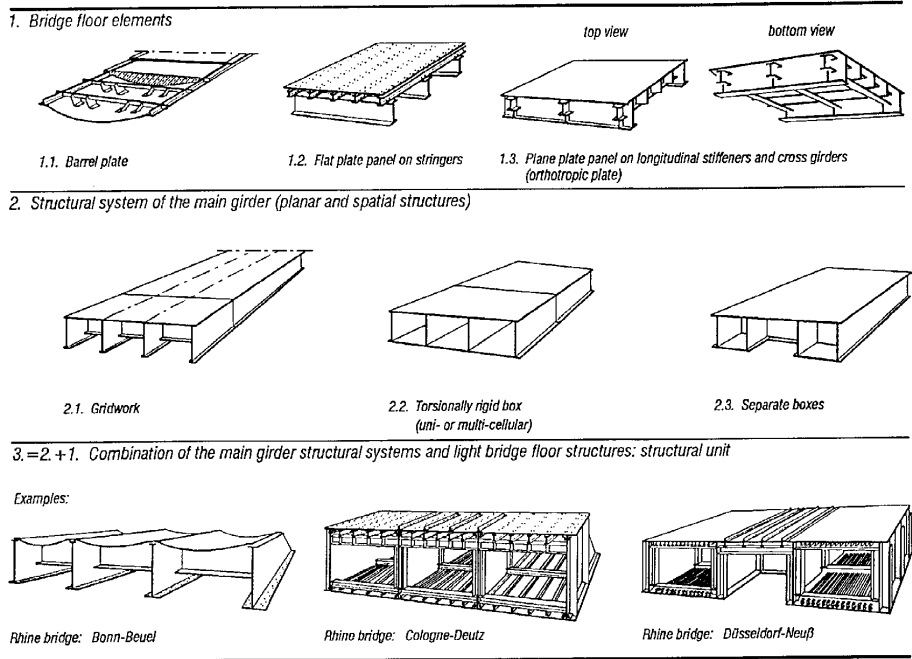
Figure 4.10 Development of highway bridges with light steel floor structure.
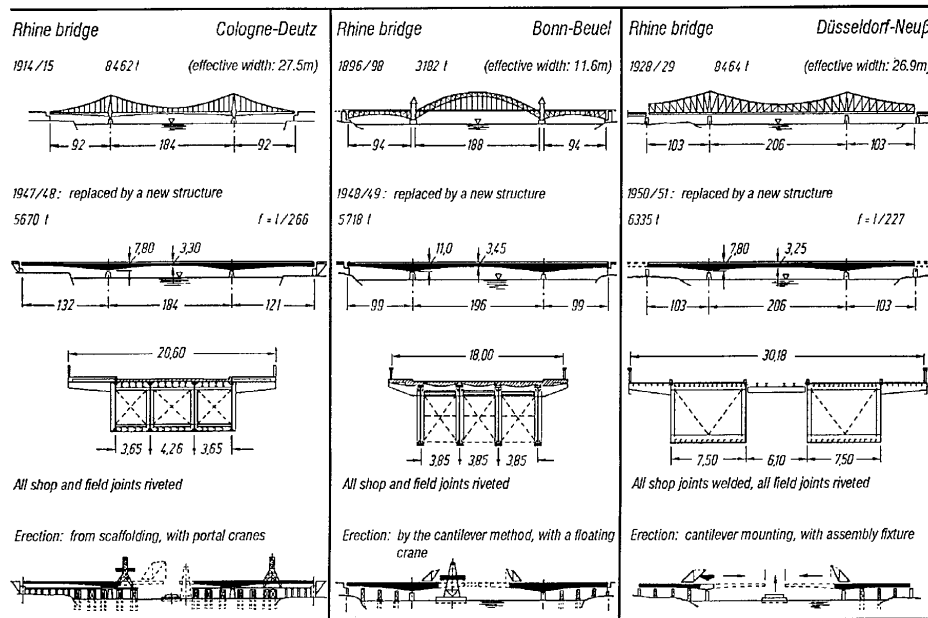
Figure 4.11 Development of large span bridges: the example of three Rhine bridges.

146
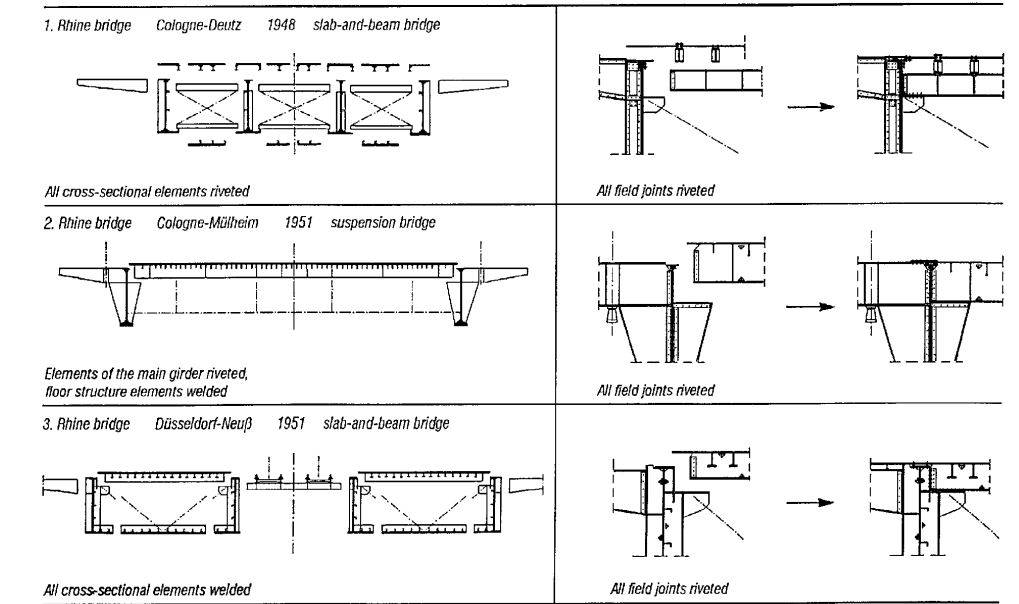
Figure 4.12 Development towards the structural continuum
Step 1: The assembly of planar cross-sectional units
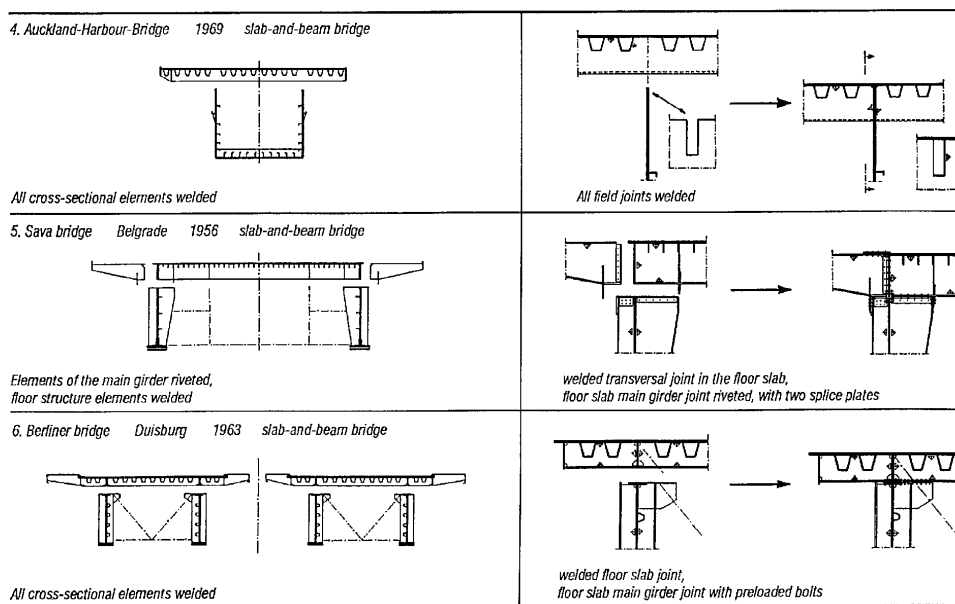
Figure 4.13 Development towards the structural continuum
Step 2: "Transversal" systems. Transition between from the planar to the spatial cross-sectional units.

| 7. Rhine bridge | Wiesbaden-Schierstein | 1962 | slab-and-beam bridge |

All cross-sectional elements welded

| 8. Rhine bridge | Düsseldorf-Oberkassel | 1973 | cable stayed bridge |

All cross-sectional elements welded
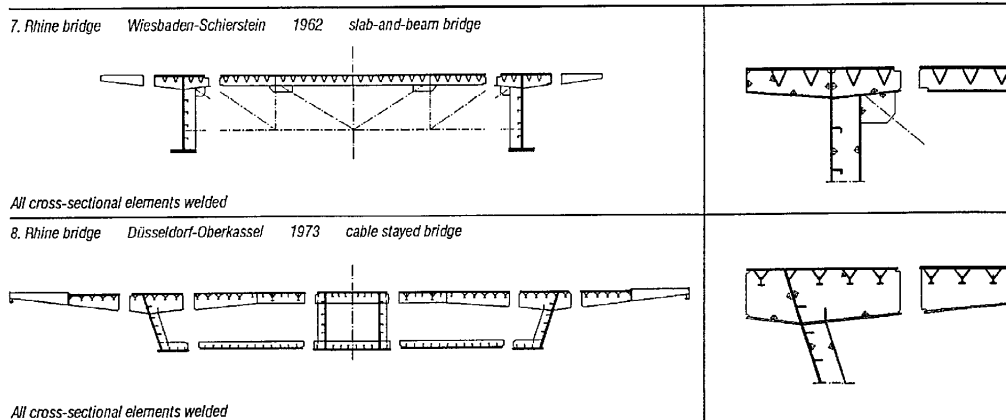
Figure 4.14 Development towards the structural continuum
Step 2: "Longitudinal" systems. Spatial cross-sectional units.

4.2 Hungarian Examples

4.2.1 'Erzsébet' bridge [Catalogue, 1998]

Location and name of the bridge
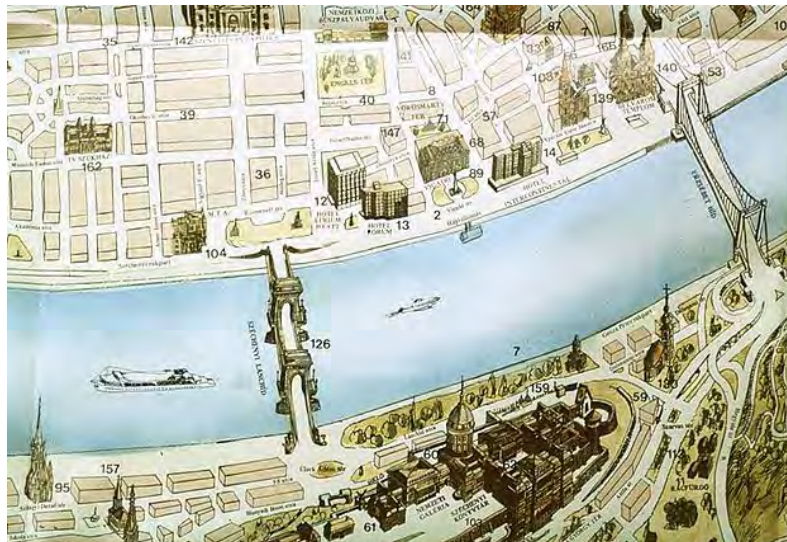
Figure 4.15 The Castle of Buda, the Lánchíd and the Erzsébet Bridge.
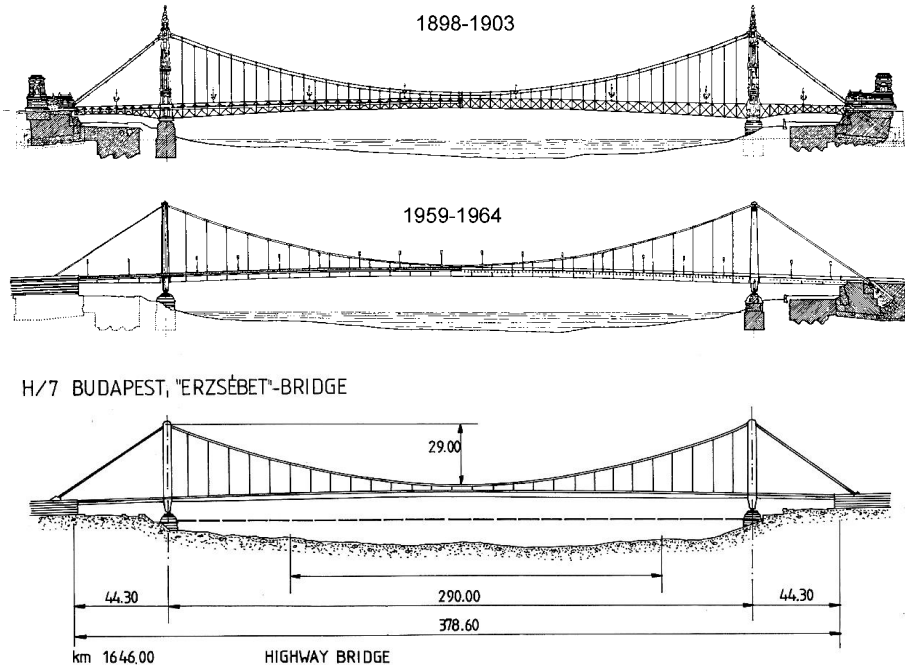
Figure 4.16 General view.

Figure 4.17 The view of Erzsébet Bridge from the Gellért Monument.

Name of the bridge	"Erzsébet" bridge
Distance:	**1646+000 km**
Country:	Hungary
City/town:	Budapest
Year of building - completion:	1898-1903
Year of rebuilding - completion:	1959-1964

Span lengths:

Figure 4.18 The view of Erzsébet Bridge from top of Gellérthegy.

Main bridge over streambed:	44.3+290.0+44.3 m
Roadway widths:	4.45+18.2+4.45 m
Designer:	UVATERV, Pál Sávoly, FÖMTERV, János Juhász
Main contractor:	Ganz-MÁVAG, Károly Massányi, János Fekete, Károly Vogt Bridge Construction Company
Construction cost:	381 million HUF

Traffic function of the bridge

Highway:

number of lanes: 6

Antecedents; the history of the bridge

Before the construction of the "Erzsébet" and "Szabadság" bridges, international tenders were invited for both bridges together. The first price winner plan was for the "Erzsébet" bridge, while the second price winner was the design for the "Szabadság" bridge. But the winner design was not realised, mainly because of the limited technological possibilities.

150

The first prize winner plan of the common tender finally has not been realized. Its main reason was, that it was a cable bridge, and at that time in Hungary cables of the required quality had not been produced. Therefore a chain bridge was built. Although during construction this change of the solution caused controversy, the realized structure later became famous and found approval.

Figure 4.19 The first prize winner plan of the 1894 tender by Kübler, Eisenlohp and Weigle.

Figure 4.20 The bridge.

The bridge, named after Queen Elizabeth of Hungary, was the largest span suspension bridge of the world for three decades, and is still considered as the most attractive suspension bridge ever built. In addition, it involved several new technical features (design by István Gállik), including the hinged pier with hinged chain connections and the special joint types of the continuous stiffening girder.

Figure 4.21 The erection of the bridge.

The plans of the realized construction were made by the Bridge Department of the Ministry of Trade Affairs, headed by Aurél Czekelius, and they applied the statical calculation method of Antal Kherndl, professor of the Technical University, who was a very important personality of the Hungarian bridge engineering.

A new design was carried out by Aurél Czekelius in the form of a chain bridge solution and it was realised. Fully propped erection method was applied.

Near the end of World War II, in January 1945 the Buda side anchorage chamber was blown up, the pylon and the chain together with the stiffening girder of the bridge felt into the river, only the pylon of the Pest side remained in the original position.

Figure 4.22 The bridge as blown up, 18 January 1945

When the bridge was blown up, the pylon of the Pest side (some 3000 metric tons) remained in its position; it was later supported by temporary structures, and was not removed until 1960.

As the original structure, by the opinion of a lot of people was one of the nicest chain bridge in the world, reconstruction was first planed in the style and form of the destroyed bridge. But the width of the roadway (11 m) was not enough the fulfill the requirements of the increasing traffic. For this and other reasons a completely new structure was designed in form of a cable suspension bridge.

Special model tests have been carried out in the laboratory of the Department of Steel Structures, TUB, to help the design of the erection of the new construction.

The model was of a scale of 1:50. Forces in the suspension cable, as well as, the characteristic deformations of the structure in different erection phases have be measured.

The technical data of the bridge
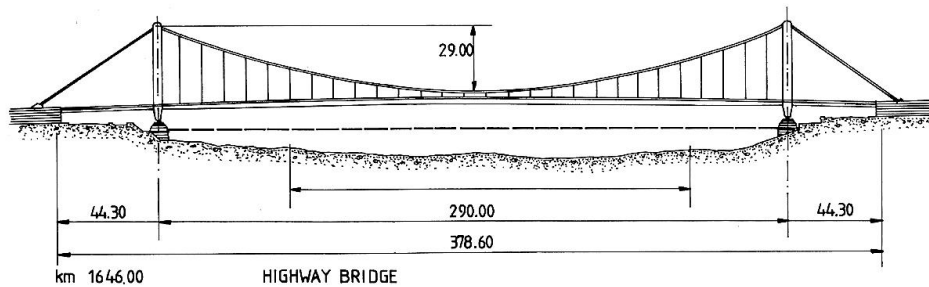
Figure 4.23 General view.
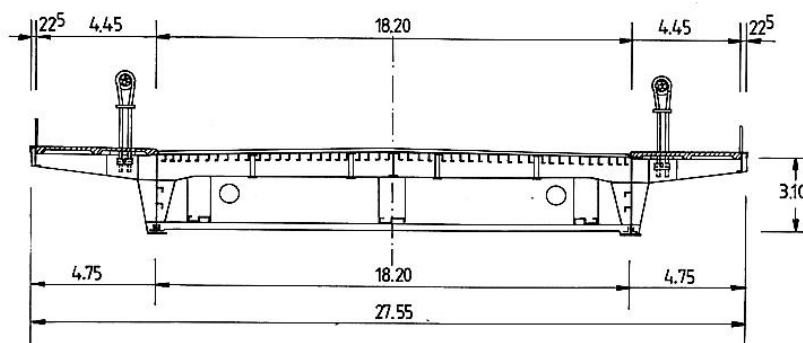
Figure 4.24 Cross section

Structural system, span lengths, widths

The two bundle of cables contains 61 elementary cables. It is formed in the shape of a regular hexagon resting on its vertex. An elementary cable contains 115 pieces of wires and it has a diameter of 54.5 mm.

Deck

The stiffening girder and the floor structure of the bridge is an orthotropic steel construction.

To prevent the slip of the asphalt layers on the deck plate, zig-zag shaped ribs were welded on the top of the deck plate.

Figure 4.25 The floor system

Foundation, substructure

The abutments needed a thorough rebuilding due to the different layout of the new bridge. After demolishing of the original ones the reinforced concrete blocks of anchorage chambers were built. The embankment piers also required a complete repair.

Bearings

At the pylons, the original hinges were applied

Figure 4.26 The new pylon, similarly to that of the old structure, is hinged.
The original hinges were re-used.

Quantities of applied materials

Weight of steel structure: 6300 t

Method of construction/erection; joints

The portal frames of the pylons were built first, each of them containing two columns, made from six elements and a transverse beam. For transferring the cables from one bank to the other, an assembly "carpet" of 420 m long was built on both sides. The two carpets were stiffened to each other in five sections by tubular trussed constructions. The cables were drawn through form Buda to Pest side, they were clamped into the disc shoe and were fixed into the anchorage chambers.
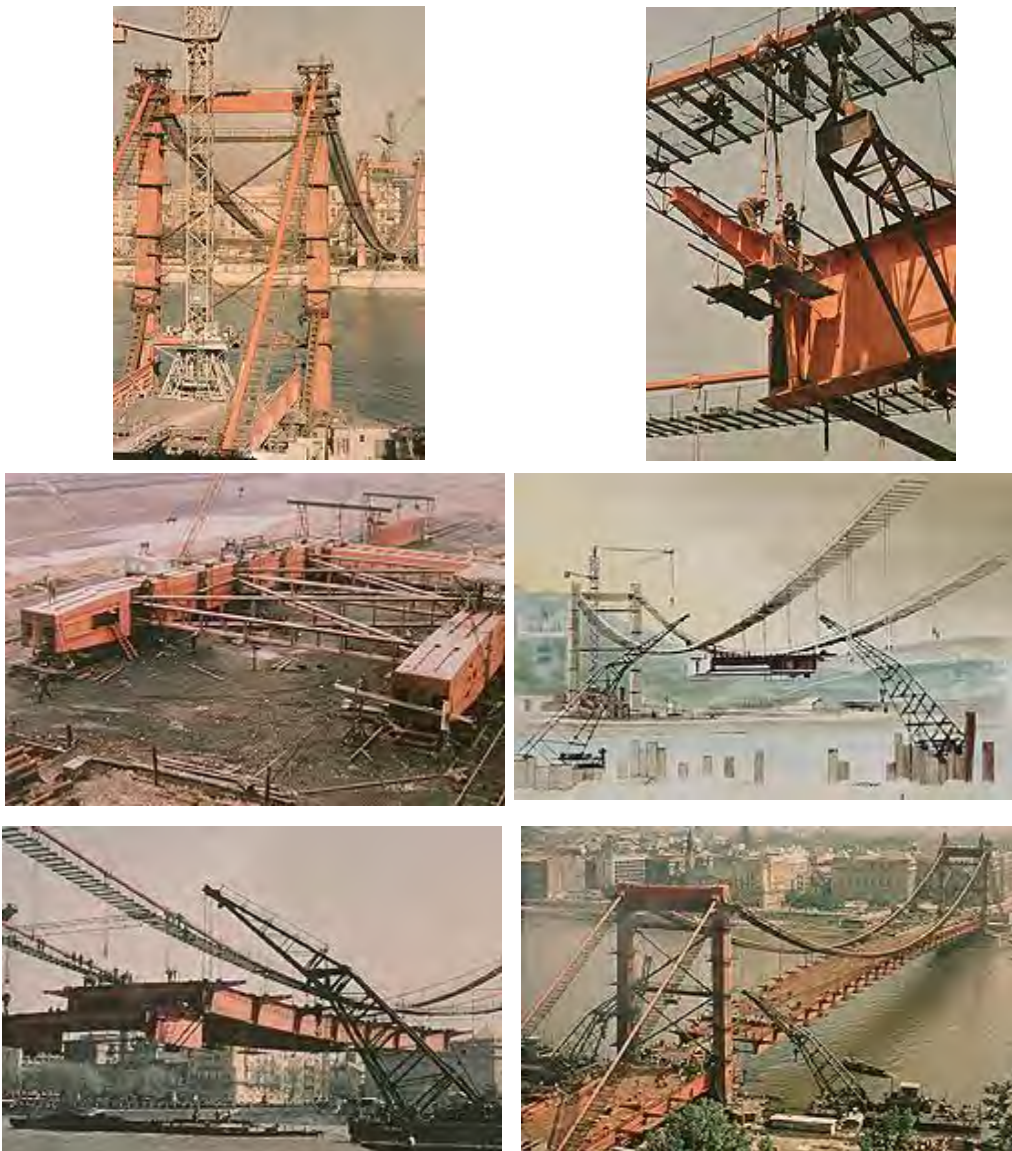
Figure 4.27 The erection of the bridge.

The stiffening girder and the floor system containing 195 assembly units, was manufactured at the yard of Ganz-MÁVAG at Lágymányos and they were shipped by barges to the building site. The units were lifted with the help of a floating crane of 100 t capacity. First the middle element was positioned and the further ones were lifted in a symmetrical order. The units were connected to each other with temporary hinges, the final connections by riveting were done, when the total structure was build and it was preloaded with 2400 t of sandy gravel ballast to achieve the final shape.

Corrosion protection

Re-dusting of the steel deck plate was performed by sand blasting, and after cleaning it was furnished with a zinc-coating.

Other parts of the steel construction were furnished with a double prime coating of red lead and a semi-synthetic painting in two layers.

Traffic situation

After reconstruction the bridge carried a two track tramway line, which was removed in 1973. This way the number of road lanes could be increased from four to six.

Test loading(s); periodical assessment of serviceability

The loading test, after finishing the construction, involved measurements of deformations and those of stresses around the intermediate supports of the main girders. Results of these later ones clearly showed that in case of such a great number of flange plates in a riveted construction the stress distribution is not linear along the flange thickness and its maximum develops around the centroid of the complete chord.

4.2.2 'Árpád' bridge

Location and name of the bridge
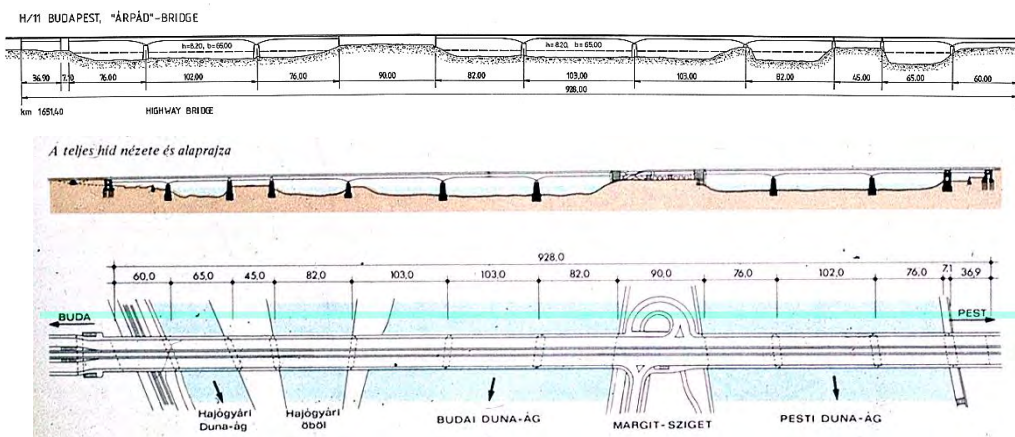
Figure 4.28 The side view of Árpád bridge.

Figure 4.29 The Árpád bridge.

Name of the bridge	"Árpád" bridge
Distance:	1651+400 km
Country:	Hungary
City/town:	Budapest
Year of building:	1939-1942
Completion:	1948-1950
Widening:	1980-1984

Span lengths:

Widening of the bridge began in 1960, according to a new concept. The original two main girders carry the loads of the trams, and the two new girders carry the road traffic

Main bridge over streambed:	60.0+65.0+45.0+82.0+2*103.0+ + 82.0+90.0+ 76.0+102.0+ +76.0+36.9 m
Roadway widths:	2.73+11.3+7.2+11.3+2.75 m
Designer:	FÕMTERV, UVATERV, Alajos Petur
Main contractor:	Bridge Construction Comp., Ganz-MÁVAG
Construction cost:	2325.365 million HUF (whole complex)
Owner of the bridge:	City of Budapest
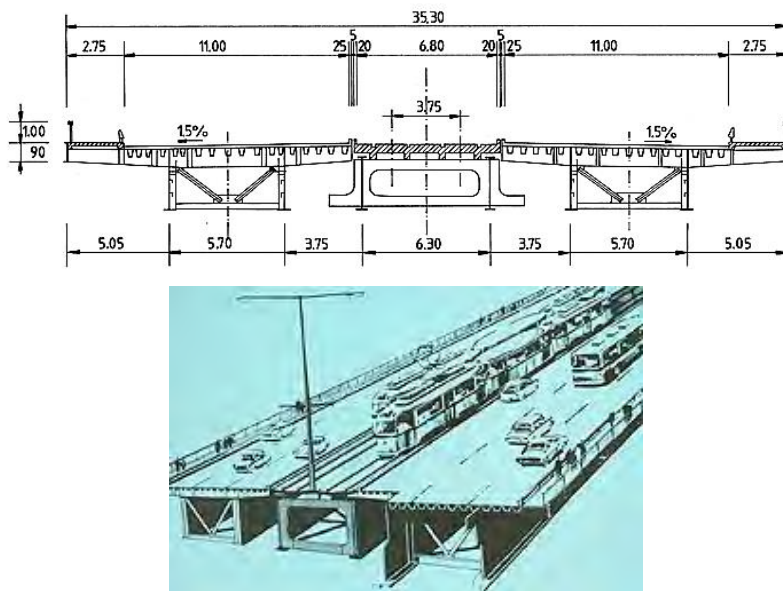
Figure 4.30 Cross sections.

Traffic function of the bridge

Highway bridge with tramway:

number of lanes:	6
number of tramway tracks:	2

Antecedents; the history of the bridge

The idea for a new bridge on the north part of the city was initiated by the fact, that the left bank was a developed industrial area, while on the right one there was a dense population. Law No. XLVIII. in 1908 ordered the construction of the bridge, but its completion was cancelled because of World War I. Later the development of the south part of the capital had a higher importance, therefore the design process started only in 1930.

The conditions were quite difficult, as the Danube has four arms in this area with very different distances to span over, and it was rather hard to decide, how the divide them, where and how to give the axis of the complete construction, etc. As not all of the conditions were clearly drawn, the designer teams should give recommendations for the solutions.

Two plans were honoured by the first prize, both of them were certain arched solutions, made by university professors János Kossalka and Gyula Wilder, and by Gyõzõ Mihailich and Iván Kotsis, with the main difference, that the arches were trusses in the first plan, while plated ones in the second. But the question, where to situate the bridge, was open. This caused delay in starting the construction and meantime some new ideas came into existence concerning the statical system of the new structure.
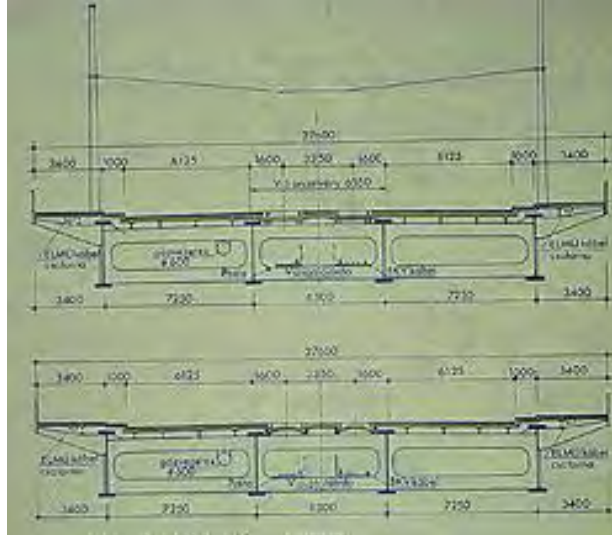
Figure 4.31 The original cross-section; continuous girder with four main girders.

Figure 4.32 The erection of Árpád bridge.

The erection of the Buda side of Árpád Bridge before the war, with four main girders as according to the original plans. The work stopped in 1942, and the structure survived the war in Budapest (Fig. 4.32.a). The erection of Árpád Bridge after the war, 1948-50. Only the two central main girders were erected (Fig. 4.32.b).

Finally taking into account, that an arch system would cause high horizontal forces to balance, which would increase the mass of foundations, it was decided, that a series of multi-span continuous plated structures would be realized. The final version of the bridge was planned by Károly Széchy, and the construction started in 1939, but after the building of the foundations it was interrupted by World War II.

The original plan of the bridge was partly realised for 1950. This structure was very narrow, its width was enough to carry the tramway tracks and two lanes of 2.22 m widths for the road

traffic. As the bridge is the northest one, crossing the Danube on the Hungarian territory, it has a very high infrastructural importance.

The technical data of the bridge
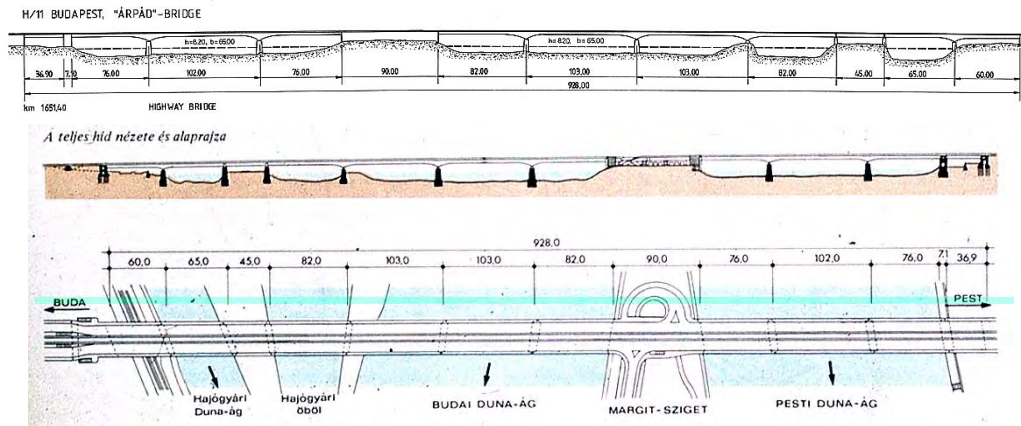
Figure 4.33 The side view of Árpád bridge.

Figure 4.34 The Pest side, the Buda side and the Hajógyári Island section of Árpád Bridge.

160

Structural system, span lengths, widths

The original part of the bridge is carrying the two tramway lines, for road traffic two new, box plated structures were built, carrying 3 lanes each.

The cross sectional layout of the new bridges is identical everywhere, only the height of the main girders and its profiles, as well as the shape of the transverse bracings is different.

The cross girders are plated ones, the distance is 4250 mm. Their height between the web of mains is 800 mm.

The height of the main plated girders varies between 3747 and 5460 mm, web thickness is 12-20 mm, and they are stiffened both horizontally and vertically.

Figure 4.35 The three independent main beams, with two main girders each, are similar.

Deck

The deck is an orthotropic steel plate, stiffened by horizontal stiffeners and the cross beams.
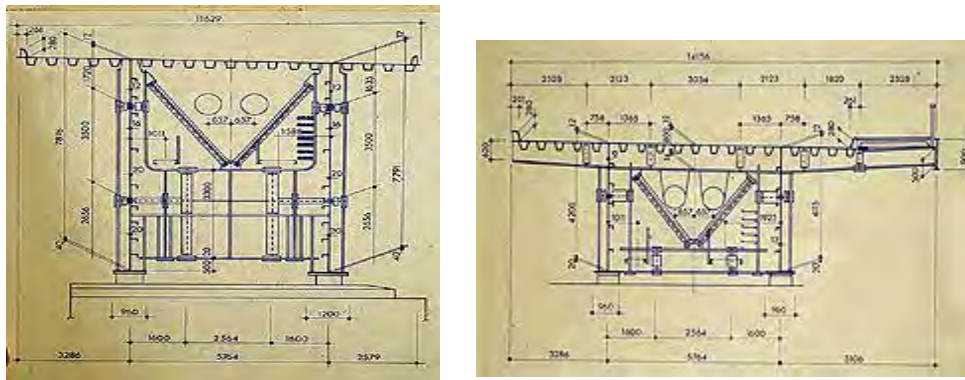
Figure 4.36 Cross section at the supports and at mid-span

Foundation, substructure

All the abutments and river piers of the old bridge were built for a total bridge width of 27.6 m. But for the new structural beams to be laid out, the pier had to be rebuilt at a height of about 1.5 m under the bearings. The middle part of the piers and abutments (under the remaining old structure) had been left unchanged

Quantities of applied materials

Weight of new steel construction: 8330 t (Grades used: A 38 B, 37 B-C, 52 C-D)

Method of construction/erection; joints

For the widening of the river bridge, a floating crane of 120 t load capacity was ordered to be built by the Bridge Construction Company in 1979. It was finished for February 1981 and was named after the constructor of the Chain Bridge, Adam Clark. The first elements of the bridge were lifted in May 1981.

Manufacturing and erection of the steel construction was carried out by Ganz-MÁVAG Steel Factory. As the bridge had to serve the traffic during widening, first the south extension structure was completed in full length, then the northern one. In the Ganz-MÁVAG yard at Lágymányos, a BK 300 type tower crane and a moving crane of 50 t capacity were built

The pre-assembled structural units were taken by ships to the building site. The construction was stated from steel pedestals, built beside the piers by incremental launching.
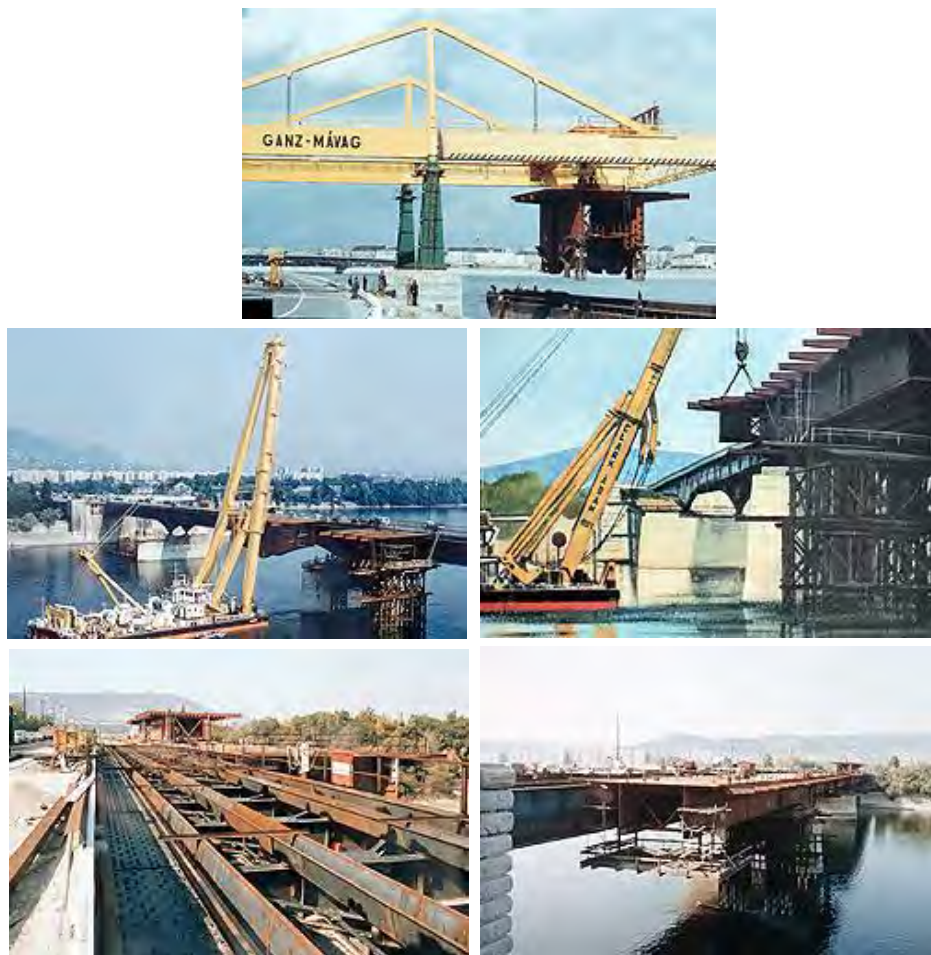
Figure 4.37 The erection of the bridge.

Corrosion protection

The orthotropic plate of the bridge is covered with a synthetic resin insulation of type VDW from Germany, which was performed in three layers after sand blasting and a degreasing by acetone. The third layer was faced with spread crushed stone to increase the adhesion between the insulation and asphalt topping.

Test loading(s); periodical assessment of serviceability

Certain parts of the complex construction were tested by different times and methods. In some cases only the characteristic deflections were measured, while other times more detailed measurements, containing measurement of strains (stresses), the vertical alignment, etc.,. were carried out.

4.2.3 'M0, Háros' motorway bridge

Location and name of the bridge

Figure 4.38 The Háros bridge.

Name of the bridge	**M0 circular motorway Danube-bridge at Háros**
Distance:	**1632+810 km**
Country:	Hungary
City/town:	Budapest
Route:	M0 circular motorway in section 15+010 km
Year of building - completion:	1987-1990

Span lengths:
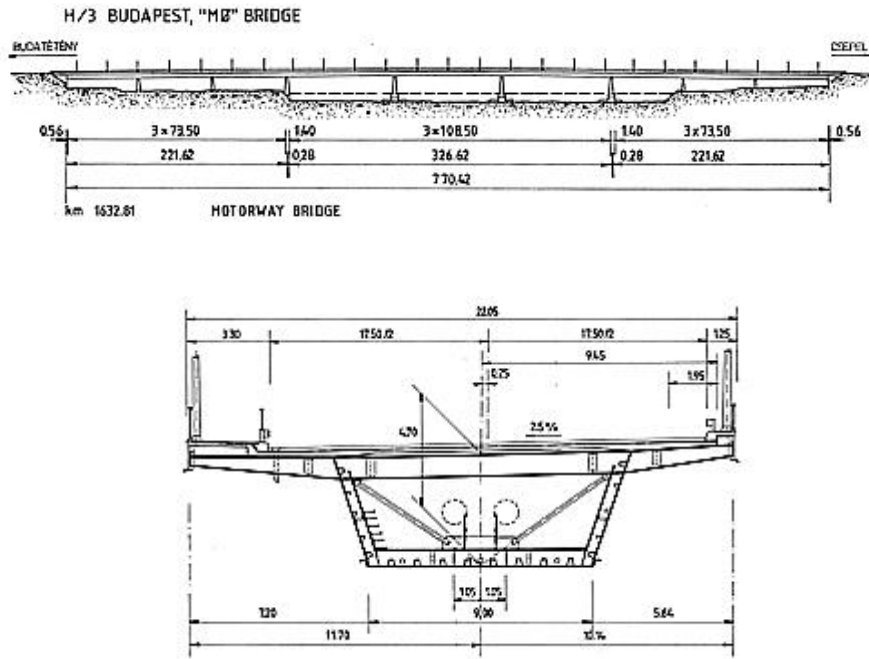
Figure 4.39 The general layout and the general cross-section of the Háros bridge.

River bridge:	3 × 108.50 m
Flood plain bridges:	3 × 73.50 m (two bridges)
Roadway widths:	4 × 17.50/4 m
Designer:	UVATERV (Engineering Consultants for Transport and Communication), Dr. Tibor Sigray (chief engineer)
Main contractor:	Bridge Construction Company
Construction cost:	883.954 million Ft
Owner of the bridge:	Motorway Directorate

Traffic function of the bridge

Highway:

roadway width:	17.50 m
number of lanes:	4

Antecedents; the history of the bridge

The idea to construct the M0 circular motorway to provide a connection between the M1 (to Vienna) and M5 (to Belgrade) motorways arised in the early seventies. The 28 km long southern sector of the belt to encircle Budapest crosses the two arms of the Danube outside of the capital. The invitation for the tenders was based upon detailed design and included two bridge system. The main Danube bridge at Háros was designed in the tender documentation, as a continuous prestressed, reinforced concrete bridge having 11 spans and constructed by the cast-in-place cantilever method. For this structure 6 alternative solutions (concrete and composite) were proposed and finally the composite construction of the tender by the Hidépitö Vállalat (Bridge Construction Company) has been found by the international jury, as the most economic one. The detailed design was carried out by UVATERV (Engineering Consultants for Transport and Communication).

The technical data of the bridge

Structural system, span lengths, widths (Fig. 4.39)

The superstructure of the bridge consists of three independent, continuous three-span bridges and its total length is 770.42 m. The main dimensions of the cross sections of the bridges are uniform. The bridges are composite ones consisting of a steel box girder of constant depth and a reinforced concrete deck slab.

The river bridge has the longest spans (3*108.50 m) of this kind in Hungary. The two flood plain bridges are identical, spanning 3*78.50 m each.

The complete width of the deck plate is 22.05 m. It supports a cycle path of total width of 3.30 m on the north side and a service walkway of 1.25 m width on the south one. The entire width for the four traffic lanes is 17.50 m.

The four traffic lanes have a constant cross fall of 2.5 % to the north direction, therefore the heights of the two webs are different, resulting an asymmetric cross section.

Quality of steel: grades 52C, 52D, 37C and A38B.

Figure 4.40 The general plan of the bridge.

Deck

Reinforced concrete deck, general thickness: 23 cm, at haunches: 29 cm, at cantilever edges: 20 cm. Prestressed by vertical movement of supports and above the intermediate supports of the

river bridge by post-tensioned tendons. Concrete quality: C25 (flood bridges) and C30 (river bridge), reinforcement quality: B 60.50.

Quality of the post-tensioned tendons over the intermediate supports of the river bridge: $1570/1770 \text{ N/mm}^2$.

Foundation, substructure

The foundation for the abutments, intermediate piers of the flood plain bridges and the common pier with the river bridge on the west side could be executed by drilling of large diameter piles started from the dry area. It was a routine job.

The foundation of the intermediate piers of the river bridge and the common pier on the east side could be executed by a basically new method. First a reinforced concrete casing element of 105 t weight and of dimensions 8 m * 18.70 m should be placed in the riverbed very accurately. In the second step 1.500 mm dia Soil-Mec piles were drilled from a catamaran. After positioning the steel upper casing element, under water concreting took place in a thickness of about 4.5 m. Pumping out the water, the reinforced concrete foundation and the rising walls were prepared in dry construction pit. Later the upper steel casing element was removed.

Figure 4.41 The piers of the bridge.

Bearings

Synthetic rubber bearing imported from East-Germany.

Fixed bearings of flood plain bridges: on the abutments, that of river bridge: intermediate pier on Buda side.

Quantities of applied materials

steel structure:	4340 t
HSFG bolts:	174.000 pieces
studs for composite connection:	80.000 pieces
reinforced concrete:	13.150 m³
reinforced concrete slab:	3950 m³
steel reinforcement:	1375 t
Soil-Mec piles:	1300 m (diameter 1200 mm) 900 m (diameter 1500 mm)

Method of construction/erection; joints

The steel box girder was divided longitudinally into construction units, not exceeding the weight of 100 t. The flood plain bridges were built up from 13 elements each, while the river bridge from 21 ones. These units were further divided by longitudinal connections during fabrication. The typical connection among the section elements in plant was welding, while in site mainly HSFG bolted connections were used, combining with welding for the elements of secondary importance.
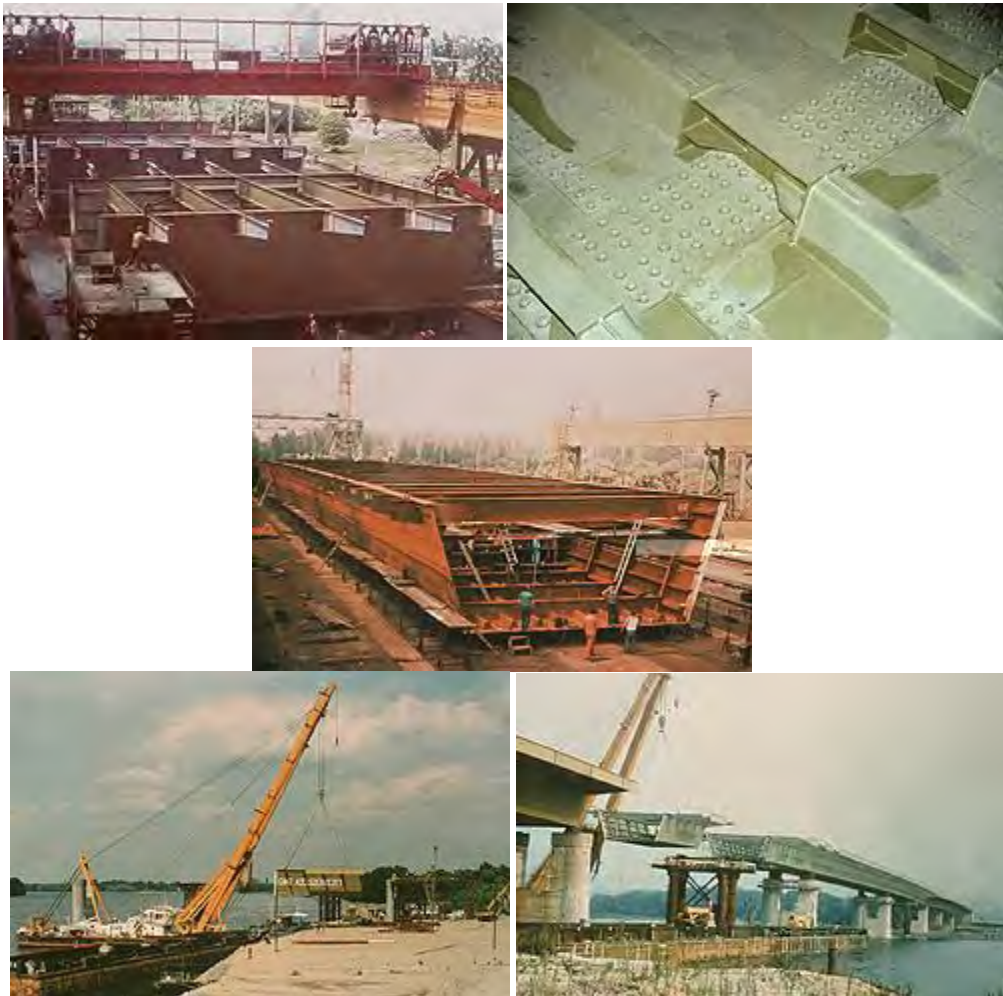
Figure 4.42 The erection of the bridge.

The construction schedules for the flood plain bridges and for the river bridge were similar, but different in details. The steel girders were erected in an overlifted position, using temporary support in the mid-spans (except for the middle span of the river bridge, which was open

permanently for navigation). Certain lengths of the deck plates were concreted in different phases to reduce the development of tension stresses in concrete slab under traffic conditions. Combination of removement of temporary supports, vertical movements of final supports and (only for river bridge) post-tensioning resulted an acceptable state in every part of the composite structure during erection and in the finished position

Traffic situation

The clearance of the navigable fairway is 100 m in each span of the river bridge. Possibility for 30 pieces of telecommunication cables and two water pipes of 1000 mm diameter has been taken into account during design.

Test loading(s); periodical assessment of serviceability

Figure 4.43 The piers of the bridge.

Time:	September 29-October 2, 1990.
applied methods:	static and dynamic loadings
vehicles, loads:	48 trucks filled with 18 t soil and weighted
nature of measurements:	deflections: 52 points on river bridge, 42 points on flood plain bridges stresses (strains): 80 points on river bridge, 60 points on flood plain bridges relative displacements at bearings natural frequency

4.2.4 'Lágymányosi' bridge

Location and name of the bridge

Name of the bridge	"Lágymányosi" bridge
Distance:	**1643+230 km**
Country:	Hungary
City/town:	Budapest
Year of building - completion:	1992 - 1995

Span lengths:
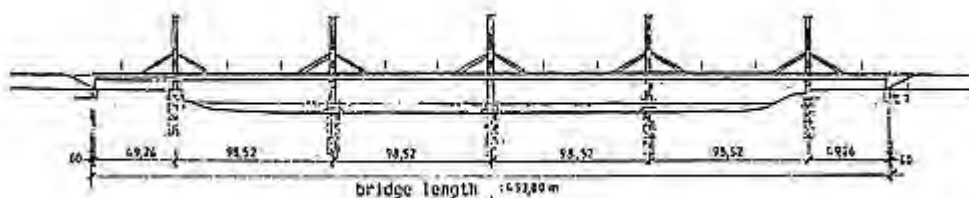
Figure 4.44 General view of the Lágymányos Bridge with the Southern Railway Bridge.

Main bridge over streambed:	49.26+4x98.52+49.26=493.80 m
Roadway widths:	2 × 8 m
Designer:	UVATERV, Dr. Tibor SIGRAI
Main contractor:	METRO Investment Co., Bridge Construction Co., Ganz Steel Construction Co.
Owner of the bridge:	City of Budapest

Traffic function of the bridge

Highway bridge with tramway:

number of lanes: 2 × 2 and a pair of tramway lanes

Antecedents; the history of the bridge

Construction of the bridge was decided as early as in 1972, when a tender was held. Its realisation is on agenda from the end of the eighties.

The axis of the bridge is in a distance of 27.98 m from the northern structure of the Southern railway bridge. This fact determined the spans of the bridge
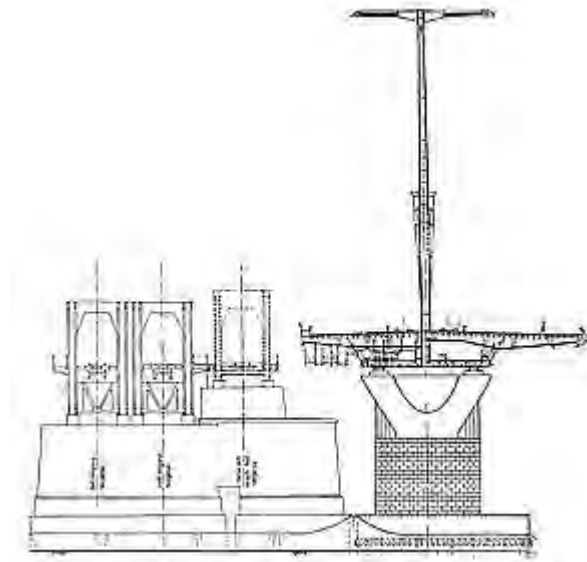
Figure 4.45 The general cross-section of the Southern Railway Bridge and the Lágymányos Bridges; the ensemble of the highway and railway bridges and aerial view of the bridge.

The technical data of the bridge

Structural system, span lengths, widths
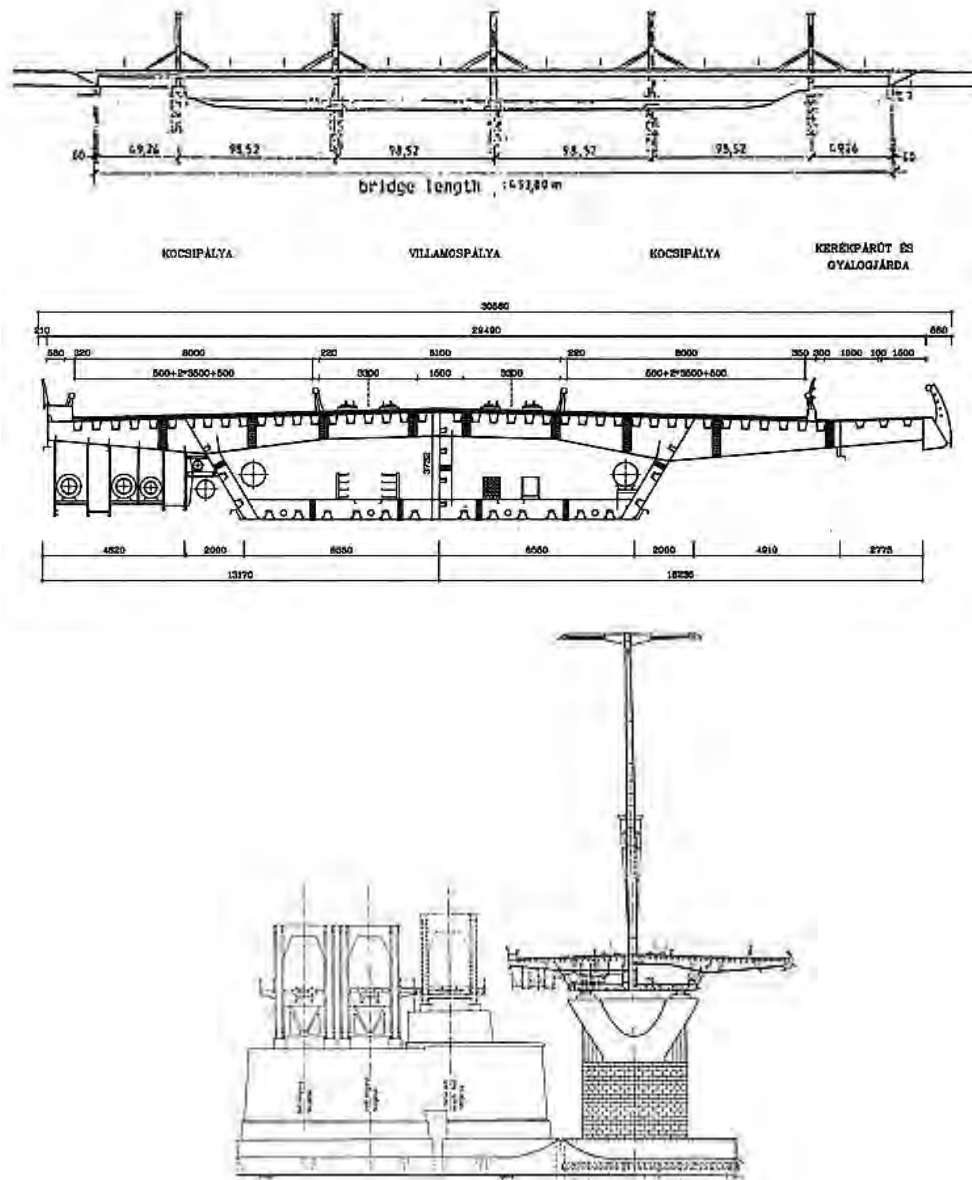
Figure 4.46 General plan and cross-section of the main girder.

The main girder is a six-span continuous asymmetric double cell box girder, having cantilevers on both sides to support the carriageways, walkway and bicycle track. Above the intermediate supports the main girder is suspended by inclined (appr. 30 °) rods, having a box section of 1.5 x 1 m. Pylons carrying the lightening have the cross section of 3 x 1 m. Their height is 35 m from the deck.

Figure 4.47 The erection of the columns

Total width of the bridge is 30.67 m.

Box width:	top: 17.1 m, bottom: 13.1 m. Webs are inclined.
Box heights:	large spans: 3.76 m, side spans: from 3.76 m decreases to 3.26 m parabolically.
Cantilever lengths:	north: 7.685 m south: 4.485 m.

Deck

Figure 4.48 Laying of the elements of box girders and Pre-assembly of the main box girder sections at the GANZ-MÁVAG plant

172

Structure, arrangement:	Orthotropic slab, trapeziodal stiffeners
Spacing of cross girders:	4.105 m

Foundation, substructure

Piers in the riverbed are situated on 48 pieces of Soil-Mec piles having a diameter 1.5 m and length of 24 m.

Abutments are r/c structures, being 31 m long, 11.78 m wide and 14.77 m high.

Figure 4.49 Lifting in of the upper casing element

Bearings

A pair of Maurer-type disk bearings is at each supported cross section, fixed ones are situated at the middle pier. Longitudinal sliding of the bridge is free in two directions.

Quantities of applied materials

Total amount of steel structure: 6500 t

Method of construction/erection; joints

Erection started on both banks from scaffolds, and was continued by free cantilever method using temporary supports. Erection units are of the length 10.21 - 14.32 m, unit weights are not exceeding the lifting capacity of floating crane "Adam Clark" (120 t) . The double cell cross section was divided into two asymmetrical parts.

Figure 4.50 The erection of the bridge.

Traffic situation

Situation of navigation: the clearance widths are the same as in case of the Southern railway bridge.

The public utilities (bicycle track and sidewalk; heating steam conduits, gas and water pipelines, electric and postal cables) are placed on Northern side.

The bridge has a unique illumination system based on special mirrors located at the tops of the pylons placed above the supports. These mirrors receive the light from reflectors located at the joints between the pylons and the inclined rods, and transmit it to the surface of the bridge, ensuring practically uniform distribution of light for the highway.

Figure 4.51 One of the lightening pylons with the mirrors and the erection of the lightening system.

Test loading(s); periodical assessment of serviceability

The construction was finished at the end of 1995, and the load tests has been carried out.
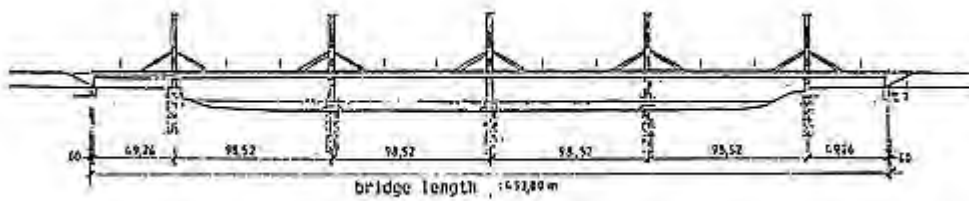
Figure 4.52 Load tests for the bridge.

4.2.5 'Szekszárd' bridge

Location and name of the bridge

Name of the bridge	Highway-bridge
Country:	Hungary
City/town:	Szekszárd
Year of building - completion:	2001 - 2003

A bridge close to Szekszárd was tendered 1988 and the construction started in 2001, will be completed early 2003.

Main data of the bridge

The bridge is situated along the M9 perspective motorway, between the main roads No.6 (parallel to the right riverside) and No.5 (parallel to the left riverside), crossing the Danube close to Szekszárd, the Tolna country-town. [Koller, 2001]

The spans are as follows: At the left side flood area 3×65.5 m, over the riverbed 80.0 m + 3×120.0 m + 80 m, and at the right side flood area 3×65.5 m, the full length is 916.0 m (Fig. 4.53). In the cross section the bicycle way, the carriageway and the sidewalk are 2.95 m + 10.0 m + 1.05 m = 14.0 m.

The realised superstructure is a continuous composite box girder (reinforced concrete deck slab and steel spines and bottom slab) over both flood areas, and over the riverbed a continuous steel box girder with an orthotropic plate deck. The structural depth is constant, approx. 4.0 m. The elevation of a bay is seen in Fig. 4.54, the steel cross section above the riverbed in Fig. 4.55 and the composite cross section above the flood area in Fig. 4.56. The piers have a deep foundation using bored piles and are made of concrete.

Span lengths:
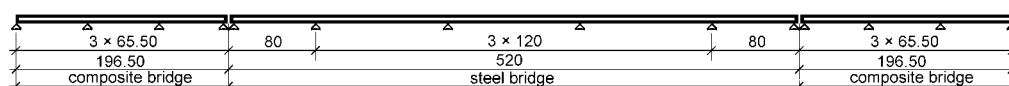
Figure 4.53 Span arrangement of the Danube bridge at Szekszárd.

Main bridge over streambed:	3×65.5 + 80 + 3x120 + 80 + 3×65.5 = 916.80 m
Roadway widths:	2.95 + 2×5.0 + 1.05 = 14.0 m
Designer:	steel bridge: Pont-TERV, Dr. Ernő KNÉBEL composite bridge: UVATERV, Zsolt KOVÁCS
Main contractor:	Magyar Hídépítő Konzorcium

Bridge length 919.60 m

continuous steel box girder with orthotropic
plate over the riverbed 520.00

120.00

6   7
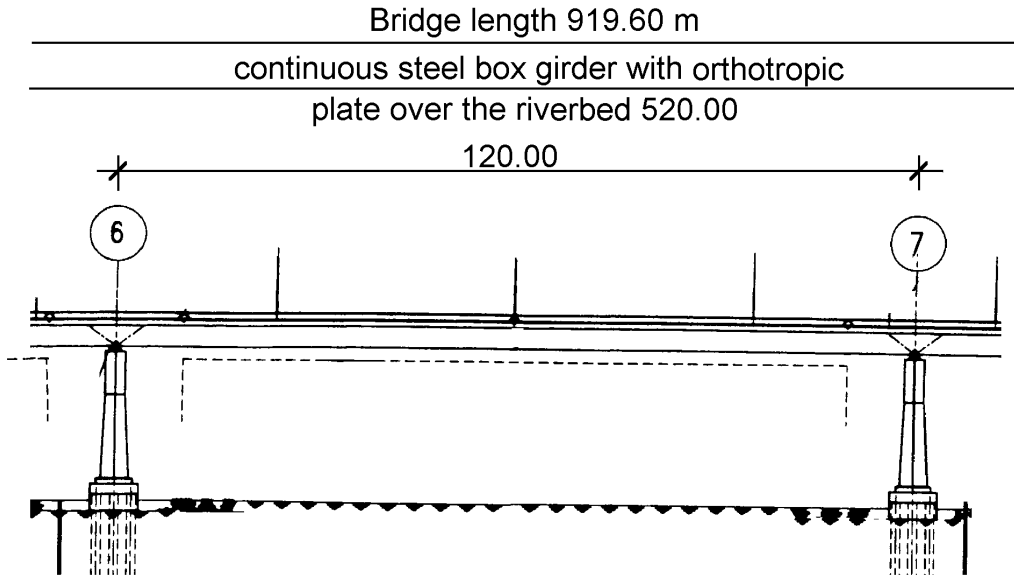
Figure 4.54 Elevation of a span of the steel bridge.

14.00

2.95   10.00

3.75   3.75

3.04   7.50   3.04

3.93   3.75

5.60
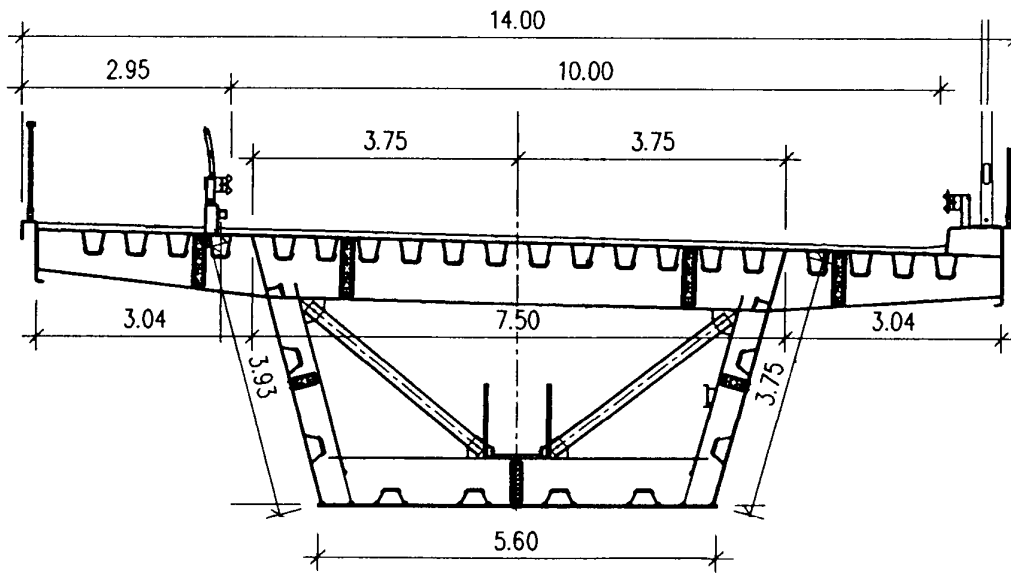
Figure 4.55 Steel cross section of the steel bridge over the riverbed.
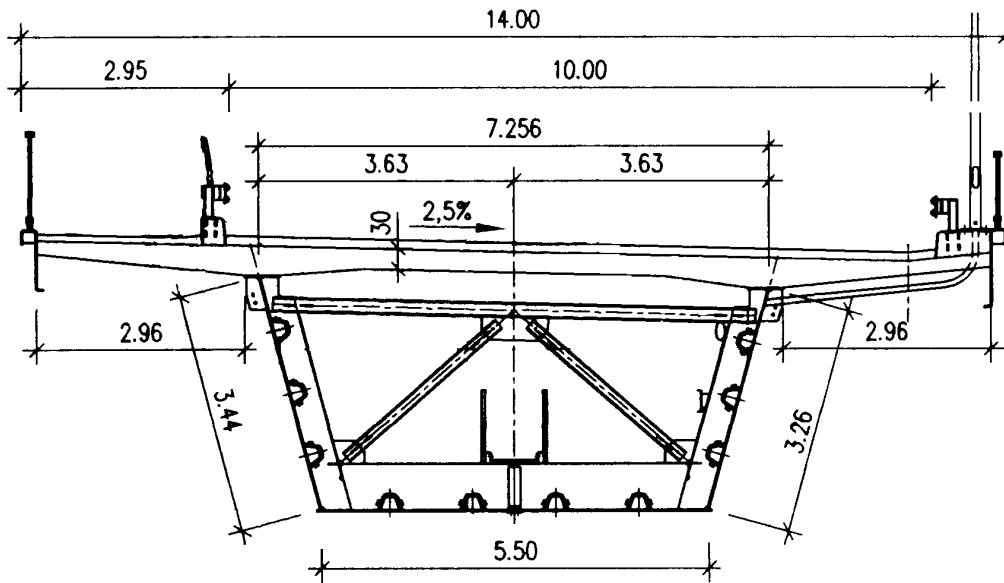
Figure 4.56 Composite cross section above the flood area.

Figure 4.57 The general view of the bridge.

Figure 4.58 The erection of the bridge before lifting the last element.

Figure 4.59 The connection of the orthotropic deck and webplate.

Figure 4.60 The lower flange plate and the cross bracing.

179

Figure 4.61 In-situ connection of steel bridge and lower flange plate of composite bridge.

Figure 4.62 Outer support of the concrete slab and the connection of the concrete slab and steel girder.

5　Refurbishment of Orthotropic Steel Bridges: Case studies from Germany

5.1 Traffic Data of the Examined Bridges

Lately, an increasing number of crack has been apparent in several steel highway bridges built between 1950 and 1970. Most affected are sway bracings, diaphragms, web stiffeners, components of orthotropic decks and crossing connections These problems are not confined to German bridges [Nather, 1991] [Iványi, 2002]. Earlier reports from the USA describe similar damage, and for some time fatigue damage detected in Japanese bridges has been reported too [Nather, 1991].

The main cause of the increasing number of damages is the development of traffic. Most bridges suffer more severe loading than was envisaged during their design due to increased traffic and higher axle loads. Other causes include inadequate fatigue design of structural details and fabrication defects. Another reason for fatigue cracks in steel bridges is inadmissible simplification of statical systems, mainly because the three-dimensional behaviour of bridges and secondary stresses are usually neglected in design practice.

Data of traffic flow and vehicle composition is necessary for bridge rehabilitation and investigation of damage. Earlier forecasts of lorry traffic on these motorways underestimated current traffic conditions. For instance, lorry traffic over the Haseltal bridge increased from 5700 lorries per day in 1978, to 9000 lorries per day in 1988. Over the period from 1980 to 1989, the number of applications for permission of special transports almost tripled [Nather, 1991].

Because of the predominant local traffic, the portion of vehicles with four and more axles did not exceed 55%. Further measurements indicated that the rate of capacity utilization was low and that the impact factor depends to a high degree on the velocity of vehicles. In assessing remaining fatigue life, development of future traffic must be considered. For instance with the European Community liberalization beginning in 1993, permissible axle loads and maximum weight of commercial vehicles will be increased.

5.2　Cracks in Connections of Cross Beams and Stiffeners.

Fatigue cracks have been detected:

- in fillet welds between the cross beam flange and the web or flange of the inside or outside main girder stiffener (Fig. 5.1, Detail No. 4)
- in the seam between web and flange of the cross beam (Fig. 5.1, Detail No. 2)
- in fillet welds between cap and connection plate of transverse stiffeners (Fig. 5.2, Type I, II, III) or sway bracings (Fig. 5.2, Type II, VI)
- in fillet welds connecting the connection plate to the main girder web (Fig. 5.2, Type III, IV)
- in the butt weld between connection plate and transverse stiffener (Fig. 5.2, Type V, VI), and
- in the connection between longitudinal and transverse web stiffeners.

Depending on the position of axle loads that may be located either between the main girders or on the cantilever, the haunches receive bending moments of changing signs. These moments are usually not considered during design of the connection. On curved bridges, the influence of local loads and forces due to the curvature are superimposed. On the Haseltal bridge (Fig. 5.1) the outside vertical stiffeners have been torn down in some spans. This led to a drop of the safety factor for lateral buckling of the bottom chord in compression. Fatigue assessment showed that fatigue cracking of the haunches could have been foreseen.

The Danube bridge near Sinzing (Fig. 5.2) has a superstructure for each lane. The main lane is located between the main girders, and every passage of a lorry results in bending stresses in the stiffeners. Field measurements and structural analyses revealed stresses larger than the yield stress even under service loading in welding outlets of nodes V and VI. Consequently, 17 of a total of 18 nodes of type VI and 47 of a total of 62 nodes of type V were cracked. The main reason for this damage was an inadequate statical system assumed during bridge design, i.e. the support points of the cross beams were assumed to be hinges.

On Fig. 5.2 node III, cracks are indicated in welded connections between vertical stiffener and cap plate. These cracks have been detected at an earlier date and repaired in 1977. Although 384 of a total of 424 welding showed cracks, no investigation of the causes of these cracks was conducted. Additionally, reinforcing plates have been mistakingly welded on top of the flanges of transverse stiffeners, and cap plates were also welded on flanges of cross beams. Thus, the cause of cracks was not eliminated, and new cracks similar to those presented in Fig. 5.2 developed. During repair work, 1990 diagonals had been fastened between transverse stiffeners and cross beams, as indicated on Fig. 5.3.

The influence of the deformation of the cross section on stresses in various structural details of the Danube bridge near Sinzing has been analyzed using the Advanced Theory of Bending, Torsion and Distorsion, which is a simple method of analysis but precise enough to study the three-dimensional behaviour of the bridge. Structural analysis indicated that the bending stresses in vertical web stiffeners reached values larger than those allowed (Figures 5.4 and 5.5).
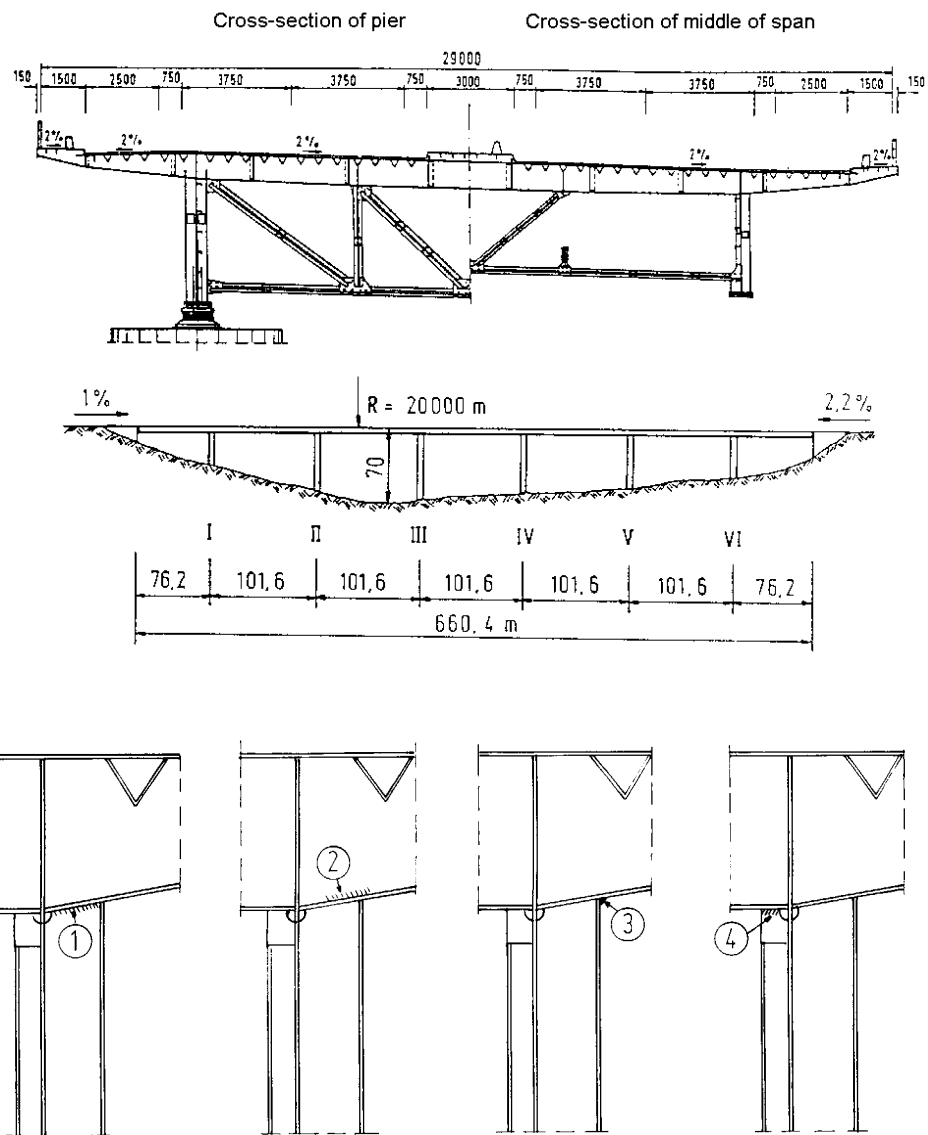
Figure 5.1 Haseltal bridge
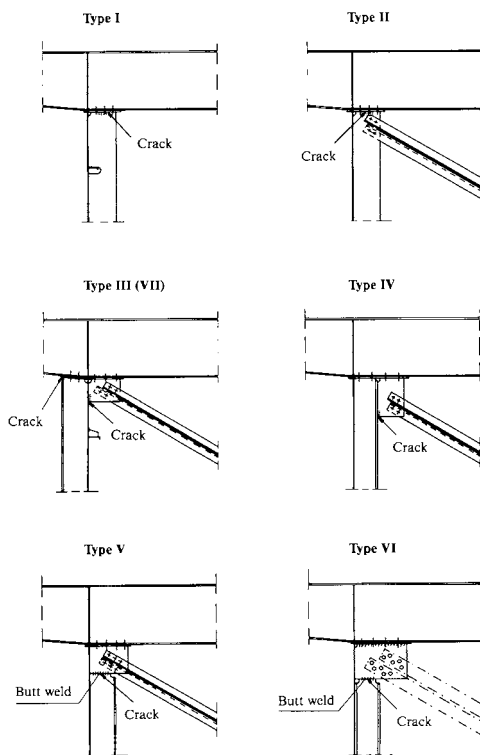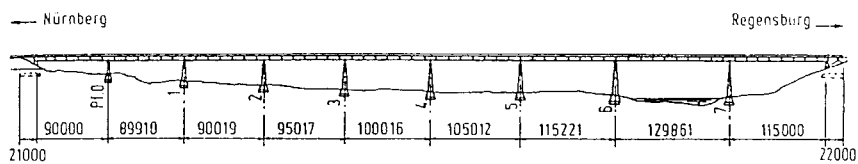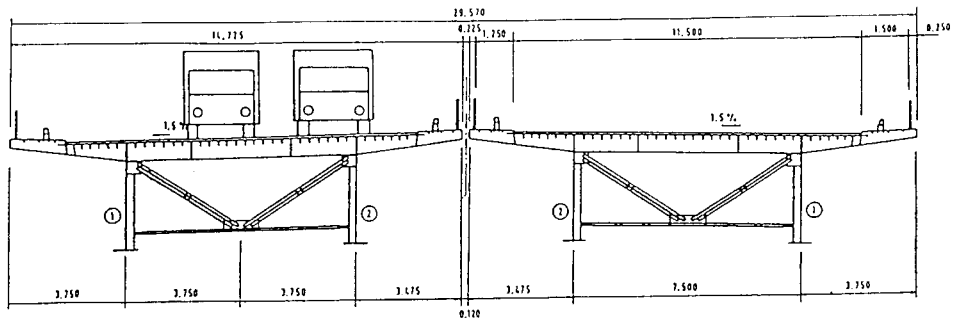
Figure 5.2 Danube bridge near Sinzing
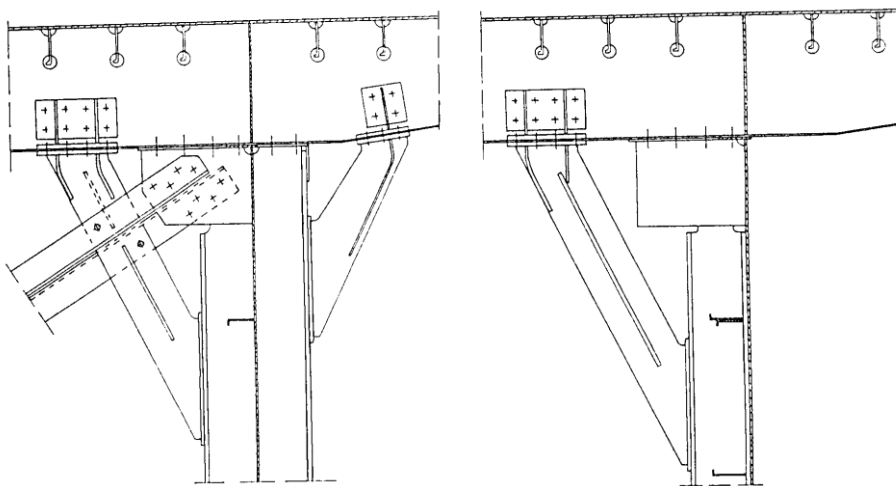
Figure 5.3 Danube bridge near Sinzing: Reconstruction of node type III (VII)
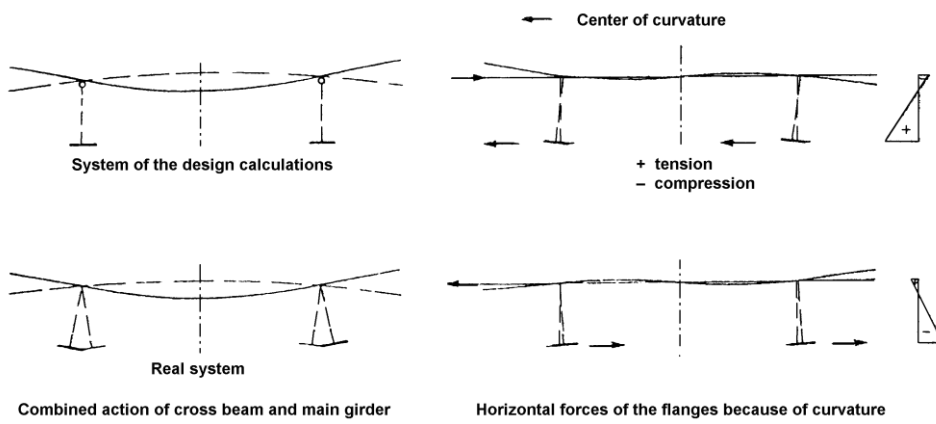
Figure 5.4 Haseltal bridge: Influences in the design calculation
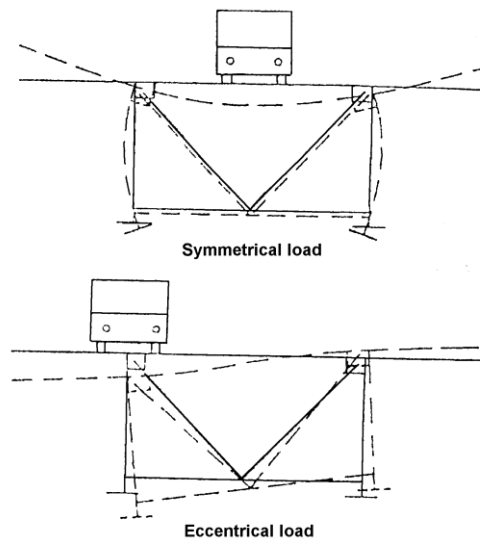
Figure 5.4 Danube bridge near Sinzing: Reconstruction of node type III (VII)

5.3 Cracks in Orthotropic Decks

Between 1960 and 1973, 25 steel bridges have been built in Germany with orthotropic deck and ribs of «Y»-(«wine glass») or «V»-shape. Ribs are cut into the floor beams, and their «V»-part is buttwelded with bevel groove welds to the floor beam webs. Outside Germany, only one bridge with «Y»-ribs and one with «V»-ribs has been built, i.e. the Bosporus Bridge (with continuous ribs) and the Komatsugawa Bridge (with backing strips).

The ideal case of a cross joint of the longitudinal V-stiffener, shown in Fig. 5.6, does not often occur. The axis of «V»-ribs tend to misalign, and an incomplete penetration may lead to fatigue cracks that are not visible from the outside. These fatigue cracks may even penetrate the cross beam web. For instance, the cracks in the rib-to-floor intersections of the Haseltal bridge could not be detected from the outside.

The ribs are directly stressed by the wheel loads. Structural analysis showed that a single passage of a vehicle causes several stress cycles of relatively high amplitude. For repair, short reinforcing plates have been welded first to the cap plate and then to both the deck plate and the «V»-rib by fillet welds (Fig. 5.7). Finally, the cap plates on both sides of the cross-beam web have been connected using high strength bolts. A fatigue assessment has been made for this connection to adapt the fatigue life of the ribs to the design life of other important structural members, i.e. 50 years. The detail category of 36 according to [ECCS, 1985] and a partial safety factor of 1.0 were chosen. From this, section modulus of the strengthened joint of 611 cm^3 has been determined, while for the original joint it was 290 cm^3.

186
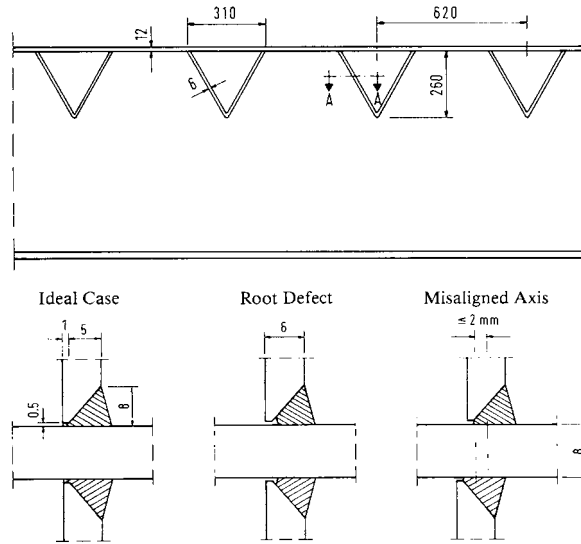
Figure 5.6 Cross joint of the longitudinal stiffener
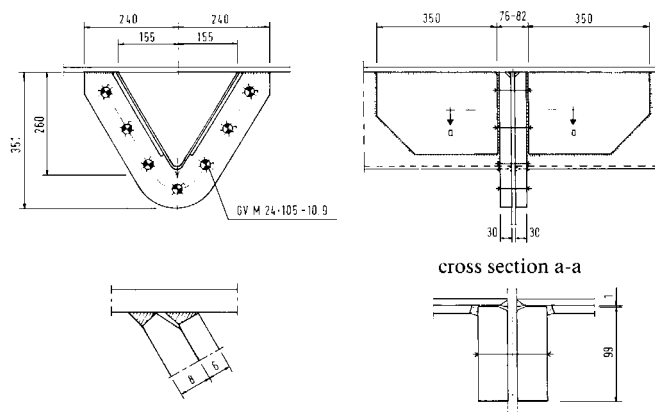
Figure 5.7 Haseltal bridge: Reconstruction of the connection of V-stiffener to cross beam

Three different designs of the intersection between «Y»-ribs and floor beams are known (Fig. 5.8). The tee-portions of structural type A are spliced by a formed piece which runs continuously through circular cutouts in the floor beams. This detail has been used in the Sinntal bridge. The tee-portions of design B and C run continuously through the cut-outs and are welded, either single-sided or on both sides, to the floor-beam web by fillet welds. Design B for example, was used for the Rhine bridge near Leverkusen. In the deck of this bridge, a multitude of cracks

developed from the lower end crater of the fillet weld, and some of them run through the inclined weld to the cover plate.
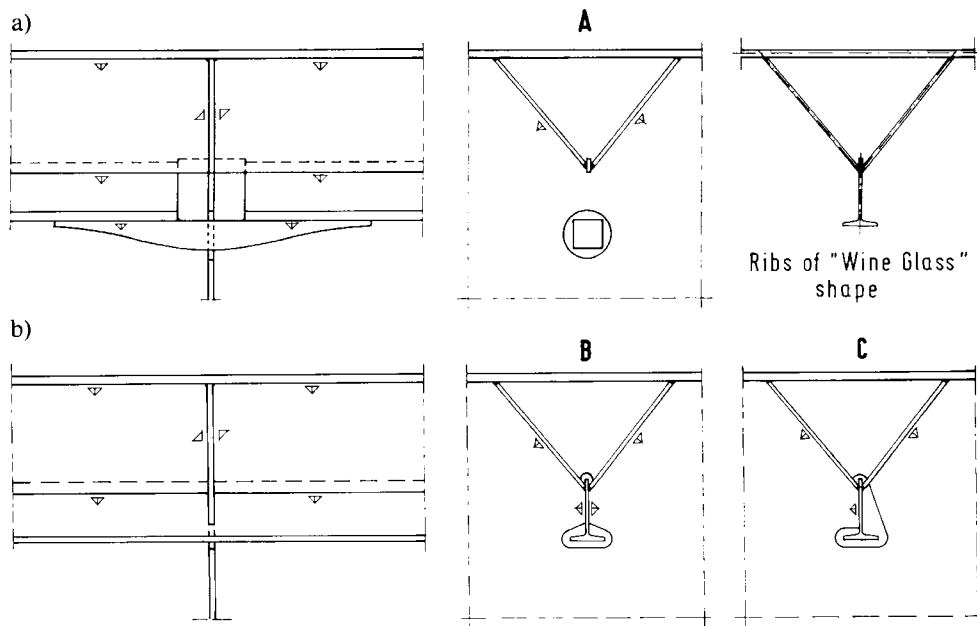
a) Splice profiles run through cutouts of the floor beam
b) T-portions run continuously through cutouts of the floor beam

Figure 5.8 Rib-to-floor-beam junctions

The numerous welds in the intersection of design A represent various possible locations for fatigue cracks. In a first phase of rehabilitation of the Sinntal bridge, cracks have been found in welds of the inclined plates of the «Y»-ribs. At some locations, the ribs were almost completely torn down. As a consequence, the grid effect of the deck was reduced which resulted in a propagation of damage similar to the opening of a zip-fastener. The accumulation of cracks in the last four spans near the southern abutment was explained by high dynamic stresses in the bridge deck caused by the traffic. It could be observed that trucks overtake one another even though no other vehicles were on the bridge.

In the second phase of rehabilitation, many new cracks have been detected which could not be attributed to fatigue. A considerable quantity of cracks may have developed as a result of the Sinntal bridge reached 115 °C on the side of the base.

The damage in the rib-to-floor intersection is typical for this type of structural detail. Cracks are not expected where the ribs with hollow sections run continuously through the cut-outs of the

floor beams. Insufficient fatigue strength of rib cuts welded to floor-beam webs, has already been described in 1961.

5.4 Strengthening of Main Girders under Traffic

Increasing traffic loads, the high probability of occasional overstressing and a high utilization of the material without considering fatigue, are the main causes that may require strengthening of bridges [Nather, 1991]. The possibilities of strengthening and broadening of bridges, even under traffic, is the main advantage of steel structures. Two methods of strengthening are described next:

1. To reinforce the Haseltal bridge, two lattice girders were mounted between the existing main girders as shown in Fig. 5.9. Transverse truss bracings have been built-in, every 9.24 m, to form a grillage with the main girders. At the centre, pier hinges were built in the lattice girders to avoid additional loading of the cross bracings at the support which could result in replacement of the existing support bracings. The support reactions of the additional lattice girders are taken over by additional support bracings, from where they are led off to the main girders and finally to the bearings.

2. Another suggestion, shown in Fig. 5.10, is to build an additional lattice girder in the centre line of the bridge together with a torsional bracing that is fixed above the bottom chords of the existing main girders. The floor-beam cantilevers are braced by diagonals to the stanchions of the torsional bracings. These stanchions and diagonals form, together with the cross beams and web stiffeners, transverse diaphragms to keep the cross sections elastic. All joints are bolted using high-strength bolts. To reduce the stress-resultant components, additional transverse bracings may be built-in. In case removal or strengthening of the existing support bracing is not possible, the new lattice girder may also be supported spatially by diagonal bracings that are directly supported by the bearings.

5.5 Final Remarks.

Experiences derived from the rehabilitation of highway steel bridges have been described. Fatigue cracks in orthotropic plates and in connections of cross beams and stiffeners have been detected, and repaired, on three steel road bridges. The main cause of the increasing number of damages, is the more severe loading of bridges due to increased traffic and higher axle loads. Other causes include inadequate fatigue design of structural details and fabrication defects. Repair and strengthening of steel bridges can be conducted relatively easily under traffic. Additionally, inadmissible simplification of statical systems is a further reason for damage on steel bridges.
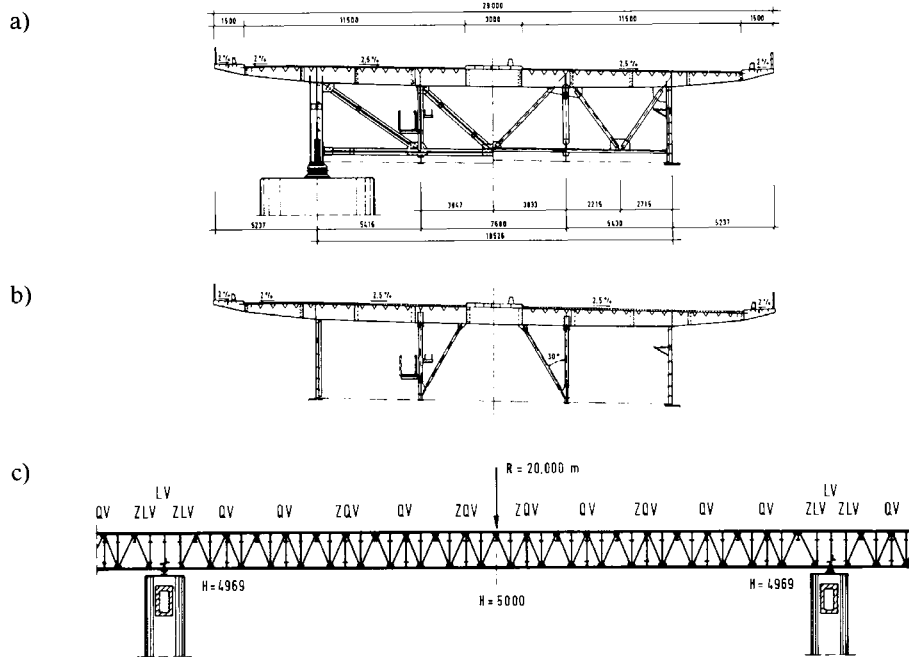
a) Transverse bracing above the support
b) Additional transverse bracing next to the support
c) Truss girder in the center span
(LV = Transverse bracing over the pier (old), QV = Transverse bracing (old, reconstructed),
ZQV = Additional transverse bracing (new), ZLV = Additional transverse bracing beside
the supports (new)

Figure 5.9 Strengthening of the Haseltal bridge

190
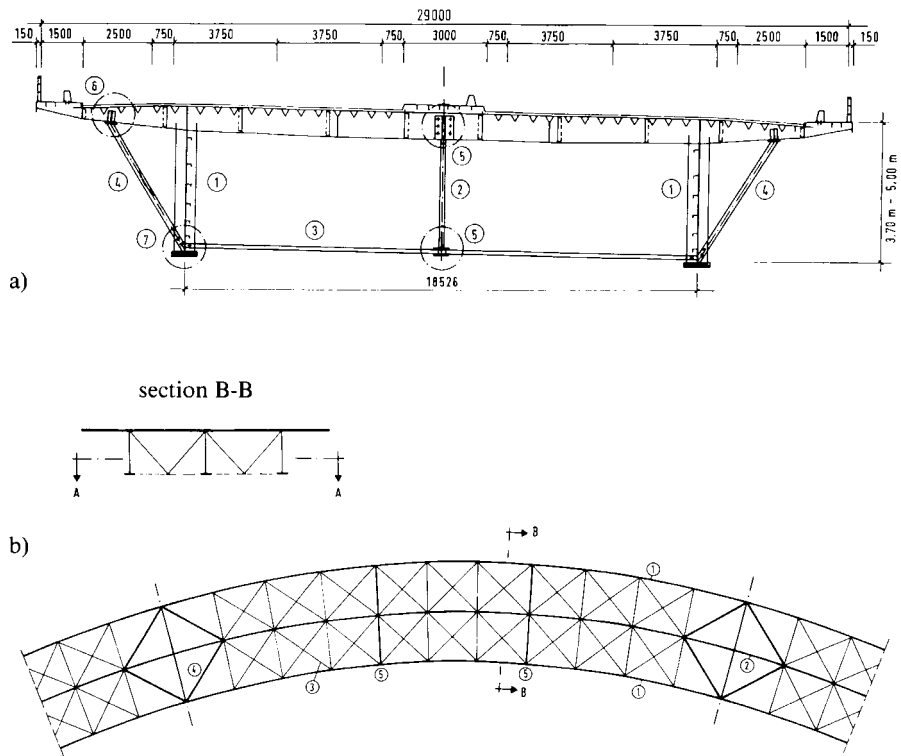
Strengthening of steel road bridges – suggestion:

a) Cross section   b) Horizontal projection

1: Plate girder
2: Truss girder (new)
3: Torsional web system (new)
4: Diagonal (new)

5: Bottom chord member (new)
6: Longitudinal girder (new, for load distribution)
7: Supporting of the truss girder (new)
8: Transverse bracing (alternative)

Figure 5.10 Strengthening of Main Girders under Traffic

191

6 Design of Steel Bridges with Structural Eurocodes

New design rules for steel bridges have been developed by CEN / TC 250 / SC 3. The result of the work in the EN-version of Eurocode 3 Part 2 (EC3-2).

For educational purpose some chapters are presented helping the knowledge of design of steel bridges. The rules concerning with design of planar plated structures without transverse loading, presented in Appendix II., and with design of planar plated structures with transverse loading, presented in Appendix III., belongs to this topic.

The summary is reviewed on the basis of Johansson et. al [1999] and Johansson et. al [2001].

The Figure 6.1 summarizes the general procedures calculating the interaction between shear force, bending moment, axial and transverse force.

The Figure 6.2 shows the flow chart of the procedure for the determination of effective cross-section properties of a longitudinally stiffened class 4 panel.

The Figure 6.3 shows the flow chart of the procedure for the determination of effective cross-section resistance in the shear buckling.

The Figure 6.4 shows the flow chart of the procedure for the determination of the cross-section resistance under patch loading.

The Figure 6.5 shows the interaction between effective widths due to shear lag effects and effective widths from plate buckling.

The presented examples are reviewed on the basis of Eisel-Müller-Sedlacek [1995] and Bancila [1996].

Example 1: Truss element (Danish-Swedish truss diagonal)
Example 2: Stiffened bottom plate of a bridge in compression (French bridge)
Example 3: Stiffened bottom plate and webs of a composite bridge

Actions

Deckplate with effective widths

Panel Subpanel

M_y, M_t, V_z, N, V_y, M_z

Longitudinal stresses	**Shear stresses with shear force including shear from torque**	**Transverse stresses with transverse forces**
Longitudinal normal stresses with gross cross-section	Shear stresses with gross cross-section	Stresses under the transverse forces
σ	τ	
Buckling of subpanel	**Buckling of plates in shear**	
ρ_{pan} reduction factor for each subpanel (Suppose: rigid supports and stiffeners)	χ_{V1} reduction factor (Suppose: rigid supports and stiffeners)	
Buckling of panel	**Shear buckling of panel**	
ρ_c reduction factor for panel buckling (Suppose: rigid supports for panels)	χ_{V2} reduction factor (Suppose: rigid supports for panels)	
Join ρ_{pan} and ρ_c	**Min $[\chi_{V1} ; \chi_{V2}] = \chi_V$**	**χ_f reduction factor**
e_n Shift in the position of neutral axis		
Verification	**Verification**	**Verification**
$\eta_1 = \dfrac{\sigma_{x.Ed}}{f_{yd}} = \dfrac{N_{Sd}}{f_{yd}A_{eff}} + \dfrac{M_{Sd} + N_{Sd}e_N}{f_{yd}W_{eff.y}} \leq 1$	$\eta_3 = \dfrac{\tau_{Ed}}{\chi_V\,f_{ywd}/\sqrt{3}} = \dfrac{V_{Sd}}{\chi_V\,bt\,f_{ywd}/\sqrt{3}} \leq 1$	$\eta_2 = \dfrac{\sigma_{z.Ed}}{f_{ywd}} = \dfrac{F_{Sd}}{f_{ywd}L_{eff}\,t} \leq 1$

$$\eta_1 + \left[1 - \frac{M_{tRd}}{M_{plRd}}\right][2\eta_3 - 1]^2 \leq 1$$

$$\eta_2 + 0,8\eta_1 \leq 1,4$$

Interaction between shear force, bending moment, axial and transverse force

Figure 6.1 Flow chart describing the general procedure for the design of plated structures according to EC3, Part 1.5.
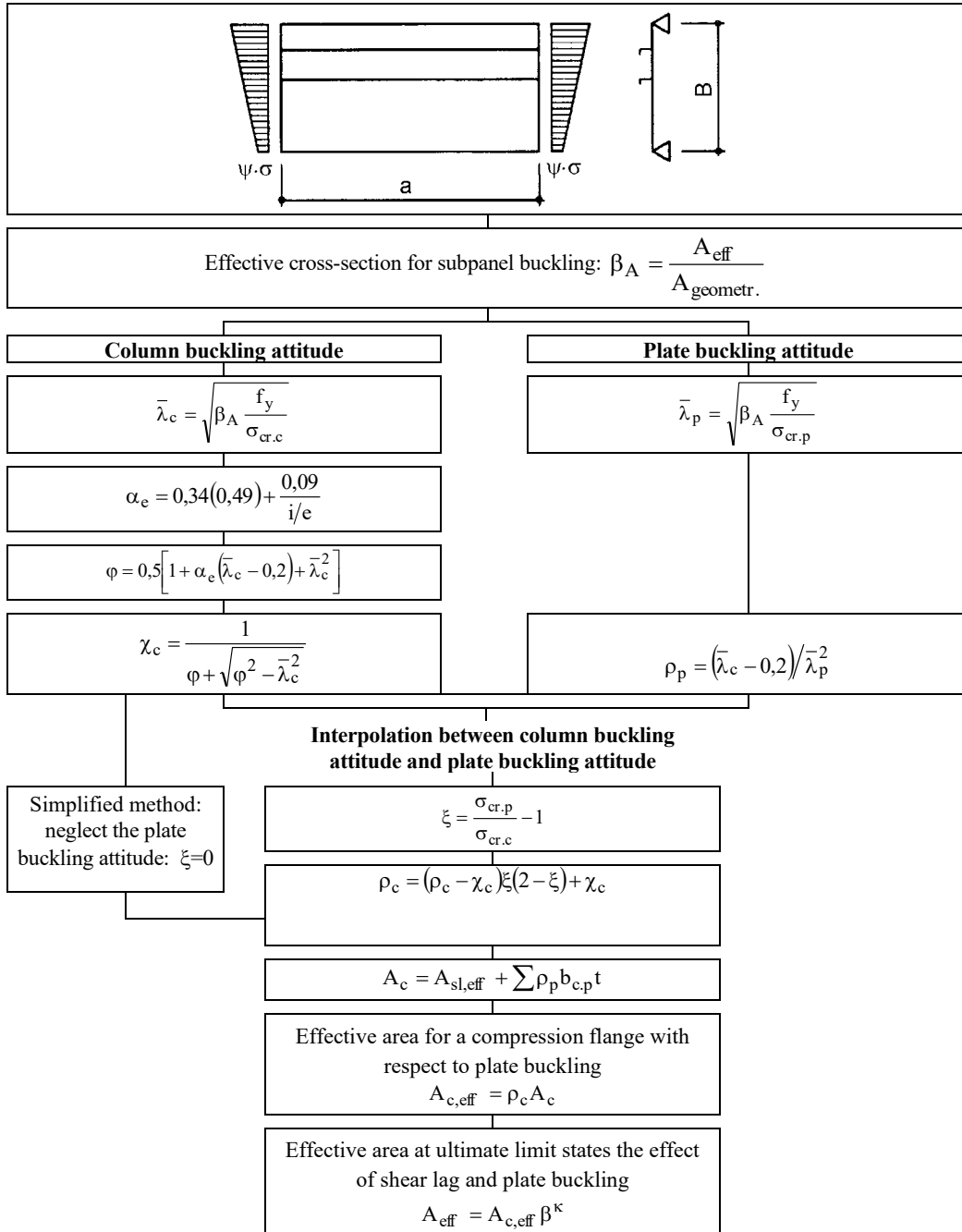
Figure 6.2 Flow chart describing the procedure for the determination of effective cross-section properties of a longitudinally stiffened class 4 panel.

Web plate | **Flange plate**

Web with transverse stiffeners at supports only | Web with transverse stiffeners at the supports and intermediate transverse and/or longitudinal stiffeners | Other cases

k_τ shear buckling coefficient:

$$k_\tau = 4{,}0 + 5{,}34\left(h_w/a\right)^2 + k_{\tau st} \quad \text{for} \quad a/h_w < 1$$

$$k_\tau = 5{,}34 + 4{,}0\left(h_w/a\right)^2 + k_{\tau st} \quad \text{for} \quad a/h_w > 1$$

$$k_{\tau st} = 9\left(\frac{h_w}{a}\right)^2 \left(\frac{I_{st}}{t_w^3 h_w}\right)^{\frac{3}{4}} \quad \text{and} \quad k_{\tau st} \geq \frac{2{,}1}{t}\left(\frac{I_{st}}{h_w}\right)^{\frac{1}{3}}$$

$$\overline{\lambda}_w = \frac{b_w}{86{,}4 \cdot t_w \varepsilon}$$

$$\overline{\lambda}_{w1} = \frac{b_w}{37{,}4 \cdot t_w \varepsilon \sqrt{k_\tau}}$$

$$\overline{\lambda}_{wl} = 0{,}76\sqrt{\frac{f_{yw}}{\tau_{cr}}}$$

$$\tau_{cr} = k_\tau \sigma_{cr}$$

Web with longitudinal stiffeners

$$\overline{\lambda}_{w2} = \frac{b_{w1}}{37{,}4 \cdot t_w \varepsilon \sqrt{k_{\tau l}}}$$

$$k_{\tau l} = k_\tau\left(b_w = b_{w1}; k_{\tau st} = 0\right)$$

$$\overline{\lambda}_w = \text{Min}\left[\overline{\lambda}_{w1}; \overline{\lambda}_{w2}\right]$$

Effective thickness factor χ_w for shear buckling

λ_w	Rigid end post	Non-rigid end post
$<0{,}83/\eta$	η	η
$0{,}83/\eta \leq \lambda_w < 1{,}08$	$0{,}83/\lambda_w$	$0{,}83/\lambda_w$
$>1{,}08$	$1{,}37/(0{,}7+\lambda_w)$	$0{,}83/\lambda_w$

$\eta = 1{,}20\ \gamma_{M1}/\gamma_{M0}$ for S235, S275 and S355
$\eta = 1{,}05\ \gamma_{M1}/\gamma_{M0}$ for S420 and S460

$$\chi_f = \frac{b_f t_f^2 f_{yf} \sqrt{3}}{c t_w b_w^2 f_{yw}}\left[1 - \left(\frac{M_{Sd}}{M_{f,Rd}}\right)^2\right]$$

$$c = \left[0{,}25 + \frac{1{,}6 b_f t_f^2 f_{yf}}{t_w b_w^2 f_{yw}}\right]a$$

$$\chi_v = \chi_w + \chi_f \leq \eta$$

$$V_{Rd} = \chi_v t_w b_w \frac{f_y}{\sqrt{3}\gamma_M}$$

Figure 6.3 Flow chart describing the procedure for the determination of effective cross-section resistance in the shear buckling.

Forces applied through one flange	Forces applied through both flange	Forces applied through one flange to an unstiffened end
$k_f = 6 + 2\left(\dfrac{h_w}{a}\right)^2$	$k_f = 3,5 + 2\left(\dfrac{h_w}{a}\right)^2$	$k_f = 2 + 6\left(\dfrac{s_s + c}{a}\right)^2$

$$F_{cr} = 0,9 k_f E \frac{t_w^3}{h_w}$$

Effective loaded length

$$m_1 = \frac{f_{yf} b_f}{f_{yw} t_w}$$

$$m_2 = 0,02\left(\frac{h_w}{t_f}\right)^2 \quad \text{for } \overline{\lambda}_F > 0,5$$

$$m_2 = 0 \quad \text{for } \overline{\lambda}_F \leq 0,5$$

$$l_y = s_s + 2t_f\left(1 + \sqrt{m_1 + m_2}\right)$$

$$l_y = s_s + 2t_f\left(1 + \sqrt{m_1 + m_2}\right)$$

$$l_y = \text{Min}\left[l_{y1}; l_{y2}; l_{y3}\right]$$

$$l_{ef} = \frac{k_f}{2}\frac{E}{f_{yw}}\frac{t_w^2}{h_w} \leq s_s + c$$

$$l_{y1} = l_{ef} + t_f\left(\sqrt{m_1 + m_2}\right)$$

$$l_{y2} = l_{ef} + t_f\left(\sqrt{\frac{m_1}{2} + \left(\frac{l_{ef}}{t_f}\right)^2 + m_2}\right)$$

$$l_{y3} = s_s + 2t_f\left(1 + \sqrt{m_1 + m_2}\right)$$

$$F_y = f_{yw} t_w l_y$$

$$\overline{\lambda}_f = \sqrt{\frac{F_y}{F_{cr}}}$$

$$\overline{\lambda}_f = \sqrt{\frac{F_y}{F_{cr}}}$$

$$\chi_f\left(\overline{\lambda}_f\right) = \frac{0,5}{\overline{\lambda}_f} \leq 1$$

$$l_{eff} = \chi_f l_y \qquad F_{Rd} = l_{eff} t_w \frac{f_{yw}}{\gamma_M}$$
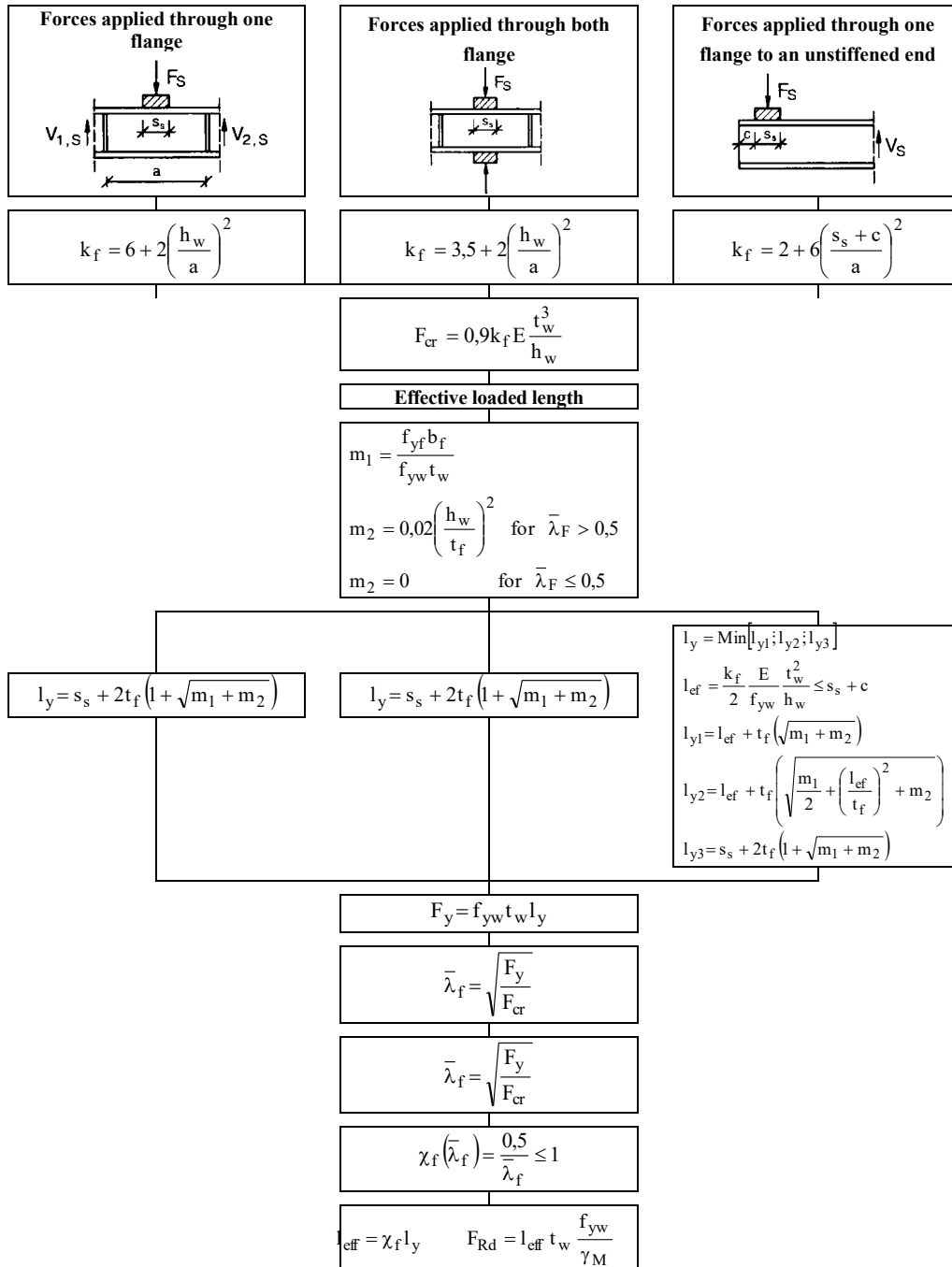
Figure 6.4 Flow chart describing the procedure for the determination of the cross-section resistance under patch loading.

Definitions of notations for shear lag	Effective length L_e for continuous beam and distribution of effective width

A_{sl}: Area of all longitudinal stiffeners

$$\alpha_0 = \sqrt{1 + \frac{A_{sl}}{b_0 t}} \qquad \kappa = \alpha_0 b_0 / L_e$$

Effective width factor β

$\kappa = \dfrac{\alpha_0 b_0}{L_e}$	Location for verification	β - Value
$\leq 0{,}02$		$\beta = 1{,}0$
$0{,}02 - 0{,}07$	Sagging bending	$\beta = \beta_1 - \dfrac{1}{1 + 6{,}4\kappa^2}$
	Hogging bending	$\beta = \beta_2 - \dfrac{1}{1 + 6{,}0\left(\kappa - \dfrac{1}{2500\kappa}\right) + 1{,}6\kappa^2}$
$> 0{,}70$	Sagging bending	$\beta = \beta_1 - \dfrac{1}{5{,}9\kappa}$
	Hogging bending	$\beta = \beta_2 - \dfrac{1}{8{,}6\kappa}$
all κ	End support	$\beta_0 = (0{,}55 + 0{,}025/\kappa)\beta_1$, but $\beta_0 < \beta_1$
all κ	Cantilever	$\beta = \beta_2$ at support, $\beta_0 = 1{,}0$ at the end

Effective width under serviceability limit state

$$b_{eff} = \beta b_0$$

Effective area under ultimate limit state

$$A_{eff} = A_{c,eff} \beta^\kappa$$

Figure 6.5 Interaction between effective widths due to shear lag effects and effective widths from plate buckling.

Example 1: Truss element (Danish-Swedish truss diagonal)

<u>Geometry</u>
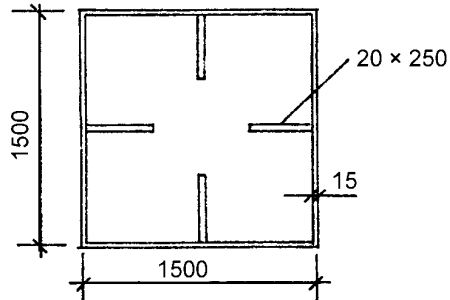
L = 15,0 m

<u>Material</u>: S 355

<u>Effective breadths</u> (5.3.6.2 (10), 5.3.5)

  plate subpanels

  b = 750 mm, t = 15 mm

$$\bar{\lambda}_p' = \frac{\bar{b}/t}{28,4 \cdot \varepsilon \cdot \sqrt{k_\sigma}} = \frac{750/15}{28,4 \cdot 0,81 \cdot \sqrt{4,0}} = 1,087$$

$$\rho' = \left(\bar{\lambda}_p' - 0,22\right)\Big/\bar{\lambda}_p'^2 = (1,087 - 0,22)/1,087^2 = 0,734$$

$$b_{eff}' = 0,734 \cdot 750 = 551 \text{ mm}$$

  stiffener subpanels

  b = 250 mm, t = 20 mm

$$\bar{\lambda}_p = \frac{\bar{b}/t}{28,4 \cdot \varepsilon \cdot \sqrt{k_\sigma}} = \frac{250/20}{28,4 \cdot 0,81 \cdot \sqrt{0,43}} = 0,829$$

$$\rho = \left(\bar{\lambda}_p' - 0,22\right)\Big/\bar{\lambda}_p'^2 = (0,829 - 0,22)/0,829^2 = 0,886$$

$$b_{eff} = 0,886 \cdot 250 = 221,5 \text{ mm}$$

[mm]
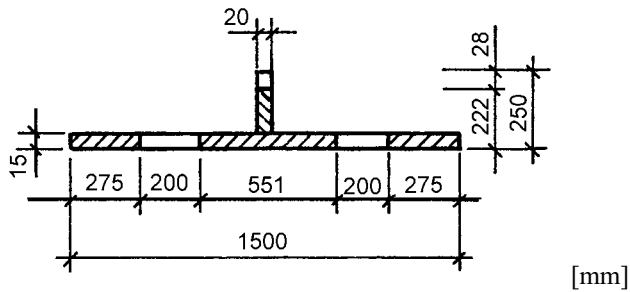
$$A_{eff} = 20 \cdot 222 + 1100 \cdot 15 = 209{,}4 \text{ cm}^2$$

Global plate buckling (5.3.6.3)

[mm]
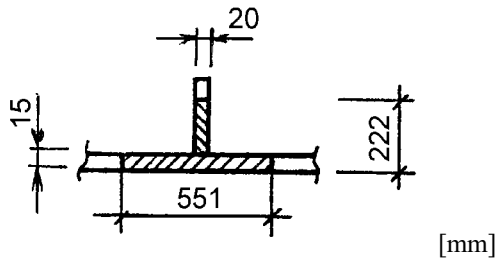
| $A_{st,eff} = 44{,}4$ cm^2 (5.3.6.3 (3))
⊥ $A_{eff} = 127{,}1$ cm^2
   $z = 3{,}88$ cm
   $I = 5398$ cm^4

Comment: (5.3.6.3 (4))
Open section stiffeners shall be proportioned so as to be fully effective.
In this case a reduction has to be done.
A reduction of the breadth is chosen.

$$\underline{\underline{N_{cr,c}}} = \frac{\pi^2 EI_{St}}{a^2} = \frac{\pi^2 \, 210000 \cdot 5398 \cdot 10^4}{15000^2} = \underline{\underline{497{,}2 \text{ kN}}}$$

$$\underline{\underline{N_{cr,p}}} = 1{,}05 \cdot E \cdot \frac{\sqrt{I_{St} \cdot t^3 b}}{b_1' \cdot b_2'} = 1{,}05 \cdot 210000 \cdot \frac{\sqrt{5398 \cdot 10^4 \cdot 15^3 \cdot 1500}}{750 \cdot 750} = \underline{\underline{6480{,}1 \text{ kN}}}$$

(5.3.6.3 (8)) and (5.3.6.3 (7))

Alternative calculation of $N_{cr,p}$ (Petersen):
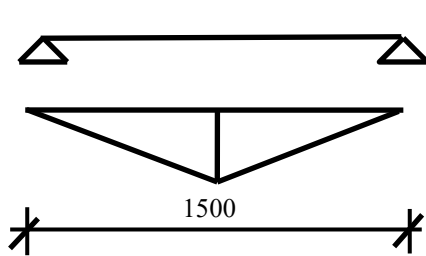
$$M = \frac{1500}{4} = 375$$

$$I = \frac{15^3}{0,91 \cdot 12} = 309,1$$

$$EI\delta = \frac{1}{3} \cdot 375^2 \cdot 1500$$

$$c = \frac{1}{\delta} = 0,923 \; \frac{1}{mm}$$

diagram Peterson (p. 468):

$$\sqrt{\frac{cl^4}{EI}} = \sqrt{\frac{0,923 \cdot 15000^4}{210000 \cdot 5398 \cdot 10^4}} = 642$$

System II $\Rightarrow \beta = 0,27$

$$\underline{\underline{N_{cr,c}}} = \frac{\pi^2 \, 210000 \cdot 5398 \cdot 10^4}{(0,27 \cdot 15000)^2} = \underline{\underline{6820,9 \; kN}}$$

The continued calculation will be done with $N_{cr,p} = 6480,1$ kN.

$$\xi = \frac{N_{cr,p}}{N_{cr,c}} - 1 = 12,03 \qquad (\rho_c \text{ will not be calculated}) \; (5.3.6.2 \; (9))$$

$$\Rightarrow \quad \xi = 1,0 \quad \Rightarrow \quad \rho = \rho_p$$

Calculation of $\overline{\lambda}_p$ with $A_{st,eff}$:

$$\overline{\lambda}_p = \sqrt{\frac{127,1 \cdot 10^2 \cdot 355}{6480,1 \cdot 10^3}} = 0,834$$

$$\rho_p = (0,834 - 0,22)/0,834^2 = 0,883 \quad (5.3.6.2 \; (7))$$

$$\rho = \rho_p = 0,883$$

$$A_c = \sum A_{st,eff} + \sum \rho_p' \cdot b_p' \cdot \rho_v \cdot t \qquad \rho_v = 1,0$$

$$A_c = 209,4 \; cm^2$$

$$A_{c,eff} = \rho \cdot A_c = 0,883 \cdot 209,4 = 184,9 \; cm^2$$

$$\underline{\underline{N_{Rd}}} = A_{c,eff} \cdot f_y / \gamma_M = 184,9 \cdot 10^2 \cdot 355/1,1 = \underline{\underline{5967,2 \; kN}}$$

(5.3.6.2 (11))

Buckling resistance (5.5)
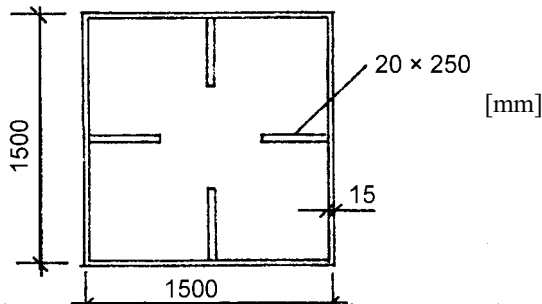
$A = 1100 \text{ cm}^2$

$I = 3770951 \text{ cm}^2$

[mm]

$i = 58{,}55 \text{ cm}$

a) Determination of A and I with the gross area (5.5.1.2 (1))

$$\lambda = \frac{s_k}{i} = \frac{15000}{585{,}5} = 25{,}6$$

$$\lambda_1 = \pi\sqrt{E/f_y} = 93{,}9 \cdot \varepsilon = 93{,}9 \cdot 0{,}81 = 76{,}1$$

$$\beta = \frac{A_{eff}}{A} = \frac{4 \cdot 184{,}9}{1100} = 0{,}672$$

$$\bar{\lambda} = \frac{\lambda}{\lambda_1}\sqrt{\beta_A} = \frac{25{,}6}{76{,}1}\sqrt{0{,}672} = 0{,}276 \qquad \text{(5.5.1.2 (2)) and (5.5.1.2 (1))}$$

$$\alpha = 0{,}34$$

$$\phi = 0{,}5 \cdot \left[1 + 0{,}34(0{,}276 - 0{,}2) + 0{,}276^2\right] = 0{,}551$$

$$\chi = \frac{1}{\phi + \sqrt{\phi^2 - \bar{\lambda}^2}} = \frac{1}{0{,}551 + \sqrt{0{,}551^2 - 0{,}276^2}} = 0{,}973$$

$$\underline{\underline{N_{b,Rd}}} = \chi \cdot \beta_A \cdot A \cdot f_y / \gamma_M = 0{,}973 \cdot 0{,}672 \cdot 1100 \cdot 10^2 \cdot 355/1{,}1 = \underline{\underline{23212 \text{ kN}}}$$

b) Determination of A and I by a cross section with equivalent thickness $t_{c,equi} = A_{c,eff}/b_c$

$$t_{c,equi} = \frac{184{,}9 \cdot 10^2}{1500} = 12{,}3 \text{ mm}$$

[mm]
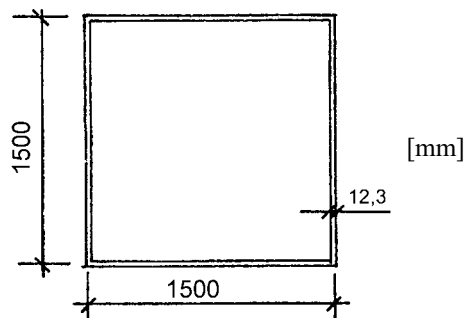
$A = 738 \text{ cm}^2$

$I = 2767547 \text{ cm}^2$

$i = 61{,}24 \text{ cm}$

201

$$\lambda = \frac{s_k}{i} = \frac{15000}{612,4} = 24,5$$

$$\lambda_1 = \pi\sqrt{E/f_y} = 93,9 \cdot \varepsilon = 93,9 \cdot 0,81 = 76,1$$

$$\beta = \frac{A_{eff}}{A} = \frac{4 \cdot 184,9}{1100} = 0,672$$

$$\bar{\lambda} = \frac{\lambda}{\lambda_1}\sqrt{\beta_A} = \frac{24,5}{76,1}\sqrt{0,672} = 0,264 \qquad (5.5.1.2\ (2))$$

$$\alpha = 0,34$$

$$\phi = 0,5 \cdot \left[1 + 0,34(0,264 - 0,2) + 0,264^2\right] = 0,546$$

$$\chi = \frac{1}{\phi + \sqrt{\phi^2 - \bar{\lambda}^2}} = \frac{1}{0,546 + \sqrt{0,546^2 - 0,264^2}} = 0,977$$

$$\underline{\underline{N_{b,Rd} = \chi \cdot \beta_A \cdot A \cdot f_y / \gamma_M = 0,977 \cdot 0,672 \cdot 1100 \cdot 10^2 \cdot 355/1,1 = \underline{\underline{23307\ kN}}}}$$

Example 2: Stiffened bottom plate of a bridge in compression (French bridge)

<u>Geometry</u>
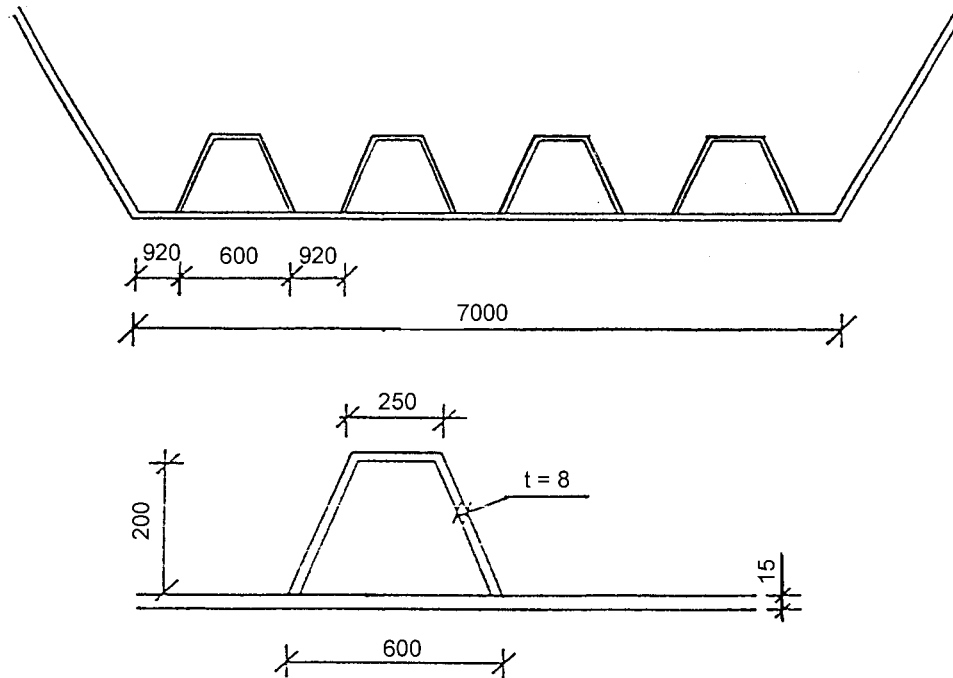
Distance between diaphragms: L = 4000 mm

Material: S 355

Global plate buckling (5.3.6.2 (1) and 5.3.6.2 (3))

$$A = 700 \cdot 15 + 4 \cdot (2 \cdot 271 + 250) \cdot 8 = 105000 + 25344 = 130344 \text{ mm}^2$$

$$z = 26,5 \text{ mm}$$

$$I_x = 46473 \text{ cm}^4$$

$$D_x = \frac{EI_x}{7000} = \frac{210000 \cdot 46473 \cdot 10^4}{7000} = 13941900 \text{ Nm}$$

$$D_y = \frac{Et^3}{12 \cdot \left(1 - \mu^2\right)} = \frac{210000 \cdot 15^3}{12 \cdot 0,91} = 64904 \text{ Nm}$$

$$\gamma = \sqrt{\frac{D_x}{D_y}} = \sqrt{\frac{13941900}{64904}} = 14,66$$

$$\alpha = \frac{a}{b} = \frac{4000}{7000} = 0,571$$

$$\psi = 1,0 \quad \Rightarrow \alpha_1 = \frac{\alpha}{\sqrt{\gamma}} = \frac{0,571}{\sqrt{14,66}} = 0,149 < 1$$

$$\Rightarrow K_{\sigma,p} = \left(\alpha + \frac{\gamma}{\alpha}\right)^2 = \left(0,571 + \frac{14,66}{0,571}\right)^2 = 688,8$$

$$\sigma_e = 189800 \cdot \left(\frac{t}{b}\right)^2 = 189800 \cdot \left(\frac{15}{7000}\right)^2 = 0,872$$

$$\underline{\underline{\sigma_{cr,p}}} = K_{\sigma,p} \cdot \sigma_e = 688,8 \cdot 0,872 = \underline{\underline{600,6 \text{ N}/\text{mm}^2}}$$

$$\underline{\underline{\sigma_{cr,c}}} = \frac{\pi^2 \cdot D_x}{a^2 \cdot t} = \frac{\pi^2 \cdot 13941900 \cdot 10^3}{4000^2 \cdot 15} = \underline{\underline{573,3 \text{ N}/\text{mm}^2}}$$

(5.3.6.2 (4) and 5.3.6.2 (5))

$$\overline{\lambda}_p = \sqrt{\frac{f_y}{\sigma_{cr,p}}} = \sqrt{\frac{355}{600,6}} = 0,769$$

$$\rho_p = \left(\overline{\lambda}_p - 0,22\right)\Big/ \overline{\lambda}_p^2 = \left(0,769 - 0,22\right)\Big/ 0,769^2 = 0,728$$

$$\overline{\lambda}_c = \sqrt{\frac{f_y}{\sigma_{cr,p}}} = \sqrt{\frac{355}{573,3}} = 0,787 \qquad\qquad (5.3.6.2 \ (7) \ \text{and} \ 5.3.6.2 \ (8))$$

$$i = \sqrt{\frac{b \cdot D_x}{A \cdot E}} = \sqrt{\frac{7000 \cdot 13941900}{130344 \cdot 210000}} = 59,71 \ \text{mm}$$
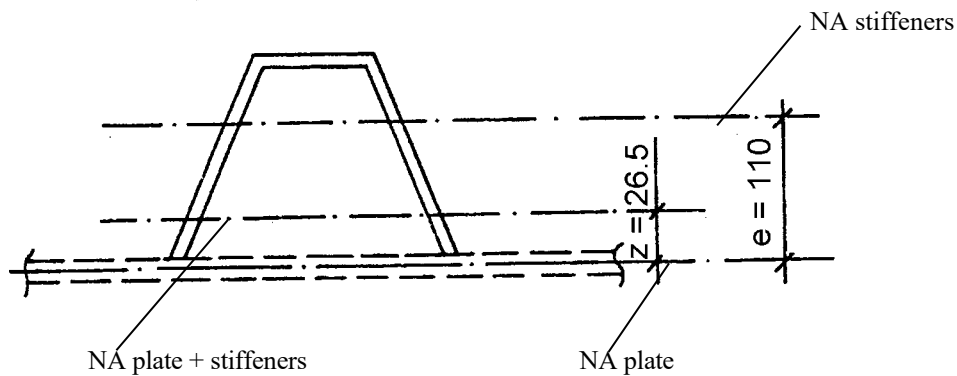
NA – neutral axis
Calculation with gross area!

$$\alpha^* = 0,34 + \frac{0,09}{i/e} = 0,34 + \frac{0,09}{59,71/110} = 0,506$$

$$\phi_c = 0,5 \cdot \left[1 + \alpha^*\left(\overline{\lambda}_c - 0,2\right) + \overline{\lambda}_c^2\right] = 0,5 \cdot \left[1 + 0,506\left(0,787 - 0,2\right) + 0,787^2\right] = 0,958$$

$$\rho_c = \frac{1}{\phi_c + \sqrt{\phi_c^2 - \overline{\lambda}_c^2}} = \frac{1}{0,958 + \sqrt{0,958^2 - 0,787^2}} = 0,665 \qquad\qquad (5.3.6.2 \ (10))$$

$$\xi = \frac{\sigma_{cr,p}}{\sigma_{cr,c}} - 1 = \frac{600,6}{573,3} - 1 = 0,048$$

$$\underline{\underline{\rho}} = \left(\rho_p - \rho_c\right)\xi\left(2 - \xi\right) + \rho_c = \left(0,728 - 0,665\right) \cdot 0,048 \cdot \left(2 - 0,048\right) + 0,665 = \underline{\underline{0,670}}$$

Local plate buckling (5.3.6.2 (10) and 5.3.5)

plate subpanels

$$\underline{b' = 920 \ \text{mm}, \ t = 15 \ \text{mm}}$$

$$\sigma'_e = 189800 \cdot \left(\frac{15}{920}\right)^2 = 50{,}45 \text{ N}/\text{mm}^2$$

$$\sigma'_{cr,p} = K'_{\sigma,p} \cdot \sigma'_e = 4{,}0 \cdot 50{,}45 = 201{,}8 \text{ N}/\text{mm}^2$$

$$\bar{\lambda}'_p = \sqrt{\frac{f_y}{\sigma_{cr,p}}} = \sqrt{\frac{355}{201{,}8}} = 1{,}326$$

$$\rho'_p = \left(1{,}326 - 0{,}22\right)/1{,}326^2 = 0{,}629$$

<u>b' = 600 mm, t = 15 mm</u>

$$\sigma'_e = 189800 \cdot \left(\frac{15}{600}\right)^2 = 118{,}6 \text{ N}/\text{mm}^2$$

$$\sigma'_{cr,p} = K'_{\sigma,p} \cdot \sigma'_e = 4{,}0 \cdot 118{,}6 = 474{,}5 \text{ N}/\text{mm}^2$$

$$\bar{\lambda}'_p = \sqrt{\frac{f_y}{\sigma_{cr,p}}} = \sqrt{\frac{355}{474{,}5}} = 0{,}865$$

$$\rho'_p = \left(0{,}865 - 0{,}22\right)/0{,}865^2 = 0{,}862$$

<u>stiffeners subpanels</u>

<u>b' = 250 mm, t = 8 mm</u>

$$\sigma'_e = 189800 \cdot \left(\frac{8}{250}\right)^2 = 194{,}4 \text{ N}/\text{mm}^2$$

$$\sigma'_{cr,p} = K'_{\sigma,p} \cdot \sigma'_e = 4{,}0 \cdot 194{,}4 = 777{,}6 \text{ N}/\text{mm}^2$$

$$\bar{\lambda}'_p = \sqrt{\frac{f_y}{\sigma_{cr,p}}} = \sqrt{\frac{355}{777{,}6}} = 0{,}676$$

$$\rho'_p = \left(0{,}676 - 0{,}22\right)/0{,}676^2 = 0{,}998$$

<u>b' = 271 mm, t = 8 mm</u>

$$\sigma_e^{'} = 189800 \cdot \left(\frac{8}{271}\right)^2 = 165,4 \, \text{N}/\text{mm}^2$$

$$\sigma_{cr,p}^{'} = K_{\sigma,p}^{'} \cdot \sigma_e^{'} = 4,0 \cdot 165,4 = 661,6 \, \text{N}/\text{mm}^2$$

$$\bar{\lambda}_p^{'} = \sqrt{\frac{f_y}{\sigma_{cr,p}}} = \sqrt{\frac{355}{661,6}} = 0,733$$

$$\rho_p^{'} = (0,733 - 0,22)/0,733^2 = 0,955$$

$$A_c = \sum A_{st,eff} + \sum \rho_p^{'} \cdot b_p^{'} \cdot \rho_v \cdot t \qquad (\rho_v = 1,0)$$
$$A_c = 4 \cdot 8 \cdot (0,998 \cdot 250 + 0,955 \cdot 2 \cdot 271) + 5 \cdot 0,629 \cdot 920 \cdot 15 + 4 \cdot 0,862 \cdot 600 \cdot 15$$
$$A_c = 989,8 \, \text{cm}^2 \qquad\qquad\qquad\qquad\qquad\qquad\qquad (5.3.6.2 \ (11))$$

$$\underline{\underline{A_{c,eff}}} = \rho \cdot A_c = 0,670 \cdot 989,9 = 663,2 \, \text{cm}^2$$

$$\underline{\underline{N_{Rd}}} = A_{c,eff} \cdot f_y/\gamma_M = 66320 \cdot 355/1,1 = \underline{\underline{21402 \, \text{kN}}}$$

<u>Consideration of shear lag effects</u>

<u>Geometry</u>
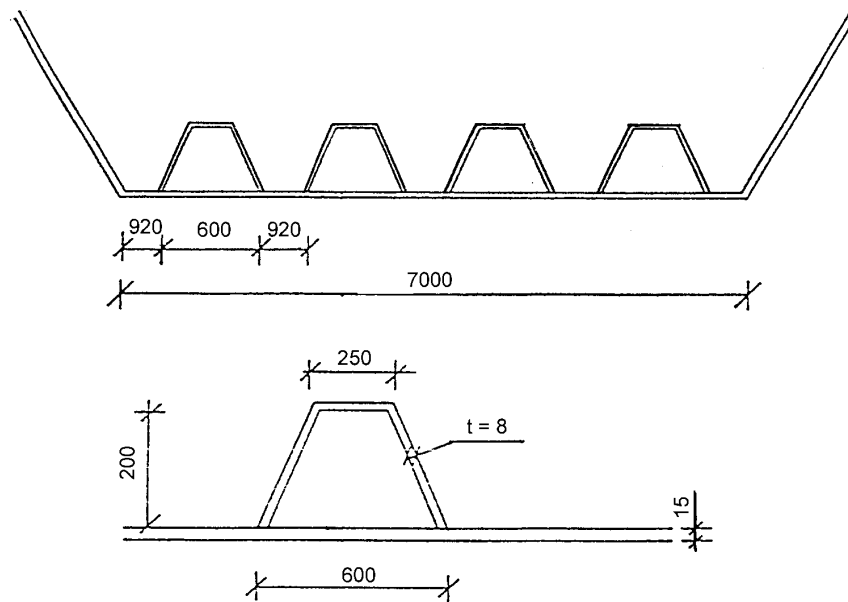
Distance between diaphragms: L = 4000 mm
<u>Material</u>: S 355
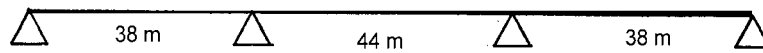
$$L_e = 0,2 \cdot 5 \cdot (38,2 + 44,0) = 20,5 \, m$$

$$\alpha_0 = \sqrt{1 + \frac{\Delta A}{b \cdot t}} = \sqrt{1 + \frac{25344/2}{3500 \cdot 15}} = 1,114$$

$$\beta_2 = \frac{1}{1 + 6,0 \cdot \dfrac{\alpha_0 \cdot b}{L_e} + 1,6 \cdot \left(\dfrac{\alpha_0 \cdot b}{L_e}\right)^2} = \frac{1}{1 + 6,0 \cdot \dfrac{1,114 \cdot 3500}{20500} + 1,6 \cdot \left(\dfrac{1,114 \cdot 3500}{20500}\right)^2} = 0,455$$

$$\rho_{comb} = \rho \cdot \beta^{\frac{\alpha_0 \cdot b}{L_e}} = 0,670 \cdot 0,455^{\frac{1,114 \cdot 3500}{20500}} = 0,670 \cdot 0,681 = 0,577$$

$$A_{c,eff} = \rho_{comb} \cdot A_c = 0,577 \cdot 989,8 = 571,1 \, cm^2$$

$$\underline{\underline{N_{Rd}}} = A_{c,eff} \cdot f_y / \gamma_M = 57110 \cdot 355/1,1 = \underline{\underline{18431 \, kN}}$$

(5.4.2.3.3 (4) and 5.4.2.4 (1))

Example 3: Stiffened bottom plate and webs of a composite bridge

Material: S 355

Distance between diaphragms: L = 4000 mm

$$A_{gross} = 3219,08 \, cm^2$$
$$z = 95,50 \, cm$$
$$I_{gross} = 28\,627\,744 \, cm^4$$

Geometry

[mm]
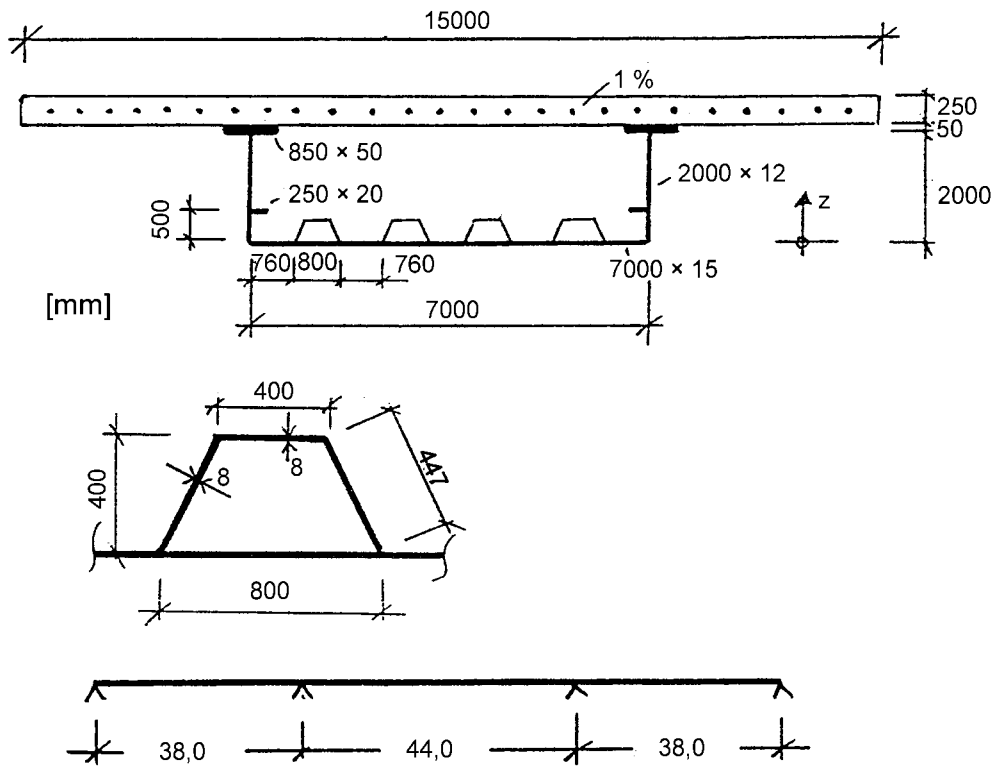
Classification (and local plate buckling) (5.3.5)
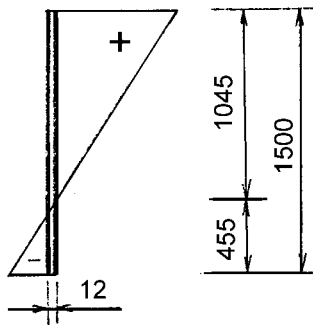
$$\psi = -2{,}297$$

$$\frac{d}{t_w} = \frac{1500}{12} = 125 < 62 \cdot \varepsilon \cdot (1 - \psi) \cdot \sqrt{(-\psi)} =$$

$$= 62 \cdot 0{,}81 \cdot (1 + 2{,}297) \cdot \sqrt{2{,}297} = 250{,}9$$

$\Rightarrow$ Class 3 (or lower class)

$$\frac{c}{t} = \frac{250}{20} = 12,5 > 14 \cdot \varepsilon = 14 \cdot 0,81 = 11,3$$

$\Rightarrow$ Class 4
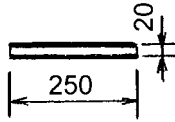
$$\psi = 1,0 \quad \Rightarrow \quad K_\sigma = 0,43$$

$$\overline{\lambda}_p = \frac{250/20}{28,4 \cdot 0,81 \cdot \sqrt{0,43}} = 0,829$$

$$\rho = \left(0,829 - 0,22\right)\big/ 0,829^2 = 0,886$$

$$\psi = 0,476 \quad \Rightarrow \quad K_\sigma = \frac{8,2}{1,05 + 0,476} = 5,37$$

$$\frac{d}{t_w} = \frac{500}{12} = 41,7 > \frac{42 \cdot \varepsilon}{0,67 + 0,33 \cdot \psi} = \frac{42 \cdot 0,81}{0,67 + 0,33 \cdot 0,476} = 41,1$$

$\Rightarrow$ Class 4
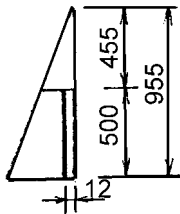
$$\overline{\lambda}_p = \frac{500/12}{28,4 \cdot 0,81 \cdot \sqrt{5,37}} = 0,782$$

$$\rho = \left(0,782 - 0,22\right)\big/ 0,782^2 = 0,919$$

$$\frac{b}{t} = \frac{760}{15} = 50,7 > 42 \cdot \varepsilon = 42 \cdot 0,81 = 34,0$$

$\Rightarrow$ Class 4
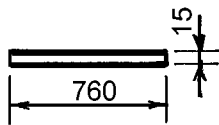
$$\psi = 1,0 \quad \Rightarrow \quad K_\sigma = 0,43$$

$$\overline{\lambda}_p = \frac{760/15}{28,4 \cdot 0,81 \cdot \sqrt{4,0}} = 1,101$$

$$\rho = \left(1,101 - 0,22\right)\big/ 1,101^2 = 0,727$$

209

$$\frac{b}{t} = \frac{800}{15} = 53,3 > 42 \cdot \varepsilon = 42 \cdot 0,81 = 34,0$$
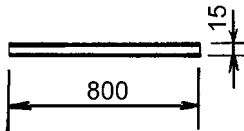
$$\Rightarrow \text{ Class 4}$$

$$\psi = 1,0 \implies K_\sigma = 0,43$$

$$\overline{\lambda}_p = \frac{800/15}{28,4 \cdot 0,81 \cdot \sqrt{4,0}} = 1,159$$

$$\rho = \left(1,159 - 0,22\right)/1,159^2 = 0,699$$

$$\frac{b}{t} = \frac{400}{8} = 50 > 42 \cdot \varepsilon = 42 \cdot 0,81 = 34,0$$
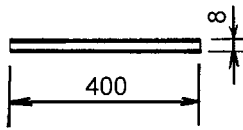
$$\Rightarrow \text{ Class 4}$$

$$\psi = 1,0 \implies K_\sigma = 0,43$$

$$\overline{\lambda}_p = \frac{400/8}{28,4 \cdot 0,81 \cdot \sqrt{4,0}} = 1,087$$

$$\rho = \left(1,087 - 0,22\right)/1,087^2 = 0,734$$

$$\psi = 0,581 \implies K_\sigma = \frac{8,2}{1,05 + 0,581} = 5,03$$
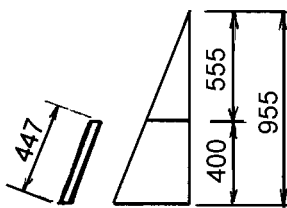
$$\frac{d}{t_w} = \frac{447}{8} = 55,9 > \frac{42 \cdot \varepsilon}{0,67 + 0,33 \cdot \psi} = \frac{42 \cdot 0,81}{0,67 + 0,33 \cdot 0,581} = 39,5$$

$$\Rightarrow \text{ Class 4}$$

$$\overline{\lambda}_p = \frac{447/8}{28,4 \cdot 0,81 \cdot \sqrt{5,03}} = 1,083$$

$$\rho = \left(1,083 - 0,22\right)/1,083^2 = 0,736$$

Global plate buckling (5.36)

210
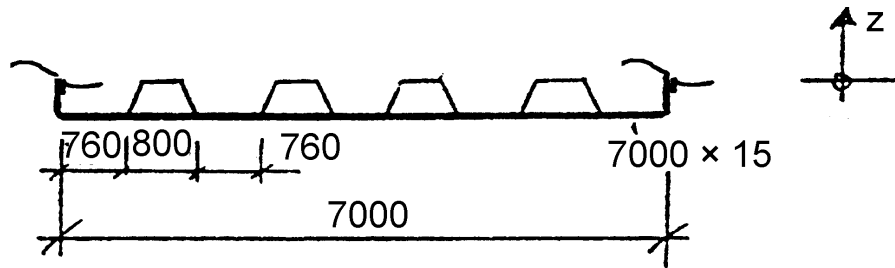
$A = 1464,1 \, \text{cm}^2$

$z = 7,41 \, \text{cm}$

$I_x = 273\,286 \, \text{cm}^4$

$D_x = \dfrac{EI_x}{7000} = \dfrac{210000 \cdot 273\,286 \cdot 10^4}{7000} = 81\,985\,800 \, \text{Nm}$ \qquad (5.3.6.2 (2))

$D_y = \dfrac{Et^3}{12 \cdot \left(1 - \mu^2\right)} = \dfrac{210000 \cdot 15^3}{12 \cdot 0,91} = 64904 \, \text{Nm}$

$\gamma = \sqrt{\dfrac{D_x}{D_y}} = \sqrt{\dfrac{81\,985\,800}{64904}} = 35,54$

$\alpha = \dfrac{a}{b} = \dfrac{4000}{7000} = 0,571$

$\psi = 1,0 \quad \Rightarrow \alpha_1 = \dfrac{\alpha}{\sqrt{\gamma}} = \dfrac{0,571}{\sqrt{35,54}} = 0,096 < 1$

$\Rightarrow K_{\sigma,p} = \left(\alpha + \dfrac{\gamma}{\alpha}\right)^2 = \left(0,571 + \dfrac{35,54}{0,571}\right)^2 = 3945,4$

$\sigma_e = 189800 \cdot \left(\dfrac{t}{b}\right)^2 = 189800 \cdot \left(\dfrac{15}{7000}\right)^2 = 0,872$

$\underline{\underline{\sigma_{cr,p}}} = K_{\sigma,p} \cdot \sigma_e = 3945,4 \cdot 0,872 = \underline{\underline{3440,4 \, \text{N}/\text{mm}^2}}$

$\underline{\underline{\sigma_{cr,c}}} = \dfrac{\pi^2 \cdot D_x}{a^2 \cdot t} = \dfrac{\pi^2 \cdot 81\,985\,800 \cdot 10^3}{4000^2 \cdot 15} = \underline{\underline{3371,5 \, \text{N}/\text{mm}^2}}$

$\bar{\lambda}_p = \sqrt{\dfrac{f_y}{\sigma_{cr,p}}} = \sqrt{\dfrac{355}{3440,4}} = 0,321 \quad \Rightarrow \rho_p = 1,0$

$$\bar{\lambda}_c = \sqrt{\frac{f_y}{\sigma_{cr,p}}} = \sqrt{\frac{355}{3371,5}} = 0,324$$

$$i = \sqrt{\frac{b \cdot D_x}{A \cdot E}} = \sqrt{\frac{7000 \cdot 81\,985\,800}{146\,410 \cdot 210\,000}} = 136,6 \text{ mm}$$
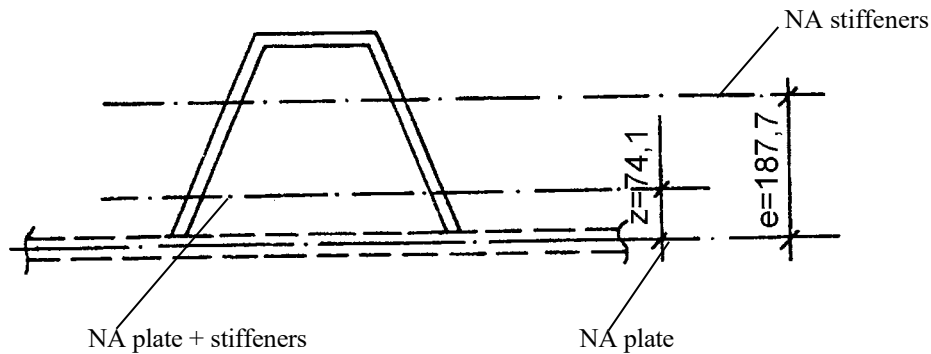
NA – neutral axis
Calculation with gross area!

$$\alpha^* = 0,34 + \frac{0,09}{i/e} = 0,34 + \frac{0,09}{136,6/187,7} = 0,464$$

$$\phi_c = 0,5 \cdot \left[1 + \alpha^*\left(\bar{\lambda}_c - 0,2\right) + \bar{\lambda}_c^2\right] = 0,5 \cdot \left[1 + 0,464\left(0,324 - 0,2\right) + 0,324^2\right] = 0,577$$

$$\rho_c = \frac{1}{\phi_c + \sqrt{\phi_c^2 - \bar{\lambda}_c^2}} = \frac{1}{0,577 + \sqrt{0,577^2 - 0,324^2}} = 0,948$$

$$\xi = \frac{\sigma_{cr,p}}{\sigma_{cr,c}} - 1 = \frac{3440,4}{3371,5} - 1 = 0,020$$

$$\underline{\underline{\rho}} = \left(\rho_p - \rho_c\right)\xi(2 - \xi) + \rho_c = \left(1,0 - 0,948\right) \cdot 0,02 \cdot (2 - 0,02) + 0,948 = \underline{\underline{0,950}}$$

$$A_c = \sum A_{st,eff} + \sum \rho_p' \cdot b_p' \cdot \rho_v \cdot t \qquad \left(\rho_v = 1,0\right)$$

$$A_c = 4 \cdot \left(0,734 \cdot 8 \cdot 400 + 2 \cdot 0,736 \cdot 8 \cdot 447\right) + 5 \cdot 0,727 \cdot 760 \cdot 15 + 4 \cdot 0,699 \cdot 800 \cdot 15$$

$$A_c = 1054,4 \text{ cm}^2$$

$$\underline{\underline{A_{c,eff}}} = \rho \cdot A_c = 0,95 \cdot 1054,4 = 1001,7 \text{ cm}^2$$

$$\underline{\underline{N_{Rd}}} = A_{c,eff} \cdot f_y/\gamma_M = 100170 \cdot 355/1,1 = \underline{\underline{32328 \text{ kN}}}$$

<u>Web</u>
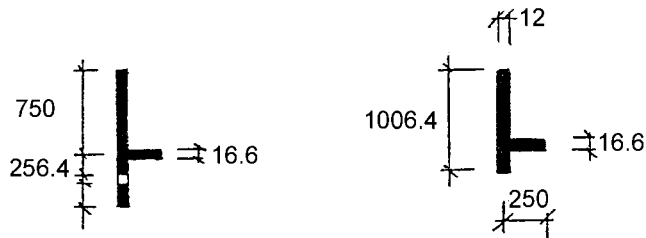
$A_{fc} = 162{,}27 \text{ cm}^2$

$z = 3{,}20 \text{ cm}$

$I_{fc} = 7001{,}9 \text{ cm}^4$

$$N_{cr,p} = 1{,}05 \cdot E \, \frac{\sqrt{I_{fc} \, t^3 b}}{b_1' \cdot b_2'} = 1{,}05 \cdot 210\,000 \, \frac{\sqrt{7001{,}9 \cdot 10^4 \cdot 12^3 \cdot 2000}}{500 \cdot 1500} = 4573{,}4 \text{ kN}$$

$$\underline{\underline{N_{cr,c}}} = \frac{\pi^2 E I_{fc}}{a^2} = \frac{\pi^2 \cdot 210\,000 \cdot 7001{,}9 \cdot 10^4}{4000^2} = \underline{\underline{9070{,}2 \text{ kN}}}$$

<u>New calculation of $N_{cr,p}$ (Petersen)</u>
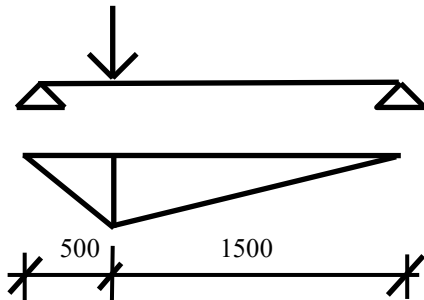
$M = 375$

$I = \dfrac{12^3}{0{,}91 \cdot 12} = 158{,}2$

$EI\delta = \dfrac{1}{3} \cdot 375^2 \cdot 2000$

$c = \dfrac{1}{\delta} = 0{,}354 \, \dfrac{1}{\text{mm}}$

$$\sqrt{\frac{cl^4}{EI}} = \sqrt{\frac{0{,}354 \cdot 4000^4}{210000 \cdot 7001{,}9 \cdot 10^4}} = 2{,}48$$

$$\Rightarrow \beta = 0{,}86$$

$$N_{cr,p} = \frac{\pi^2 \, 210\,000 \cdot 7001,9 \cdot 10^4}{(0,86 \cdot 4000)^2} = 12\,263,6 \text{ kN}$$

$$\bar{\lambda}_p = \sqrt{\frac{A_{fc} \cdot f_y}{N_{cr,p}}} = \sqrt{\frac{162,27 \cdot 10^2 \cdot 355}{12263,6 \cdot 10^3}} = 0,685$$

$$\rho_p = (0,685 - 0,22)/0,685^2 = 0,991$$

$$\bar{\lambda}_c = \sqrt{\frac{A_{fc} \cdot f_y}{N_{cr,c}}} = \sqrt{\frac{162,27 \cdot 10^2 \cdot 355}{9070,2 \cdot 10^3}} = 0,797$$

NA plate stiffeners

NA stiffener

NA plate
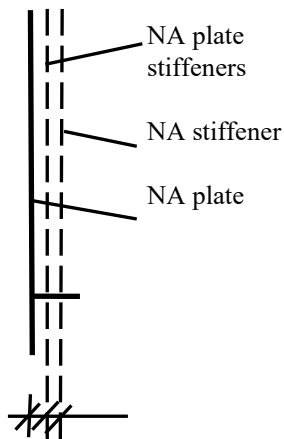
$$A_{gross} = 290 \text{ cm}^2$$

$$I_{gross} = 9098 \text{ cm}^4$$

$$i = \sqrt{\frac{I_{gross}}{A_{gross}}} = \sqrt{\frac{9098}{290}} = 5,6 \text{ cm}$$

$$e = 103,4 \text{ mm}$$

21,6 103,4

$$\alpha^* = 0,34 + \frac{0,09}{i/e} = 0,34 + \frac{0,09}{56/103,4} = 0,506$$

$$\phi_c = 0,5 \cdot \left[1 + \alpha^* \left(\bar{\lambda}_c - 0,2 \right) + \bar{\lambda}_c^2 \right] = 0,5 \cdot \left[1 + 0,506(0,797 - 0,2) + 0,797^2 \right] = 0,969$$

$$\rho_c = \frac{1}{\phi_c + \sqrt{\phi_c^2 - \bar{\lambda}_c^2}} = \frac{1}{0,969 + \sqrt{0,969^2 - 0,797^2}} = 0,658$$

$$\xi = \frac{\sigma_{cr,p}}{\sigma_{cr,c}} - 1 = \frac{12263,6}{9070,2} - 1 = 0,352$$

$$\rho = (\rho_p - \rho_c)\xi(2 - \xi) + \rho_c = (0,991 - 0,948) \cdot 0,352 \cdot (2 - 0,352) + 0,658 = \underline{\underline{0,851}}$$

214

$$A_c = \sum A_{st,eff} + \sum \rho_p' \cdot b_p' \cdot \rho_v \cdot t \qquad (\rho_v = 1,0)$$

$$A_c = 0,886 \cdot 250 \cdot 20 + 1500 \cdot 12 + 0,919 \cdot 500 \cdot 12$$

$$A_c = 279,44 \ cm^2$$

$$\underline{\underline{A_{c,eff}}} = \rho \cdot A_c = 0,851 \cdot 279,44 = \underline{\underline{237,8 \ cm^2}}$$

<u>Shear lag effects</u>
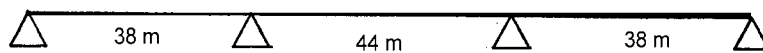
$$L_e = 0,2 \cdot 5 \cdot (38,2 + 44,0) = 20,5 \ m$$

$$\alpha_0 = \sqrt{1 + \frac{\Delta A}{b \cdot t}} = \sqrt{1 + \frac{2 \cdot 8 \cdot (400 + 2 \cdot 447)}{3500 \cdot 15}} = 1,181$$

$$\beta_2 = \frac{1}{1 + 6,0 \cdot \dfrac{\alpha_0 \cdot b}{L_e} + 1,6 \cdot \left(\dfrac{\alpha_0 \cdot b}{L_e}\right)^2} = \frac{1}{1 + 6,0 \cdot \dfrac{1,181 \cdot 3500}{20500} + 1,6 \cdot \left(\dfrac{1,181 \cdot 3500}{20500}\right)^2} = 0,440$$

$$\rho_{comb} = \rho \cdot \beta^{\frac{\alpha_0 \cdot b}{L_e}} = 0,950 \cdot 0,440^{\frac{1,181 \cdot 3500}{20500}} = 0,950 \cdot 0,847 = 0,804$$

$$A_{c,eff} = \rho_{comb} \cdot A_c = 0,804 \cdot 1054,4 = 847,7 \ cm^2$$

<u>Shear buckling resistance of the web</u>

a = 4000 $\dfrac{a}{d} = 2,0$

d = 2000
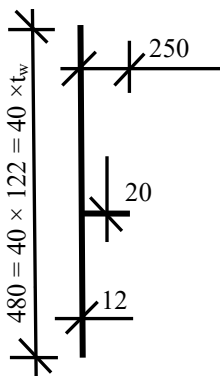
$$I_{st} = 6793,2 \ cm^4$$

$$\underline{\underline{K_{\tau,st}}} = 9 \cdot \left(\frac{d}{a}\right)^2 \left(\frac{I_{st}}{t_w^3 \cdot d}\right)^{3/4} = 9 \cdot \left(\frac{1}{2}\right)^2 \left(\frac{6793,2}{12^3 \cdot 2000}\right)^{3/4} = \underline{\underline{21,00}}$$

$$K_{\tau,st,min} = \frac{2,1}{t_w} \cdot \left(\frac{I_{st}}{d}\right)^{1/3} = \frac{2,1}{12} \cdot \left(\frac{6793,2 \cdot 10^4}{2000}\right)^{1/3} = 5,67$$

$$K_\tau = 5,34 + 4,0 \cdot \left(\frac{d}{a}\right)^2 + K_{\tau,st} = 5,34 + 4,0 \cdot \left(\frac{1}{2}\right)^2 + 21,00 = 27,34$$

$$\lambda_w = \frac{d}{37,4 \cdot t_w \cdot \varepsilon \cdot \sqrt{K_\tau}} = \frac{2000}{37,4 \cdot 12 \cdot 0,81 \cdot \sqrt{27,34}} = 1,052$$

Largest subpanel

$$a = 4000$$
$$d_1 = 1500 \qquad \frac{a}{d_1} = 2,667$$

$$K_{\tau 1} = 5,34 + 4,0 \cdot \left(\frac{d_1}{a}\right)^2 + K_{\tau,st} = 5,34 + 4,0 \cdot 0,375^2 = 5,903$$

$$\lambda_w = \frac{d_1}{37,4 \cdot t_w \cdot \varepsilon \cdot \sqrt{K_{\tau 1}}} = \frac{1500}{37,4 \cdot 12 \cdot 0,81 \cdot \sqrt{5,903}} = 1,698$$

$$\rho_v = \frac{1,37}{0,7 + \lambda_w} = \frac{1,37}{0,7 + 1,698} = 0,571$$

References

Adotte, G.D. (1967). Second–Order Theory in Orthotropic Plates. *Journal of the Structural Division*, Proc. ASCE, 93 (October 1967), pp. 343-362.

Bancila, R.: "Noile norme Europeene: EC 3/2 extras selectiv" Al II-lea Seminar de Poduri "Directii actuale in calculul si prosecturea podurilor", Universitatea "Politehnica" Timisoara, martie 1996, pp. 97-149

Bares, R. and Massonnet, C. (1968). Analysis of beam grids and orthotropic plates by the Guyon-Massonnet-Bares, SNTL, Prague, 1968 and Crosby-Lockwood, London, 1968

Bittner, E. (1938). Momententafeln und Einflussflachen fur Kreuzweise Bewehrte Eisenbetonplatten, Springer, Wien

Boobnov, I.G. (1902). On the Stresses in a Ship's Bottom Plating Due to Water pressure, *Transactions of the Institutions of Naval Architects*, London, Vol. 44

Boussinesq, J.V. (1879). Complements a une etude sur la theorie de l'equilibre et du mouvement des solides elastiques don't certaines dimensions sont tres-petites par rapport a l'autre, *Journal de Mathematiques*, T-5, Paris

Bölcskei, E. (1968). Beton- vasbeton és feszítettbeton hidak (in Hungarian), Tankönyvkiadó, Budapest

BS 5400 (1982). Steel, concrete and composite bridges, Part 3.

Cartledge, P. (1973). Steel box girder bridges. Proceedings of the International Conference, The Institution of Civil Engineers, London, p. 315.

Catalogue. Bridges on the Danube CD-ROM (1998). *International Conference, Regensburg*. Editor-in-Chief: Prof. M. Iványi.

Cauchy, A.L. (1828). De la pression dans un systeme de point materiels, *Excersices de Mathematique*, Paris

Cheung, Y.K. (1968). The Finite Strip Method in the Analysis of Elastic Plates With Two Simply Supported Ends. Proc. ICE, 40, December 1968, p.1

Cornelius, W. (1952). Die Berechnung der ebenen Flächentragwerke mit Hilfe der Theorie der Orthogonal-anisotropen Platte, *Der Stahlbau*, Vol. 2, pp. 21-26, Vol. 3, pp. 43-48, Vol. 4, pp. 60-64.

Domanovszky, S. (1984). Manufacturing and erection of steel structures (in Hungarian), *Mérnöki kézikönyv Vol. II (Palotás, L. editor) Steel structures*, Műszaki Könyvkiadó, Budapest

Dörnen, A. (1955). Stahlüberbau der Weserbrücke Porta, *Der Stahlbau*, p. 97.

ECCS (1985). <<Recommendation for the Fatigue Design of Steel Structures.>> *European Convention for Constructional Steelwork*, Brussels, Publication No.43.

Eibl, J. (1983). Bericht des Ad-Hoc-Ausschusses "Mitwirkende Plattenbreite", Bonn.

Eisel, H., Müller, C. and Sedlacek, G.: *Worked examples to demonstrate the use of design rules of Eurocode 3 – Part 2.*, Institute of Steel Construction, RWTH Aachen, 1995.

ENV 1993-1-7:April 1998. Eurocode 3: Design of steel structures – Part 1-7: Supplementary rules for planar plated structural elements with transverse loading

ESDEP (1994). European Steel Design Education Programme Vol. 10. Plates and Shells, *British Steel*, administered by the Steel Construction Institute

Eurocode 1, Part 3.2 (1992). Traffic Loads on Road Bridges, Draft July 1992, CEN Bruxelles.

Faltus, F. (1927). Lastverteilende Querverbindungen, *II. Int. Tagung für Brückenbau und Hochbau*, Wien, pp. 200-203

Geckeler, J.W. (1928). Elastiuzitastheorie anisotroper Körper, *Handbuch der Physik*, Band VI, Berlin

Gehring, F. (1860). De acquationibus differentialibus quibus aequilibrium et motus laminae crystallinac definitur, Berlin

Guyon, Y. (1946a). Calcul des Ponts Larges a pouters Multiples Solidarisees par des Entretoises, *Annales des Ponts et Chaussees*, No. V, Septembre-Octobre 1946, pp. 553-612.

Guyon, Y. (1946b). Calcul des Ponts-Dalles, *Annales des Ponts et Chaussees*, Vol. 36., pp. 683-718.

Günther, G.H. (1985). Beanspruchung von Stahlbrücken beim Einbau bituminöser Fahrbahnbeläge aufgrund gemessener Temperaturverteilungen, *BAST*, B 3.1-3440.

Günther, G.H., Bild, S. and Sedlacek, G. (1987). Durability of asphaltic pavements on orthotropic decks of steel bridges. *J. Constr. Steel Res.*, 85.

Halász, O., Hunyadi, F. (1959). Ortotrop pályalemezes hidak szerkezeti és számítási kérdései (in Hungarian), Mérnöki Továbbképző Intézet kiadványa, Felsőoktatási Jegyzetellátó Vállalat, Budapest

Hawranek, H. and Steinhardt, O. (1958). Theorie und Berechnung der Stahlbrücken, Springer, Berlin

Huber, M.T. (1914). Die Grundlagen einer Rationellen Berechnung der Kreuzwiese Bewehrten Eisenbetonplatten. *Zeitschrift des Osterreichischen Ingenieur-u. Architeken-Vereines*, Vol. 66, No. 30

Huber, M.T. (1922). Teorya Plyt, Lvov

Huber, M.T. (1923). Die Theorie der Kreuzweise bewehrten Eisenbetonplatten. *Der Bauingenieur*, Nos. 12, 13

Huber, M.T. (1929). Problems der Statik technish wichtiger orthotropen Platten, Warsaw

Huber, M.T. (1950). Theorie de L'elasticite, (in Polish), Cracow, Vol. I,1948, Vol. II. 1950)

Huber, M.T. (1956). Pisma, Tom II., Polska Akademia Nauk, Warszawa

Huber, M.T. (1957). Pisma, Tom III., Polska Akademia Nauk, Warszawa

Iványi, M. (2002). Refurbishment of Steel Bridges, in Mazzolani, F.M. and Iványi, M., editors: *Refurbishment of Buildings and Bridges*, Springer Wien New York, CISM Courses No. 435, pp. 61-150.

Iványi, M., Agócs, Z. Balaz, I. (1990). Torsion of Steel Beams (in Hungarian), Budapest-Bratislava, Mérnöki Továbbképző Intézet, BME.

Johansson, B., Maquoi, R., Sedlacek, G., Müller, C. and Schneider, R.: *Die Behandlung des Beulens bei dünnewardingen, Stahlkonstructionen in ENV 1993-Teil 1,5. (Eurocode 3-1-5)*, Stahlbau 68 (1999), Heft 11.

Johansson, B., Maquoi, R., and Sedlacek, G.: New design rules for plated structures in Eurocode 3, *Journal of Constructional Steel Research*, **Vol.57, No.3**, March 2001, pp. 279-311.

Kahmann, R. (1973). Schweißverfahren bei der Jegsttalbrücke, *Der Bauingenieur*, p. 269.

Karman, Th. (1910). Festigkeitsprobleme in Maschinenbau; Encyklopädie der mathematischen Wissenschaften, Teilband IV. 4, Teubner, Leipzig, p. 348-350.

Koller, I. (2001). Main data of the Danube bridge Szekszárd (In Hungarian) UVATERV.

Köppel, K. and Yamada, M. (1960). Anisotrope Flussbedingung, *Der Stahlbau*, No. 6, June 1960, pp. 173-179.

Kunert, K. (1967). Einige Überlegungen zur Projektierung von Stahlbrücken am Beispiel der Mainbrücke Hocheim, *Der Bauingenieur*, p. 313.

Lechnitsky, S.G. (1947). Anisotropic Plates, 2nd Edition, Moscow (In Russian)

Lechnitsky, S.G. (1963). Theory of Elasticity of an Anisotropic Body, Holden-Day Inc., San Francisco

Leonhardt, F. (1938). Die vereinfachte Berechnung zweiseitig gelagerter Trägerroste, *Die Bautechnik,* pp. 535-557, 648.

Levy, M. (1899). Comptes rendus, Vol.129, pp- 535-539

Lindner, J. and Bamm, D. (1982). Berechnung von orthotropen Platten und Trägerrosten, *Stahlbau Handbuch,* Band 1, Köln, pp. 217-240.

Massonnet, Ch. (1950a). Contribution au calcul des ponts a poutres multiples, *Annales des Travaux,* Publics de Belgique, Juin, Octobre, Decembre.

Massonnet, Ch. (1950b). Methods de calcul des ponts á poutres multiples tenant compte de leur résistance á la torsion, *Publications International Association for Bridge and Structural Engineering,* Vol. 10.

Massonnet, Ch. (1950c). Methods de calcul des ponts á poutres multiples tenant compte de leur résistance á la torsion, *Mémoires AIPC X,* Zurich, pp. 147-182.

Massonnet, Ch. (1955). Le Dimensionnement Pratique Des Ponts a Poutres Multiples et Des Ponts-Dalles en Tenant Compte de Leur Rigidite Torsionelle, *Construczioni in Cemento Armato,* No. 7, Rendiconti e Publicazioni, Milano, pp. 77-114.

Massonnet Ch. (1968). Thin-walled deep plate girders. *Proc. of 8th Congress of the IABSE, New York*, pp. 194-209.

Massonnet Ch. and Maquoi, R. (1973). New theory and tests on the ultimate strength of stiffened box girders in Proceedings, ″Steel box girder bridges″ International Conference. The Institute of Civil Engineers, London, pp. 131-143.

Maquoi, R. (1971). Measurement of the initial deflections of stiffened panels of large box girders (in French). *IABSE Publications*, **31**, Part 2, 141-151.

Maquoi, R. and Massonnet Ch. (1971). Non-linear theory of post-buckling resistance of large stiffened box girders (in French). *IABSE Publications*, Zürich

Maquoi, R. and Massonnet Ch. (1972). Design of plate and box girders for ultimate strength. *Proc. of IABSE Colloquium, London, March 1971*, Leemann, Zürich

Maquoi, R. and Massonnet Ch. (1982). Une evaluation simple de la largeur efficace due au traînage de cisaillement, *Constrùction Métallique*, No. 2.

Nakai, H. and Yoo, C.H. (1988). Analysis and Design of Curved Steel Bridges. McGraw-Hill Book Company

Nather F. (1991). Rehabilitation and Strengthening of Steel Road Bridges. In *Structural Engineering International*, Volume 1, No.3, 24-30.

Patentschrift No. 847014 (1948). Dr. Cornelius/MAN. *Straßenbrücke mit Flachblech*.

Pelikan, W. and Esslinger, M. (1957). Die Stahlfahrbahn – Berchnung und Konstruktion, *MAN Forschungsheft*, No. 7.

Pflüger, A. (1947). About the buckling problem of the anisotropic rectangular plate (in German), *Ing. Arch.* Vol. 16, pp 111-120.

prENV 1993-2:1997. Eurocode 3: Design of steel structures – Part 2: Steel bridges

prENV 1993-1-5:1997. Eurocode 3: Design of steel structures – Part 1-5: General rules – Supplementary rules for planar plated structures without transverse loading

prENV 1993-1-7:1998. Eurocode 3: Design of steel structures – Part 1-7: General rules – Supplementary rules for planar plated structural elements with transverse loading

Pucher, A. (1938). Die Momenteneinflussfelder rechteckiger Platten, No. 90 *der Reihe "Deutscher Ausschussfur Eisenbetonbau"*, Wilhelm Ernst u. Sohn, Berlin

Roloff, M. (1942). Erfahrungen mit Leichtfahrbahnen strählerner Reichsautobahnbrücken, *Die Bautechnik*, p. 433.

Roik, K. and Sedlacek, G. (1970). Erweiterung der technischen Biege- und Verdrehtheorie unter Berücksichtigung von Schubverformungen, *Die Bautechnik*, 47.

Rostovtsev, G.G. (1940). Calculation of a thin plate sheeting supported by rods (in Russian) Tondy, Leningrad, Inst. Juzkererov, Grazhdanskogo Vasdaghnogo Flota, No. 20.

Rostovtsev, G.G. (1968). in Anisitropic plates by Leknitskii, S.G., Gordon and Breach, p. 291.

Schaechterle and Leonhardt (1936). Leichte Fahrbahndecken auf stählernen Straßenbrücken, *Die Bautechnik*, p. 246.

Sedlacek, G. (1972). Bemerkenswerte Straßenbrücken aus Stahl der letzten 10 Jahre, *Technishe Mitteilungen Krupp*, p. S. 53.

Sedlacek, G. (1982). Zweiachsige Biegung und Torsion, *Stahlbau Handbuch Band 1*, Köln.

Sedlacek, G. (1992). Orthotropic Plate Bridge Decks, In Dowling, P.J., Harding, J.E. and Bjorhovde, R., editors: Construction Steel Design. An International Guide, Elsevier Applied Science, London and New York.

Sedlacek, G. and Bild, S. (1984). Simplified rules for the determination of the effective width of bridge decks caused by shear lag ″Verba volant, scripta manent″ Imprimeries Cérés s.p.r.-Liége, pp. 333-348.

Sedlacek, G. and Merzenich, G. (1991). Gutachten zu den Lastannahmen für die Verbreiterung der Rheinbrücke Mainz-Weisenau, RWTH Aachen (unpublished).

Skaloud, M. and Novotny, R. (1965). Post-critical behaviour ofan initially curved uniformly compressed panel, reinforced in its middle by longitudinal stiffener (in German), *Acta Tech.*, ČSAV, No. 2

Skaloud, M. (1970). Post-buckled behaviour of stiffened webs, Academia Nakladatelstoi Ceskoslovenske Akademie VED, Prague

Szabó, J. and Visontai, J. (1962). Válogatott fejezetek a tartók sztatikája köréből (in Hungarian), Tankönyvkiadó, Budapest.

Tesar, A. (1977), Kovové konštrukcie a mosty, *Moderné ocel'ové mosty, II. cast'* (in Slovak), ES SVŠT, Bratislava.

Troitsky, M.S. (1976). Stiffened Plates: Bending, Stability and Vibrations, Elsevier Scientific Publishing Company, Amsterdam-Oxford-New York, pp. 114-122.

Troitsky, M.S. (1987). Orthotropic Bridges. Theory and Design, The James F. Lincoln Arc Weld Found, Cleveland, Ohio.

Visontai, J. (1965). V. Ortotrop lemezek számításának menete (in Hungarian) (Dénes E., Korányi I., Tóth B., Visontai J.: Acélhidak), Mérnöki Továbbképző Intézet Kiadványa, Tankönyvkiadó, Budapest, pp. 145-170.

Weitz, F.-R. (1966). Entwicklungstendenzen des Stahlbrückenbaus am Beispiel der Rheinbrücke Wiesbaden-Schierstein, *Der Stahlbau*, Vol. 35, No. 10, pp. 289-301, Vol. 12. pp. 357-365.

Weitz, F.-R. (1974). Neuzeitliche Gesichtspunkte im schweiβenden Brückenbau, *Der Stahlbau*, Vol. 43, No. 3, pp. 73-81.

Weitz, F.-R. (1975). Entwurfsgrundlangen und Entscheidungskriterien für Konstruktionssysteme im Groβbrückenbau unter besonderer Berücksichtigung der Fertigung, *Dissertation*, Darmstadt.

Voigt, W. (1910). Lehrbuch der Kristallphysik, Lepzig

Wolchuk, R. (1990). Lessons from weld cracks in orthotropic decks on three European bridges. *Journal of Structural. Engineering*, 75.

Wolmir, A.S. (1962). Flexibile plates and shells (in German), VEB für Bauwesen, Berlin

Zienkiewicz, O.C. and Cheung, Y.K. (1964). The Finite Element Method for Analysis of Elastic Isotropic and Orthotropic Slabs, Proc. Int. Civ. Eng., London, Vol. 28, August 1964.

Appendixes

Appendix I.

Eurocode 3: Design of steel structures – Part 2
   STEEL BRIDGES
   prENV 1993-2 (1997-03-27)

Appendix II.

Eurocode 3: Design of steel structures – Part 1.5 (EC3-1-5)
   Planar plated structures without transverse loading
   [prENV 1993-1-5:1997]

Appendix III.

Eurocode 3: Design of steel structures – Part 1.7 (EC3-1-7)
   Planar plated structural elements with transverse loading
   [prENV 1993-1-7:April 1998]

Appendix I.

Eurocode 3: Design of steel structures – Part 2
       STEEL BRIDGES
       prENV 1993-2 (1997-03-27)

Extract

I.1 Serviceability Limit States [prENV 1993-2:1997, Section 4]

I.1.1 Basis

A bridge shall be designed and constructed such that all relevant serviceability limit states are satisfied. In general the following serviceability requirements should be taken into account:

  a) restriction to elastic behaviour in order to exclude:
   - excessive yielding;
   - deviations from the intended geometry by residual deflections;
   - accumulation of deformations;
  b) limitation of deflections and curvature in order to exclude:
   - unwanted dynamic impacts due to traffic (also deflection limits together with natural frequencies);
   - infringement of required clearances;
   - cracking of brittle layers (of asphaltic pavements for example);
   - impairment of drainage;
  c) limitation of natural frequencies in order to exclude:
   - vibrations due to traffic or wind perceptible to pedestrians or passengers in cars;
   - fatigue damages caused by resonance phenomena;
   - excessive noise emission from plated elements;
  d) limitation of plate slenderness in order to exclude:
   - visible buckling of plates;
   - breathing of plates (also in view of fatigue);
   - reduction of stiffness due to plate buckling, that may result in an increase of deflection;
  e) achievement of sufficient durability by appropriate detailing to reduce corrosion and excessive wear;
  f) ease of maintenance and repair throughs:
   - accessibility of structural parts to permit maintenance, inspection and renewal (of corrosion protection and asphaltic pavements, for example);
   - exchangeability of bearings, anchors, individual cables, expansion joints and the like, that might have a limited service life, with the minimum practicable interruption to use of the structure.

In appropriate cases, serviceability limit states may be verified by numerical assessment. Where more appropriate, serviceability aspects may be dealt with in the conceptual design of the bridge, or by suitable detailing.

I.1.2 Calculation models

Deflections should be determined by linear elastic analysis, using gross cross-section properties reduced to take account of shear lag effects. Stress-resultants at serviceability limit states should be determined from a linear elastic analysis, using gross cross-section properties as specified in ENV 1993-1-5. The stresses should then be obtained using effective cross-section properties determined taking account of shear lag. Simplified calculation models may be used for stress calculations provided that the effects of the simplification are conservative.

I.1.3 Limitation for reversible behaviour

The nominal stresses in all elements of the bridge resulting from characteristic (rare) load combinations $\sigma_{Ed,ser}$ and $\tau_{Ed,ser}$, calculated making due allowance where relevant for the effects of shear lag in wide flanges and the secondary effects implied by deflections (for instance secondary moments in trusses), should be limited as follows:

$$\sigma_{Ed,ser} \leq \frac{f_y}{\gamma_{M,ser}}$$

$$\tau_{Ed,ser} \leq \frac{f_y}{\sqrt{3} \cdot \gamma_{M,ser}} \quad , \qquad \text{/I.1/}$$

$$\sqrt{\left(\sigma_{Ed,ser}\right)^2 + 3 \cdot \left(\tau_{Ed,ser}\right)^2} \leq \frac{f_y}{\gamma_{M,ser}}$$

The partial factor for serviceability limit states may be taken as: $\gamma_{M,ser} = 1,0$. The nominal stress range $\Delta\sigma_{fre}$ due to the representative values of variable loads specified for the frequent load combination should be limited to $1,5 \, f_y / \gamma_{M,ser}$. For non-preloaded bolted connections loaded in shear, the bolt forces due to the characteristic (rare) load combination should be limited to:

$$F_{b,Rd,ser} \leq 0,7 \, F_{b,Rd} \qquad \text{/I.2/}$$

in which $F_{b,Rd}$ is the bearing resistance for ultimate limit states verifications. For slip-resistant preloaded bolted connections category B, the assessment for serviceability shall be carried out using the characteristic (rare) load combination.

I.1.4 Limitation of web breathing

The slenderness of unstiffened or stiffened web plates should be limited to avoid excessive breathing that might result in fatigue at or adjacent to the web-to-flange connections. Unless a more accurate calculation method is used, the following simplified procedure may be applied. The stresses $\sigma_{x,Ed,ser}$ and $\tau_{Ed,ser}$ in a web panel, see Fig. I.1, should be calculated using the frequent load combination.
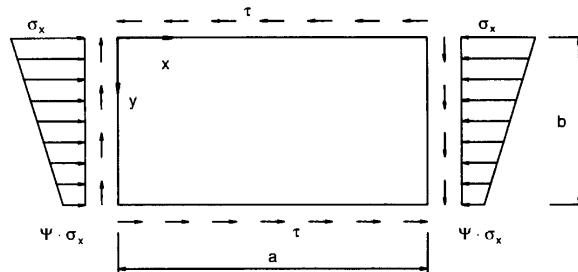
Figure I.1 Stress state for a panel [Fig. 4.1].

If either of these stresses is not constant along the length of the panel, the design value should be taken as the maximum of:

– the greater of the values at a distance equal to the lesser of a/2 or b/2 from a transverse edge, in which a is the longitudinal dimension of the panel and b is the transverse dimension;
– half of the maximum value within the length of the panel.

For a sub-panel, its dimensions $a_{i,k}$ and $b_{i,k}$ should be used in place of a and b.
The following criterion should be satisfied:

$$\left(\frac{\sigma_{Ed,ser}}{k_\sigma \cdot \sigma_E}\right)^2 + \left(\frac{\tau_{Ed,ser}}{k_\tau \cdot \sigma_E}\right)^2 \leq 1{,}15 \qquad\qquad \text{/I.3/}$$

with:

$$\sigma_E = \frac{\pi^2 E}{12\left(1-v^2\right)}\left(\frac{t}{b_p}\right)^2 \approx \frac{189800}{\left(b/t\right)^2}$$

in which k_τ and k_σ are given by the following:

– for unstiffened plates:
  – k_σ is given in table 5.3.2 of ENV 1993-1-1;
  – k_τ is given in 5.6.3(3) of ENV 1993-1-1;
– for stiffened plates: see ENV 1993-1-5;

and b_p is the smaller of a and b.

I.1.5 Limits for clearance gauges

Specified clearance gauges shall be maintained without encroachment by any part of the structure under the effects of the characteristic (rare) load combination.

I.1.6 Limits for visual impression

If it is necessary to avoid the visual impression of sagging, consideration should be given to precambering. In calculating the precambering, the effects of shear deformation and of slip in riveted or bolted connections should be considered. For connections with rivets or fitted bolts a fastener slip of 0,2 mm should be assumed. For preloaded bolts no slip need be considered. In modelling the distribution of permanent weight and stiffness in a bridge, the non-uniform distribution resulting from changes in plate thickness, reinforcement and the like should be taken into account.

I.1.7 Performance criteria for railway bridges

Specific performance criteria for deformations and vibrations for railway bridges may be obtained from annex G of ENV 1991-3. Requirements for the limitation of possible noise emission should be given in the project specification.

I.1.8 Performance criteria for road bridges

I.1.8.1 General

Excessive deformations should be avoided if they might:

- endanger traffic when the surface is iced;
- affect the dynamic load on the bridge;
- affect the dynamic behaviour to an extent that might cause discomfort to users;
- lead to cracks in asphaltic surfacings;
- adversely affect the drainage of water from the bridge deck.

Calculations of deformations should be carried out using the frequent load combination. To ensure the durability of asphaltic pavements on road bridges, the difference between the deflections of two adjacent stringers or stiffeners should be limited. Unless otherwise specified the minimum stiffness of stringers should be as indicated in Fig. I.2. The natural frequencies and deflections of the bridge structure should be limited to avoid discomfort of users.

I.1.8.2 Deflection limits to avoid excessive impact from traffic

The roadway should be designed such that it exhibits uniform deflection behaviour along the length with no abrupt changes in stiffness or smoothness of surface giving rise to impact. Sudden changes in slope of the surface deck and changes of level at expansion joints should be eliminated. Transverse girders at the end of the bridge should be designed such that the deflection does not exceed:

- the deflection limit specified for the proper functioning of the expansion joint;
- 5 mm.

Where the deck structure is irregularly supported (for instance by additional bracings at intermediate bridge piers) the deck area adjacent to these additional deck supports should be

designed for the enhanced impact factors given in ENV 1991-3 for the area close to expansion joints.

I.1.8.3 Resonance effects

Mechanical resonance of the main girders of bridges should be taken into account when relevant. Where light bracing members, cable stays or similar items have natural frequencies that are close to the frequency of any mechanical excitation (for instance regular passage of vehicles over deck joints) consideration should be given to artificial damping of the members (by means of oscillation dampers, for example).
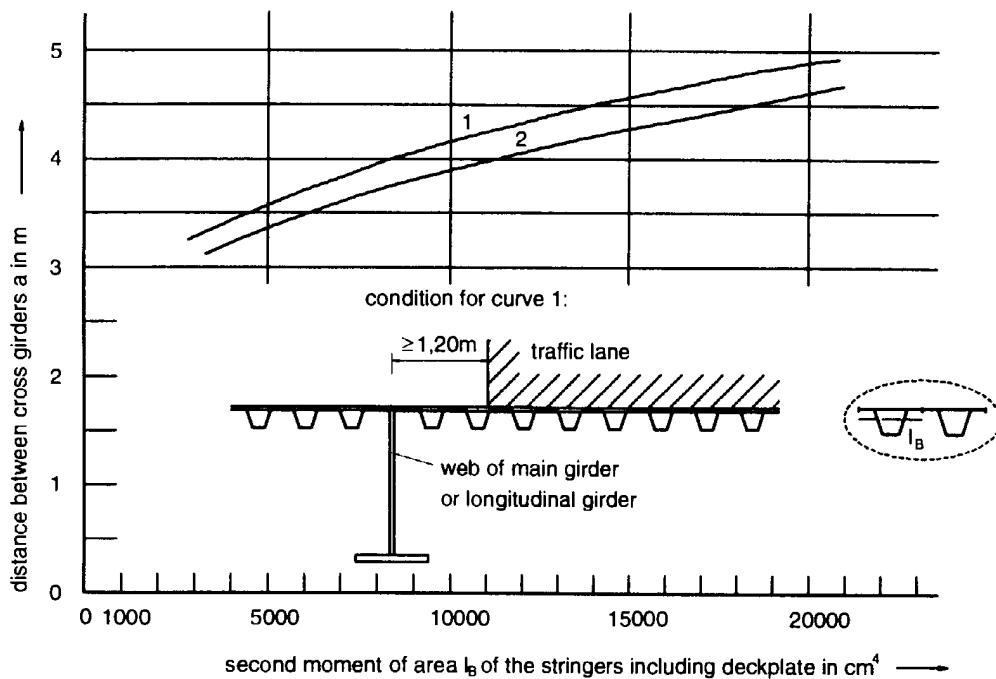
NOTES: 1) Curve 1 applies to stringers or stiffeners that are located under the most heavily loaded traffic lane and within 1,2 m of a web of the main girder.
2) Curve 2 applies to all other stringers or stiffeners.
3) The figure applies to any type of stiffeners.

Figure I.2 Minimum stiffness of stringers [Fig. 4.2].

I.1.9 Performance criteria for pedestrian bridges

For footbridges and cycle track bridges vibration that might produce discomfort may be eliminated either through the structural design or by providing suitable damping devices.

I.1.10 Performance criteria for effects of wind

Vibrations of slender members induced by vortex excitation should be limited to values below those that generate stresses of sufficient magnitude to cause fatigue. For the determination of fatigue loads from vortex excitation reference should be made to annex F. Aerodynamic effects caused by flutter or galloping or by divergency should be treated as ultimate limit state conditions. Appropriate checks should be carried out according to the procedures given in ENV 1991-2-4.

I.1.11 Accessibility of joint details and surfaces

All steelwork shall be designed and detailed to minimise the risk of corrosion and to permit inspection and maintenance. All parts should satisfy at least one of the following alternatives:

– accessible for inspection, cleaning and painting;
– effectively sealed against corrosion (for instance the interior of boxes or hollow portions);
– made of steel with adequate corrosion-resistant properties;
– be thicker than required structurally, to allow for future corrosion.

None of the above provisions need be applied to temporary bridges or to those with an appropriately short design life.

I.1.12 Drainage

The surfaces of carriageways and footpaths shall be sealed to prevent the ingress of surface water. Bridge decks shall be drained in such a way that surface water cannot damage structural elements. Arrangements for drainage should take into account the slope of the bridge deck, the position, diameter and slope of the waste pipes, the drainage of expansion joints and the discharge of waste water. Free fall drains should carry waste water to a point clear of the underside of the structure so that no structural element and no supporting structure is hit by water under any conditions of wind and weather.

Waste pipes should be designed so that they can be easily cleaned out. The distance between centres of cleaning openings should be stated in the project specification. Where waste pipes are used in box girder bridges, provisions shall be made to avoid accumulation of water in the event of a leak in a pipe. For road bridges, drains should be provided outside each expansion joint, on both sides where necessary. For railway bridges up to 40 m long carrying ballasted tracks, the deck may be assumed to be self-draining and no further drainage provisions need be provided. Provision should be made for drainage of all closed cross-sections.

I.2 Ultimate Limit States

I.2.1 Structural elements [prENV 1993-2:1997]

I.2.1.1 Structural system: Orthotropic plates [prENV 1993-2:1997, Section 5.2.3.1]

In verifying the stresses in the orthotropic plate as the load distributing deck the following effects should be taken into account:

a) membrane stresses in the stringers and in the deckplate from bending moments caused by local loads and from axial forces from cooperation as flange of the main girder (longitudinal stringers) or cross girder (transverse stringers).

b) membrane stresses in the cross girders with cut-outs at the intersections with the stringers. This might imply the consideration of a Vierendeel-behaviour.

Bending stresses in the deckplate and the walls of the stringers need not be considered, provided that minimum distances of stiffeners are observed. The cross girders together with the vertical stiffeners of the webs, may be part of transverse frames, for which the frame behaviour and its consequences for restraining moments at the interconnection at the frame knees and for U-frame behaviour in case of open bridge-sections should be considered.

I.3 Special considerations for structural detailing of orthotropic decks [prENV 1993-2:1997, Annex G]

A) Road bridges

<u>Deckplate</u>

In the view of both fatigue cracking in the deckplate and cracking of the asphalt layer, the thickness of the deckplate should be limited to

$t_{min} \geq 12$ mm for asphalt layer ≥ 70 mm
$t_{min} \geq 14$ mm for asphalt layer ≥ 40 mm

The spacing of the support of the deckplate by webs of stringers should be:
$e \leq 300$ mm for $t = 12$ mm and $e/t < 25$, Fig. I.3.

For temporary bridges the plate thickness t may be smaller than indicated previously however the ratio $e/t < 25$ should be fulfilled.

For permanent bridges the stringers should only be provided transversally to the traffic lanes if agreed by the competent authority. When the recommendations mentioned before are satisfied, the bending moments in the deckplate need not be verified.

Transverse splices with weld running in crosslane direction are on Fig. I.4. Double-V weld or single V-weld with root jointing and additional weld or single V-weld with ceramic backing strip.

- 100 % inspection required.
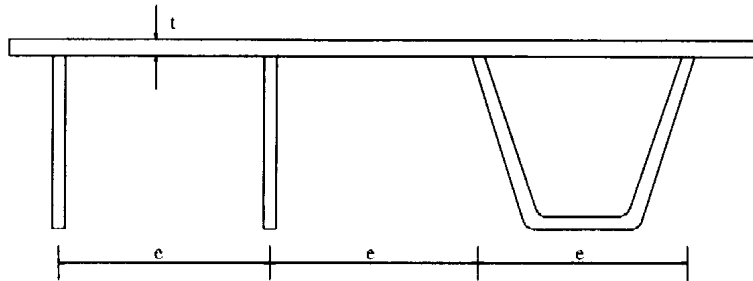
Figure I.3 [Fig. G.1].
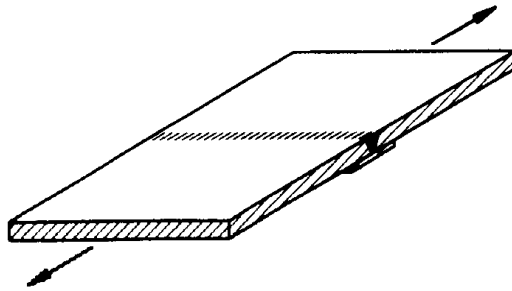
Figure I.4 [Fig. G.2].

Longitudinal splices with welds running in in-lane direction are on Fig. I.5. Methods as for transverse splices or single V-weld with steel backing strip with the following requirements:

– Tack weld in the final butt weld
– Special attention to be given to corrosion protection
– Standard inspection requirements
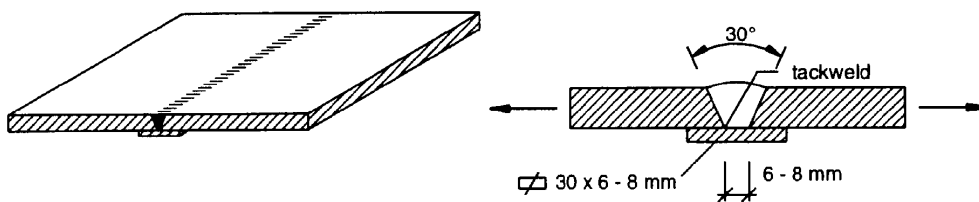
Figure I.5 [Fig. G.3].

Stiffeners

Stiffeners made of hollow sections type V, trapezoidal or round should have a minimum plate thickness t ≥ 6 mm. The radius for cold forming should be R/t ≥ 4. For open section stiffeners the plate thickness should be t ≥ 10 mm. Stiffeners should satisfy the minimum stiffness requirements in [prENV 1993-2:1997, Section 4.8].

Gap between stiffener and deckplate before welding ≤ 1 mm. Weld throat: 1.25 x thickness of the stiffener. The weld penetration: see Fig. I.6.

General requirements   Manual requirements   Automatic welding
                                                               (if proved by procedure test)
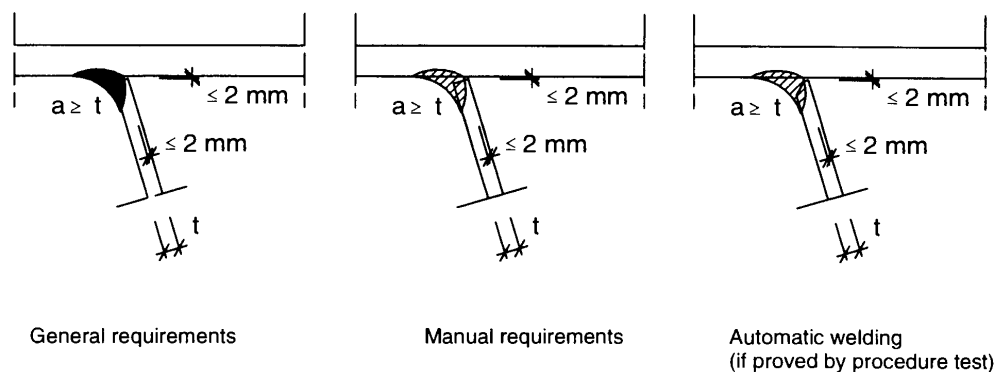
Figure I.6 [Fig. G.4]**.**

Welding process/inspection:

– For automatic welding:
  – Standard inspection requirements

– For manual welding:
  – 100 % inspection to confirm weld penetration and throat thickness

– For manual welding in overhead position:
  – Edge preparation must be provided for the total length of the weld and 50 % inspection is required.
  – Special attention must be payed to starts and stops (grinding).
  – No undercuts permitted.

Length of the stiffener - stiffener connection: ≥ 200 mm, see Fig. I.7. Weld length connecting stiffener: 100 - 200 mm. Root gap between splice plate and connecting stiffener: 6 mm, see Fig. I.8. Backing strip: thickness 3 mm, width ≥ 30 mm; fit-up gap ≤ 1 mm; misali0gnment between stiffener and splice ≤ 1 mm. Tack weld is located within the butt weld, over the full length of the butt weld and has the same quality as the butt weld. The welding process/inspection:

– M.M.A.W. is allowed with 100 % inspection
– MIG/MAG is preferred with 50 % inspection

Welding procedure:
- 1. First weld between stiffener and splice plate
  2. Second weld between stiffener and splice plate
  3. Deckplate weld
- Special requirements must be made for several straight passes, not using weaving techniques
- Special attention must be paid to starts and stops (grinding)

General requirements are tolerances for fit up 1 mm and side welds 50 % inspection
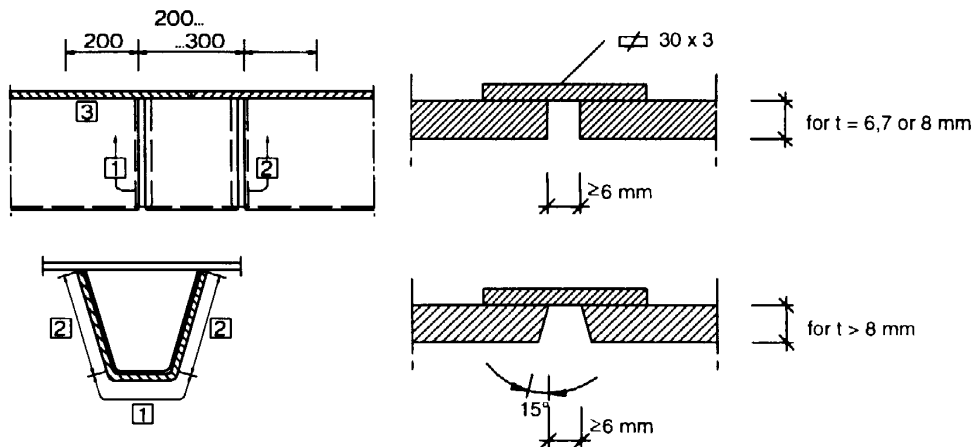
Figure I.7 [Fig. G.5].   **Figure I.8** [Fig. G.6].

Stiffener-crossbeam connections with cope holes connection

Stiffener should be continuous, passing through cut outs in the webs of the crossbeams. A cope hole should be provided around the soffit of the stiffener, but cope holes close to the deck plate are not permitted. The cope holes should have the following recommended dimensions:

– V-stiffener: continuous radius (75 mm) on the same centre as the soffit of the stiffener.
– Trapezoidal stiffener: for the minimum size of the cope hole see figure I.9.
– Round stiffener (bottom radius 100 mm): radius of 35 mm at each side centred on the lower end of the straight part of the stiffener web. Connecting radius of 140 mm on the same centre as the soffit of the stiffener.

The following requirements apply:

– Special attention to be given to providing a smooth edge to cope holes. Any notches to be ground smooth.
– Welds to be returned around the edges of cope holes in the web.
– Weld throat thickness to be ≥ 50 % of diaphragm plate thickness.
– No undercut permitted.

229

By the above mentioned recommendations and the ULS-assessment of the welds the formation of fatigue cracks in the welds due to shear from shear forces and torsion and from restraints from deflections of the stringers prevented. By the above mentioned recommendations and the ULS and SLS-assessments of the stringers the formation of fatigue cracks in the stringer web (vertical before the weld toe) is prevented.
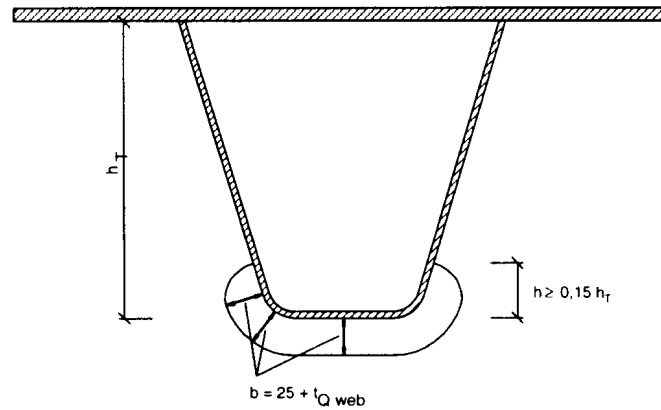
Figure I.9 [Fig. G.7].
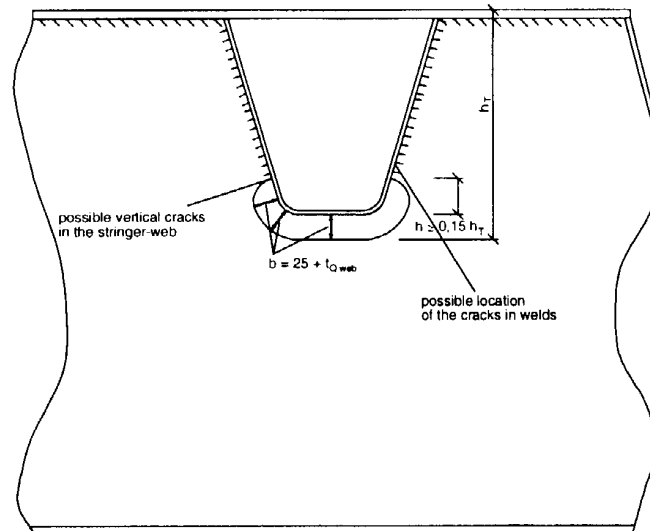
Figure I.10 [Fig. G.8].

Provisions for the crossbeam in case of cope holes

The stiffness of crossbeams and in particular of the web should be sufficient to prevent the formation of horizontal fatigue cracks in the web of the stringers at the returns of the welds, due to variable imposed deformations from the crossbeam web, Figure I.11. By applying the ULS-

assessment rules for the web of the cross beam taking account of the Vierendeel action, the formation of such cracks will be prevented.
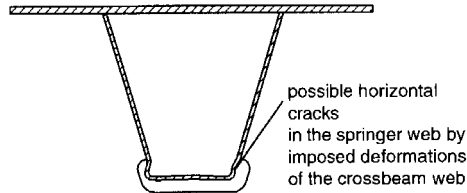
Figure I.11 [Fig. G.9].

Connections without cope holes

Stringers should be continuous, passing through cutouts in the webs of the crossbeams. Best fatigue behaviour is achieved, when <u>trapezoidal</u> stiffeners or <u>round</u> stiffeners are used without cutouts at the bottom of the stiffeners (welded all around). For this solution the maximum gap between the webplate and the stiffener is 3 mm and the minimum throat thickness is 50 % of the thickness of the cross-beam web. Standard inspection requirements apply.

Short stiffeners fitted between cross-beams

In exceptional cases, for instance shallow decks for light traffic, short stiffeners fitted between cross-beams may be used when following requirements are satisfied:

– - crossbeam spacing ≤ 2,75 m
– - stiffener to cross-beam welds to be full-penetration welds with a prepared end on the stiffener, see Fig. I.12.
– - the sequence of assembly and welding should be decided with advice from the fabricator to prevent excessive shrinkage effects.
– - 100 % inspection required for stiffener to cross-beam welds.
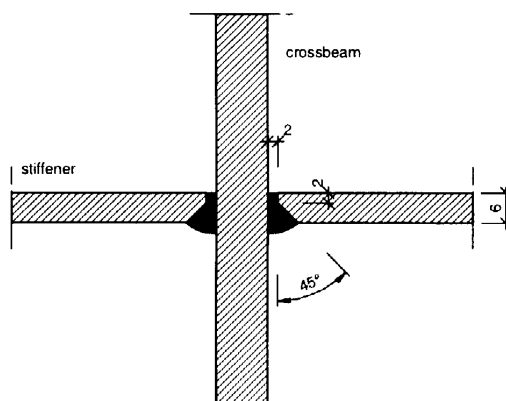
Figure I.12 [Fig. G.10].

Crossbeams

In case of continuous stringers with cutouts the crossbeams should be designed for the Vierendeel-action resulting from the cutouts, Fig. I.13. The design stresses are the result from the Vierendeel- actions multiplied with the stress concentration factors (SCF). The values of the SCF's are depending on the form and the location of the cope hole.
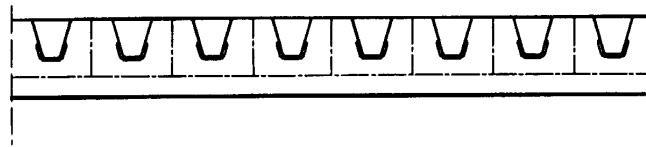
Figure I.13 [Fig. G.11].

To avoid fatigue cracks at the cutouts the following recommendations have to be satisfied:

- – - the requirement for limiting the stresses to yielding in the ultimate limit state in the critical sections A-A and B-B, Fig. I.14;
- – - the determination of an optimum for the web thickness by the combination of the in-plane and out-of-plane behaviour;
- – - the above mentioned recommendations for structural detailing of the cutouts.

In case of continuous stringers without cope holes the strength of critical sections A-A and B-B may be determined using an effective breadths of the stringer web $b_{eff} = 5$ t.
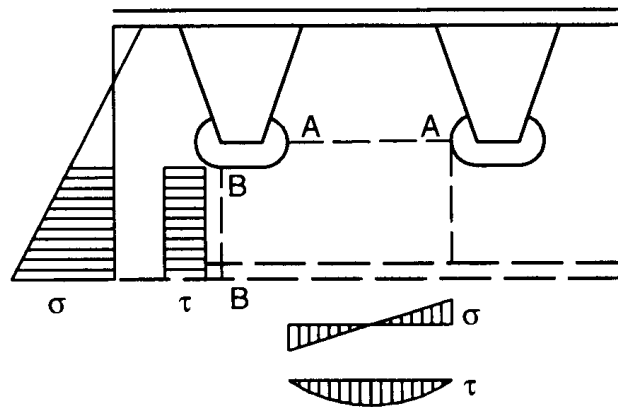
Figure I.14 [Fig. G.12].

Crossbeam to deckplate connection: the gap before welding ≤ 1 mm. Continuous double fillet weld: a = 0.5 × crossbeam thickness.

The connection between the crossbeam and the vertical stiffeners of the web, that from a transverse frame shall be designed for the restraining moments. Fatigue restraint design as

indicated in Fig. I.15 has to be applied. If the lower flanges of the crossbeam and main girder are at the same level the radius for the edges should be R = 8 mm, see Fig. I.16.
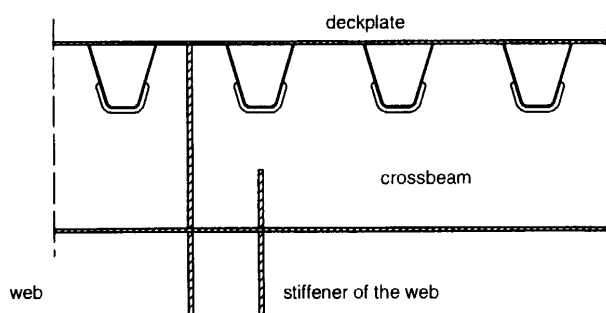
Figure I.15 [Fig. G.13].
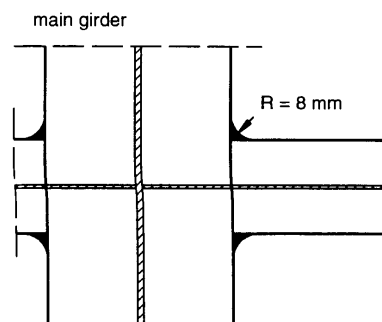
Figure I.16 [Fig. G.14]**.**

B) Railway bridges

All clauses for road bridges apply apart from more conservative rules to follow. In the following also additional rules for railway bridges are presented.

Deckplate

The thickness of the deckplate should be limited to $t_{min} \geq 14$ mm and $t_{min} \geq e/40$, where e is the maximum distance between the stiffeners.

Stiffeners

Non-continuous stringers are allowed; however they have a low fatigue classification. In connections with cope holes circular or apple forms of cutouts are recommended for railway bridges (Fig. I.17a to d). Their radii should be 40 to 50mm. Connections without cope holes in the web of the cross girder (Fig. I.17e and f) are allowed if welding is carried out in such a way that residual welding stresses are limited. Unsymmetrical cutouts (Fig. I.l7g) are not recommended for railway bridges.

In case of trapezoidal stiffeners with cutouts in the web of crossbeams these cutouts shall meet the requirements of Fig. I.18. In case the weld is not prepared as indicated in Fig. I.18 sufficient weld penetration should be ensured otherwise.

The geometry of trapezoidal stiffeners should fulfill the requirements of Fig. I.19.

Stiffener-to-stiffener connections shall be made at a location $0.15 \times e_{QT}$ to $0,25 \times e_{QT}$ away from a crossbeam.

233
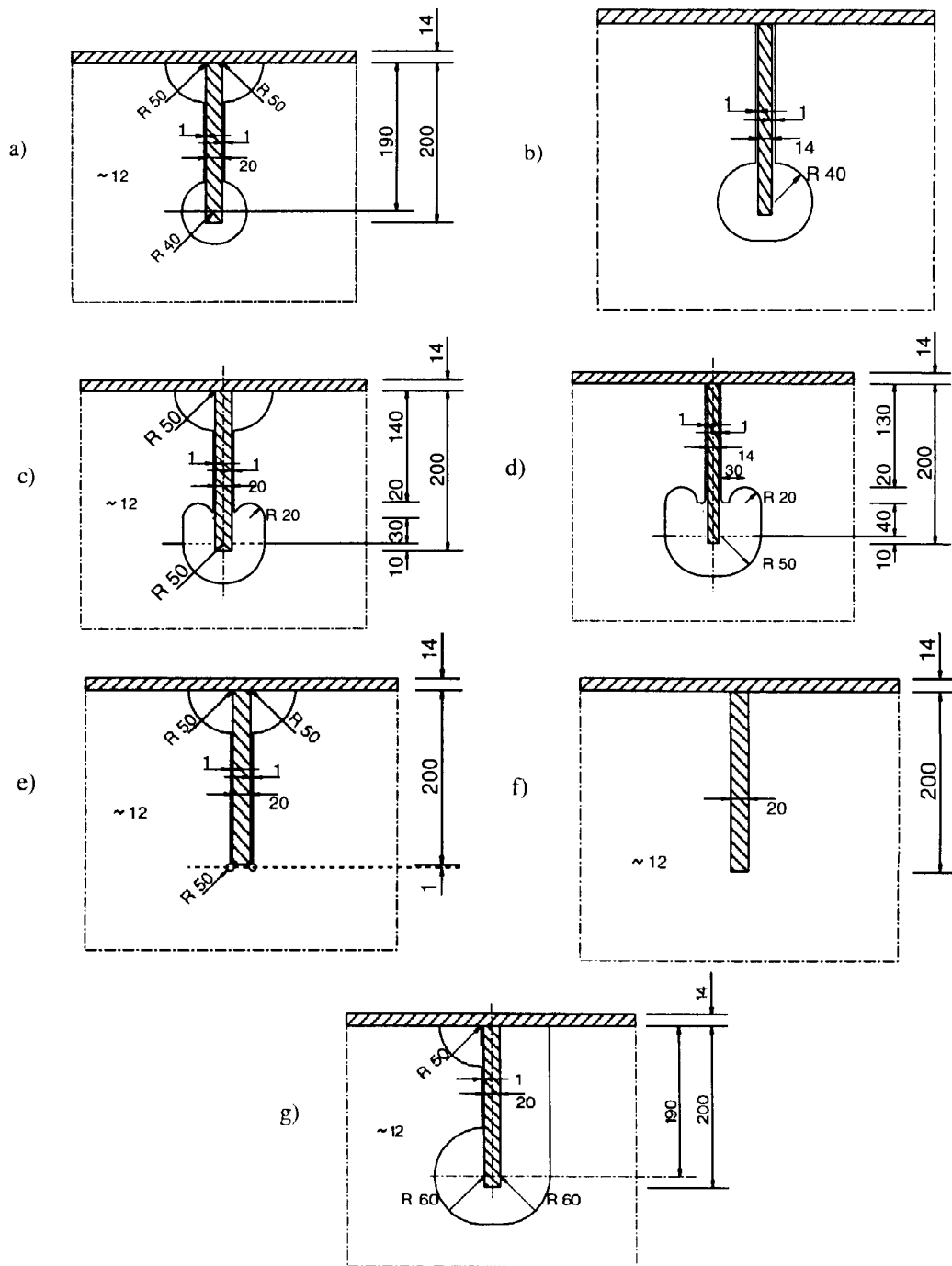
Figure I.17 [Fig. G.15].
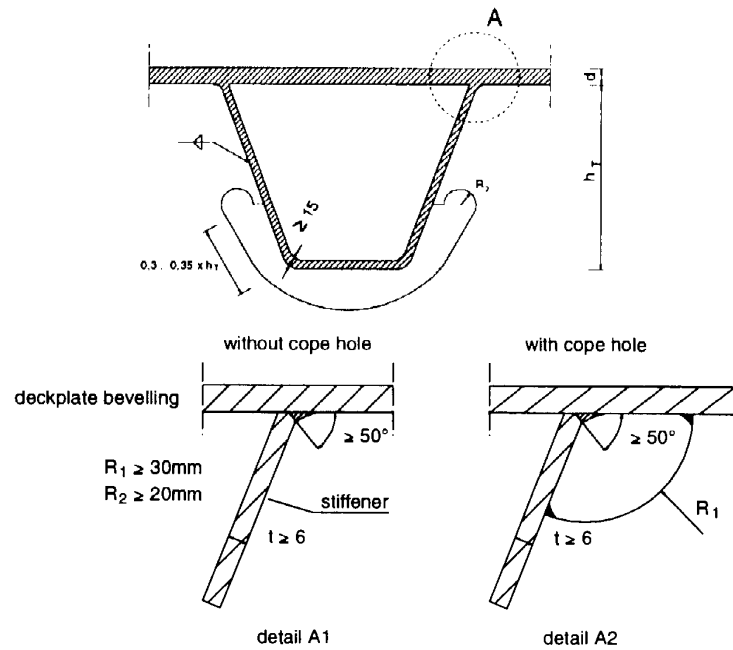
Figure I.18 [Fig. G.16].

Crossbeams

The geometry of crossbeams should fulfil the requirements of Fig. I.19.
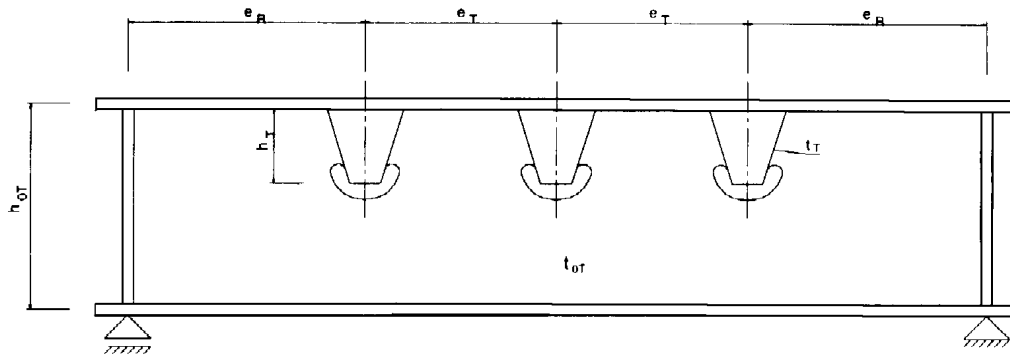
Requirements for geometry of crossbeams and stiffeners:

$600 \le e_T \le 900$ mm; $e_R \ge e_T$ $2500 \le e_{QT} \le 3500$ mm

$h_T/h_{QT} < 0.4$ $6 \le t_T \le 10$ mm $16 \le t_{QT} \le 20$ mm

Figure I.19 [Fig. G.17].

I.4 Design of diaphragms in box girders at supports [prENV 1993-2:1997, Annex H]

H.1 General

Diaphragms should be provided at supports of box girders to transfer applied loads to the bearings. Subject to the limitations and provisions of H.2, unstiffened and stiffened diaphragms should be designed in accordance with H.5 and H.6, respectively, on the basis of the loadings and effective sections given in H.3 and H.4, respectively. The diaphragm/web junctions should meet the provisions of H.7. Deck cross beams and/or cantilevers supporting the deck and located in the plane of a diaphragm should meet the provisions of H.8. The geometric notation used is shown in Fig. I.20.

H.2 Limitations

H.2.1 Box girders

Box girders should be of nominally rectangular cross section or of nominally trapezoidal cross-section with webs in single planes inclined at less than 45° from the vertical, and when unstiffened, should be nominally symmetrical about a vertical axis (i.e. ignoring cross fall or superelevation). Box girders should be of a single cell form with or without interconnecting cross members and cantilevers and should not be subject to internal pressure effects due to sealing.

H.2.2 Diaphragms and bearings

The plane of the diaphragm should be within ±5° to the normal to the axis of the girder in elevation, within ±10° in plan, and within ±5° of a vertical plane. The diaphragm should be in a single plane, except as permitted in H.2.4 for starter plates.

Each diaphragm should be supported on a single or twin bearings under each box. Bearings under unstiffened diaphragms should be symmetrically placed about the vertical axis of the diaphragm. The contact width j of a stiffened diaphragm above a bearing, as defined in Fig. I.20, should not exceed half the depth of the diaphragm with a single bearing nor one-quarter of the depth of the diaphragm with twin bearings. A bearing below a stiffened diaphragm should not extend across the width of the diaphragm beyond the line of attachment of a bearing stiffener by more than $15 t_p \varepsilon_p$, where:

- t_p is the thickness of the diaphragm plate
- $\varepsilon_p = (235/f_{yp})^{0.5}$
- f_{yp} is the nominal yield strength of the diaphragm plate,

H.2.3 Cross beams and cantilevers

Where the deck projects beyond the box web and is supported on cross beams and/or cantilevers which are in the plane of a diaphragm, the flanges of such members should provide a continuous

236

load path through each box web and across the diaphragm for the forces they are required to carry. These members should be assumed to be supported by the diaphragm/box web junctions (see H.7 and H.8).
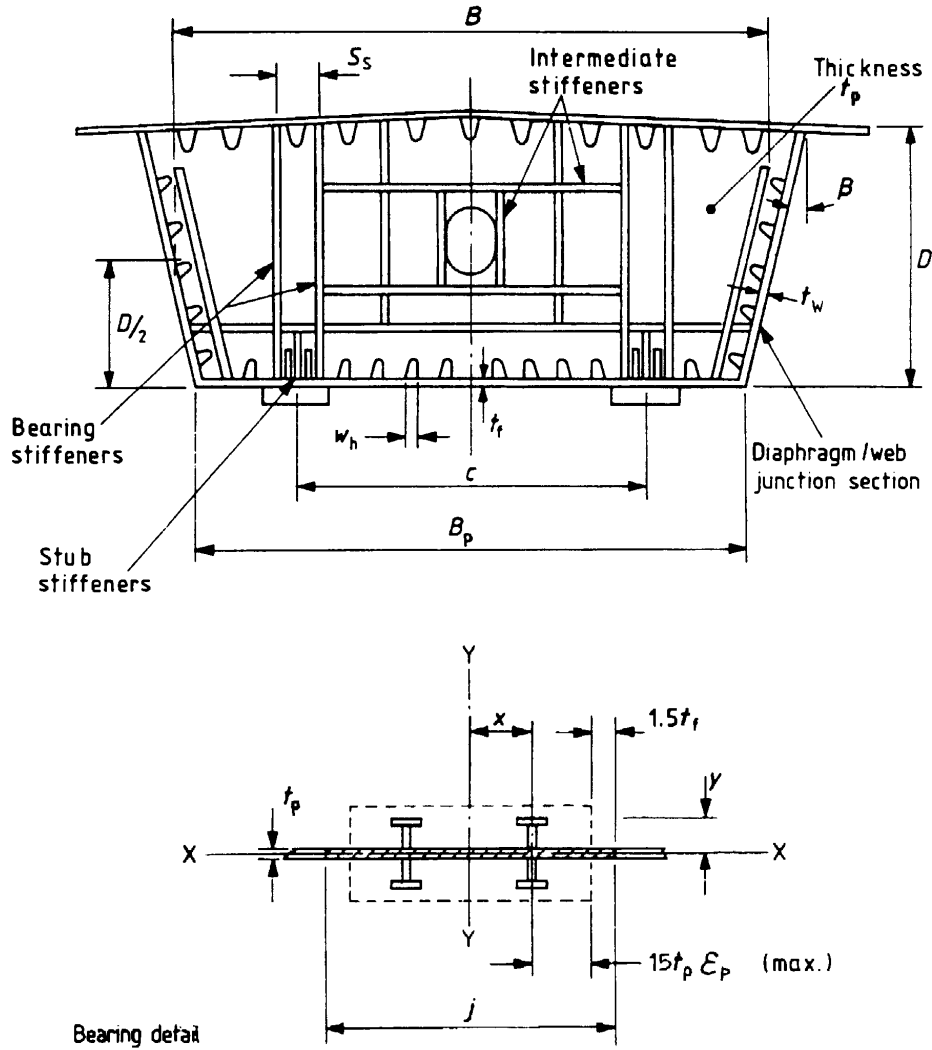
Figure I.20. Geometric notation for diaphragms [Fig. H.1]

237

H.2.4 Starter plates

Where starter plates are to be used to connect a diaphragm to the box walls, they should either be:

- a) positioned in the plane of the diaphragm and be butt-welded or connected by double cover plates to the diaphragm; or
- b) lap jointed to the diaphragm, provided that a suitable system of stiffening is designed to withstand, in addition to any other load effects, all the moments resulting from the eccentricity of connection.

H.2.5 Stiffeners to diaphragms

All stiffeners to plate diaphragms should be in accordance with 5.3.6.2 of ENV 1993-2. Bearing stiffeners should be symmetrically placed about the diaphragm plate, unless a special analysis is made of the effects of any eccentricity with respect to that plate.

H.2.6 Plating in diaphragms

The thickness of plating in an unstiffened diaphragm should be uniform throughout.

H.2.7 Openings in unstiffened diaphragms

Openings in unstiffened diaphragms should be in accordance with the following:

- a) only one circular opening may be provided on each side of the vertical centreline of the diaphragm within the upper-third of the height of the diaphragm;
- b) the diameter of any such opening should not exceed the least of: $6t_p$; D/20; B/20.
 where
    - tp is the diaphragm plate thickness
    - D is the depth of the diaphragm (see Fig. I.20)
    - B is the width of the diaphragm taken as the average of the widths at the top and bottom flange levels for boxes with sloping webs;
- c) cut-outs for longitudinal stiffeners on the box walls should have the stiffeners connected to the diaphragm plate by one of he following methods:
    - welding, along at least one-third of the perimeter of the cut-out;
    - cleating to the longitudinal stiffener with at least two bolts or rivets per side of the connection, or by full perimeter welding of the cleat.

In addition, the length of the free edge of any cut-out should not exceed $10t_p\varepsilon_p$, when any part of this free edge is within a distance $12t_p\varepsilon_p$, from any part of a bearing plate,
    where t_p is the diaphragm plate thickness.

H.2.8 Openings in stiffened diaphragms

Openings in stiffened diaphragms should be in accordance with the following.
    a) With the exception of openings permitted in item (d), openings should not be positioned within the areas shown shaded in Fig. I.21.
    b) Unstiffened openings should be circular and of diameter not exceeding the least of: $6t_p$; $a/20$; $b/20$.
    except when

$$\sigma_e \leq \frac{f_{yp}}{2\gamma_m}$$

for which the limiting diameter is twice the limits given above, where
a and b are the panel dimensions

$$\sigma_e = \sqrt{\sigma_{p1}^2 + \sigma_{p2}^2 - \sigma_{p1}\sigma_{p2} + 3\tau_p^2}$$

σ_{p1}, σ_{p2}, and τ_p are the stresses in the diaphragm plate derived in accordance with H.6.2 f_{yp} is the nominal yield strength of the diaphragm plate.
    Not more than one such opening should be positioned in a single plate panel.
    c) Stiffened openings should:
      - be framed on all sides by stiffeners;
      - have circular corners of radius at least one-quarter of the least dimension of the hole, with no re-entrant corners;
      - be positioned such that the distance of any edge from an adjacent wall of the box is at least 0.7 times the maximum dimension of the hole parallel to the wall, plus the distance from the wall to the tips of any cut-outs in the diaphragm for longitudinal stiffeners (see Fig. I.21), unless the adjacent plate is designed for secondary in-plane stresses.
    d) Cut-outs for longitudinal stiffeners should be in accordance with H.2.7(c).

H.3 Loading on diaphragms

H.3.1 Derivation

The load effects in diaphragms and associated parts of box girders should be derived from global analysis undertaken in accordance with 5.2 of ENV 1993-2. The design methods of H.5 and H.6 use strength provisions that are compatible only with the assumed methods of stress derivation contained therein. Stresses derived by finite element analyses should not be substituted directly for these derived stresses.
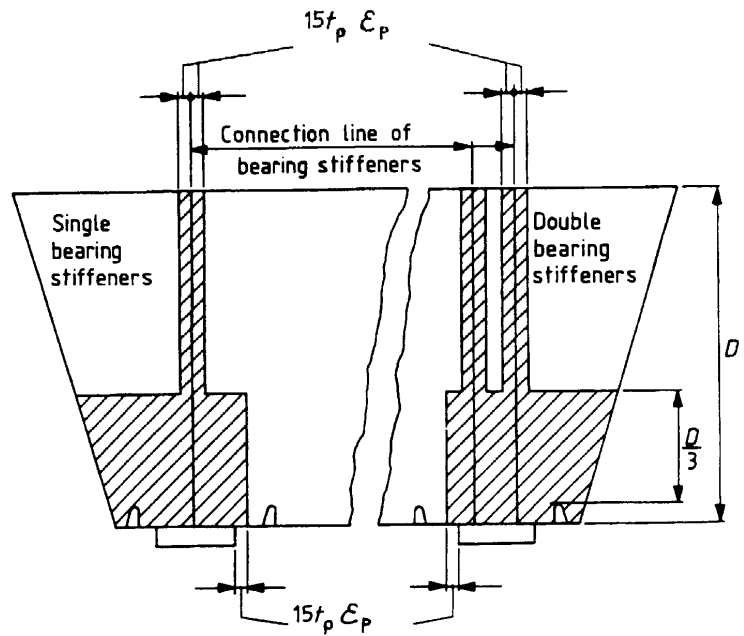
(a) Twin bearings
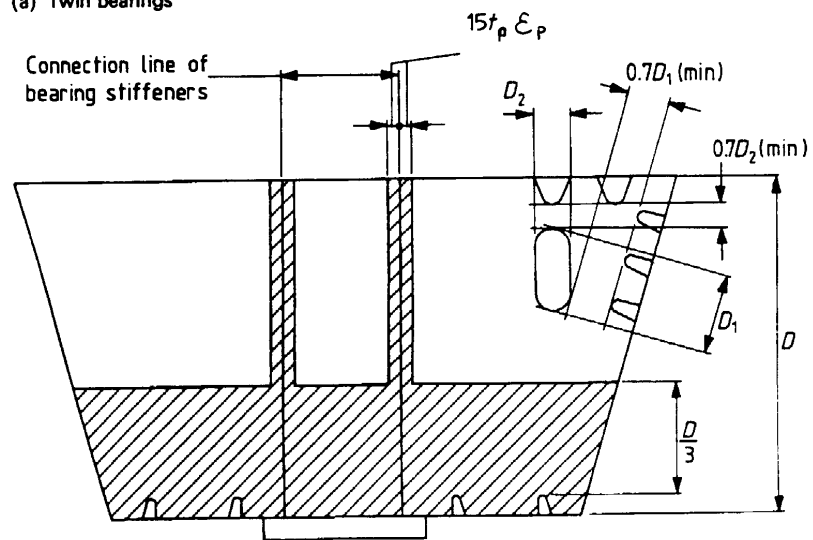
(b) Single central bearing and positioning of large openings

NOTE 1. Openings are not permitted in shaded areas.

NOTE 2. Dimensions are taken from top of cut-outs where present.

Figure I.21. Openings in stiffened diaphragms [Fig. H.2]

240

H.3.2 Effects to be considered

Diaphragms should be designed to resist, with due account being taken of any lack of symmetry in the cross section or in the bearing arrangement, the combined effects of the following.

   a) All externally applied loads and the associated bearing reactions.
   b) Changes in bearing reactions and web shears due to:
   – creep, shrinkage and differential temperature;
   – settlement and other movement of supports.
   c) Errors in installation of bearings, comprising:
   – bearing misalignment in plan;
   – errors in level of a single bearing, or in the mean levels of more than one bearing at any support;
   – bearing inclination;
   – departures from common planarity of twin or multiple bearings.
   d) Changes in longitudinal slope of box flanges at the diaphragm.
   e) Errors of longitudinal camber in continuous construction. Allowance for this may be made by assuming, at the bearings, a vertical displacement of a support relative to two adjacent supports of 1/5000 times the sum of the adjacent spans.
   f) Out-of-plane moments due to any or all of the following, as appropriate:
   – longitudinal movements of the bridge;
   – changes in slope of the bridge;
   – eccentricity due to bearing misalignment along the span or due to the shape of the bearing; the combined eccentricity for these may be taken as:
        - half the width of the flat bearing surface plus 10 mm for flat topped rocker bearing in contact with flat bearing surface; or
        - 3 mm for radiused upper bearing resting on flat or radiused lower part;
        - l0 mm for flat upper bearing resting on radiused lower part.
   – interconnection between deck and diaphragm stiffeners;
   – any intended eccentricity of the centroidal axes of the effective section of the bearing stiffeners with respect to the diaphragm plate.

H.4 Effective sections

H.4.1 General

For determining the stresses in a diaphragm, the effective elastic section modulus and effective area of a vertical cross-section, and the effective vertical and horizontal shear areas, should be derived in accordance with H.4.2 and H.4.3. For determining the stresses in stiffeners, their effective sections shall be derived in accordance with H.4.4 or H.4.5, as appropriate. In H.4.2 and H.4.3 the references to transverse tension and compression apply to directions normal to the longitudinal axis of the girder.

H.4.2 Vertical sections

The determination of the effective area A_e and the effective section modulus Z_e of a vertical cross-section of a diaphragm, should be based on effective areas of box flanges and diaphragm plate as given in H.4.2.2 to H.4.2.5.

In calculating an effective area of a box flange, an effective width we should be determined separately for each side of the diaphragm and should not exceed any of the following:
    a) one-quarter of the distance of the section under consideration from the nearest web/flange junction;
    b) half the distance to an adjacent diaphragm or cross beam for any flange in transverse tension, or for a composite flange in transverse compression;
    c) outside an end diaphragm, the actual width of plate provided;
    d) $15t_f\varepsilon_f$ for a non-composite flange in transverse compression. This limit may be increased to one-quarter of the distance to an adjacent diaphragm or cross beam provided that the transverse compressive stress (using the increased width) does not exceed the lesser of:
        - one-quarter of the longitudinal compressive strength of the flange;

$$- 0.5\left(\frac{t_f}{b}\right)^2 E$$

        where
        t_f is the thickness of the flange plate; $\varepsilon_f = (235/f_{yf})^{0.5}$; f_y is the nominal yield strength of the flange plate; b is the spacing of the longitudinal flange stiffeners or the distance between box webs for an unstiffened flange.

The effective area of a box flange should be determined as follows
    a) The effective area of steel plate on each side of the diaphragm should be taken as: $K_c t_f w_e$
    where
        - t_f is the flange thickness
        - w_e is the effective width on the appropriate side of the diaphragm derived from H.4.2.2
        - K_c is a coefficient taken as 1.0, except in the case of a non-composite flange in transverse compression with an effective width greater than $15t_f\varepsilon_f$ when the value of K_c should be obtained from Fig. I.22 with the dimension a taken as the spacing of longitudinal flange stiffeners and dimension *b* taken as the distance from the diaphragm to an adjacent cross beam or diaphragm. In using Fig. I.22, the restrained curve should be used for diaphragms at internal supports of continuous beams and the unrestrained curve for diaphragms at end supports
    b) Any transverse flange stiffeners within the effective width should be ignored.
    c) In composite construction, the effective flange area may include the area of steel reinforcement within the total effective width, and, if subjected to transverse compression, may also include the transformed area of concrete within the total effective width.
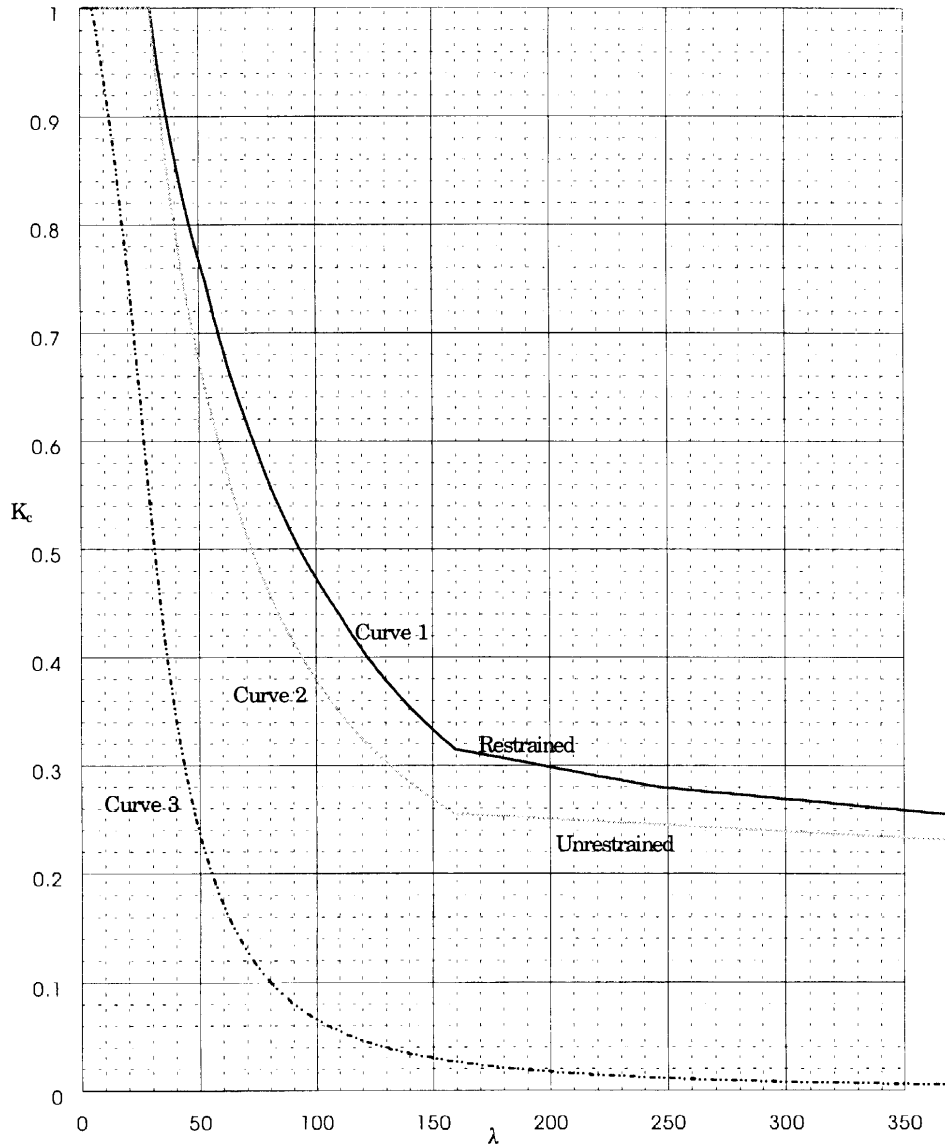
NOTE: The value of K_c to be used is the higher of the values obtained using either:
  (a) curve 1 or 2 as relevant, with $\lambda = b/(t_f\varepsilon_f)$ or
  (b) curve 3, with $\lambda = a/(t_f\varepsilon_f)$, where a is the panel dimension in the direction of stress considered; b is the panel dimension normal to the direction of stress.
(a) will always give the higher value for K_c when $a/b \geq 0.5$. For $a/b < 0.5$, (a) or (b) may give a higher value.

Figure I.22. Coefficient K_c for panels under direct compression [Fig. H.3]

243

Holes within the vertical section of a diaphragm should be deducted. When a stiffened opening is provided, diaphragm plating extending within the framing stiffeners by more than $15t_f\varepsilon_f$ should be ignored.

In the case of box girders with inclined webs, no part of the webs should be included in the vertical section of a diaphragm.

H.4.3 Shear area

The effective vertical and horizontal shear areas A_{ve} and A_{he} should be taken as the net areas of a vertical and horizontal cross section, respectively, of diaphragm plating only.

H.4.4 Diaphragm stiffeners

The effective section of a stiffener on a diaphragm should be taken to comprise the stiffener with widths of diaphragm plate on each side of the stiffener where available, not exceeding the lesser of:

    a) half the distance from the stiffener to an adjacent stiffener or to the wall of the box; or

    b) $15\varepsilon_p$ times the thickness of the diaphragm plate.

   Additionally, for a bearing stiffener, the effective width of plate assumed on the side towards the web should not exceed half the distance from the stiffener to the web/bottom flange junction. The sectional area of discontinuous diaphragm stiffeners should be ignored.

H.4.5 Diaphragm/web junction

The effective section of this part should be taken to comprise both of the following:

    a) a width of web plating each side of the diaphragm (where available) of up to 16 times the web thickness;

    b) the area of a stiffener, together with a width of diaphragm plate equal to $25t_p$, when there is a stiffener on the diaphragm parallel to the web within $25t_p$ of the web, or a width of diaphragm plate equal to $15t_p\varepsilon_p$ when there is no stiffener parallel to and within $25t_p$ of the web, where t_p is are the thickness of the diaphragm plate.

H.5 Unstiffened diaphragms

H.5.2 Reference values of in-plane stresses

The stresses in an unstiffened diaphragm, resulting from the load effects given in H.3, should be determined at the reference point indicated in Fig. I.23, in accordance with H.5.2.2 to H.5.2.4, for each of the appropriate reference stresses required.

The reference value of the in-plane <u>vertical stress</u> σ_{Rl} should be taken as follows:

    a) for a diaphragm with a single central bearing:

$$\sigma_{R1} = \frac{R_v\left(1 + 4\,e/t_p\right)}{\left(j - \sum w_h\right)t_p} + 0.77\left(\frac{T_b\,j}{2I_{yp}}\right)$$

    b) for a diaphragm with a pair of twin symmetrical bearings:

$$\sigma_{R1} = \frac{R_v\left(1 + 4\,e/t_p\right)}{\left(j - \sum w_h\right)t_p}$$

where

R_v is the total vertical load transmitted by the diaphragm to one bearing (including the effects of torque on twin bearings)

T_b is the torsional reaction at a single central bearing

j is the width of contact of the bearing pad plus 1.5 times the thickness of the bottom flange at each end if available (see Fig. I.20)

$\sum w_h$ is the sum of the widths of any cut-outs for stiffeners within the width j at the level immediately above the flange.

t_p is the thickness of the diaphragm plate

I_{yp} is the second moment of area of the diaphragm plate of width j excluding cut-outs, about the Y-axis (see Fig. I.20)

e is the eccentricity of bearing reaction along the span, which should include the effects of:

       - movements of the beam relative to the bearing due to changes in temperature;

       - changes in the point or line of contact at the spherical or cylindrical surface of a bearing due to slope of the beam when deflected by load;

       - uneven seating which may occur on a flat bearing surface;

       - inaccuracy which may occur in positioning of the beam relative to the bearing.
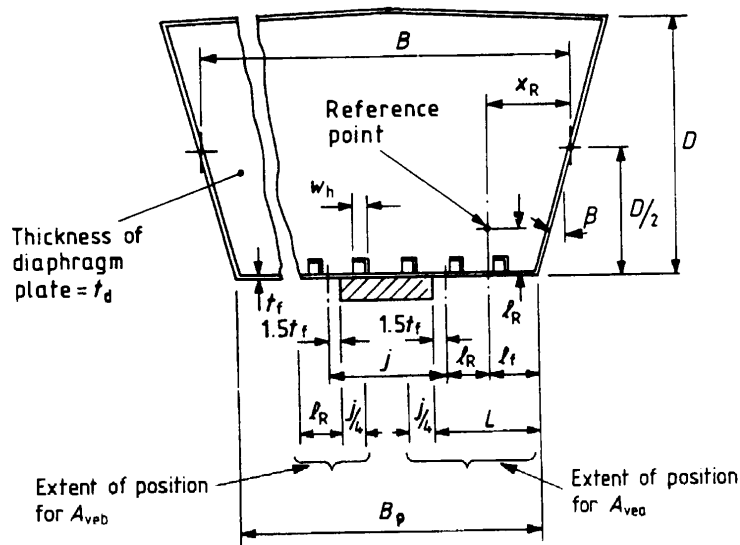
NOTE. ℓ_R is taken as the least of:

$$7{\cdot}5\,t_P\,\varepsilon_P\,,\ \frac{D}{8}\ \text{or}\ \frac{L}{2}$$

Figure I.23. Reference point and notation for unstiffened diaphragms [Fig. H.4]

245

The reference value of the in-plane <u>horizontal</u> stress σ_{R2} should be taken as:

$$\sigma_{R2} = \left[\left(\frac{K_p \sum R_v}{2} + \frac{T}{B}\right)x_R + Q_{fv}\frac{\ell_f}{2}\right]\frac{1}{Z_e} + \frac{\sum R_v \tan\beta}{2A_e}$$

where

K_p is a factor to allow for the effects of boundary shears and should be taken as 2.0 in the absence of any special analysis;

$\sum R_v$ is the total vertical force transmitted by the diaphragm to the bearings;

Q_{fv} is the vertical force transmitted to the diaphragm by the portion of the bottom flange over a width ℓ_f when there is a change of flange slope;

ℓ_f is the horizontal distance from the reference point to the nearest edge of the bottom flange;

B is as defined in H.2.7;

T is the torque transmitted to the diaphragm in shear through the box walls and from cross beam and/or cantilever loading;

x_R is the distance parallel to the bottom flange from the reference point to the web mid-point (see Fig. I.23);

Z_e and A_e are the effective section modulus and the effective area respectively of the diaphragm and flanges at the vertical cross section through the reference point, derived in accordance with H.4.2;

β is the inclination of the box web to the vertical.

a) Except as required by (b), the reference value of the in-plane <u>shear stress</u> τ_R should be taken as follows:

$$\tau_R = \left(\frac{\sum R_v}{2} + Q_{fv} + \frac{T}{2B}\right)\frac{1}{A_{vea}} + \frac{Q_h}{A_{he}}$$

where

$\sum R_v$, Q_{fv} and T are as defined above;

B is as defined in H.2.7;

Q_h is the shear force due to transverse horizontal loads on the bridge transmitted from the top flange to the diaphragm;

A_{vea} is the minimum value of the effective vertical shear area, as given in H.4.3, for any section of diaphragm plating taken between the web and a point $j/4$ inside the outer edge of the bearing (see Fig. I.23);

j is as defined above;

A_{he} is the effective horizontal shear area, as given in H.4.3 for the section of diaphragm plating through the reference point.

b) In addition, in the case of diaphragms on twin symmetrical bearings where there is a change in slope of the bottom flange, an alternative value τ_{Rf} should be derived from:

$$\tau_{Rf} = \left(\frac{T}{c} + \frac{Q_{bv}}{2} - \frac{T}{2B} \right) \frac{1}{A_{veb}} + \frac{Q_h}{A_{he}}$$

where

T   is as defined above;

Q_{bv} is the total vertical force transmitted to the diaphragm by the portion of the bottom flange between the inner edges of the bearings when there is a change in flange slope;

c   is the distance between centres of bearings;

A_{veb} is the minimum value of the effective vertical shear area, as given in H.4.3, for any section of diaphragm plating taken within a distance ℓ_R from the inner edge of a bearing (i.e. towards the diaphragm centreline) and a distance $j/4$ inside the same inner edge of the bearing (see Fig. I.23);

ℓ_R is as defined in Fig. I.23.

This value τ_{Rf} should be adopted if it exceeds the value of τ_R determined in (a).

H.5.3 Buckling coefficient

In checking the adequacy of an unstiffened plate diaphragm, a coefficient *K* is required which is given by:

$K = K_1 K_2 K_3 K_4$

where

$$K_1 = 3.4 + \frac{2.2D}{B_p} \; ;$$

$$K_2 = 0.4 + \frac{j}{2B_p} \text{ for single central bearings;}$$

$$K_2 = 0.4 + \frac{c - j/3}{B_p} \text{ for twin bearings;}$$

$$K_3 = 1.0 - \frac{\beta}{100} \; ;$$

$$K_2 = 1.0 - \frac{fP_p}{\sum R_v + T/\ell_b} \left(\frac{2B}{B_p} - 1 \right) \; ;$$

D, B_p, B and β (in degrees) are as defined in Fig. I.23;

j   is as defined above;

f   = 0.55 when $D/B \leq 0.7$;

       = 0.86 when $D/B \geq 1.5$ with intermediate values found by linear interpolation

ℓ_b = $j/2$ for single central bearings, or

       = c for twin bearings

$\sum R_v$ and T are as defined above

c   is the distance between centres of bearings

$$P_p = W_p + \sum\left(\frac{P}{K_5}\right)$$

W_p is the total uniformly distributed load applied to the top of the diaphragm

P   is any local load applied to the top of a diaphragm

$$K_5 = 0.4 + \frac{w}{2B - B_p}$$

w   is the actual width of the load *P* plus an allowance for the dispersal through a concrete flange ac an angle of 45° to the vertical, and through a steel flange at an angle of 60° to the vertical.

H.5.4 Yielding of diaphragm plate

The value of σ_{Rl} and $\sqrt{\sigma_{R2}^2 + 3\tau_R^2}$ should not exceed the lesser of:

$$\frac{f_{yp}}{\gamma_m}, \qquad \text{or} \qquad \frac{f_{yp}}{\gamma_m}\left[1.2 - \frac{\left(\sum R_v + T/\ell_b\right)D}{1.25KEt_p^3}\right]$$

where

σ_{Rl}, σ_{R2} and τ_R are the reference values of stress and T are as defined above

$\sum R_v$ and K are as derived in H.5.3

D   is as defined in Fig. I.23

t_p and f_{yp} are, respectively, the thickness and nominal yield strength of the diaphragm plate.

H.5.5 Buckling of diaphragm plate

The value of $\sum R_v + T/\ell_b$ should not exceed: $\dfrac{0.7KEt_p^3}{D\gamma_m}$

where

ℓ_b and K are as derived in H.5.3

t_p is the thickness of the diaphragm plate

D   is as defined in Fig. I.23

$\sum R_v$ and T are as defined above.

H.6 Stiffened diaphragms

H.6.1 General

Diaphragms in accordance with H.2.1 to H.2.6 and H.2.8 and stiffened by an orthogonal system of stiffeners, generally as indicated in Fig I.20, should be designed such that the diaphragm plate meets the yield criterion of H.6.4 and the buckling criterion of H.6.5, using the appropriate stresses determined from H.6.2.

In addition, all types of stiffeners, as defined in (a), (b) and (c) below, should be designed such that they meet the yield criterion of H.6.6 and the buckling criterion of H.6.7, using the appropriate stresses determined from H.6.3. Web/flange junctions should, additionally, be in accordance with H.7.3 and H.7.4.

Stiffening may consist of (see Fig. I.23):

a) bearing stiffeners, which span from a box flange immediately above a bearing, to the flange at deck level;

b) stub stiffeners, which are short vertical stiffeners above bearings;

c) intermediate stiffeners, which may be either primary or secondary. Stiffeners spanning between box walls or, if horizontal, between a box web and a bearing stiffener, or between bearing stiffeners should be treated as primary. All other stiffeners should be treated as secondary.

H.6.2 Stresses in diaphragm plates

Vertical stresses σ_{p1} may be neglected with the exception of those due to:

a) a change in slope of the main girder flange; and

b) local wheel loads applied above the diaphragm, which should be calculated in accordance with 4.4 of ENV 1993-1-5.

Horizontal stresses σ_{p2} should be calculated under the action of the following.

a) The in-plane primary moment M on the diaphragm which should be taken as:

$$M = \left(K_p Q_v + 2Q_T\right)x_w + K_p Q_c x_c + \sum_{i=1,n}\left(P_i x_i\right) - R_v x_b + \left(\frac{Q_{fv}\ell_f}{2}\right)$$

where (as shown in Fig. I.24)

Q_v is the total vertical component of symmetric shear transmitted into the diaphragm from one web

Q_T is the vertical component of torsional shear transmitted into the diaphragm from one web, given by T/(2B)

x_w is the horizontal distance, from the section under consideration to the mid point of the web

Q_c is the vertical component of any cross beam or cantilever shear

x_c is the horizontal distance from the section under consideration to the root of the cross beam or cantilever

P_i is a locally applied deck load between the section under consideration and the web

x_i is the horizontal distance from the section under consideration to the locally applied deck load P_i;

R_v is the total vertical load transmitted to one bearing by the diaphragm

x_b is the distance from the section under consideration to the inner edge of the nearest bearing plus $j/4$ for sections between"uwin bearings, or is zero for all other sections, and for diaphragms with a single bearing

Kp, Q_{fv}, and ℓ_f are as defined above

j is as defined above

The horizontal bending stress σ_{2b} should be taken as:

$$\sigma_{2b} = \frac{M}{Z_e}$$

where

Z_e is the effective section modulus of a vertical cross-section of the diaphragm and flanges, at the point under consideration, derived in accordance with H.4.2.

b) The horizontal component of girder shear when the webs are inclined. The horizontal stress σ_{2q} from this component should be taken as:

$$\sigma_{2q} = \frac{Q_v \tan\beta}{A_e}$$

where

Q_v is as defined in (a)

A_e is the effective area of a vertical cross section of the diaphragm and flanges, at the point under consideration, derived in accordance with H.4.2

β is the inclination of the box web to the vertical.

The <u>total horizontal stress</u> σ_{p2} at the point under consideration should be taken as:

$$\sigma_{p2} = \sigma_{2b} + \sigma_{2q}$$
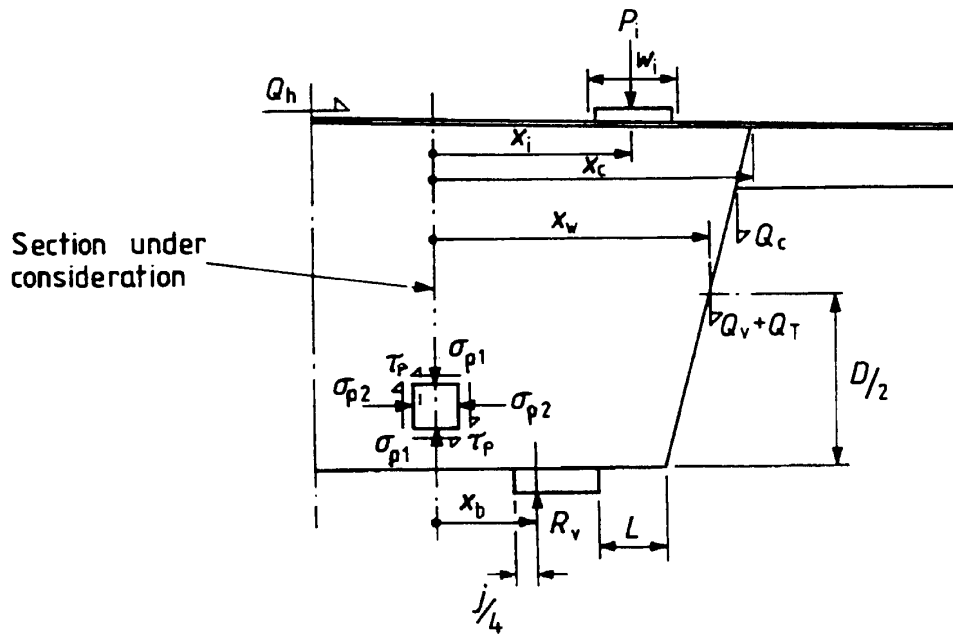
Figure I.24. Load effects and notation for stiffened diaphragms [Fig. H.5]

250

<u>Shear stresses</u> should be calculated under the action of the shear flow q at the section of the diaphragm under consideration. This shear flow q should be taken as constant over the net depth or width of the diaphragm, and as follows:

a) In sections between a box web and an outer bearing stiffener:

$$q = \frac{Q_v + Q_T + Q_{fv} + Q_c + \sum P_i}{D_e} + \frac{Q_h}{B_e}$$

b) In sections between inner bearing stiffeners where there are twin bearings:

$$q = \left(\frac{Q_v}{4} + \frac{Q_{bv}}{2} + \frac{T}{c} - Q_T \right) \frac{1}{D_e} + \frac{Q_h}{B_e}$$

c) In sections between pairs of bearing stiffeners above one of a pair of bearings, up to the height of longitudinal flange stiffener cut-outs:

$$q = \left(\frac{5Q_v}{8} + \frac{T}{2c} \right) \frac{1}{D_e} + \frac{Q_h}{j - \sum w_h}$$

d) In sections between pairs of bearing stiffeners above a single bearing, up to the height of longitudinal flange stiffener cut-outs:

$$q = \left(\frac{Q_v}{4} + \frac{T}{s_s} - Q_T \right) \frac{1}{D_e} + \frac{Q_h}{j - \sum w_h}$$

where
Q_v, Q_T, Q_c, P_i, Q_{fv}, T, Q_h, Q_{bv} and c are defined above
D_e and B_e are the net depth and width of the diaphragm at the point under consideration
j and $\sum w_h$ are defined above
s_s is the distance between stiffener centroids.

The shear stress τ_p in the sections referred to in above mentioned (a), (b), (c) or (d) should be taken as:

$$\tau_p = \frac{q}{t_p}$$

where t_p is the thickness of the diaphragm plate in the panel under consideration.

In sections other than those referred to in above mentioned (a), (b), (c), or (d) τ_p may be neglected.

<u>*H.6.3 Stresses in diaphragm stiffeners*</u>

<u>Vertical stresses in bearing stiffeners</u> σ_{1s} in a bearing stiffener should be taken as:

$$\sigma_{1s} = \frac{P_s}{A_{se}}$$

where
P_s is the total vertical force in the group of bearing stiffeners
A_{se} is the effective cross-sectional area of the group of bearing stiffeners, derived in accordance with H.4.4.

In the absence of openings in the diaphragm between the group of bearing stiffeners and the adjacent web, the vertical force P_s may be assumed to vary linearly from the value of the reaction at the bearing to the value of any reaction transmitted from the deck to the top of the bearing stiffener.

If there are any openings in the diaphragm between the group of bearing stiffeners and the adjacent web, no variation of load over the depth of such openings should be assumed. The variation over the remaining parts of the diaphragm should be assumed to be linear of constant slope. In the case of a diaphragm above a single bearing, an additional vertical stress σ_{1sT} in a bearing stiffener should be taken as:

$$\sigma_{1sT} = \frac{T_s x}{I_{yse}}$$

where

T_s is the value of the moment in the plane of the diaphragm on the group of bearing stiffeners

x   is the horizontal distance of the stiffener under consideration from the centroidal axis, normal to the plane of the diaphragm, of the stiffener group (see Fig. I.20)

I_{yse} is the effective second moment of area of the stiffener group about the same centroidal axis, derived in accordance with H.4.4.

Where stub stiffeners are used, the stress calculated as above may be reduced locally by including the area of such stiffeners, provided their connections to the diaphragm plate are adequate to transfer their share of the bearing reaction.

The bending stresses in bearing stiffeners σ_{bs} in a bearing stiffener due to an out-of-plane moment should be taken as:

$$\sigma_{bs} = \frac{M_s y}{I_{xse}}$$

where

M_s is the proportion of the out-of-plane moment carried by the group of bearing stiffeners

y   is the distance of the extreme fibre of the stiffener under consideration from the centroidal axis, parallel to the plane of the diaphragm, of the stiffener group (see Fig. I.20)

I_{xse} is the effective second moment of area of the stiffener group about the same centroidal axis, derived in accordance with H.4.4.

A proportion of the out-of-plane moment may be assumed to be carried by the flange longitudinal stiffeners, provided due account is taken of this in their design. Stub stiffeners should not be considered to carry any part of the out-of-plane moment carried by a bearing stiffener group unless they have an adequate out-of-plane shear connection to the bearing stiffeners and/or the box walls.

The equivalent axial stress for buckling check σ_{se} to be used in the buckling check of all stiffeners, should be taken as the maximum value within the middle-third of the length ℓ_s, of the stiffener, calculated from:

$$\sigma_{se} = \sigma_a + \frac{1}{A_{se}}\left[\frac{\sigma_q \ell_s^2 t_p k_s}{\alpha_{max}}\left(1 + \frac{\sum A_s}{\ell_s t_p}\right) + \tau_h t_p h_h\right]$$

where, for all stiffeners,

A_{se} is the effective cross-sectional area of the stiffener derived in accordance with H.4.4

ℓ_s is the length of the stiffener between points of effective restraint

t_p is the thickness of the diaphragm plate

k_s is obtained from Fig. I.25 using the slenderness parameter $\lambda = \ell_s / r_{se}\varepsilon_s$,

r_{se} is the radius of gyration of the effective section of the stiffener about its centroidal axis parallel to the plane of the diaphragm, derived in accordance with H.4.4

ε_s $= (235/f_{ys})^{0.5}$

f_y is the nominal yield strength of the stiffener.

$\sum A_s$ is the sum of the areas of all stiffeners which intersect the stiffeners being designed, within the length ℓ_s not including any adjacent diaphragm plate

σ_{p2} is derived above, for the level being considered, and taken as positive when compressive

σ_{2s} is the average value of σ_{p2} within the middle-third of the length ℓ_s

σ_a, σ_q, α_{max}, τ_h and h_h are defined as follows for the appropriate type of stiffener.

(a) For bearing stiffeners:
   σ_a $= \sigma_{1s} + \sigma_{1sT}$, σ_{1s} and σ_{1sT} are as derive above
   σ_q $= \sigma_{2s}$
   α_{max} is the maximum spacing of vertical stiffeners which would ensure the adequacy of the diaphragm plate and any horizontal stiffeners, and may conservatively be taken as the actual spacing of vertical stiffeners
   τ_h and h_h are taken as zero.

(b) For all intermediate stiffeners:
   α_{max} is one-half of the sum of the panel widths on each side of the stiffener. Where the widths vary over the length ℓ_s, the average value of the middle-third should be used
   τ is the average shear stress in the panels on either side of the stiffener
   τ_h is zero except in the case of the stiffeners framing openings where τ_h is the shear stress which would occur in the plating adjacent to the stiffener if the opening had been fully plated
   h_h is zero except in the case of the stiffeners framing openings where h_h is the dimension of the opening parallel to the stiffener.

253
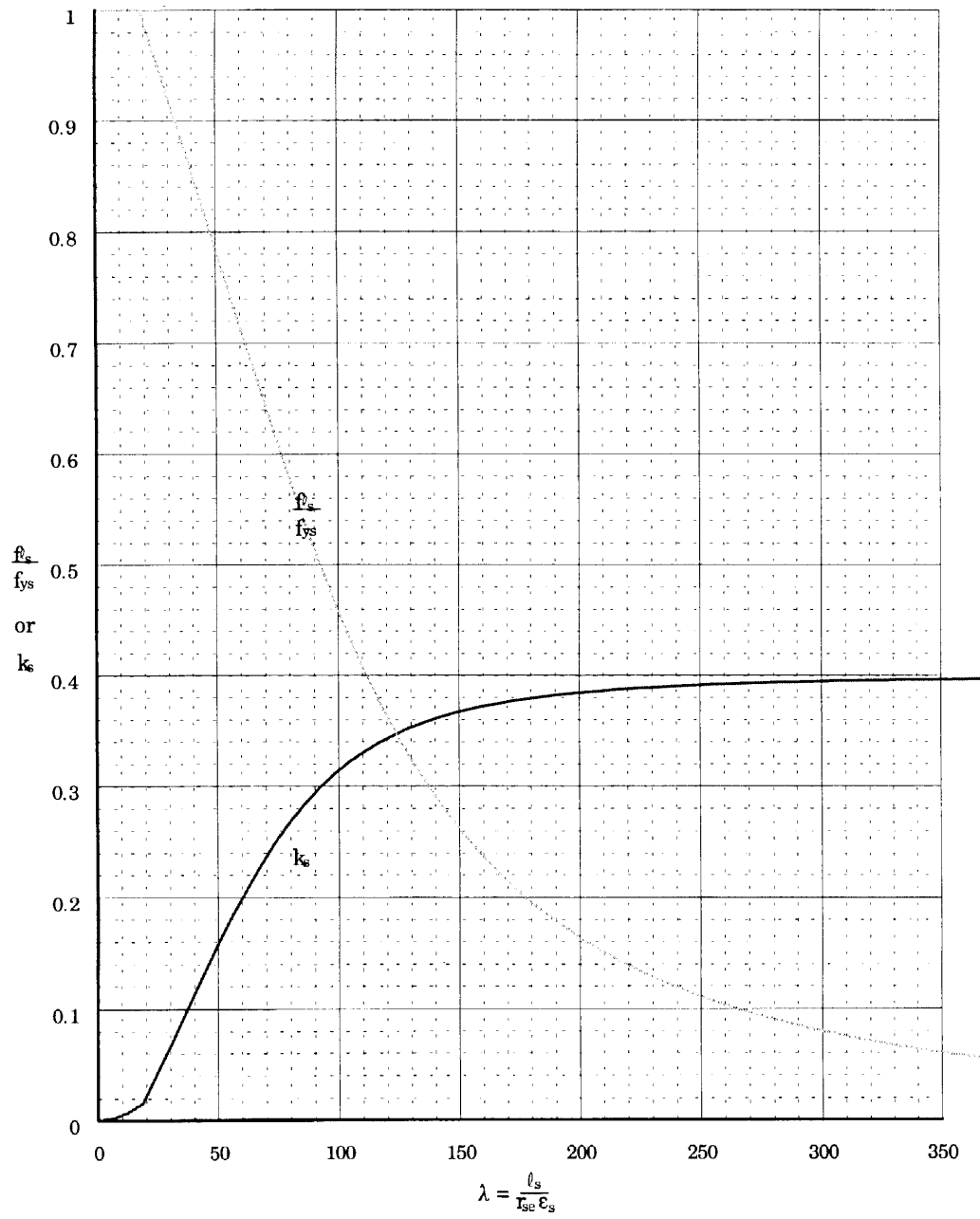
Figure I.25. Parameters for the design of diaphragm stiffeners [Fig. H.6]

(c) For horizontal intermediate stiffeners only:

$$\sigma_a \quad = \sigma_{p2}$$
$$\sigma_q \quad = \tau$$

(d) For vertical intermediate stiffeners only:

$$\sigma_a \quad = 0$$

$$\sigma_q = \tau + \sigma_{2s} + \frac{\sigma_{2b.max} + \sigma_{2b.min}}{12}$$

$\sigma_{2b\ max}$ and $\sigma_{2b\ min}$ are the maximum and minimum values of σ_{2b} derived above, within the length ℓ_s and taken as positive when compressive.

H.6.4 Yielding of diaphragm plate

Plate panels between stiffeners, or between stiffeners and the box walls, should be designed such that at all points in every panel:

$$\sigma_{p1}^2 + \sigma_{p2}^2 - \sigma_{p1}\sigma_{p2} + 3\tau^2 \leq \left(\frac{f_{yp}}{\gamma_m}\right)$$

where

σ_{p1} = σ_{1s} + σ_{q1sT} for parts of plate panels forming part of the effective section of any bearing stiffener, or is the vertical in-plane stress due to local deck loads and change in flange slope, if relevant, for all remaining parts of plate panels

σ_{1s} is defined above

σ_{1sT} is as derived above, but with the value of x in that clause taken as the dimension from the centroidal axis to the extreme fibre of the effective section of the stiffener group

σ_{p2} is defined above

τ_p is defined above

f_{yp} is the nominal yield strength of the diaphragm plate.

H.6.5 Buckling of diaphragm plate

Plate panels need not be checked for buckling provided that:
  a) the cross section of the girder is nominally rectangular;
  b) the ratio of the depth of the diaphragm D to the minimum plate thickness t_p is less than 100 ε_p
  c) the overhang L (see Fig. I.23 or I.24) from the outer edge of the bearing to the box web is less than $D/2$;
  d) stiffening is limited to the bearing stiffeners themselves, and any member providing continuity of cross beam or cantilever flanges through the diaphragm;
  e) there is no change in flange slope at the diaphragm.

A bearing stiffener section should be designed such that, at any point along its length:

$$\sigma_{ls} + \sigma_{lsT} + \sigma_{bs} \leq \frac{f_{ys}}{\gamma_m}$$

where

σ_{ls} and σ_{lsT} are as defined above

σ_{bs} is as defined above

f_{ys} is the nominal yield strength of the stiffener.

The bearing stress at the point of contact with a flange should be verified in accordance with 4.4.6(6) of ENV 1993-1-5.

H.6.7 Buckling of diaphragm stiffeners

The stiffener section should be such that, at any point within the middle-third of the length of the stiffener:

$$\frac{\sigma_{se}}{f_{ls}} + \frac{\sigma_{bs}}{f_{ys}} \leq \frac{1}{\gamma_m}$$

where

σ_{se} is as defined above

σ_{bs} is as defined above for a bearing stiffener, or is taken as zero for an intermediate stiffener

f_{ls} is obtained from Fig. I.25 using the slenderness parameter $\lambda = \ell_s / r_{se}\varepsilon_s$,

ℓ_s is the length of the stiffener between points of effective restraint

r_{se} is the radius of gyration of the effective section of the stiffener about its centroidal axis parallel to the plane of the diaphragm, derived in accordance with H.4.4.

H.7 Diaphragm/web junctions

The diaphragm/web junction should be designed as a stiffener to the box web, spanning between box flanges, unsupported in the plane of the diaphragm, and with effective section derived as in H.4.5.

H.7.2 Loading effects to be considered

The junction should withstand the effects of the following.

    a) All loads transmitted to the diaphragm from the cross beams and/or cantilevers in the plane of the diaphragm. Such loads should be assumed to be applied at the centroidal axis of the effective section, and to vary linearly from a maximum at the top of the junction, to zero at the bottom.

b) Any forces resulting from tension field action in the adjacent web panels. Such forces should be assumed to be applied in the plane of the box web, and to be constant over the height of the junction.

c) An equivalent axial force representing the destabilizing influence of the web. This force should be assumed to be applied at the centroidal axis of the effective section, and to be constant over the height of the junction.

H.7.3 Strength of diaphragm/web junction

The maximum stress at any point on the cross section of the junction, at any section in its length, should not exceed f_{ys}/γ_m, where f_{ys} is the nominal yield strength of the junction section.

The effective junction section should be such that:

$$\frac{P}{A_{se}f_{\ell s}} + \frac{M}{Z_{se}f_{ys}} \le \frac{1}{\gamma_m}$$

where

P and M are, respectively, the maximum force on the effective junction section and the maximum moment about the centroidal axis parallel to the web due to all the effects specified in H.7.2, within the middle-third of the length of the junction

A_{se} is the effective area of the junction section (see H.4.5)

Z_{se} is the lowest section modulus of the effective junction section about the centroidal axis parallel to the web (see H.4.5)

$f_{\ell s}$ is obtained from Fig. I.25 using the slenderness parameter $\lambda = \ell_s /r_{se}\varepsilon_s$,

ℓ_s is the total length of the junction section

r_{se} is the radius of gyration of the effective junction section about its centroidal axis parallel to the web, derived in accordance with H.4.5

f_y,   is the nominal yield strength of the junction section.

H.7.4 Junction restraint provided by diaphragm stiffeners

Diaphragm/web junctions should be designed in accordance with H.7.1 to H.7.3, except that full width horizontal stiffeners in the diaphragm may be assumed to offer restraint to the junction in the plane of the diaphragm, provided that the equivalent axial stress σ_{se} in such stiffeners is increased by an amount equal to:

$$\frac{0.025P}{nA_{se}}$$

where

P is as defined in H.7.3

n is the number of full width horizontal stiffeners

A_{se} is the effective area of the horizontal stiffeners, derived in accordance with H.4.4.

In this case ℓ_s in H.7.3 may be taken as the distance between such stiffeners.

H.8 Continuity of cross beams and cantilevers

When continuity of cross beams and cantilevers is provided in the plane of a diaphragm, in accordance with H.2.3, that portion within the box walls should be in accordance with the following.

a) The force in the member providing continuity to the bottom flange of the transverse member should be taken as the moment in the transverse member at the box wall divided by the distance between the mid-plane of the top and bottom flanges of the member. If the force is different at the two box walls a linear variation along the length may be assumed.

b) If the member providing the continuity in (a) is also required as a horizontal stiffener for a diaphragm designed in accordance with H.6, it should be designed to withstand, in addition to the load given in (a), an axial force equal to $A_{se}\sigma_{se}$.

where

   A_{se} is the effective cross-sectional area of the continuity member derived in accordance with H.4.4

   σ_{se} is as specified above.

c) The member providing the continuity in (a) should be designed as a compression member in accordance with 5.5.1 of ENV1993-1-1, and should be assumed to be unrestrained out of the plane of the diaphragm unless provided with effective intermediate restraint. If these restraints are provided by bearing or primary vertical diaphragm stiffeners, such stiffeners should each be designed to resist, in addition to all other forces given in H.I.3, a force equal to 2.5% of the maximum axial load in the continuity member including that given in (b), if appropriate. This force should be applied, out of the plane of the diaphragm, at the point of intersection of the continuity member and the stiffener providing the restraint. The stiffener should be designed to satisfy the criterion:

$$\frac{\sigma_{se}}{f_{\ell s}} + \frac{\sigma_{bs} + \sigma_{b2}}{f_{ys}} \leq \frac{1}{\gamma_m}$$

where

   σ_{b2} is the bending stress induced in the stiffener by the above force, taken as the maximum value within the middle-third of the lengths of the stiffener

   σ_{bs}, $f_{\ell s}$, σ_{se}, and fys are as defined in H.I.7.

Appendix II.

Eurocode 3: Design of steel structures – Part 1.5 (EC3-1-5)
Planar plated structures without transverse loading
[prENV 1993-1-5:1997]

Extract

II.1 General

Definitions

For the purpose of this standard, the following definitions apply:

elastic critical stress: Stress at which an elastic structure without imperfections becomes unstable according to small deformation theory.

gross cross-section: The total cross-sectional area of a member but excluding longitudinal stiffeners that are not continuous, battens and splice material.

effective cross-section: The gross cross-section reduced for the effects of plate buckling and shear lag.

membrane stress: Stress at mid-depth of the plate.

plated structure: A structure that is built up from nominally flat plates which are welded together. The plates may be stiffened or unstiffened.

stiffener: A plate or rolled section attached to a plate with the purpose of delaying or preventing buckling of the plate or reinforcing it against local loads. A stiffener is denoted:

- longitudinal if its direction is parallel to that of the member;
- transverse if its axis is perpendicular to that of the member.

stiffened plate: Plate with transverse and/or longitudinal stiffeners.

subpanel: Unstiffened plate surrounded by flanges or stiffeners.

Symbols

Complementary to those given in ENV 1993-1-l, the following symbols are used:

A_{s1} is the total area of all the longitudinal stiffeners within the flange width b_0;

A_{st} is the gross cross sectional area of one transverse stiffener;

A_{eff} is the effective cross-section area;

b is the width of the plate;

b_w is the clear width between welds;

b_{eff} effective width for elastic shear lag;

F_{Sd} is the design transverse force;

f_{yd} is the design value of the yield strength f_y/γ_{M1}. Further index f and w indicate flange and web, respectively;

h_w is the clear web depth between flanges;

L_{eff} is the effective length for resistance to transverse forces;

$M_{f.Rd}$ is the design plastic moment resistance of a cross-section consisting of the flanges only;

$M_{pl.Rd}$ is the plastic resistance of the cross-section (irrespective of cross-section class);

M_{Sd} is the design bending moment;

N_{Sd} is the design axial force;

t is the thickness of the plate;

t_{eff} is the effective thickness for shear buckling;

V_{Sd} is the design shear force;

W_{eff} is the effective section modulus;
β is the effective width factor for elastic shear lag;
η is the relation between resistance in shear and yield strength in tension;
$\gamma_{M,ser}$ is the partial factor for resistance at serviceability states.

II.2 Basis of design

Modelling for elastic global analysis

The effects of shear lag and of local buckling on the stiffness shall be taken into account if this significantly influences the global analysis. The effects of shear lag of flanges in elastic global analysis may be taken into account by the use of an effective width. For simplicity this effective width may be assumed to be uniform over the length of the beam.

For each span of a beam the effective width of flanges should be taken as the lesser of the full width and *L*/8 per side of the web, where *L* is the span or twice the distance from the support to the end, for a cantilever. For the global analysis the effect of plate buckling on the stiffness may be ignored in normal plated structures. If the effective cross-sectional area according to 4.2 of an element in compression is less than 0,5 times the gross cross-sectional area, the reduction of the stiffness due to plate buckling should be considered.

Verification of cross-sectional resistance

<u>General</u>

At ultimate limit states the verification of cross-sectional resistance shall take the following effects into account:

    a) longitudinal stresses $\sigma_{x,Ed}$ considering shear lag and plate buckling
    b) transverse stresses $\sigma_{z,Ed}$ considering their distribution and plate buckling
    c) shear stresses τ_{Ed} considering plate buckling
    d) combined effects of a), b) and c) acting in the same cross-section where relevant.

The verification should in general be performed as follows

$$\eta_1 = \frac{\sigma_{x,Ed}}{f_{yd}} = \frac{N_{Sd}}{f_{yd}A_{eff}} + \frac{M_{Sd} + N_{Sd}e_N}{f_{yd}W_{eff}} \le 1,0 \qquad \text{/II.1/}$$

$$\eta_2 = \frac{\sigma_{z,Ed}}{f_{vwd}} = \frac{F_{Sd}}{f_{vwd} \cdot L_{eff} \cdot t} \le 1,0 \qquad \text{/II.2/}$$

$$\eta_3 = \frac{\tau_{Ed}}{f_{ywd}} = \frac{V_{Sd}}{f_{ywd} \cdot b \cdot t_{eff}} \le 1,0 \qquad \text{/II.3/}$$

where:
A_{eff} is the effective cross-section area;
b is the width of the plate (for a web the clear distance between flanges);
e_N is the shift in the position of neutral axis;

F_{Sd} is the design transverse force;
f_{yd} is the design yield strength f_y/γ_{Ml};
L_{eff} is the effective length for resistance to transverse forces;
M_{Sd} is the design bending moment;
N_{Sd} is the design axial force;
t is the thickness of the plate;
t_{eff} is the effective thickness for shear buckling;
V_{Sd} is the design shear force including shear from torque;
W_{eff} is the effective section modulus.

Longitudinal stresses at ultimate limit states

In calculating longitudinal stresses, account should be taken of the effects of shear lag and plate buckling by the use of an effective width. The effective area A_{eff} should normally be determined assuming a cross-section subject only to stresses due to axial compression N_{Sd}. For non-symmetrical cross-sections, the possible shift e_N of the centroid of the effective area A_{eff} relative to the centre of gravity of the gross section, see Fig. II.1. The resulting additional moment should be taken into account in the cross-section verification using expression /II.1/. The effective section modulus W_{eff} should normally be determined assuming a cross-section subject only to bending stresses due to M_{Sd}, see Fig. II.2.

As an alternative the effective cross-section may be determined for the resulting state of stress from N_{Sd} and M_{Sd} acting simultaneously. The effects of e_N should be taken into account.

The stress in a flange should be calculated using the elastic section modulus with reference to midline of the flange. Hybrid girders may have flange material with yield strength f_{yf} up to 2 f_{yw} provided that:

a) the increase of flange stresses caused by yielding of the web is taken into account
b) f_{yf} (rather than f_{yw}) is used in determining the effective area of the web.

In hybrid girders, the increase of deformations due to yielding of the web may be ignored.
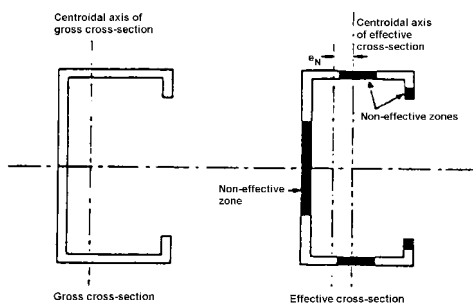
Figure II.1. Class 4 cross-sections [Fig. 2.1]
– axial force
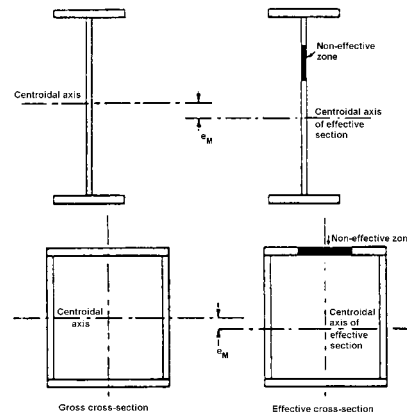
Figure II.2. Class 4 cross-sections [Fig. 2.2]
– bending moment

262

Verification methods for interaction

Provided that η_3 does not exceed 0,5 the design resistance to bending moment and axial force need not be reduced to allow for the shear force. If η_3 is more than 0,5 the combined effect of bending and shear in a web of an I or box girder should satisfy:

$$\eta_1 + \left[1 - \frac{M_{fRd}}{M_{plRd}}\right][2\eta_3 - 1]^2 \leq 1,0 \qquad \text{/II.4/}$$

where:

$M_{f.Rd}$ is the design plastic moment resistance of a cross-section consisting only of the flanges;

$M_{pl.Rd}$ is the plastic resistance of the cross-section (irrespective of cross-section class).

The above criterion should be fulfilled in every cross-section, but it need not be checked closer to an interior support than $h_w/2$. The plastic resistance $M_{f.Rd}$ of the cross-section consisting of the flanges only should be taken as the design yield strength times the effective area of the smaller flange times the distance between the centroids of the flanges.

If an axial force N_{Sd} is applied, then $M_{pl.Rd}$ should be replaced by the reduced plastic resistance moment $M_{N.Rd}$ according to 5.4.8.1 (2) of ENV 1993-1-1:1992 and M_{fRd} should be reduced according to 4.3.4(2). If the axial force is so large that the whole web is in compression the above mentioned plastic resistance $M_{f.Rd}$ should be applied.

A flange in a box girder should be verified using (2.4) taking $M_{fRd} = 0$ and τ_{Ed} as the average shear stress in the flange but not less than half the maximum shear stress in the flange. In addition the subpanels should be checked using the average shear stress within the subpanel calculated using $t_{eff,w}$ determined for shear buckling of the subpanel, assuming the longitudinal stiffeners to be rigid according to 4.3.3.

If the girder is subjected to a concentrated transverse force in combination with bending and axial force, the resistance should be verified using the following interaction expression:

$$\eta_2 + 0,8\eta_1 \leq 1,4 \qquad \text{/II.5/}$$

Stress verification for serviceability and fatigue limit states

The verification of the section for stresses at serviceability and fatigue limit states should be based on the effective cross-section taking elastic shear lag into account.

For biaxial states of stress the effective stress σ_e for verification of yielding should be determined using the following expression:

$$\sigma_{e,Ed} = \left[\sigma_{x,Ed}^2 + \sigma_{y,Ed}^2 - \sigma_{x,Ed}.\sigma_{y,Ed} + 3\tau_{Ed}\right]^{0,5} \qquad \text{/II.6/}$$

Stresses should be entered with signs, tension is positive.

The effective stress $\sigma_{e,Ed}$ should satisfy:

$$\sigma_{e,Ed} \leq f_y/\gamma_{M,ser} \qquad \text{/II.7/}$$

where:

$\gamma_{M,ser}$ is the partial factor for resistance at serviceability limit states.

II.3 Effects of shear lag on stress distribution and resistance

Effective width for shear lag at serviceability and fatigue limit states

The effective width b_{eff} for elastic shear lag should be determined from:

The effective width factor β should be obtained from table II.1 using values of κ determined using:

$$\kappa = \alpha_0 b_0/L_e \qquad \text{/II.8/}$$

with:

$$\alpha_0 = (1 + A_{sl}/b_0 t)^{0.5}$$

in which A_{sl} is the area of all longitudinal stiffeners within the width b_0 and all other symbols are as defined in Fig. II.4.

Provided that no span is longer than 1,5 times an adjacent span and no cantilever is longer than half the adjacent span the effective lengths Le may be determined from Fig. II.3. In other cases L_e should be an estimate of the distance between adjacent points of zero bending moment.
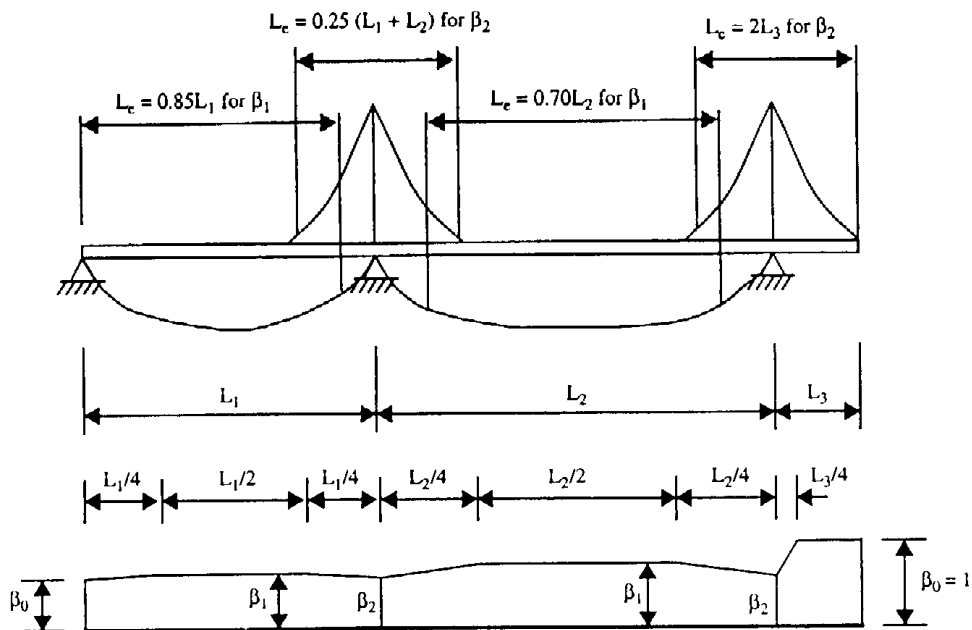
Figure II.3. Effective length L_e for continuous beam and distribution of effective width. [Fig. 3.1]
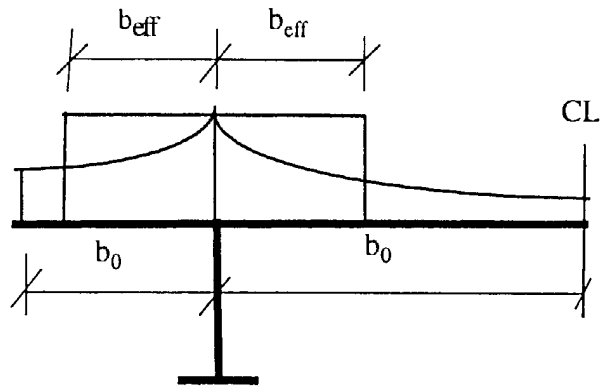
Figure II.4. Definitions of notations for shear lag. [Fig. 3.2]

Table II.1 Effective width factor β.

$\dfrac{\alpha_0 \cdot b_0}{L_e} = \kappa$	location for verification	β value
$\leq 0,02$		$\beta = 1,0$
$(0,02) - 0,70$	sagging bending	$\beta = \beta_1 = \dfrac{1}{1 + 6,4\kappa^2}$
	hogging bending	$\beta = \beta_2 = \dfrac{1}{1 + 6,0\left(\kappa - \dfrac{1}{2500\,\kappa}\right) + 1,6\kappa^2}$
$> 0,70$	sagging bending	$\beta = \beta_1 = \dfrac{1}{5,9\kappa}$
	hogging bending	$\beta = \beta_2 = \dfrac{1}{8,6\kappa}$
all κ	end support	$\beta_0 = (0,55 + 0,25/\kappa)\beta_1$ but $b_0 < \beta_1$
all κ	cantilever	$\beta = \beta_0$ at support $\beta = 1,0$ at the end

Stress distribution in case of shear lag

The transverse distribution of stresses due to shear lag should be obtained from Fig. II.5.

$\beta > 0.20$
$\sigma_2 = 1{,}25 \, (b - 0.20) \, \sigma_1$
$\sigma \, (y) = \sigma_2 + (\sigma_1 - \sigma_2) \, (1 - y/b)^4$

$\beta < 0.20$
$\sigma_2 = 0$
$\sigma \, (y) = \sigma_1 \, (1 - y/b_1)^4$
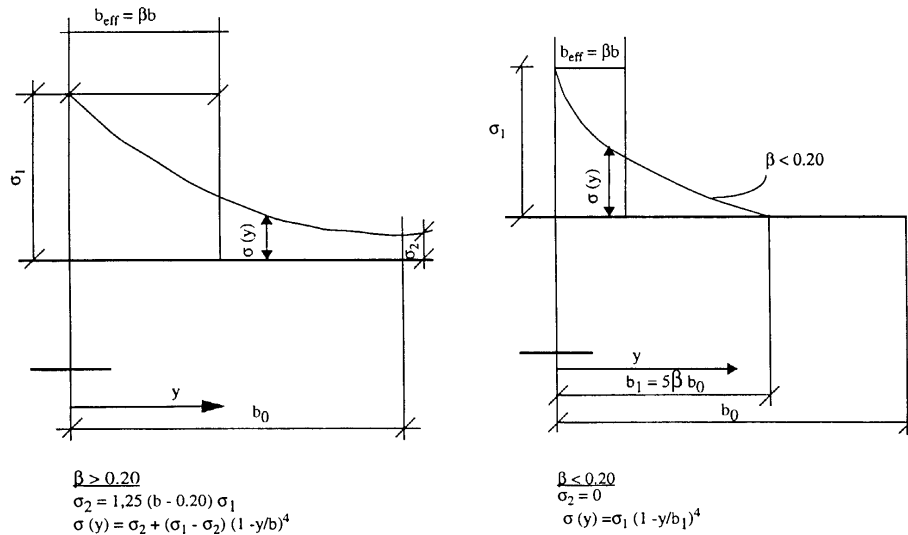
Figure II.30 Transverse distribution of stresses due to shear lag. [Fig. 3.3]

In-plane load introduction

The elastic stress distribution in a stiffened or unstiffened plate due to local introduction of in-plane forces, see Fig. II.6, should be determined from:

$$\sigma_{z,Ed} = F_{Sd} \big/ \left(b_{eff} \cdot t + A_{st,0} \right) \qquad \text{/II.9/}$$

with:

$$b_{eff} = s_e \left(1 + \left(z / s_e n \right)^2 \right)^{0,5}$$

$$n = 0{,}636 \left(1 + 0{,}878 \cdot A_{st,1} / t \right)^{0,5}$$

$$s_e = l_f + 2t_f$$

where:

$A_{st,1}$ is the gross cross-sectional area of stiffeners per unit width;

$A_{st,0}$ is the gross cross sectional area of the stiffeners directly loaded taking into account a load spread 1:1 through the thickness of the flange.

Shear lag effects at ultimate limit state

At ultimate limit states the effect of shear lag and plate buckling should be taken into account by using an effective area A_{eff} given by:

266

$$A_{eff} = A_{c,eff} \cdot \beta^{\kappa} \text{ but } A_{eff} \geq \beta A_{c,eff} \qquad \qquad \text{/II.10/}$$

where:

$A_{c,eff}$ is the effective area for a compression flange with respect to plate buckling from 4.2

β is the effective width factor for elastic shear lag from 3.2

κ is the ratio defined in 3.2(2)

Expression (II.10) is also applicable for flanges in tension in which case $A_{c,eff}$ should be replaced by the gross area of the tension flange.
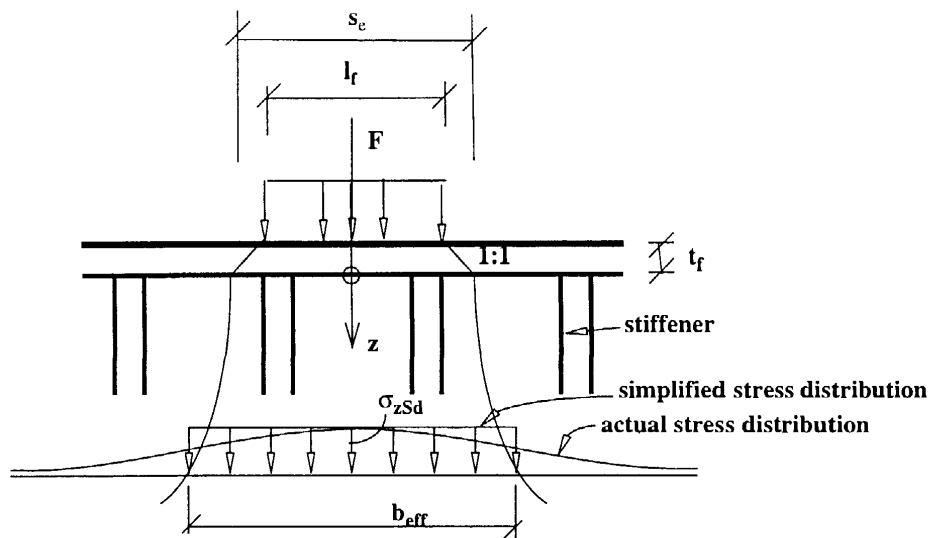
Figure II.6 Transverse distribution of stresses due to shear lag. [Fig. 3.4]

II.4 Resistance to plate buckling

Buckling of plates in compression

<u>*Effective cross-section of Class 4 cross-sections without longitudinal stiffeners*</u>

The effective cross-section properties of Class 4 cross-sections without longitudinal stiffeners should be based on the effective areas of the compression elements and their locations within the effective cross-section.

The effective areas and locations of flat compression elements should be obtained using Table II.2 for internal elements and Table II.3 for outstand elements. The effective area of a plate or part of it in compression with area A_c should be obtained from:

$$A_{c,eff} = \rho \, A_c \qquad\qquad \text{/II.11/}$$

where:

ρ is the reduction factor for plate buckling.

As an approximation, the reduction factor p may be obtained as follows:

when $\qquad \overline{\lambda}_p \leq 0{,}673 \qquad\qquad\qquad \rho = 1 \qquad\qquad$ /II.12/

when $\qquad \overline{\lambda}_p > 0{,}673 \qquad\qquad\qquad \rho = \left(\overline{\lambda}_p - 0{,}22\right)\!\big/\overline{\lambda}_p^{\,2} \qquad$ /II.13/

with:

$$\overline{\lambda}_p = \left[\frac{f_y}{\sigma_{cr}}\right]^{0,5} = \frac{b_p/t}{28{,}4\varepsilon\sqrt{k_\sigma}} \qquad\qquad \text{/II.14/}$$

b_p is the appropriate width as follows (for definitions, see table 5.3.1 of ENV 1993-1-1:1992)

b_w	for webs;
b	for internal flange elements (except RHS);
b - 3 t	for flanges of RHS;
c	for outstand flanges;
(b + h)/2	for equal-leg angles;
h or (b + h)/2	for unequal-leg angles;
k_σ	is the buckling factor corresponding to the stress ratio ψ from table II.2 or table II.3 as appropriate;
t	is the thickness;
σ_{cr}	is the elastic critical plate buckling stress.

For flange elements, the stress ratio ψ used in table II.2 or table II.3 should be based on the properties of the gross cross-section, reduced for shear lag according to 3.5 if relevant.

For web elements the stress ratio ψ used in table II.2 should be obtained using the effective area of the compression flange and the gross area of the web.

The plate slenderness $\overline{\lambda}_p$ of an element may be replaced by:

$$\overline{\lambda}_{p,red} = \overline{\lambda}_p \sqrt{\sigma_{com,Ed}\big/f_{yd}} \qquad\qquad \text{/II.15/}$$

where:

$\sigma_{com.Ed}$ is the maximum design compressive stress in the element determined using effective areas of all the compression elements.

This procedure generally requires an iterative calculation in which ψ is determined again at each step from the stresses calculated on the effective cross-section defined at the end of the previous step.

However, when verifying the design buckling resistance of a member using 5.5 of ENV 1993-1-1, the plate slenderness $\bar{\lambda}_p$ should always be used.

Table II.2 Internal compression elements.
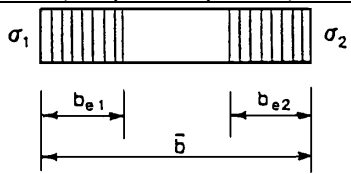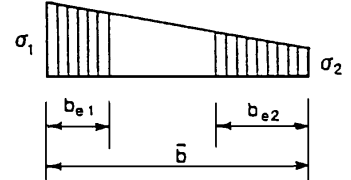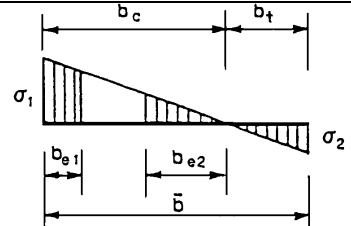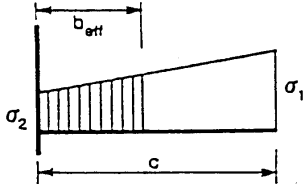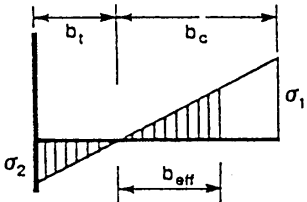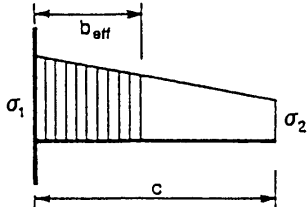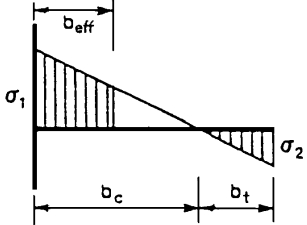
Stress distribution (compression positive)			Effective width b_{eff}		
			$\underline{\psi = 1}$ $b_{eff} = \rho b$ $b_{e1} = 0{,}5b_{eff}$ $b_{e2} = 0{,}5b_{eff}$		
			$\underline{0 \leq \psi < 1}$ $b_{eff} = \rho b$ $b_{e1} = 2b_{eff} / (5 - \psi)$ $b_{e2} = b_{eff} - b_{e1}$		
			$\underline{\psi < 0}$ $b_{eff} = \rho b_c = \rho b / (1 - \psi)$ $b_{e1} = 0{,}4b_{eff}$ $b_{e2} = 0{,}6b_{eff}$		
$\psi = \sigma_2 / \sigma_1$	1	$1 > \psi > 0$	0	$0 > \psi > -1$	-1	$-1 > \psi > -2$
Buckling factor k_σ	4,0	$8{,}2/(1{,}05 + \psi)$	7,81	$7{,}81 - 6{,}29\psi + 9{,}78\psi^2$	23,9	$5{,}98(1 - \psi)^2$
Alternatively for $1 \geq \psi \geq -1$, $k_\sigma = \dfrac{16}{\left[(1+\psi)^2 + 0{,}112(1-\psi)^2\right]^{0{,}5} + (1+\psi)}$						

Table II.3 Outstand compression elements.

Stress distribution (compression positive)	Effective width b_{eff}
	$1 > \psi \geq 0$ $b_{eff} = \rho c$
	$\psi < 0$ $b_{eff} = \rho b_c = \rho c /(1 - \psi)$

$\psi = \sigma_2 / \sigma_1$	1	0	−1	$1 > \psi > -1$
Buckling factor k_σ	0,43	0,57	0,85	$0,57 - 0,21\psi + 0,07\psi^2$

Stress distribution	Effective width b_{eff}
	$1 > \psi \geq 0$ $b_{eff} = \rho c$
	$\psi < 0$ $b_{eff} = \rho b_c = \rho c /(1 - \psi)$

$\psi = \sigma_2 / \sigma_1$	1	$1 > \psi > 0$	0	$0 > \psi > -1$	−1
Buckling factor k_σ	0,43	$0,578 /(0,34 + \psi)$	1,70	$1,70 - 5\psi + 17,1\psi^2$	23,8

Effective cross-section of Class 4 cross-sections with longitudinal stiffeners

The effective cross-section properties of class 4 cross-sections with longitudinal stiffeners should be based on the effective areas of the compression elements. As a first step the effective cross-sectional areas A_{eff} should be determined by a reduction factor ρ_{pan} for each subpanel to account for plate buckling between the stiffeners. In a second step the plate should be considered as an equivalent orthotropic plate and a reduction factor ρ_c for overall plate buckling of the equivalent plate should be determined.

The area of each subpanel between the stiffeners or panels forming the stiffener should be reduced by a reduction factor ρ_{pan} to account for possible plate buckling where ρ_{pan} is taken as equal to the value of ρ determined in accordance with 4.2.1 (3)

Plates with multiple longitudinal stiffeners
The elastic critical plate buckling stress of the equivalent plate is:

$$\sigma_{cr,p} = k_{\sigma,p}\sigma_E \qquad \text{/II.16/}$$

where:

$k_{\sigma,p}$ is the buckling coefficient ignoring buckling between stiffeners obtained from appropriate charts for buckling coefficients, by relevant computer simulations or according to annex Al.l

b, t   are defined in Fig. II.32
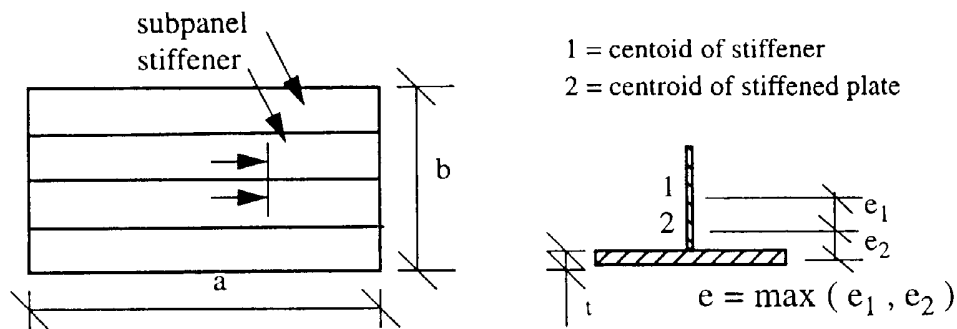
Figure II.7 Notations for longitudinally stiffened plates. [Fig. 4.1]

The relative plate slenderness $\overline{\lambda}_p$ of the equivalent plate is defined as:

$$\overline{\lambda}_p = \sqrt{\frac{\beta_A f_y}{\sigma_{cr,p}}} \qquad \text{with} \qquad \beta_A = \frac{A_{eff}}{A} \qquad \text{/II.17/}$$

where:

A   is the gross area of the compressed part of the stiffened plate;

A_{eff} is the effective area of the same part of the plate taking plate buckling of subpanels into account.

The elastic critical column buckling stress $\sigma_{cr,c}$ of the equivalent plate should be taken as the buckling stress of the same plate with the supports along the longitudinal edges removed. For uniform compression $\sigma_{cr,c}$ may be obtained using:

$$\sigma_{cr,c} = \frac{\pi^2 E I_x}{A a^2}$$ /II.18/

where:

I_x is the second moment of gross area for bending in the longitudinal direction of the stiffened plate

A stress gradient along the plate may be taken into account by the use of an effective length. The relative column slenderness $\overline{\lambda}_c$ of the equivalent plate is defined as:

$$\overline{\lambda}_c = \sqrt{\frac{\beta_A f_y}{\sigma_{cr,c}}}$$ /II.19/

The reduction factor χ_c should be obtained from 5.5.1.2(1) of ENV 1993-1-1 where α is replaced by:

$$\alpha_e = 0,49 + \frac{0,09}{i/e} \qquad \text{with} \qquad i = \sqrt{\frac{I_x}{A}}$$ /II.20/

where:

e   is the largest distance from the respective centroids of the plating and the one-sided stiffener (or of the centroids of either set of stiffeners when on both sides) to the neutral axis of the stiffened plate, see Fig. II.7. The factor α_e accounts for an initial bow imperfection of a/500.

The final reduction factor ρ_c should be obtained by interpolation between χ_c and ρ according to:

$$\rho_c = (\rho - \chi_c)\xi(2 - \xi) + \chi_c$$ /II.21/

where:

$$\xi = \frac{\sigma_{cr.p}}{\sigma_{cr.c}} - 1$$ /II.22/

The parameter ξ should not be taken as less than 0 nor larger than 1.

<u>Effective cross-sectional area</u>

The effective cross-sectional area of the compression zone of the stiffened plate should be taken as:

$$A_{c,eff} = \rho_c A_c \qquad\qquad /II.23/$$

in which A_c is composed of the effective cross-sectional areas of all the stiffeners and subpanels that are fully or partially in the compression zone.

The area A_c should be obtained from:

$$A_{c,eff} = \rho_c A_c \qquad\qquad /II.24/$$

where:
$A_{sl,eff}$ is the effective cross-section of all longitudinal stiffeners
$b_{c,pan}$ is the width of the compressed part of each subpanel
ρ_{pan} is the reduction factor for each subpanel.

The reduction of the area of the compressed part through ρ_c may be taken as a uniform reduction retaining the overall geometry. The effective cross-sectional area of the tension zone of the stiffened plate element should be taken as the gross area of the tension zone. The effective section modulus W_{eff} may be taken as the second moment of area of the effective cross section divided by the distance from its centroid to the mid depth of the flange.

Plates with one or two stiffeners in the compression zone
If the plate has only one or two longitudinal stiffeners the procedure in 4.2.2.3 may be simplified by replacing the elastic critical plate buckling stress in 4.2.2.3(2) with the elastic critical stress for a fictitious column elastically restrained by the plate. The cross-section of the fictitious column should be obtained from 4.2.2.5(2)-(3). The critical stress may be obtained from annex A2.

The gross cross-section of the fictitious column (for calculation of A and I_{sl}) should be taken as the gross area of the stiffener A_{sl} and adjacent parts of the plate. If the subpanel is fully in compression, half the width is taken as part of the fictitious column. If the stresses change from compression to tension within the subpanel, one third of the compressed part should be taken as part of the fictitious column, see Fig. II.8.

The effective area of the fictitious column should be taken as the effective cross-section of the stiffener $A_{sl,eff}$ and the adjacent effective parts of the plate, see Fig. II.8. The slenderness of the plate elements in the fictitious column may be determined according to 4.2.1 (6) with $\sigma_{com,Ed}$ calculated for the gross cross-section of the plate.

If $\rho_c f_{yd}$ with ρ_c according to 4.2.2.3(6) is greater than the average stress in the fictitious column $\sigma_{c,Ed}$ no further reduction of the effective area of the fictitious column should be made. Otherwise the reduction according to expression /II.23/ is replaced by:

$$A_{c,eff} = \rho_c f_{yd} A_c / \sigma_{c,Ed} \qquad\qquad /II.25/$$

The reduction mentioned in above should be applied only to the area of the fictitious column. No reduction need be applied to other compressed part of the plate, other than that for buckling of subpanels.

a.   b.   c.
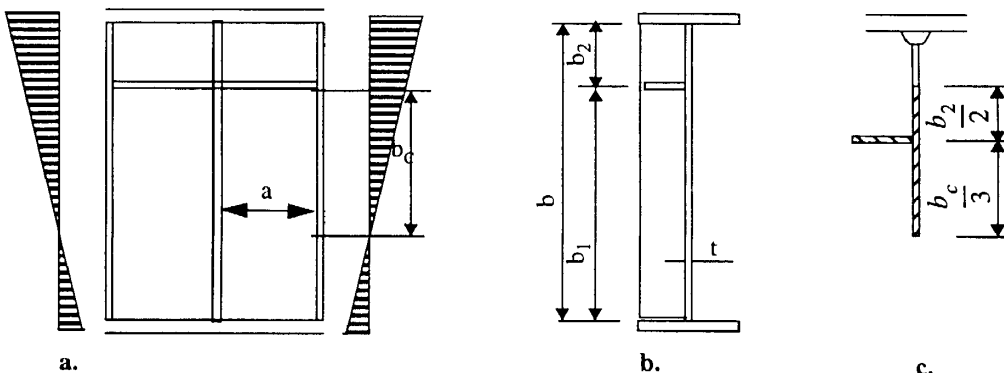
Figure II.8 Notations for plate with single stiffener. [Fig. 4.2]

Requirements for transverse stiffeners

In order to form rigid supports for longitudinal stiffeners, transverse stiffeners should satisfy the stiffness and strength requirements as given below. The cross-section of the transverse stiffener should be taken as including an associated part of plate $b_{eff}=30\varepsilon t$, see Fig. II.15.

Cut-outs of the stiffeners should be taken into account. The transverse stiffener should be treated as a simply supported beam with an initial sinusoidal imperfection w_0 equal to $s/300$, where s is the smallest of a_1, a_2 or b, see Fig. II.9
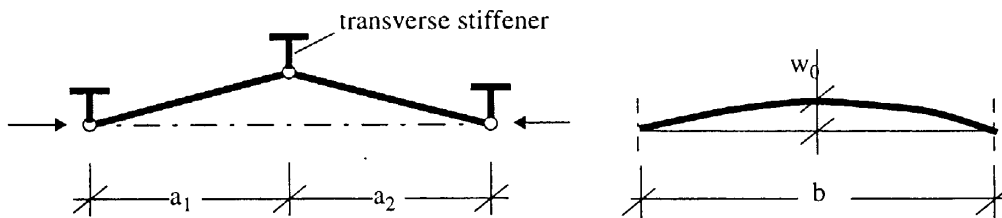
Figure II.9 Transverse stiffener. [Fig. 4.3]

The transverse stiffener should carry the deviation forces from the adjacent compressed panels under the assumption that both adjacent transverse stiffeners are rigid and straight. The compressed panels and the longitudinal stiffeners are considered to be simply supported at the transverse stiffeners. It should be verified that both the following criteria are satisfied:

- - that the maximum stress in the stiffener should not exceed f_{yd}
- - that the additional deflection should not exceed $b/300$

Both criteria may be assumed to be satisfied provided that the second moment of area I_{st} of the transverse stiffeners is not less than:

$$I_{st} = \frac{\sigma_m}{E}\left(\frac{b}{\pi}\right)^4\left[1 + w_0\,\frac{300}{b}\,u\right] \qquad\qquad \text{/II.26/}$$

with: $\qquad \sigma_m = \frac{\sigma_{cr,c}}{\sigma_{cr,p}}\,\frac{N_{Sd}}{b}\left[\frac{1}{a_1} + \frac{1}{a_2}\right], \qquad\qquad u = \frac{\pi^2 E e_{max}}{f_{yd}\,300\,b} \geq 1{,}0$

where:

e_{max} is the distance of the extreme fibre of the stiffener to the centroid of the stiffener.

N_{Sd} is the largest design compressive force of the adjacent panels but not less than the largest compressive stress times half the effective area of the panel including stiffeners;

$\sigma_{cr,c}$, $\sigma_{cr,p}$ are defined above.

Requirements for longitudinal stiffeners

In order to avoid torsional buckling of stiffeners with open class 4 cross-sections the following criterion should be satisfied:

$$\frac{I_T}{I_p} \geq 11{,}0\left(\frac{t}{b}\right)^2 \qquad\qquad \text{/II.27/}$$

where:

b   is the width of plate between stiffeners;

I_p is the polar second moment of area of the stiffener (excluding the plate) around the edge fixed to the plate;

I_T is the torsional constant (St. Venant) for the stiffener without plate;

t   is the thickness of plate between stiffeners.

Webs may have discontinuous longitudinal stiffeners, provided that those are not included in the cross section carrying longitudinal stresses. A large trapezoidal stiffener may be considered as two separate stiffeners or as one stiffener located at the middle of the stiffener.

Stiffeners at support

Stiffeners at support should be designed to carry the reaction force together with the possible bending moment arising from bearing eccentricity. If the stiffeners are assumed to provide lateral restraint to the top flange they should be designed for stiffness and strength in conformity with the assumptions in the beam design.

Buckling of plates in shear

Plates with b_w/t greater than $41\varepsilon/\eta$ for an unstiffened web, or $18\varepsilon\sqrt{k_\tau}/\eta$ for a stiffened web, shall be checked for resistance to shear buckling and shall be provided with transverse stiffeners at the supports. For notation η, see 4.3.3(1) and k_τ see 4.3.3(3).

For webs with or without stiffeners shear buckling should be taken into account by reducing the web thickness to an effective web thickness t_{eff} for shear obtained using:

$$t_{eff} = t_{eff.w} + t_{eff.f} \qquad \text{/II.28/}$$

in which $t_{eff.w}$ is a contribution from the web and $t_{eff.f}$ is a contribution from the flanges, determined according to 4.3.3 and 4.3.4, respectively. For simplicity the contribution from the flanges $t_{eff.f}$ may be neglected.

a) Cross-section notations   b) Rigid end post   c) Non-rigid end post
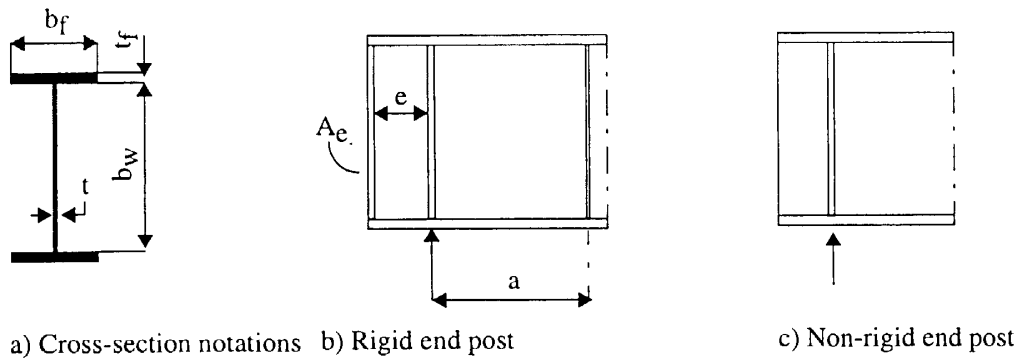
Figure II.10 Criteria for end-stiffener. [Fig. 4.4]

Contribution of the web to the effective thickness

For webs with transverse stiffeners at supports only and for webs with intermediate transverse and/or longitudinal stiffeners, the contribution of the web to the effective thickness for shear $t_{eff.w}$ Should be obtained from

$$t_{eff,w} = \chi_v t \qquad \text{/II.29/}$$

in which χ_v is the effective thickness factor for shear buckling according to Table II.4 or Fig. II.11.

A distinction should be made between:

    a) rigid end posts. This case is also applicable for panels not at the end of the girder and at an intermediate support of a continuous girder;

    b) non rigid end posts.

Table II.4 Effective thickness factor χ_v for shear buckling.

$\bar{\lambda}_w$	Rigid end post	Non-rigid end post
$< 0{,}48/\eta$	η	η
$0{,}48/\eta \leq \bar{\lambda}_w < 1{,}08$	$0{,}48/\bar{\lambda}_w$	$0{,}48/\bar{\lambda}_w$
$\geq 1{,}08$	$0{,}79/\left(0{.}7 + \bar{\lambda}_w\right)$	$0{,}48/\bar{\lambda}_w$
$\eta = 0{,}70$ for S235, S275 and S355		
$\eta = 0{,}60$ for S420 and S460		
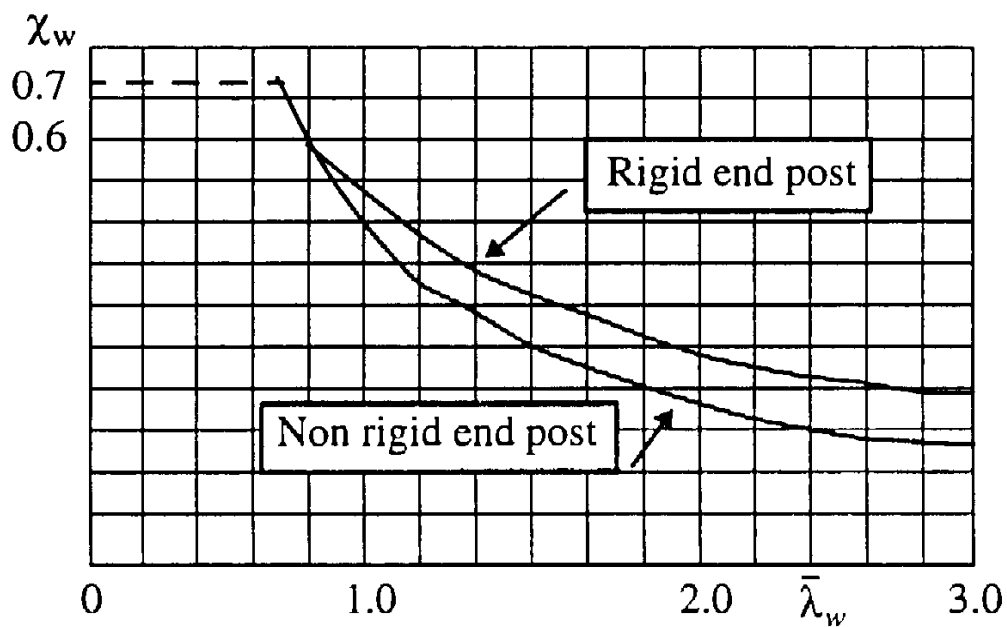
Figure II.11 Effective thickness factor for shear buckling. [Fig. 4.5]

The slenderness parameter $\bar{\lambda}_w$ in Table II.4 and Fig. II.11 should be determined from:

$$\bar{\lambda}_w = 0{,}76\left(f_{yw}/\tau_{cr}\right)^{0{,}5} \qquad \text{/II.30/}$$

in which τ_{cr} is the critical shear buckling stress obtained from:

$$\tau_{cr} = k_\tau \sigma_E \qquad \text{/II.31/}$$

in which σ_E should be taken from 4.2.2.3(2) and k_τ from (5) or (6).

For webs with transverse stiffeners at supports only the slenderness parameter $\bar{\lambda}_w$ may be taken as:

$$\bar{\lambda}_w = \frac{b_w}{86.4 t \varepsilon}$$
/II.32/

For webs with transverse stiffeners at the supports and intermediate transverse and/or longitudinal stiffeners the slenderness parameter $\bar{\lambda}_w$ may be taken as:

$$\bar{\lambda}_w = \frac{b_w}{37.4 \varepsilon \sqrt{k_\tau}}$$
/II.33/

in which k_τ is the smallest buckling coefficient for the web panel surrounded by rigid supports (flange or transverse stiffeners).

If k_τ is governed by a buckling mode that include stiffener buckling the difference between k_τ for the stiffened panel and that for the same panel without longitudinal stiffeners should be multiplied by 1/3. Formulae for k_τ taking this reduction into account in annex A3 may be used.

For webs with longitudinal stiffeners the slenderness parameter $\bar{\lambda}_w$ should not be taken as less than

$$\bar{\lambda}_w = \frac{b_{w1}}{37.4 \varepsilon \sqrt{k_{\tau 1}}}$$
/II.34/

where the shear buckling coefficient $k_{\tau 1}$ refers to the largest subpanel with depth b_{w1} and length a, see Fig. II.12. Annex A3 may be used with $k_{\tau st} = 0$.
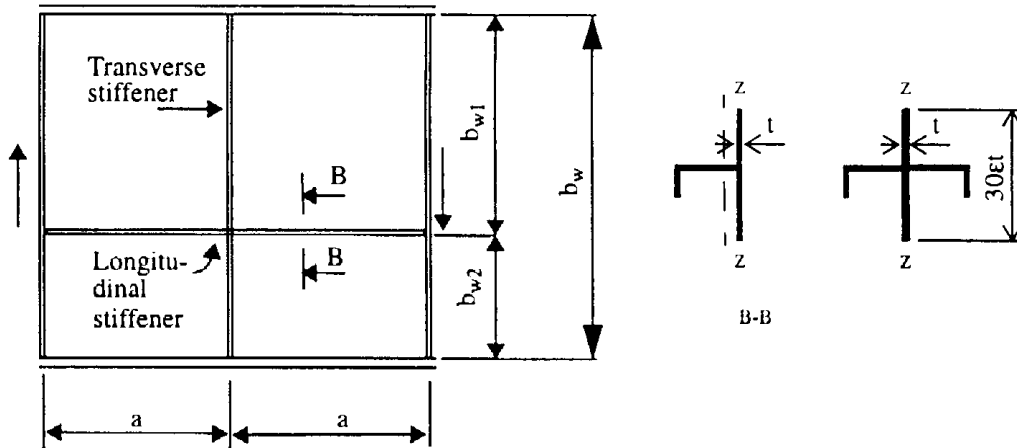
Figure II.12 Web with transverse and longitudinal stiffeners. [Fig. 4.6]

Contribution of flange to the effective web thickness

If the flanges are not completely utilized by bending moment ($M_{Sd} < M_{f.Rd}$) there is a contribution $t_{eff.f}$ of the flanges to the effective thickness obtained from:

$$t_{eff.f} = \chi_{vf} t \qquad \text{/II.35/}$$

with:

$$\chi_{vf} = \frac{b_f t_f^2 f_{yf}}{cth_w \eta f_{yw}} \left[1 - \left[\frac{M_{Sd}}{M_{f.Rd}} \right]^2 \right] \qquad \text{/II.36/}$$

$$c = \left[0,25 + \frac{1,6 b_f t_f^2 f_{yf}}{cth_w^2 f_{yw}} \right] a \qquad \text{/II.37/}$$

in which b_f and t_f are taken for the smaller flange.

If an axial force N_{Sd} is also applied, the value of $M_{f,Rd}$ should be reduced by a factor:

$$\left| 1 - \frac{N_{Sd}}{[A_{f1} + A_{f2}] f_{yfd}} \right| \qquad \text{/II.38/}$$

where: A_{f1} and A_{f2} are the areas of the flanges.

Stiffeners

Rigid end post

The rigid end post should act as a bearing stiffener resisting the reaction at the girder support, and as a short beam resisting the longitudinal membrane stresses in the plane of the web.

A rigid end post may comprise of two double-sided transverse stiffeners that form the flanges of a short beam of length h_w, see Fig. II.10 (b). The strip of web plate between the stiffeners forms the web of the short beam. Alternatively, an end post may be in the form of an inserted section, connected to the end of the web plate. Each stiffener should have a cross sectional area of at least $4 h_w t^2/e$ where e is the distance between the stiffeners and $e > 0.1 h_w$, see Fig. II.10 (b).

Non-rigid end post

A non-rigid end posts may be a single stiffener as shown in Fig. II.10 (c). It may be assumed to act as a bearing stiffener resisting the reaction at the girder support.

Intermediate transverse stiffeners

Intermediate stiffeners acting as rigid supports of interior panels of the web should be checked for resistance and stiffness.

Other intermediate transverse stiffeners may be considered flexible, their stiffness being considered in the calculation of k_τ in 4.3.3 (4). Intermediate stiffeners acting as rigid supports for the web panel should have a second moment of area fulfilling the following:

$$\text{if} \qquad a/h_w < \sqrt{2} \qquad\qquad I_{st} \geq 1{,}5 h_w^3 t^3 / a^2 \qquad\qquad \text{/II.39/}$$

$$\text{if} \qquad a/h_w \geq \sqrt{2} \qquad\qquad I_{st} \geq 0{,}75 h_w t^3 \qquad\qquad \text{/II.40/}$$

The resistance of intermediate rigid stiffeners should be checked for an axial force equal to V_{Sd} minus $f_{ywd} h_w t_{eff,w}$ calculated assuming the stiffener under consideration removed.

Longitudinal stiffeners
Longitudinal stiffeners may be either rigid or flexible. In both cases their stiffness should be taken into account when determining the slenderness $\bar{\lambda}_w$ in 4.3.3. If the value of $\bar{\lambda}_w$ is governed by the subpanel then the stiffener may be considered as rigid. The strength should be checked for direct stresses if the stiffeners are taken into account for resisting direct stress

Welds

The welds may be designed for the nominal shear flow V_S / h_w if V_S does not exceed $f_{ywd} h_w t_{eff,w}$. For larger values the weld between flanges and webs should be designed for the shear flow $\eta f_{yw} t$ unless the state of stress is investigated in detail.

Resistance of webs to transverse forces

The resistance of an unstiffened or stiffened web to transverse forces applied through a flange, is given by 2.2.1 (2) with L_{eff} determined from the following rules, which are applicable for rolled beams and welded girders provided that the flanges are held in position in the lateral direction either by their own stiffness or by bracings.

A distinction should be made between three types of load application, as follows:
   a) Forces applied through one flange and resisted by shear forces in the web, see Fig. II.13(a);
   b) Forces applied to one flange and transferred through the web directly to the other flange, see Fig. II.13(b).
   c) Forces applied through one flange close to an unstiffened end, see Fig. II.13(c)

For box girders with inclined webs the resistance of both the web and flange should be checked. The internal forces to be taken into account are the components of the external load in the plane of the web and flange respectively. In addition the effect of the transverse force on the moment resistance of the member should be considered.

$$k_F = 6 + 2\left[\frac{h_w}{a}\right]^2 \qquad k_F = 3.5 + 2\left[\frac{h_w}{a}\right]^2 \qquad k_F = 2 + 6\frac{s_s + c}{h_w} \leq 6$$
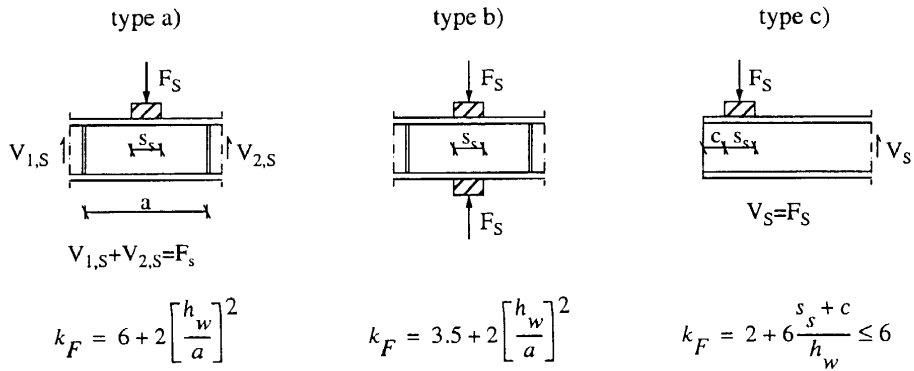
Figure II.13 Buckling coefficients for types of load applications. [Fig. 4.7]

Length of stiff bearing

The length of stiff bearing, s_s, on the flange is the distance over which the applied force is effectively distributed and it may be determined by dispersion of load through solid steel material at a slope of 1:1, see Fig. II.14. However, s_s should not be taken as larger than h_w.

If several concentrated loads are closely spaced, the resistance should be checked for each individual load as well as for the total load. In the latter case ss should be taken as the centre-to-centre distance between the outer loads.
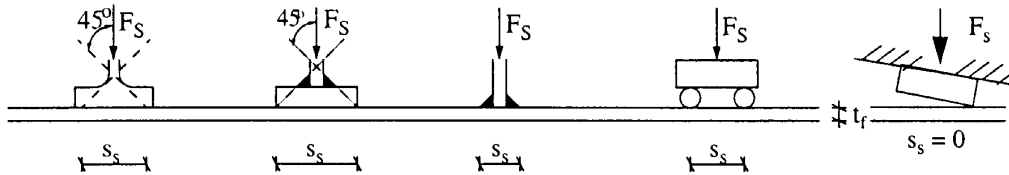
Figure II.14 Length of stiff bearing. [Fig. 4.8]

Effective length for resistance

The effective length for resistance should be obtained from:

$$L_{eff} = \chi_F l_y \qquad\qquad /\text{II.41}/$$

with:

$$\chi_F = \frac{0,5}{\lambda_F} \leq 1 \qquad\qquad /\text{II.42}/$$

281

$$\lambda_F = \sqrt{\frac{l_y t_w f_{yw}}{F_{cr}}} \tag{/II.43/}$$

$$F_{cr} = 0{,}9 k_F E \frac{t_w^3}{h_w} \tag{/II.44/}$$

The factor k_F should be obtained from Fig. II.13.

Effective loaded length

The effective loaded length l_y should be calculated using two dimensionless parameters m_1 and m_2 obtained from:

$$m_1 = \frac{f_{yf} b_f}{f_{yw} t_w} \tag{/II.45/}$$

$$m_2 = 0{,}02 \left[\frac{h_w}{t_f}\right]^2 \quad \text{if } \lambda_F > 0{,}5 \text{ else } m_2 = 0 \tag{/II.46/}$$

For box girders, b_f in equation /II.45/ should be limited to $25 t_f$ on each side of the web. For cases a) and b) in Fig. II.13 l_y should be obtained using:

$$l_y = s_s + 2 t_f \left[1 + \sqrt{m_1 + m_2}\right] \tag{/II.47/}$$

For case c) l_y should be obtained by the smaller of equations /II.47/, /II.49/ and /II.50/. However s_s in /II.48/ should be taken as zero if the loading device does not follow the change in slope of the girder end, see Fig. II.14.

$$l_{ef} = \frac{k_F}{2} \frac{E}{f_{yw}} \frac{t_w^2}{h_w} \le s_s + c \tag{/II.48/}$$

$$l_y = l_{ef} + t_f \sqrt{\frac{m_1}{2} + \left[\frac{l_{ef}}{t_f}\right]^2 + m_2} \tag{/II.49/}$$

$$l_y = l_{ef} + t_f \sqrt{m_1 + m_2} \tag{/II.50/}$$

Transverse stiffeners

If the design resistance of an unstiffened web is insufficient transverse stiffeners should be provided. At a plastic hinge location in the beam, stiffeners should be provided if the relative local load η_2 in 2.2 is larger than 0,5.

282

When checking the buckling resistance, the effective cross-section of a stiffener may be taken as including a width of web plate equal to $30\varepsilon t_w$, arranged with $15\varepsilon t_w$ each side of the stiffener, see Fig. II.15. At the ends of the member (or openings in the web) the dimension of $l5\varepsilon t_w$ should be limited to the actual dimension available. If the stiffener itself is class 4, the effective section of 4.2.1 (3) should be used.
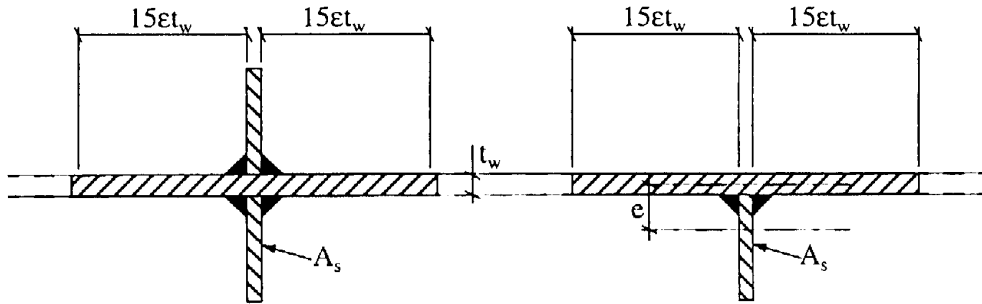
Figure II.15 Effective cross-section of transverse stiffener. [Fig. 4.9]

The out-of-plane buckling resistance should be determined from 5.5.1 of ENV 1993-1-1 :1992, using buckling curve c and a buckling length l of not less than 0,75 h_w, or more if appropriate for the conditions of restraint. Where single sided or other asymmetric stiffeners are used, the resulting eccentricity should be allowed for using 5.5.4 of ENV 1993-1-1:1992.

In addition to checking the buckling resistance, the cross-section resistance of a load bearing stiffener should also be checked adjacent to the loaded flange. The width of web plate included in the effective cross-section should be limited to l_y and allowance should be made for any openings cut in the stiffener to clear the web-to-flange welds.

Flange induced buckling

To prevent the possibility of the compression flange buckling in the plane of the web, the ratio h_w/t_w of the web should satisfy the following criterion:

$$\frac{h_w}{t_w} \leq k\left(E/f_{yf}\right)\sqrt{A_w/A_{fc}}$$ /II.51/

where:

A_w is the area of the web
A_{fc} is the area of the compression flange

The value of the factor k should be taken as follows:

– - Plastic rotation utilized   0,3
– - Plastic moment resistance utilized   0,4
– - Elastic moment resistance utilized   0,55

When the girder is curved in elevation, with the compression flange on the concave face, the following criterion should be checked in addition to 4.4.7(1).

$$\frac{h_w}{t_w} \le \frac{k\left(E/f_{yf}\right)\sqrt{A_w/A_{fc}}}{\sqrt{1 + h_w E / \left[3\, r\, f_{yf}\right]}} \qquad \text{/II.52/}$$

in which r is the radius of curvature of the compression flange.

If the girder has transverse or longitudinal web stiffeners, the limiting value of h_w/t_w may be increased.

Annex A Buckling coefficients

A1 Buckling coefficient for plates with multiple stiffener loaded by direct stresses

For stiffened plates with equidistant multiple longitudinal stiffeners the plate buckling coefficient $k_{\sigma,p}$ may be approximated by

$$k_{\sigma,p} = \frac{2\left[\left(1+\alpha^2\right)^2 + \gamma\right]}{\alpha^2\left(\psi+1\right)\left(1+\delta\right)} \qquad \text{if } \alpha < \left(1+\gamma\right)^{0,25} \qquad \text{/II.53/}$$

$$k_{\sigma,p} = \frac{4\left(1+\sqrt{1+\gamma}\right)}{\left(\psi+1\right)\left(1+\delta\right)} \qquad \text{if } \alpha > \left(1+\gamma\right)^{0,25} \qquad \text{/II.54/}$$

with:

$$\psi = \frac{\sigma_2}{\sigma_1} > 0\,; \qquad \gamma = \frac{I_x}{I_p} > 50\,; \qquad \delta = \frac{A_{sl}}{A_p}\,; \qquad \alpha = a/b > 1\,.$$

where:

I_x is the second moment of area for bending in the longitudinal direction for the whole panel;

I_p is the second moment of area for bending of the plate =

A_{sl} is the gross area of all longitudinal stiffeners (without plate);

A_p is the gross area of the plate = bt;

σ_1 is the larger edge stress;

σ_2 is the smaller edge stress;

a, *b* and *t* are as defined in Fig. II.7.

A2 Critical stress for stiffener regarded as a fictitious column restrained by the plate

In the case of one longitudinal stiffener only located in the compression zone and ignoring stiffeners in the tension zone, the elastic critical plate buckling stress is:

$$\sigma_{cr,p} = \frac{1,05E}{A} \frac{\sqrt{I_{sl}t^3 b}}{b_1 b_2} \qquad\qquad \text{if } a \geq a_c \qquad\qquad /\text{II.55}/$$

$$\sigma_{cr,p} = \frac{\pi^2 E I_{sl}}{A a^2} + \frac{E t^3 b a^2}{4\pi^2 \left[1 - v^2\right] A b_1^2 b_2^2} \qquad\qquad \text{if } a \geq a_c \qquad\qquad /\text{II.56}/$$

$$a_c = 4,33\left[I_{sl}b_1^2 b_2^2 / \left(t^3 b\right)\right]^{0,25} \qquad\qquad /\text{II.57}/$$

where:

I_{sl} is the second moment of area of the gross cross-section of the fictitious column defined in 4.2.2.5(2) about an axis through its centroid and parallel to the plane of the plate;

b_1, b_2 are the distances from longitudinal edges to the stiffener ($b_1 + b_2 = b$).

In the case of two longitudinal stiffeners, both in compression, each stiffener is first considered assuming the other one to be rigid and the procedure for one stiffener is used. In a further step both stiffeners are considered as lumped together, with an area and a second moment of area equal to the sum of those of the individual stiffeners. The location of the lumped stiffener is the position of the resultant of the axial forces in the stiffeners. The elastic critical plate buckling stress is the lowest of the ones computed for the three cases. If one of the stiffeners is in tension the procedure will be conservative.

A3 Shear buckling coefficient for stiffened panels

For plates with rigid transverse stiffeners with or without longitudinal stiffeners in between, the shear buckling coefficient k_τ is:

$$k_\tau = 5,34 + 4,00\left(h_w/a\right)^2 + k_{\tau st} \qquad\qquad \text{when } a/h_w \geq 1 \qquad\qquad /\text{II.58}/$$

$$k_\tau = 4,00 + 5,34\left(h_w/a\right)^2 + k_{\tau st} \qquad\qquad \text{when } a/h_w < 1 \qquad\qquad /\text{II.59}/$$

with:

$$k_{\tau st} = 9\left[\frac{h_w}{a}\right]^2 \left[\frac{I_{sl}}{t^3 h_w}\right]^{3/4} \qquad \text{but not less than } \frac{2,1}{t}\left[\frac{I_{sl}}{h_w}\right]^{1/3} \qquad\qquad /\text{II.60}/$$

where

a   is the distance between transverse stiffeners (see Fig. II.12);

I_{sl} is the second moment of area of the longitudinal stiffener with regard to the z-axis, see Fig. II.12(b). For webs with two or more equal stiffeners, not necessarily equally spaced, I_{sl} is the sum of the stiffness of the individual stiffeners.

Appendix III.

Eurocode 3: Design of steel structures – Part 1.7 (EC3-1-7)
　　　　Planar plated structural elements with transverse loading
　　　　[prENV 1993-1-7:April 1998]

Extract

III.1 General

Scope

Part 1-7 of ENV 1993 provides principles and application rules for the structural design of thin unstiffened and stiffened plates which are loaded by out of plane actions. It is to be used in conjunction with EC3 - Part 1.1 and the relevant application standards. Any action consideration, such as:

– definition of an action
– combination of actions
– partial safety factors on actions

  are to be taken from EC 1 as far as general rules are concerned, and the relevant parts of EC 3 as far as specific application rules are concerned.

  This Part 1.7 is concerned with the requirements of an appropriate design against the ultimate limit state taking account of the following failure modes:

– plastic collapse or tensile rupture
– cyclic plasticity / low cycle fatigue
– buckling
– fatigue.

  The rules in this Part 1.7 refer to thin plate segments in plated structures which may be stiffened or unstiffened. These plate segments may be individual plates or parts of a plated structure. They are loaded by out of plane actions. The verification of unstiffened and stiffened plated structures loaded only by in-plane effects shall be carried out with the design rules given in ENV 1993-1-5. In ENV 1993-1-7 rules for the interaction between the effects of inplane and transverse loading are given. The temperature range within which the rules of this Part 1.7 are allowed to be applied are defined in the relevant EC 3 application parts.

  Wind loading and bulk solids flow may, in general, be treated as quasi-static actions. For fatigue, the dynamic effects must be taken into account according to the relevant application parts of EC3. The stress resultants arising from the dynamic behaviour are then treated in this part as quasi-static.

Definitions

Stress components

Membrane stresses in rectangular plate
    σ_{mx} is the membrane stress in the x-direction due to membrane forces n_x.
    σ_{my} is the membrane stress in the y-direction due to membrane forces n_y.
    τ_{mxy} is the membrane shear stress due to membrane forces n_{xy}.
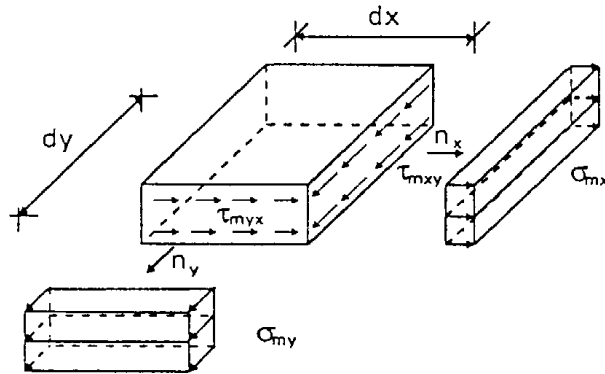
Figure III.1 Definition of membrane stresses. [Fig. 1.1]

Normal and shear stresses in rectangular plates due to bending

σ_{bx} is the stress in the x-direction due to bending moment m_x.

σ_{by} is the stress in the y-direction due to bending moment m_y.

τ_{bxy} is the shear stress due to the bending moment m_{xy}.

τ_{bxz} is the shear stress due to shear forces q_x.

τ_{byz} is the shear stress due to shear forces q_y.
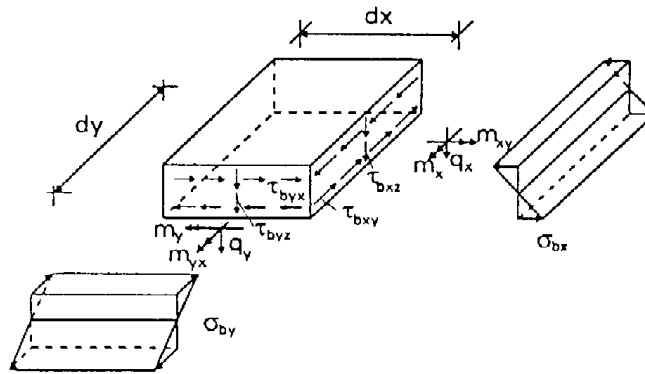
Figure III.2 Definition of normal and shear stresses due to bending. [Fig. 1.2]

Structural forms

– **Plated structure**: A structure that is built up from nominally flat plates which are welded together. The plates may be stiffened or unstiffened, see Fig. III.3.

– **Plate segment**: A plate segment is a flat plate, which may be unstiffened or stiffened. A plate segment may be regarded as an individual part of a plated structure.

- **Stiffener**: A plate or section attached to a plate with the purpose of preventing buckling of the plate or reinforcing it against local loads. A stiffener is denoted:
  - longitudinal if its direction is parallel to that of the member
  - transverse if its axis is perpendicular to that of the member.
- **Stiffened plate**: Plate with transverse and/or longitudinal stiffeners.
- **Subpanel**: Unstiffened plate surrounded by flanges or stiffeners.
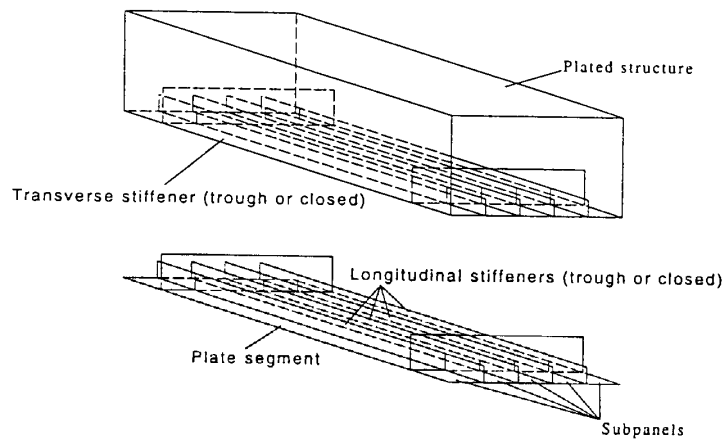
Figure III.3 Components of a plated structures. [Fig. 1.3]

Terminology

- **Plastic collapse**: a failure mode in the ultimate limit state where the structure looses its ability to resist increased loading due to yielding of the material.
- **Tensile rupture**: a failure mode in the ultimate limit state where the plate experiences failure due to tension.
- **Cyclic plasticity**: Where repeated yielding is caused by cycles of loading and unloading.
- **Buckling**: Where the structure suddenly looses its stability under compression and/or shear.
- **Fatigue**: Where cyclic loading causes cracking or failure of the plate.

Actions

- **Transverse loading**: The load applies normal to the middle surface of a plate segment.
- **In-plane forces**: Forces, which apply parallel to the middle surface of the plate segment. They are induced by in-plane effects (for example temperature and friction effects) or by global loads applied at the plated structure.

Creek lower case letter

a   aspect ratio of a plate segment (a/b);
ε strain
λ_R load amplification factor
ρ reduction factor for plate buckling;
σ_i Normal stress in the direction *i*;
τ Shear stress;
γ_M safety factor for resistance;

Latin upper case letter

E   Modulus of elasticity

Latin lower case Letter

a   length of a plate segment, see Fig.III.4 and III.5;
b   width of a plate segment, see Fig. III.4 and III.5;
f_y yield stress;
n_i membrane force in the direction i [kN/m];
m   bending moment [kNm/m];
q_i shear force in direction i [kN/m];
t   thickness of a plate segment, see Fig. III.4 and III.5;
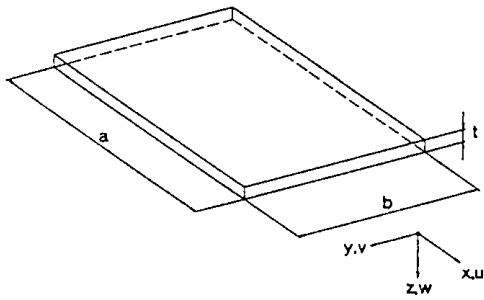
Figure III.4 Dimensions and axes
of unstiffened plate segments. [Fig. 1.4]
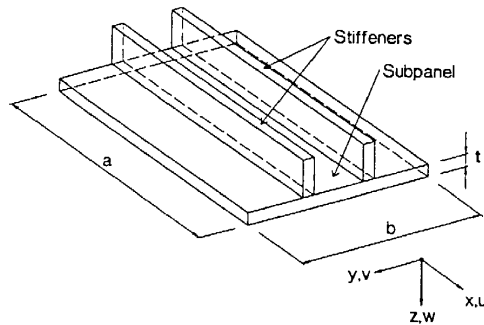
Figure III.5 Dimensions and axes of stiffened
plate segments; stiffeners may
be trough or closed stiffeners [Fig. 1.5]

III.2 Basis of Design

Ultimate limit state

Plastic collapse or tensile rupture

Plastic collapse is defined as the condition in which part of the structure develops excessive plastic deformations, associated with development of a plastic mechanism. The plastic collapse load is usually derived from a mechanism based on small deflection theory. Tensile rupture is defined as the condition in which the plated structure fails through tensile rupture, leading to separation of the two parts of the structure. Both failure modes involve loss of equilibrium between the imposed loadings and the maximum attainable internal resultants in the plate, and only equilibrium considerations are concerned.

Cyclic plasticity /low cycle fatigue

Cyclic plasticity / low cycle fatigue is defined as the limit condition for repeated cycles of loading and unloading produce yielding in tension or in compression or both at the same point, thus causing plastic work to be repeatedly done on the structure. This alternative yielding may lead to local cracking by exhaustion of the material's energy absorption capacity, and is thus a low cycle fatigue restriction. The stresses which are associated with this limit state develop under a combination of all actions and the compatibility conditions for the structure.

Buckling

Buckling is defined as the condition in which all or parts of the structure develop large displacements, caused by instability under compressive or shear stresses in the plate. It leads eventually to incapacity to sustain an increase in the stress resultants.

Fatigue

Fatigue is defined as the limit condition caused by the development and / or growth of cracks by repeated cycles of increasing and decreasing stresses.

Serviceability limit states

Out of plane deflection

The limit value of the out of plane deflection w is defined as the condition in which the effective use of a plate segment is governed on its out of plane detlection *w*. It depends usually on the field of application and shall be given in the relevant standard.

Excessive vibrations is defined as the limit condition in which either the failure of a plated structure occurs by fatigue at adjacent connections caused by excessive vibrations of the plate or serviceability limits apply. The slenderness of a plate segment should be limited to avoid excessive vibrations.

III.3 Modelling of structural analysis

Calculations shall be carried out using appropriate design models involving all relevant variables. The models used shall be appropriate for predicting the structural behaviour and the limit states considered. If the boundary conditions can be conservatively defined a plated structure may be subdivided into individual plate segments that may be assumed independently. The overall stability of the complete structure shall be checked as defined in the relevant parts of Eurocode 3.

Calculation of internal stresses or stress resultants

The internal stresses or stress resultants of a plated structure shall be calculated for the relevant combination of actions. The calculation model and basic assumptions for determining internal stresses or stress resultants should represent the expected structural response in the ultimate limit state loading.

The models shall be sufficiently precise to predict the plate behaviour, commensurate with the standard of workmanship likely to be achieved, and with the reliability of the information on which the design is based. Structural models may be simplified to the extent that it can be shown that the simplifications used will give conservative estimates of the effects of actions.

If necessary, the calculation model shall be supplemented by tests involving all relevant variables. Elastic global analysis may generally be used for plated structures. Plastic global analysis should not be used where fatigue resistance is important. Possible deviations from the assumed directions or positions of actions shall be considered.

Plate boundary conditions

The plated structure shall be designed in such a way as to ensure that boundary conditions assumed in the design calculations are achieved in the construction. If a plated structure is subdivided into individual plate segments the boundary conditions e.g for stiffeners assumed for the individual plate segments in the design calculations shall be achieved in the drawings and execution.

Design models for plated structures

The internal stresses of a plate segment in a plated structure should be determined with one of the following design models:

– standard formulas for plates,
– global analysis,

– simplified models.

The design models given above shall take into account a linear or non linear bending theory for plates. A linear bending theory is based on small-deflection assumptions and relates loads to deformations in a proportional manner. A non-linear bending theory is based on large-deflection assumptions and the effects of deformation on equilibrium are taken into account.

The design models given above may be based on the types of analysis given in Table III.1.

Table III.1 Types of analysis

Type of analysis	Bending theory	Material law	Plate geometry
Linear elastic plate analysis (LA)	linear	linear	perfect
Geometrically non-linear elastic analysis (GNA)	non-linear	linear	perfect
Materially non-linear analysis (MNA)	linear	non-linear	perfect
Geometrically and materially non-linear analysis (GMNA)	non-linear	non-linear	perfect
Geometrically non-linear elastic analysis with imperfections (GNIA)	non-linear	linear	imperfect
Geometrically and materially non-linear analysis with imperfections (GMNIA)	non-linear	non-linear	imperfect

<u>Design by standard formulas</u>

For an individual plate segment of a plated structure the internal stresses may be calculated for the relevant combination of design actions with appropriated design formulae based on the types of analysis given in Table III.1.

In case of a two dimensional stress field resulting from a membrane theory analysis the equivalent v. Mises stress $\sigma_{eq,Sd}$ may be determined by

$$\sigma_{eq,Sd} = \frac{1}{t}\sqrt{n_{x,Sd}^2 + n_{y,Sd}^2 - n_{x,Sd}n_{y,Sd} + 3n_{xy,Sd}^2} \qquad \text{/III.1/}$$

In case of a two dimensional stress field resulting from an elastic plate theory the equivalent v. Mises stress $\sigma_{eq,Sd}$ may be determined, as follows:

$$\sigma_{eq,Sd} = \sqrt{\sigma_{x,Sd}^2 + \sigma_{y,Sd}^2 - \sigma_{x,Sd}\sigma_{y,Sd} + 3\tau_{xy,Sd}^2} \qquad \text{/III.2/}$$

where

$$\sigma_{x,Sd} = \frac{n_{x,Sd}}{t} \pm \frac{m_{x,Sd}}{t^2/4}$$

$$\sigma_{y,Sd} = \frac{n_{y,Sd}}{t} \pm \frac{m_{y,Sd}}{t^2/4}$$

$$\tau_{xy,Sd} = \frac{n_{xy,Sd}}{t} \pm \frac{m_{xy,Sd}}{t^2/4}$$

and $n_{x,Sd}$, $n_{y,Sd}$, $n_{xy,Sd}$, $m_{x,Sd}$, $m_{y,Sd}$ and $m_{xy,Sd}$ are defined above.

<u>Design by global analysis: numerical analysis</u>

If the internal stresses of a plated structure are determined by a numerical analysis which is based on a materially linear analysis, the highest equivalent v. Mises stress $\sigma_{eq,Sd}$ of the plated structure shall be calculated for the relevant combination of design actions.

The equivalent v. Mises stress $\sigma_{eq,Sd}$ defined by the stress components which occurred at one point in the plated structure.

$$\sigma_{eq,Sd} = \sqrt{\sigma_{x,Sd}^2 + \sigma_{y,Sd}^2 - \sigma_{x,Sd}\sigma_{y,Sd} + 3\tau_{Sd}^2} \qquad \text{/III.3/}$$

where $\sigma_{x,Sd}$ and $\sigma_{y,Sd}$ are positive in case of tension.

If a numerical analysis is used for the verification of buckling, the effects of practically unavoidable imperfections shall be taken into account. These imperfection may be:

(a) geometrical imperfections:

- deviations from the nominal geometric shape of the plate (predeformation, out of plane deflections)
- irregularities of welds (minor excentricities)
- deviations from nominal thickness

(b) material imperfections:

- residual stresses because of rolling, pressing , welding, straightening
- inhomogenities and anisotropies

If no better method is known, the geometrical and material imperfections shall be taken into account by an initial equivalent geometric imperfection of the perfect plate. The shape of the initial equivalent geometric imperfection shall be derived from the relevant buckling mode.
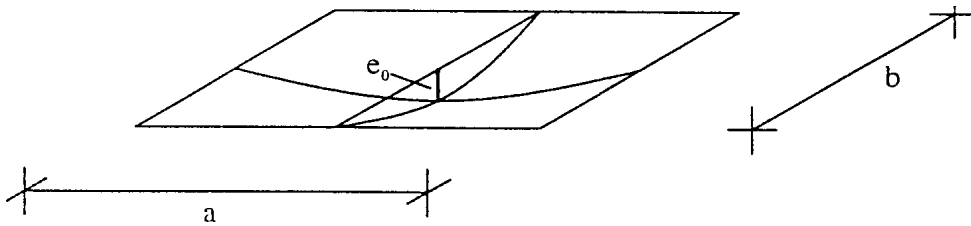
Figure III.6 Initial equivalent geometric bow imperfection e_0 of a plate segment [Fig. 3.1]

The amplitude of the initial equivalent geometric imperfection e_0 of a rectangular plate segment may be derived by numerical calibrations with test results from test pieces that may be

considered as representative for fabricative from the plate buckling curve of Eurocode 3 - Part 1.5, as follows:

$$e_0 = \frac{\left(1 - \rho \bar{\lambda}_p^2\right)(1 - \rho)}{\rho \zeta} \qquad \text{/III.4/}$$

where

$$\zeta = \frac{6b^2\left(b^2 + v \cdot a^2\right)}{t\left(a^2 + b^2\right)^2} \qquad \text{and} \qquad \alpha < \sqrt{2}$$

and:

    ρ is the reduction factor for plate buckling,
    a,b   are geometric properties of the plate, see Fig. III.4,
    t   is the thickness of the plate,
    α is the aspect ratio a/b < $\sqrt{2}$.

As a conservative assumption the amplitude may be taken as e_0 = a/250 where a $\leq$ b. The pattern of the equivalent geometric imperfections shall, if relevant, be adapted to the constructional detailing and to imperfections expected from fabricating or manufacturing. In all cases the reliability of a finite element analysis shall be checked with known results from tests or compared analysis.

Design by simplified design models

The internal forces or stresses of a plated structure loaded by transverse loads and inplane loads may be calculated with a simplified design model, that gives conservative estimates.

Therefore the plated structure may be subdivided into individual plate segments, which may be stiffened or unstiffened. The individual plate segments may be designed with the following design models:

a) Unstiffened plate segments

An unstiffened rectangular plate under transverse loads may be modelled as an equivalent beam in the direction of the dominate load distribution, if the following conditions are fulfilled:

   – the aspect ratio a/b of the plate is greater than 2;
   – the plate is loaded by a uniform distributed transverse load, which may be linear or constant;
   – the strength, stability and stiffness of the frame or beam on which the plate segment is supported fulfils the assumed boundary conditions of the equivalent beam.

The internal forces and moments of the equivalent beam shall be determined with an elastic analysis as defined in ENV 1993-1-1. If the direction of the dominant load distribution is transverse to the direction of the inplane compression forces, the interaction between the effects

of inplane loads and out of plane loads may be neglected. If the direction of the dominant load distribution is parallel to the direction of the inplane compression forces, the interaction formula specified in Part 1-1 clause 5.5.4 may be applied to the equivalent beam.

b) Stiffened plate segments

A stiffened plate or a stiffened plate segment of a plated structure may be modelled as a grillage if it is regularly stiffened in the transverse and longitudinal direction. In determining the cross-sectional value A_i of the cooperating plate of an individual member i of the grillage the effects of shear lag shall taken into account by the reduction factor β according to ENV 1993-1.5. For a member i of the grillage which is arranged in parallel to the direction of inplane compression forces, the cross-sectional value A_i shall also be determined taking account of the effective width of the adjacent subpanels due to plate buckling according to ENV 1993-1.5.

The interaction of shear lag effects and plate buckling effects, see Fig. III.7, should be considered by the effective area A_i from equation /III.5/.

$$A_i = \left[\rho_c\left(A_{L,eff} + \sum\rho_{pan,i}b_{pan,i}t_{pan,i}\right)\right]\beta^\kappa \qquad \text{/III.5/}$$

where

$A_{L,eff}$ is the effective area of the stiffener due to local plate buckling of the stiffener;

ρ_c is the reduction factor due to global plate buckling of the stiffened plate segment;

$\rho_{pan,i}$ is the reduction factor due to local plate buckling of the subpanel i;

$b_{pan,i}$ is the width of the subpanel i;

$t_{pan,i}$ is the thickness of the subpanel i;

β is the effective width factor for the effect of shear lag.

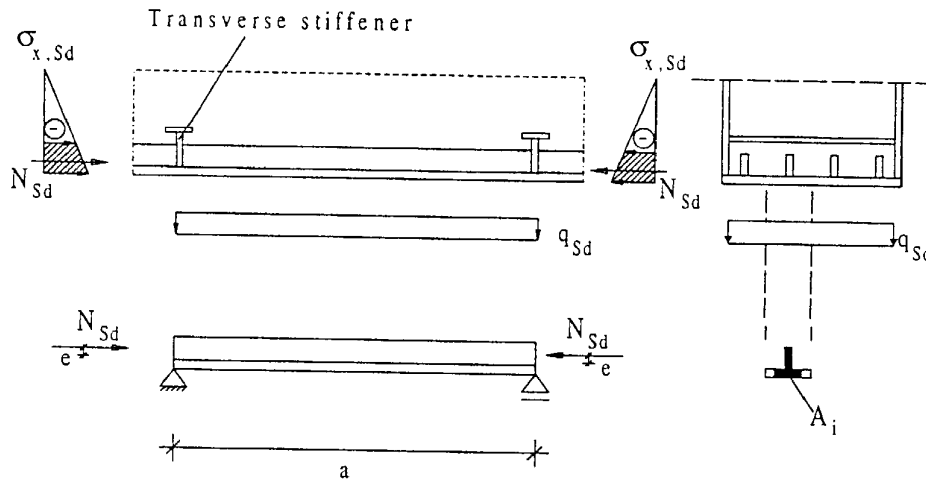κ is the ratio defined in 3.2(2) of ENV 1993 – 1.5.

Figure III.7 Definition of the cross-section A_i [Fig. 3.2]

The verification of a member i of the grillage may be performed using the interaction formula in clause 5.5.4 of ENV 1993-1.1 taking into account the following loading conditions:

– effects of transverse loadings

296

– equivalent axial force in the cross-section A_i due to normal stresses in the plate:
$$N_{Sd} = \int \sigma_x dA_i$$
– eccentricity e of the equivalent axial force N_{Sd} according to ENV 1993-1.5.

If the stiffeners of a plate or a plate segment are only arranged in parallel to the direction of inplane compression forces, the stiffened plate may be modelled as an equivalent beam on elastic springs, see ENV 1993-2. If the stiffeners of a stiffened plate segment are positioned in the transverse direction to the compression forces, the interaction between the compression forces and bending moments in the unstiffened plate segments between the stiffeners should be verified.

III.4 Serviceability limit states

Plated steel structures should meet the serviceability limit state criteria in 4.1 of ENV 1993-1-1.

The requirements for the out of plane deflection *w* of a plate segment in a plated structure shall be defined by the relevant application standard or by the competent authority, the designer or the client. The limit state of excessive vibrations shall be verified with the requirements given by the competent authority, the designer or the client.

III.5 Ultimate limit state

All parts of a plated structure shall be so proportioned that the basic design requirements for ultimate limit states are satisfied. The partial factor γ_M for resistance of plated structures shall be taken from the relevant parts of EC 3 - Part l. For connections of plated structures the partial factor γ_M shall be obtained from section 6 of ENV 1993-1-l. Members and connections subject to fatigue shall also satisfy the requirements given in section III.

Plastic collapse or tensile rupture

<u>General</u>

In an elastic design the resistance of a plate segment in a plated structure against plastic collapse or tensile rupture under combined axial forces and bending is defined by the v. Mises equivalent stress $\sigma_{eq,Rd}$ as:

$$\sigma_{eq,Rd} = 1,0 \cdot f_y / \gamma_{M0} \qquad \text{/III.6/}$$

At every point in a plated structure the design stress $\sigma_{eq,Sd}$ shall satisfy the condition:

$$\sigma_{eq,Sd} \leq \sigma_{eq,Rd} \qquad \text{/III.7/}$$

where $\sigma_{eq,Sd}$ is the largest value of v. Mises equivalent stress.

Supplementary rules for the design by global analysis

If a numerical analysis is based on materially linear analysis the resistance against plastic collapse or tensile rupture shall be checked for the requirement given in /III.7/.

If a materially nonlinear analysis is based on a design stress-strain relationship with f_{yd}, the plated structure shall be subject to a load arrangement F that may be taken from the design values of actions F_{Sd}, and the load may be incrementally increased to determine the load amplification factor λR of the plastic limit state F_{Rd}.

The result of the numerical analysis shall satisfy the condition:

$$F_{Sd} \leq F_{Rd} \qquad\qquad \text{/III.8/}$$

where $F_{Sd} = \lambda_R \times F$ and λ_R is the load amplification factor.

Supplementary rules for the design by simplified design models

If an unstiffened plate is designed as an equivalent beam, the cross-section resistance of the equivalent beam shall be checked for the combination of inplane loading and out of plane loading effects with the design rules given in ENV 1993-1-1.

If a stiffened plate segment is modelled as a grillage as described above the cross-section resistance and the buckling resistance of the individual members i of the grillage shall be checked for the combination of inplane and out of plane loading effects using the interaction formula in clause 5.5.4 of ENV 1993-1.1.

If a stiffened plate segment is designed as a an equivalent beam as described above the cross-section resistance and the buckling resistance of the equivalent beam shall be checked for the combination of inplane and out of plane loading effects using the interaction formula in clause 5.5.4 of ENV 1993-1.1.

Cyclic plasticity / low cycle fatigue

In a materially linear design the resistance of a plate segment in a plated structure against cyclic plasticity / low cycle fatigue may be verified by the v. Mises stress range limitation $\Delta\sigma_{Rd}$.

$$\Delta\sigma_{Rd} = 2{,}0 \cdot f_y / \gamma_{M0} \qquad\qquad \text{/III.9/}$$

At every point in a plated structure the design stress range $\Delta\sigma_{Rd}$ shall satisfy the condition:

$$\Delta\sigma_{Sd} \leq \Delta\sigma_{Rd} \qquad\qquad \text{/III.10/}$$

where $\Delta\sigma_{Sd}$ is the largest value of the v. Mises equivalent stress range at the relevant point of the plate segment due to the relevant combination of design actions.

Where a materially nonlinear computer analysis is performed, the plate shall be subject to the design values of the varying and fixed actions. The largest change in the v. Mises plastic strain during one load cycle at any point in the structure shall be used as design value of the plastic strain range $\Delta\varepsilon_{Sd}$.

Unless a more sophisticated low cycle fatigue assessment is performed, the design value of the plastic strain range shall satisfy the condition:

$$\Delta\varepsilon_{Sd} = 2,0 \cdot f_y / E \cdot \gamma_{M0}$$ /III.11/

Buckling resistance

If a plate segment of a plated structure is loaded by in-plane effects, its resistance to plate buckling shall be verified with the design rules given in ENV 1993-1-5. The shear buckling resistance of a plate segment shall be verified with the design rules given in ENV 1993-1-5. For the interaction between the effects of inplane and out of plane loading, see section ***Modelling of structural analysis***.

If the plate buckling resistance for combined in plane and out of plane loading is checked by a numerical analysis, the design actions F_{Sd} shall satisfy the condition:

$$F_{Sd} \leq F_{Rd}$$ /III.12/

The plate buckling resistance F_{Rk} of a plated structure is defined as:

$$F_{Rd} = k\,F_{Rk}/\gamma_{M1}$$ /III.13/

where

F_{Rk} is the characteristic buckling resistance of the plated structure
k   is the calibration factor.

The characteristic buckling resistance F_{Rk} shall be derived from a load-deformation curve which is calculated for the relevant point of the structure taking into account the relevant combination of design actions F_{Sd}. In addition, the analysis shall taken into account the imperfections. The characteristic buckling resistance F_{Rk} is defined by either of the three following criterion:

– maximum load of the load-deformation-curve (limit load);
– bifurcation load if occurring during the loading path before reaching the limit point of the load-deformation-curve;
– largest tolerable deformation if occurring the loading path before reaching the bifurcation load or the limit load.

The reliability of the numerically determined critical buckling resistance shall be checked:

(a) either by calculating other plate buckling cases, for which characteristic buckling resistance values $F_{k.known}$ are known, with the same program basically similar imperfection assumptions. The check cases should be similar in their buckling controlling parameters (e.g non-dimensional plate slenderness, post buckling behaviour, imperfection-sensitivity, material behaviour)
(b) or by comparison of calculated values with test results $F_{k,known}$. Regarding the similarity of the check cases, the same statements as made above are valid.

Depending on the results of the reliability checks a calibration factor k shall be evaluated from:

$$k = F_{k,known,check} / F_{Rk,check} \qquad\qquad /III.14/$$

where $F_{k,known,check}$ are results from prior knowledge and $F_{Rk,check}$ are the results of the numerical calculations.

If a stiffened plate segment is subdivided into subpanels and equivalent effective stiffeners the buckling resistance of the stiffened plate segment shall be checked with the design rules given in ENV 1993-1-5, neglecting the bending effects due to the transverse loads which applied at the plate segments. Further, the buckling resistance of the equivalent effective stiffener of the plate shall be checked with the design rules given in ENV 1993-1-l.

Fatigue

For plated structures the requirements for fatigue shall be obtained from the relevant application parts of Eurocode 3. If no other requirements are given by the application parts of Eurocode 3 or by the competent authority, the client or the designer no fatigue assessment is required for up to 10000 cycles.

III. Annex A: Types of analysis for the design of plated structures

The internal stresses of stiffened and unstiffened plates may be determined with the following types of analysis:

- LA: Linear elastic analysis;
- GNA: Geometrically nonlinear analysis;
- MNA: Materially nonlinear analysis;
- GMNA: Geometrically and materially nonlinear analysis;
- GNIA: Geometrically nonlinear analysis elastic with imperfections included;
- GMNIA: Geometrically and materially nonlinear analysis with imperfections included.

Linear elastic plate analysis (LA)

The linear elastic analysis models the behaviour of thin plate structures on the basis of the plate bending theory, related to the perfect geometry of the plate. The linearity of the theory results from the assumptions of the linear elastic material law and the linear small deflection theory.

The LA analysis satisfies the equilibrium as well as the compatibility of the deflections. The stresses and deformations varies linear with the transverse loading. As an example for the LA analysis the following fourth-order partial differential equation is given for an isotropic thin plate that subject only to a transverse load p(x,y):

$$\frac{\partial^4 w}{\partial x^4} + \frac{\partial^4 w}{\partial x^2 \partial y^2} + \frac{\partial^4 w}{\partial y^4} = \frac{p(x,y)}{D} \qquad\qquad /III.15/$$

where $D = \dfrac{Et^3}{12(1-v^2)}$.

Geometrically nonlinear analysis (GNA)

The geometrically nonlinear elastic analysis is based on the principles of the plate bending theory of the perfect structure using the linear elastic material law and the nonlinear, large deflection theory.

The GNA analysis satisfies the equilibrium as well as the compatibility of the deflections under consideration of the deformation of the structure. The large deflection theory takes into account the interaction between flexural and membrane actions. The deflections and stresses varies in a non linear manner with the magnitude of the transverse pressure. As an example for the GNA analysis the following fourth-order partial differential equation system is given for an isotropic thin plate that subject only to a transverse load p(x,y).

$$\frac{\partial^4 w}{\partial x^4} + \frac{\partial^4 w}{\partial x^2 \partial y^2} + \frac{\partial^4 w}{\partial y^4} - \frac{1}{D}\left[\frac{\partial^2 f}{\partial y^2}\frac{\partial^2 w}{\partial x^2} - 2\left(\frac{\partial^2 f}{\partial x \partial y}\frac{\partial^2 w}{\partial x \partial y}\right) + \frac{\partial^2 f}{\partial x^2}\frac{\partial^2 w}{\partial y^2}\right] = \frac{p(x,y)}{D} \quad \text{/III.16a/}$$

$$\frac{\partial^4 f}{\partial x^4} + \frac{\partial^4 f}{\partial x^2 \partial y^2} + \frac{\partial^4 f}{\partial y^4} = E\left[\left(\frac{\partial^2 w}{\partial x \partial y}\right)^2 - \frac{\partial^2 w}{\partial x^2}\frac{\partial^2 w}{\partial y^2}\right] \quad \text{/III.16b/}$$

where f is the Airy's stress function, and

$$D = \frac{Et^3}{12(1-v^2)}.$$

Materially nonlinear analysis (MNA)

The materially nonlinear analysis is based on the plate bending theory of the perfect structure with the assumption of small deflections – like in Linear elastic plate analysis (LA) – however, it takes into account the nonlinear behaviour of the material.

Geometrically and materially nonlinear analysis (GMNA)

The geometrically and materially nonlinear analysis is based on the plate bending theory of the perfect structure with the assumptions of the nonlinear, large deflection theory and the nonlinear, elasto-plastic material law.

Geometrically nonlinear analysis elastic with imperfections included (GNIA)

The geometrically nonlinear analysis with imperfections included is equivalent to the GNA analysis defined in Geometrically nonlinear analysis (GNA), however, the geometrical model used the geometrically imperfect structure, for instance a pre-deformation applies at the plate which is governed by the relevant buckling mode.

The GNIA analysis is used in cases of dominating compression or shear stresses in some of the plated structures due to in-plane effects. It delivers the elastic buckling loads of the "real" imperfect plated structure.

Geometrically and materially nonlinear analysis with imperfections included (GMNIA)

The geometrically and materially nonlinear analysis with imperfections included is equivalent to the GMNA analysis defined in Geometrically and materially nonlinear analysis (GMNA), however, the geometrical model used the geometrically imperfect structure, for instance a pre-deformation applies at the plate which is governed by the relevant buckling mode.

The GMNIA analysis is used in cases of dominating compression or shear stresses in a plate due to inplane effects. It delivers the elasto-plastic buckling loads of the "real" imperfect structure.

III. Annex B: Internal stresses of unstiffened rectangular plates (Small deflection theory)

This annex provides design formulas for the calculation of internal stresses of unstiffened rectangular plates based on the small deflection theory for plates. Therefore the effects of membrane forces are not taken into account in the design formulas given in this annex.

Design formulas are provided for the following load cases:

– uniformly distributed loading on the entire plate
– central patch loading distributed uniformly over a patch area

The deflection w of a plate segment and the bending stresses σ_{bx} and σ_{by} in a plate segment may be calculated with the coefficients given in the tables of following sections. The coefficients take into account a poisson's ratio ν of 0.3.

Definitions

q_{Sd}	is the design value of the distributed load
p_{Sd}	is the design value of the patch loading
a	is the smaller side of the plate
b	is the longer side of the plate
t	is the thickness of the plate
E	is the Elastic modulus
k_w	is the coefficient for the deflection of the plate given in dependence of the boundary conditions of the plate in the data tables.

$k_{\sigma bx}$ is the coefficient for the bending stress σ_{bx} of the plate given in dependence of the boundary conditions of the plate in the data tables.

$k_{\sigma by}$ is the coefficient for the bending stress σ_{by} of the plate given in dependence of the boundary conditions of the plate in the data tables.

Uniformly distributed loading

Out of plane deflection

The deflection w of a plate segment which is loaded by uniformly distributed loading may be calculated as follows:

$$w = k_w \frac{q_{Sd} a^4}{Et^3} \qquad\qquad \text{/III.17/}$$

In comparison to the thickness of the plate segment the deflection w shall be small, because the design formulas base on small deflection theory.

Internal stresses

The bending stresses σ_{bx} and σ_{by} in a plate segment may be determined with the following equations:

$$\sigma_{bx,Sd} = k_{\sigma bx} \frac{q_{Sd} a^2}{t^2} \qquad\qquad \text{/III.18/}$$

$$\sigma_{by,Sd} = k_{\sigma by} \frac{q_{Sd} a^2}{t^2} \qquad\qquad \text{/III.19/}$$

For a plate segment the equivalent stress may be calculated with the bending stresses given in above as follows:

$$\sigma_{eq,Sd} = \sqrt{\sigma_{bx,Sd}^2 + \sigma_{by,Sd}^2 - \sigma_{bx,Sd}\sigma_{by,Sd}} \qquad\qquad \text{/III.20/}$$

The points for which the state of stress are defined in the data tables are located either on the centre lines or on the boundaries, so that due to symmetry or the postulated boundary conditions, the bending shear stresses τ_b are zero.

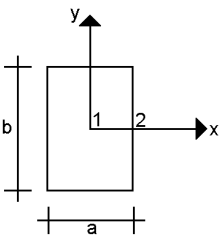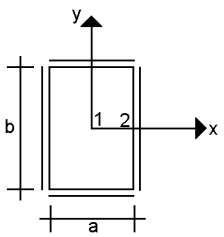*Coefficients k for uniformly distributed loadings*

Table III.2 Coefficients k

<table>
<tr><td colspan="4">Loading: Uniformly distributed loading</td></tr>
<tr><td colspan="2"></td><td colspan="2">Boundary conditions:

- All edges are rigidly supported and rotationally free</td></tr>
<tr><td>b/a</td><td>k_{w1}</td><td>$k_{\sigma bxl}$</td><td>$k_{\sigma byl}$</td></tr>
<tr><td>1.0</td><td>0.04434</td><td>0.286</td><td>0.286</td></tr>
<tr><td>1.5</td><td>0.08438</td><td>0.486</td><td>0.299</td></tr>
<tr><td>2.0</td><td>0.11070</td><td>0.609</td><td>0.278</td></tr>
<tr><td>3.0</td><td>0.13420</td><td>0.712</td><td>0.244</td></tr>
</table>

Table III.3 Coefficients k

<table>
<tr><td colspan="5">Loading: Uniformly distributed loading</td></tr>
<tr><td colspan="3"></td><td colspan="2">Boundary conditions:

- All edges are rigidly supported and rotationally fixed.</td></tr>
<tr><td>b/a</td><td>k_{w1}</td><td>$k_{\sigma bxl}$</td><td>$k_{\sigma byl}$</td><td>$k_{\sigma bx2}$</td></tr>
<tr><td>1.0</td><td>0.01375</td><td>0.1360</td><td>0.1360</td><td>- 0.308</td></tr>
<tr><td>1.5</td><td>0.02393</td><td>0.2180</td><td>0.1210</td><td>- 0.454</td></tr>
<tr><td>2.0</td><td>0.02763</td><td>0.2450</td><td>0.0945</td><td>- 0.498</td></tr>
</table>

| 3.0 | 0.02870 | 0.2480 | 0.0754 | - 0.505 |

Table III.4 Coefficients k

Loading: Uniformly distributed loading				
			Boundary conditions: - Three edges are rigidly supported and rotationally free and one edge is rigidly supported and rotationally fixed.	
b/a	k_{w1}	$k_{\sigma bxl}$	$k_{\sigma byl}$	$k_{\sigma bx4}$
1.5	0.04894	0.330	0.177	- 0.639
2.0	0.05650	0.368	0.146	- 0.705

Table III.5 Coefficients k

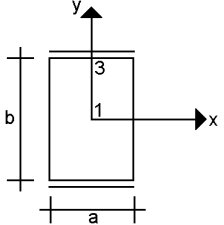| Loading: Uniformly distributed loading				
			Boundary conditions: - Two edges are rigidly supported and rotationally free and two edges are rigidly supported and rotationally fixed.	
b/a	k_{w1}	$k_{\sigma bxl}$	$k_{\sigma byl}$	$k_{\sigma bx4}$
1.0	0.02449	0.185	0.185	- 0.375
1.5	0.04411	0.302	0.180	- 0.588
2.0	0.05421	0.355	0.152	- 0.683

Table III.6 Coefficients k
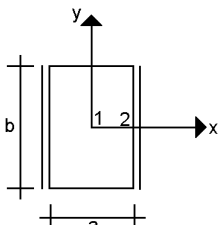
Loading: Uniformly distributed loading				
			Boundary conditions: - Two edges are rigidly supported and rotationally free and two edges are rigidly supported and rotationally fixed.	
b/a	k_{w1}	$k_{\sigma bxl}$	$k_{\sigma byl}$	$k_{\sigma by3}$
1.0	0.02089	0.145	0.197	- 0.420
1.5	0.05803	0.348	0.274	- 0.630
2.0	0.09222	0.519	0.284	- 0.717

Table III.7 Coefficients k

Loading: Uniformly distributed loading				
			Boundary conditions: - Two edges are rigidly supported and rotationally free and two edges are rigidly supported and rotationally fixed.	
b/a	k_{w1}	$k_{\sigma bxl}$	$k_{\sigma byl}$	$k_{\sigma bx2}$
1.5	0.02706	0.240	0.106	- 0.495
2.0	0.02852	0.250	0.0848	- 0.507

Central patch loading

Out of plane deflection

The deflection w of a plate segment which is loaded by a central patch loading may be calculated as follows:

$$w = k_w \frac{p_{Sd} a^2}{E t^3} \qquad \text{/III.21/}$$

Internal stresses

The bending stresses σ_{bx} and σ_{by} in a plate segment may be determined by the following formulas:

$$\sigma_{bx,Sd} = k_{\sigma bx} \frac{p_{Sd}}{t^2} \qquad \text{/III.22/}$$
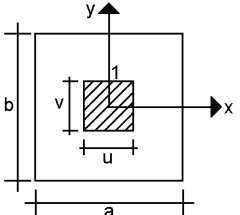
$$\sigma_{by,Sd} = k_{\sigma by} \frac{p_{Sd}}{t^2} \qquad \text{/III.23/}$$

For a plate segment the equivalent stress may be calculated with the bending stresses given above as follows:

$$\sigma_{eq,Sd} = \sqrt{\sigma_{bx,Sd}^2 + \sigma_{by,Sd}^2 - \sigma_{bx,Sd}\sigma_{by,Sd}} \qquad \text{/III.24/}$$

Coefficients k for patch loading

<p style="text-align:center">Table III.8 Coefficients k</p>

Loading: Central patch loading				
			Boundary conditions: - All edges are rigidly supported and rotationally free.	
			Parameters: $\alpha = u/a,\ \beta = v/a$	
b/a	$\alpha \times \beta$	k_{w1}	$k_{\sigma bxl}$	$k_{\sigma byl}$
1	0.1×0.1	0.1254	1.72	1.72
	0.2×0.2	0.1210	1.32	1.32
	0.3×0.3	0.1126	1.04	1.04
	0.2×0.3	0.1167	1.20	1.12
	0.2×0.4	0.1117	1.10	0.978
1.5	0.1×0.1	0.1664	1.92	1.70
	0.2×0.2	0.1616	1.51	1.29
	0.3×0.3	0.1528	1.22	1.01
	0.2×0.3	0.1577	1.39	1.09
	0.2×0.4	0.1532	1.29	0.953
2.0	0.1×0.1	0.1795	1.97	1.67
	0.2×0.2	0.1746	1.56	1.26
	0.3×0.3	0.1657	1.28	0.985
	0.2×0.3	0.1708	1.45	1.07
	0.2×0.4	0.1665	1.35	0.929
3.0	0.1×0.1	0.184	1.99	1.66
	0.2×0.2	0.1791	1.58	1.25
	0.3×0.3	0.1701	1.30	0.975

| | 0.2×0.3 | 0.1753 | 1.47 | 1.06 |
| | 0.2×0.4 | 0.1711 | 1.37 | 0.918 |

III. Annex C: Internal stresses of unstiffened rectangular plates (Large deflection theory)

This annex provides design formulas for the calculation of internal stresses of unstiffened rectangular plates based on the large deflection theory for plates. The following loading conditions are considered:

– uniformly distributed loading on the entire plate
– central patch loading distributed uniformly over the patch area

The bending and membrane stresses in a plate and the deflection w of a plate may be calculated with the coefficients given in the tables of the following sections. The coefficients take into account a poisson's ratio ν of 0.3.

Definitions

q_{Sd} the design value of the distributed load.
p_{Sd} the design value of the patch loading.
a   the smaller side of the plate.
b   the longer side of the plate.
t   the thickness of the plate.
E   the Elastic modulus.
k_w the coefficient for the deflection of the plate given in dependence of the boundary conditions of the plate in the data tables.
$k_{\sigma bx}$ the coefficient for the bending stress σ_{bx} of the plate given in dependence of the boundary conditions of the plate in the data tables.
$k_{\sigma by}$ the coefficient for the bending stress σ_{by} of the plate given in dependence of the boundary conditions of the plate in the data tables.
$k_{\sigma mx}$ the coefficient for the membrane stress σ_{mx} of the plate given in dependence of the boundary conditions of the plate in the data tables.
$k_{\sigma my}$ the coefficient for the membrane stress σ_{my} of the plate given in dependence of the boundary conditions of the plate in the data tables.

Uniformly distributed loading

Out of plane deflection

The deflection w of a plate segment which is loaded by uniformly distributed loading may be calculated as follows:

$$w = k_w \frac{q_{Sd}a^4}{Et^3} \qquad\qquad \text{/III.25/}$$

Internal stresses

The bending stresses σ_{bx} and σ_{by} in a plate segment may be determined with the following equations:

$$\sigma_{bx,Sd} = k_{\sigma bx} \frac{q_{Sd}a^2}{t^2} \qquad\qquad \text{/III.26/}$$

$$\sigma_{by,Sd} = k_{\sigma by} \frac{q_{Sd}a^2}{t^2} \qquad\qquad \text{/III.27/}$$

The membrane stresses σ_{mx} and σ_{my} in a plate segment may be determined as follows:

$$\sigma_{mx,Sd} = k_{\sigma mx} \frac{q_{Sd}a^2}{t^2} \qquad\qquad \text{/III.28/}$$

$$\sigma_{my,Sd} = k_{\sigma my} \frac{q_{Sd}a^2}{t^2} \qquad\qquad \text{/III.29/}$$

At the loaded surface of a plate the total stresses are calculated with the above mentioned bending and membrane stresses as follows:

$$\sigma_{x,Sd} = -\sigma_{bx,Sd} + \sigma_{mx,Sd} \qquad\qquad \text{/III.30/}$$

$$\sigma_{y,Sd} = -\sigma_{by,Sd} + \sigma_{my,Sd} \qquad\qquad \text{/III.31/}$$

At the no-loaded surface of a plate the total stresses are determined with the bending and membrane stresses as follows:

$$\sigma_{x,Sd} = \sigma_{bx,Sd} + \sigma_{mx,Sd} \qquad\qquad \text{/III.32/}$$

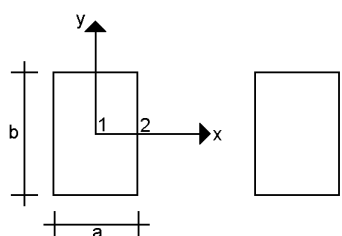$$\sigma_{y,Sd} = \sigma_{by,Sd} + \sigma_{my,Sd} \qquad\qquad \text{/III.33/}$$

For a plate the equivalent stress $\sigma_{eq,Sd}$ may be calculated with the stresses given above as follows:

$$\sigma_{eq,Sd} = \sqrt{\sigma_{x,Sd}^2 + \sigma_{y,Sd}^2 - \sigma_{x,Sd}\sigma_{y,Sd}} \qquad\qquad \text{/III.34/}$$

The points for which the state of stress are defined in the data tables are located either on the centre lines or on the boundaries, so that due to symmetry or the postulated boundary conditions, membrane shearing stresses τ_m as well as bending shear stresses τ_b are zero. The algebraic sum of the appropriate bending and membrane stresses at the points considered in the data tables gives the values of maximum and minimum surface stresses at these points.

Coefficients k for uniformly distributed loadings

Table III.9 Coefficients k

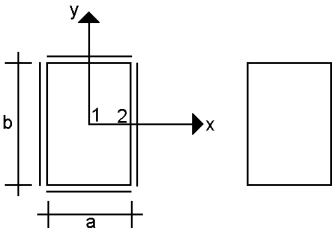| Loading: Uniformly distributed loading						
			Boundary conditions: FBC: All edges are rigidly supported and rotationally free. MBC: Zero direct stresses, zero shear stresses			
			Parameters: $$Q = \dfrac{q_{Sd}a^4}{Et^4}$$			
b/a	Q	k_{w1}	$k_{\sigma bxl}$	$k_{\sigma byl}$	$k_{\sigma mxl}$	$k_{\sigma myl}$	$k_{\sigma my2}$
1.0	20	0.0396	0.2431	0.2431	0.0302	0.0302	- 0.0589
	40	0.0334	0.1893	0.1893	0.0403	0.0403	- 0.0841
	120	0.0214	0.0961	0.0961	0.0411	0.0411	-0.1024
	200	0.0166	0.0658	0.0658	0.0372	0.0372	- 0.1004
	300	0.0135	0.0480	0.0480	0.0335	0.0335	- 0.0958
	400	0.0116	0.0383	0.0383	0.0306	0.0306	- 0.0915
1.5	20	0.0685	0.3713	0.2156	0.0243	0.0694	-0.1244
	40	0.0546	0.2770	0.1546	0.0238	0.0822	- 0.1492
	120	0.0332	0.1448	0.0807	0.0170	0.0789	- 0.1468
	200	0.0257	0.1001	0.0583	0.0141	0.0715	- 0.1363
	300	0.0207	0.0724	0.0440	0.0126	0.0646	- 0.1271
	400	0.0176	0.0569	0.0359	0.0117	0.0595	- 0.1205
2.0	20	0.0921	0.4909	0.2166	0.0085	0.0801	- 0.1346
	40	0.0746	0.3837	0.1687	0.0079	0.0984	- 0.1657
	120	0.0462	0.2138	0.0959	0.0073	0.0992	- 0.1707

	200	0.0356	0.1516	0.0695	0.0067	0.0914	- 0.1610
	300	0.0287	0.1121	0.0528	0.0061	0.0840	- 0.1510
	400	0.0245	0.0883	0.0428	0.0061	0.0781	- 0.1434

Table III.10 Coefficients k

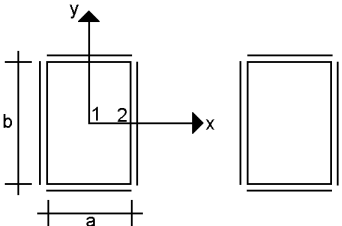| Loading: Uniformly distributed loading							
			Boundary conditions: FBC: All edges are rigidly supported and rotationally free. MBC: All edges remains straight. Zero average direct stresses, zero shear stresses				
			Parameters: $Q = \dfrac{q_{Sd}a^4}{Et^4}$				
b/a	Q	k_{w1}	$k_{\sigma bxl}$	$k_{\sigma byl}$	$k_{\sigma mxl}$	$k_{\sigma myl}$	$k_{\sigma mx2}$	$k_{\sigma my2}$
1	20	0.0369	0.2291	0.2291	0.0315	0.0315	0.0352	- 0.0343
	40	0.0293	0.1727	0.1727	0.0383	0.0383	0.0455	- 0.0429
	120	0.0170	0.0887	0.0887	0.0360	0.0360	0.0478	- 0.0423
	200	0.0126	0.0621	0.0621	0.0317	0.0317	0.0443	- 0.0380
	300	0.0099	0.0466	0.0466	0.0280	0.0280	0.0403	- 0.0337
	400	0.0082	0.0383	0.0383	0.0255	0.0255	0.0372	- 0.0309
1.5	20	0.0554	0.3023	0.1612	0.0617	0.0287	0.0705	- 0.0296
	40	0.0400	0.2114	0.1002	0.0583	0.0284	0.0710	- 0.0293
	120	0.0214	0.1079	0.0428	0.0418	0.0224	0.0559	- 0.0224
	200	0.0157	0.0778	0.0296	0.0345	0.0191	0.0471	- 0.0188
	300	0.0122	0.0603	0.0224	0.0296	0.0167	0.0408	- 0.0161
	400	0.0103	0.0505	0.0188	0.0267	0.0152	0.0369	- 0.0147
2	20	0.0621	0.3234	0.1109	0.0627	0.0142	0.0719	- 0.0142
	40	0.0438	0.2229	0.0689	0.0530	0.0120	0.0639	- 0.0120
	120	0.0234	0.1163	0.0336	0.0365	0.0086	0.0457	- 0.0083
	200	0.0172	0.0847	0.0247	0.0305	0.0075	0.0384	- 0.0067
	300	0.0135	0.0658	0.0195	0.0268	0.0067	0.0335	- 0.0058
	400	0.0113	0.0548	0.0164	0.0244	0.0064	0.0305	- 0.0050
3	20	0.0686	0.3510	0.1022	0.0477	0.0020	0.0506	- 0.0007
	40	0.0490	0.2471	0.0725	0.0420	0.0020	0.0441	0.0000

b/a	Q	k_{w1}	$k_{\sigma bx1}$	$k_{\sigma by1}$	$k_{\sigma mx1}$	$k_{\sigma my1}$	$k_{\sigma bx2}$	$k_{\sigma my2}$
	120	0.0267	0.1317	0.0390	0.0320	0.0027	0.0335	0.0010
	200	0.0196	0.0954	0.0283	0.0271	0.0044	0.0285	0.0027
	300	0.0153	0.0733	0.0217	0.0242	0.0059	0.0256	0.0044
	400	0.0127	0.0605	0.0178	0.0221	0.0066	0.0235	0.0051

Table III.11 Coefficients k

Loading: Uniformly distributed loading

Boundary conditions:

FBC: All edges are rigidly supported and rotationally fixed.

MBC: Zero direct stresses, zero shear stresses

Parameters: $Q = \dfrac{q_{Sd}a^4}{Et^4}$

b/a	Q	k_{w1}	$k_{\sigma bx1}$	$k_{\sigma by1}$	$k_{\sigma mx1}$	$k_{\sigma my1}$	$k_{\sigma bx2}$	$k_{\sigma my2}$
1	20	0.0136	0.1336	0.1336	0.0061	0.0061	- 0.3062	- 0.0073
	40	0.0131	0.1268	0.1268	0.0113	0.0113	- 0.3006	- 0.0137
	120	0.0108	0.0933	0.0933	0.0212	0.0212	- 0.2720	- 0.0286
	200	0.0092	0.0711	0.0711	0.0233	0.0233	- 0.2486	- 0.0347
	300	0.0078	0.0547	0.0547	0.0233	0.0233	- 0.2273	- 0.0383
	400	0.0069	0.0446	0.0446	0.0226	0.0226	- 0.2113	- 0.0399
1.5	20	0.0234	0.2117	0.1162	0.0061	0.0133	- 0.4472	- 0.0181
	40	0.0222	0.1964	0.1050	0.0098	0.0234	- 0.4299	- 0.0322
	120	0.0173	0.1406	0.0696	0.0124	0.0385	- 0.3591	- 0.0559
	200	0.0144	0.1103	0.0537	0.0116	0.0415	- 0.3160	- 0.0620
	300	0.0122	0.0879	0.0430	0.0105	0.0416	- 0.2815	- 0.0636
	400	0.0107	0.0737	0.0364	0.0098	0.0409	- 0.2583	- 0.0635
2	20	0.0273	0.2418	0.0932	0.0010	0.0108	- 0.4935	- 0.0150
	40	0.0265	0.2330	0.0897	0.0017	0.0198	- 0.4816	- 0.0277
	120	0.0223	0.1901	0.0740	0.0032	0.0392	- 0.4223	- 0.0551
	200	0.0192	0.1578	0.0621	0.0039	0.0456	- 0.3780	- 0.0647
	300	0.0165	0.1306	0.0518	0.0042	0.0483	- 0.3396	- 0.0690
	400	0.0147	0.1120	0.0446	0.0044	0.0487	- 0.3132	- 0.0702
3	20	0.0288	0.2492	0.0767	- 0.0015	0.0027	- 0.5065	- 0.0033

	40	0.0290	0.2517	0.0795	- 0.0022	0.0066	- 0.5095	- 0.0084
	120	0.0281	0.2440	0.0812	- 0.0010	0.0247	- 0.4984	- 0.0331
	200	0.0260	0.2230	0.0750	0.0000	0.0368	- 0.4702	- 0.0497
	250	0.0247	0.2096	0.0707	0.0002	0.0415	- 0.4520	- 0.0564

Table III.12 Coefficients k

Loading: Uniformly distributed loading								
				Boundary conditions: FBC: All edges are rigidly supported and rotationally fixed. MBC: All edges remains straight. Zero average direct stresses, zero shear stresses				
				Parameters: $Q = \dfrac{q_{Sd} a^4}{E t^4}$				
b/a	Q	k_{w1}	$k_{\sigma bx1}$	$k_{\sigma by1}$	$k_{\sigma mx1}$	$k_{\sigma my1}$	$k_{\sigma bx2}$	$k_{\sigma mx2}$	$k_{\sigma my2}$
1	20	0.0136	0.1333	0.1333	0.0065	0.0065	- 0.3058	0.0031	- 0.0055
	40	0.0130	0.1258	0.1258	0.0118	0.0118	- 0.3000	0.0059	- 0.0103
	120	0.0105	0.0908	0.0908	0.0216	0.0216	-0.2704	0.0123	- 0.0202
	200	0.0087	0.0688	0.0688	0.0234	0.0234	- 0.2473	0.0151	- 0.0233
	300	0.0073	0.0528	0.0528	0.0231	0.0231	- 0.2267	0.0169	- 0.0244
	400	0.0063	0.0430	0.0430	0.0223	0.0223	- 0.2119	0.0176	- 0.0246
1.5	20	0.0230	0.2064	0.1125	0.0137	0.0097	- 0.4431	0.0118	- 0.0082
	40	0.0210	0.1833	0.0957	0.0218	0.0155	- 0.4195	0.0200	- 0.0133
	120	0.0149	0.1175	0.0532	0.0275	0.0202	- 0.3441	0.0295	- 0.0185
	200	0.0118	0.0876	0.0369	0.0259	0.0195	- 0.3028	0.0304	- 0.0182
	300	0.0096	0.0678	0.0275	0.0238	0.0180	- 0.2710	0.0300	- 0.0173
	400	0.0083	0.0562	0.0221	0.0220	0.0168	- 0.2492	0.0291	- 0.0163
2	20	0.0262	0.2288	0.0853	0.0140	0.0060	- 0.4811	0.0149	- 0.0052
	40	0.0234	0.1994	0.0701	0.0206	0.0086	- 0.4492	0.0234	- 0.0077
	120	0.0162	0.1276	0.0404	0.0238	0.0094	- 0.3611	0.0299	- 0.0086
	200	0.0129	0.0963	0.0296	0.0223	0.0085	- 0.3162	0.0289	- 0.0079
	300	0.0105	0.0752	0.0230	0.0208	0.0077	- 0.2824	0.0274	- 0.0072
	400	0.0090	0.0627	0.0190	0.0196	0.0071	- 0.2600	0.0259	- 0.0066
3	20	0.0272	0.2331	0.0700	0.0102	0.0010	- 0.4878	0.0111	- 0.0008

	40	0.0247	0.2071	0.0615	0.0149	0.0011	- 0.4575	0.0167	- 0.0009
	120	0.0177	0.1396	0.0413	0.0186	0.0009	- 0.3727	0.0202	- 0.0005
	200	0.0143	0.1074	0.0319	0.0184	0.0009	- 0.3272	0.0197	- 0.0003
	300	0.0117	0.0848	0.0251	0.0176	0.0008	- 0.2924	0.0192	- 0.0002
	400	0.0101	0.0709	0.0210	0.0169	0.0008	- 0.2687	0.0182	0.0000

Central patch loading

Out of plane deflection

The deflection w and the stresses shall be determined with the formulas provided calculated of a plate which is loaded by a central patch loading may be calculated as follows:

$$w = k_w \frac{p_{Sd} a^4}{E t^3} \qquad \text{/III.35/}$$

Internal stresses

The bending stresses σ_{bx} and σ_{by} in a plate segment may be determined with the following equations:

$$\sigma_{bx,Sd} = k_{\sigma bx} \frac{p_{Sd} a^2}{t^2} \qquad \text{/III.36/}$$

$$\sigma_{by,Sd} = k_{\sigma by} \frac{p_{Sd} a^2}{t^2} \qquad \text{/III.37/}$$

The membrane stresses σ_{mx} and σ_{my} in a plate segment may be determined as follows:

$$\sigma_{mx,Sd} = k_{\sigma mx} \frac{p_{Sd} a^2}{t^2} \qquad \text{/III.38/}$$

$$\sigma_{my,Sd} = k_{\sigma my} \frac{p_{Sd} a^2}{t^2} \qquad \text{/III.39/}$$

At the loaded surface of a plate the total stresses are calculated with the above mentioned bending and membrane stresses as follows:

$$\sigma_{x,Sd} = -\sigma_{bx,Sd} + \sigma_{mx,Sd} \qquad \text{/III.43/}$$

$$\sigma_{y,Sd} = -\sigma_{by,Sd} + \sigma_{my,Sd} \qquad \text{/III.41/}$$

At the no-loaded surface of a plate the total stresses are determined with the bending and membrane stresses as follows:

$$\sigma_{x,Sd} = \sigma_{bx,Sd} + \sigma_{mx,Sd} \qquad \text{/III.42/}$$

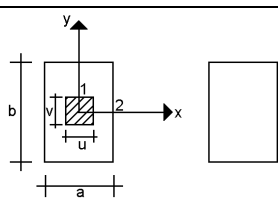$$\sigma_{y,Sd} = \sigma_{by,Sd} + \sigma_{my,Sd} \qquad \text{/III.43/}$$

For a plate the equivalent stress $\sigma_{eq,Sd}$ may be calculated with the stresses given above as follows:

$$\sigma_{eq,Sd} = \sqrt{\sigma_{x,Sd}^2 + \sigma_{y,Sd}^2 - \sigma_{x,Sd} \sigma_{y,Sd}} \qquad \text{/III.44/}$$

The points for which the state of stress are defined in the data tables are located either on the centre lines or on the boundaries, so that due to symmetry or the postulated boundary conditions, membrane shearing stresses τ_m as well as bending shear stresses τ_b are zero. The algebraic sum of the appropriate bending and membrane stresses at the points considered in the data tables gives the values of maximum and minimum surface stresses at these points.
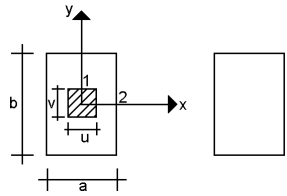
Coefficients k for uniformly distributed loadings

Table III.13 Coefficients k

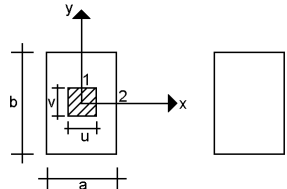| Loading: Central patch loading						
			Boundary conditions: FBC: All edges are rigidly supported and rotationally free. MBC: Zero direct stresses, zero shear stresses			
			Parameters: $\alpha = u/a$; $\beta = v/a$, **b/a = 1**			
$\alpha \times \beta$	P	k_{w1}	$k_{\sigma bxl}$	$k_{\sigma byl}$	$k_{\sigma mxl}$	$k_{\sigma myl}$
0.1×0.1	10	0.1021	1.4586	1.4586	0.1548	0.1548
	20	0.0808	1.2143	1.2143	0.1926	0.1926
	60	0.0485	0.8273	0.8273	0.2047	0.2047
	100	0.0372	0.6742	0.6742	0.1978	0.1978
	150	0.0298	0.5693	0.5693	0.1892	0.1892
	200	0.0255	0.5005	0.5005	0.1823	0.1823
0.2×0.2	10	0.0998	1.0850	1.0850	0.1399	0.1399
	20	0.0795	0.8593	0.8593	0.1729	0.1729
	60	0.0478	0.5108	0.5108	0.1756	0.1756
	100	0.0364	0.3881	0.3881	0.1624	0.1624
	150	0.0293	0.3089	0.3089	0.1505	0.1505
	200	0.0249	0.2614	0.2614	0.1412	0.1412
0.3×0.3	10	0.0945	0.8507	0.8507	0.1144	0.1144
	20	0.0759	0.6614	0.6614	0.1425	0.1425
	60	0.0459	0.3702	0.3702	0.1425	0.1425
	100	0.0351	0.2704	0.2704	0.1300	0.1300
	150	0.0282	0.2101	0.2101	0.1186	0.1186
	200	0.0240	0.1747	0.1747	0.1102	0.1102
0.2×0.3	10	0.0971	0.9888	0.9128	0.1224	0.1288
	20	0.0776	0.7800	0.7101	0.1512	0.1602
	60	0.0468	0.4596	0.4021	0.1488	0.1624
	100	0.0358	0.3468	0.2957	0.1368	0.1512
	150	0.0287	0.2760	0.2307	0.1248	0.1389
	200	0.0245	0.2340	0.1926	0.1152	0.1310

0.2×0.4	10	0.0939	0.9119	0.7961	0.1078	0.1183
	20	0.0755	0.7216	0.6142	0.1320	0.1487
	60	0.0457	0.4235	0.3355	0.1287	0.1516
	100	0.0350	0.3201	0.2435	0.1166	0.1408
	150	0.0280	0.2541	0.1868	0.1045	0.1301
	200	0.0239	0.2156	0.1545	0.0968	0.1213

Table III.14 Coefficients k

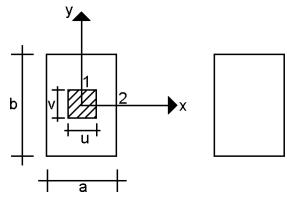| Loading: Central patch loading						
			Boundary conditions: FBC: All edges are rigidly supported and rotationally free. MBC: Zero direct stresses, zero shear stresses			
			Parameters: α = u/a; β = v/a, **b/a = 1.5**			
α×β	P	k_{wl}	$k_{\sigma bxl}$	$k_{\sigma byl}$	$k_{\sigma mxl}$	$k_{\sigma myl}$
0.1×0.1	10	0.1303	1.5782	1.3855	0.1517	0.1921
	20	0.1018	1.3056	1.1373	0.1786	0.2295
	60	0.0612	0.8986	0.7701	0.1824	0.2380
	100	0.0469	0.7411	0.6273	0.1747	0.2295
	150	0.0378	0.6298	0.5287	0.1670	0.2193
	200	0.0323	0.5568	0.4641	0.1594	0.2125
0.2×0.2	10	0.1281	1.1974	1.0049	0.1344	0.1780
	20	0.1007	0.9453	0.7766	0.1555	0.2116
	60	0.0605	0.5783	0.4554	0.1465	0.2103
	100	0.0462	0.4485	0.3457	0.1329	0.1974
	150	0.0372	0.3624	0.2748	0.1208	0.1845
	200	0.0317	0.3111	0.2322	0.1133	0.1742
0.3×0.3	10	0.1229	0.9589	0.7737	0.1074	0.1525
	20	0.0972	0.7405	0.5828	0.1232	0.1818
	60	0.0585	0.4282	0.3161	0.1110	0.1788
	100	0.0449	0.3221	0.2353	0.0988	0.1667
	150	0.0361	0.2550	0.1828	0.0878	0.1535
	200	0.0309	0.2147	0.1525	0.0805	0.1444
0.2×0.3	10	0.1260	1.1037	0.8360	0.1154	0.1657
	20	0.0994	0.8688	0.6322	0.1321	0.1984
	60	0.0598	0.5296	0.3553	0.1168	0.1973
	100	0.0459	0.4114	0.2649	0.1043	0.1853
	150	0.0369	0.3336	0.2082	0.0931	0.1722

α×β	P				
	200	0.0314	0.2877	0.1755	0.0848	0.1624
0.2×0.4	10	0.1235	1.0294	0.7271	0.0993	0.1563
	20	0.0977	0.8101	0.5432	0.1109	0.1877
	60	0.0590	0.4954	0.2983	0.0955	0.1877
	100	0.0453	0.3857	0.2220	0.0826	0.1754
	150	0.0365	0.3148	0.1744	0.0722	0.1630
	200	0.0311	0.2722	0.1468	0.0658	0.1544

Table III.15 Coefficients k

Loading: Central patch loading					
		Boundary conditions: FBC: All edges are rigidly supported and rotationally free. MBC: Zero direct stresses, zero shear stresses			
		Parameters: α = u/a; β = v/a, **b/a = 2**			
α×β	P	k_{w1}	$k_{\sigma bxl}$	$k_{\sigma byl}$	$k_{\sigma mxl}$	$k_{\sigma myl}$
0.1×0.1	10	0.1438	1.6351	1.3560	0.1517	0.1904
	20	0.1154	1.3692	1.1106	0.1773	0.2288
	60	0.0725	0.9633	0.7498	0.1753	0.2438
	100	0.0564	0.7979	0.6112	0.1675	0.2355
	150	0.0456	0.6797	0.5127	0.1596	0.2271
	200	0.0390	0.6028	0.4492	0.1517	0.2188
0.2×0.2	10	0.1414	1.2542	0.9752	0.1326	0.1751
	20	0.1138	1.0078	0.7510	0.1513	0.2104
	60	0.0716	0.6427	0.4410	0.1373	0.2167
	100	0.0555	0.5054	0.3339	0.1232	0.2054
	150	0.0449	0.4134	0.2646	0.1108	0.1928
	200	0.0384	0.3572	0.2230	0.1030	0.1827
0.3×0.3	10	0.1362	1.0227	0.7506	0.1062	0.1517
	20	0.1104	0.8090	0.5615	0.1190	0.1822
	60	0.0698	0.4941	0.3093	0.1024	0.1862
	100	0.0542	0.3789	0.2275	0.0883	0.1753
	150	0.0421	0.3046	0.1783	0.0794	0.1645
	200	0.0374	0.2586	0.1487	0.0717	0.1546
0.2×0.3	10	0.1395	1.1702	0.8164	0.1146	0.1231
	20	0.1129	0.9396	0.6153	0.1262	0.1990
	60	0.0712	0.6003	0.3488	0.1088	0.2044
	100	0.0553	0.4742	0.2611	0.0943	0.1947

α×β	P					
	150	0.0447	0.3901	0.2065	0.0841	0.1830
	200	0.0383	0.3379	0.1744	0.0754	0.1733
0.2×0.4	10	0.1375	1.0976	0.7051	0.0959	0.1551
	20	0.1117	0.8829	0.5267	0.1053	0.1886
	60	0.0706	0.5670	0.2945	0.0851	0.1942
	100	0.0549	0.4496	0.2220	0.0729	0.1849
	150	0.0445	0.3713	0.1765	0.0635	0.1737
	200	0.0381	0.3227	0.1496	0.0554	0.1644

Table III.16 Coefficients k

Loading: Central patch loading						
			Boundary conditions:			
			FBC: All edges are rigidly supported and rotationally free.			
			MBC: Zero direct stresses, zero shear stresses			
			Parameters: α = u/a; β = v/a, **b/a = 2.5**			
α×β	P	k_{w1}	$k_{\sigma bxl}$	$k_{\sigma byl}$	$k_{\sigma mxl}$	$k_{\sigma myl}$
0.1×0.1	10	0.1496	1.6636	1.3463	0.1552	0.1826
	20	0.1235	1.4109	1.1006	0.1811	0.2175
	60	0.0861	1.0428	0.7453	0.1811	0.2374
0.2×0.2	10	0.1470	1.2814	0.9650	0.1359	0.1688
	20	0.1218	1.0491	0.7400	0.1548	0.2000
	60	0.0849	0.7205	0.4363	0.1390	0.2088
0.3×0.3	10	0.1419	1.0504	0.7410	0.1092	0.1443
	20	0.1182	0.8489	0.5519	0.1222	0.1726
	60	0.0827	0.5681	0.3052	0.1014	0.1775
0.2×0.3	10	0.1455	1.1981	0.8056	0.1161	0.1579
	20	0.1210	0.9820	0.6053	0.1294	0.1876
	60	0.0847	0.6806	0.3487	0.1088	0.1982
0.2×0.4	10	0.1434		0.6949	0.0986	0.1469
	20	0.1199	0.9261	0.5168	0.1069	0.1763
	60	0.0844	0.6480	0.2993	0.0849	0.1873

References

Adotte, G.D. (1967). Second–Order Theory in Orthotropic Plates. *Journal of the Structural Division*, Proc. ASCE, 93 (October 1967), pp. 343-362.

Bancila, R.: "Noile norme Europeene: EC 3/2 extras selectiv" Al II-lea Seminar de Poduri "Directii actuale in calculul si prosecturea podurilor", Universitatea "Politehnica" Timisoara, martie 1996, pp. 97-149

Bares, R. and Massonnet, C. (1968). Analysis of beam grids and orthotropic plates by the Guyon-Massonnet-Bares, SNTL, Prague, 1968 and Crosby-Lockwood, London, 1968

Bittner, E. (1938). Momententafeln und Einflussflachen fur Kreuzweise Bewehrte Eisenbetonplatten, Springer, Wien

Boobnov, I.G. (1902). On the Stresses in a Ship's Bottom Plating Due to Water pressure, *Transactions of the Institutions of Naval Architects*, London, Vol. 44

Boussinesq, J.V. (1879). Complements a une etude sur la theorie de l'equilibre et du mouvement des solides elastiques don't certaines dimensions sont tres-petites par rapport a l'autre, *Journal de Mathematiques*, T-5, Paris

Bölcskei, E. (1968). Beton- vasbeton és feszítettbeton hidak (in Hungarian), Tankönyvkiadó, Budapest

BS 5400 (1982). Steel, concrete and composite bridges, Part 3.

Cartledge, P. (1973). Steel box girder bridges. Proceedings of the International Conference, The Institution of Civil Engineers, London, p. 315.

Catalogue. Bridges on the Danube CD-ROM (1998). *International Conference, Regensburg*. Editor-in-Chief: Prof. M. Iványi.

Cauchy, A.L. (1828). De la pression dans un systeme de point materiels, *Excersices de Mathematique*, Paris

Cheung, Y.K. (1968). The Finite Strip Method in the Analysis of Elastic Plates With Two Simply Supported Ends. Proc. ICE, 40, December 1968, p.1

Cornelius, W. (1952). Die Berechnung der ebenen Flächentragwerke mit Hilfe der Theorie der Orthogonal-anisotropen Platte, *Der Stahlbau*, Vol. 2, pp. 21-26, Vol. 3, pp. 43-48, Vol. 4, pp. 60-64.

Domanovszky, S. (1984). Manufacturing and erection of steel structures (in Hungarian), *Mérnöki kézikönyv Vol. II (Palotás, L. editor) Steel structures*, Műszaki Könyvkiadó, Budapest

Dörnen, A. (1955). Stahlüberbau der Weserbrücke Porta, *Der Stahlbau*, p. 97.

ECCS (1985). <<Recommendation for the Fatigue Design of Steel Structures.>> *European Convention for Constructional Steelwork*, Brussels, Publication No.43.

Eibl, J. (1983). Bericht des Ad-Hoc-Ausschusses "Mitwirkende Plattenbreite", Bonn.

Eisel, H., Müller, C. and Sedlacek, G.: *Worked examples to demonstrate the use of design rules of Eurocode 3 – Part 2.*, Institute of Steel Construction, RWTH Aachen, 1995.

ENV 1993-1-7:April 1998. Eurocode 3: Design of steel structures – Part 1-7: Supplementary rules for planar plated structural elements with transverse loading

ESDEP (1994). European Steel Design Education Programme Vol. 10. Plates and Shells, *British Steel*, administered by the Steel Construction Institute

Eurocode 1, Part 3.2 (1992). Traffic Loads on Road Bridges, Draft July 1992, CEN Bruxelles.

Faltus, F. (1927). Lastverteilende Querverbindungen, *II. Int. Tagung für Brückenbau und Hochbau*, Wien, pp. 200-203

Geckeler, J.W. (1928). Elastiuzitastheorie anisotroper Körper, *Handbuch der Physik*, Band VI, Berlin

Gehring, F. (1860). De acquationibus differentialibus quibus aequilibrium et motus laminae crystallinac definitur, Berlin

Guyon, Y. (1946a). Calcul des Ponts Larges a pouters Multiples Solidarisees par des Entretoises, *Annales des Ponts et Chaussees*, No. V, Septembre-Octobre 1946, pp. 553-612.

Guyon, Y. (1946b). Calcul des Ponts-Dalles, *Annales des Ponts et Chaussees*, Vol. 36., pp. 683-718.

Günther, G.H. (1985). Beanspruchung von Stahlbrücken beim Einbau bituminöser Fahrbahnbeläge aufgrund gemessener Temperaturverteilungen, *BAST*, B 3.1-3440.

Günther, G.H., Bild, S. and Sedlacek, G. (1987). Durability of asphaltic pavements on orthotropic decks of steel bridges. *J. Constr. Steel Res.*, 85.

Halász, O., Hunyadi, F. (1959). Ortotrop pályalemezes hidak szerkezeti és számítási kérdései (in Hungarian), Mérnöki Továbbképző Intézet kiadványa, Felsőoktatási Jegyzetellátó Vállalat, Budapest

Hawranek, H. and Steinhardt, O. (1958). Theorie und Berechnung der Stahlbrücken, Springer, Berlin

Huber, M.T. (1914). Die Grundlagen einer Rationellen Berechnung der Kreuzwiese Bewehrten Eisenbetonplatten. *Zeitschrift des Osterreichischen Ingenieur-u. Architeken-Vereines*, Vol. 66, No. 30

Huber, M.T. (1922). Teorya Plyt, Lvov

Huber, M.T. (1923). Die Theorie der Kreuzweise bewehrten Eisenbetonplatten. *Der Bauingenieur*, Nos. 12, 13

Huber, M.T. (1929). Problems der Statik technish wichtiger orthotropen Platten, Warsaw

Huber, M.T. (1950). Theorie de L'elasticite, (in Polish), Cracow, Vol. I,1948, Vol. II. 1950)

Huber, M.T. (1956). Pisma, Tom II., Polska Akademia Nauk, Warszawa

Huber, M.T. (1957). Pisma, Tom III., Polska Akademia Nauk, Warszawa

Iványi, M. (2002). Refurbishment of Steel Bridges, in Mazzolani, F.M. and Iványi, M., editors: *Refurbishment of Buildings and Bridges*, Springer Wien New York, CISM Courses No. 435, pp. 61-150.

Iványi, M., Agócs, Z. Balaz, I. (1990). Torsion of Steel Beams (in Hungarian), Budapest-Bratislava, Mérnöki Továbbképző Intézet, BME.

Johansson, B., Maquoi, R., Sedlacek, G., Müller, C. and Schneider, R.: *Die Behandlung des Beulens bei dünnewardingen, Stahlkonstructionen in ENV 1993-Teil 1,5. (Eurocode 3-1-5)*, Stahlbau 68 (1999), Heft 11.

Johansson, B., Maquoi, R., and Sedlacek, G.: New design rules for plated structures in Eurocode 3, *Journal of Constructional Steel Research*, **Vol.57, No.3**, March 2001, pp. 279-311.

Kahmann, R. (1973). Schweißverfahren bei der Jegsttalbrücke, *Der Bauingenieur*, p. 269.

Karman, Th. (1910). Festigkeitsprobleme in Maschinenbau; Encyklopädie der mathematischen Wissenschaften, Teilband IV. 4, Teubner, Leipzig, p. 348-350.

Koller, I. (2001). Main data of the Danube bridge Szekszárd (In Hungarian) UVATERV.

Köppel, K. and Yamada, M. (1960). Anisotrope Flussbedingung, *Der Stahlbau*, No. 6, June 1960, pp. 173-179.

Kunert, K. (1967). Einige Überlegungen zur Projektierung von Stahlbrücken am Beispiel der Mainbrücke Hocheim, *Der Bauingenieur*, p. 313.

Lechnitsky, S.G. (1947). Anisotropic Plates, 2nd Edition, Moscow (In Russian)

Lechnitsky, S.G. (1963). Theory of Elasticity of an Anisotropic Body, Holden-Day Inc., San Francisco

Leonhardt, F. (1938). Die vereinfachte Berechnung zweiseitig gelagerter Trägerroste, *Die Bautechnik,* pp. 535-557, 648.

Levy, M. (1899). Comptes rendus, Vol.129, pp- 535-539

Lindner, J. and Bamm, D. (1982). Berechnung von orthotropen Platten und Trägerrosten, *Stahlbau Handbuch,* Band 1, Köln, pp. 217-240.

Massonnet, Ch. (1950a). Contribution au calcul des ponts a poutres multiples, *Annales des Travaux,* Publics de Belgique, Juin, Octobre, Decembre.

Massonnet, Ch. (1950b). Methods de calcul des ponts á poutres multiples tenant compte de leur résistance á la torsion, *Publications International Association for Bridge and Structural Engineering,* Vol. 10.

Massonnet, Ch. (1950c). Methods de calcul des ponts á poutres multiples tenant compte de leur résistance á la torsion, *Mémoires AIPC X,* Zurich, pp. 147-182.

Massonnet, Ch. (1955). Le Dimensionnement Pratique Des Ponts a Poutres Multiples et Des Ponts-Dalles en Tenant Compte de Leur Rigidite Torsionelle, *Construczioni in Cemento Armato,* No. 7, Rendiconti e Publicazioni, Milano, pp. 77-114.

Massonnet Ch. (1968). Thin-walled deep plate girders. *Proc. of 8th Congress of the IABSE, New York*, pp. 194-209.

Massonnet Ch. and Maquoi, R. (1973). New theory and tests on the ultimate strength of stiffened box girders in Proceedings, ″Steel box girder bridges″ International Conference. The Institute of Civil Engineers, London, pp. 131-143.

Maquoi, R. (1971). Measurement of the initial deflections of stiffened panels of large box girders (in French). *IABSE Publications*, **31**, Part 2, 141-151.

Maquoi, R. and Massonnet Ch. (1971). Non-linear theory of post-buckling resistance of large stiffened box girders (in French). *IABSE Publications*, Zürich

Maquoi, R. and Massonnet Ch. (1972). Design of plate and box girders for ultimate strength. *Proc. of IABSE Colloquium, London, March 1971*, Leemann, Zürich

Maquoi, R. and Massonnet Ch. (1982). Une evaluation simple de la largeur efficace due au traînage de cisaillement, *Constrùction Métallique*, No. 2.

Nakai, H. and Yoo, C.H. (1988). Analysis and Design of Curved Steel Bridges. McGraw-Hill Book Company

Nather F. (1991). Rehabilitation and Strengthening of Steel Road Bridges. In *Structural Engineering International*, Volume 1, No.3, 24-30.

Patentschrift No. 847014 (1948). Dr. Cornelius/MAN. *Straßenbrücke mit Flachblech*.

Pelikan, W. and Esslinger, M. (1957). Die Stahlfahrbahn – Berchnung und Konstruktion, *MAN Forschungsheft*, No. 7.

Pflüger, A. (1947). About the buckling problem of the anisotropic rectangular plate (in German), *Ing. Arch.* Vol. 16, pp 111-120.

prENV 1993-2:1997. Eurocode 3: Design of steel structures – Part 2: Steel bridges

prENV 1993-1-5:1997. Eurocode 3: Design of steel structures – Part 1-5: General rules – Supplementary rules for planar plated structures without transverse loading

prENV 1993-1-7:1998. Eurocode 3: Design of steel structures – Part 1-7: General rules – Supplementary rules for planar plated structural elements with transverse loading

Pucher, A. (1938). Die Momenteneinflussfelder rechteckiger Platten, No. 90 *der Reihe "Deutscher Ausschussfur Eisenbetonbau"*, Wilhelm Ernst u. Sohn, Berlin

Roloff, M. (1942). Erfahrungen mit Leichtfahrbahnen strählerner Reichsautobahnbrücken, *Die Bautechnik*, p. 433.

Roik, K. and Sedlacek, G. (1970). Erweiterung der technischen Biege- und Verdrehtheorie unter Berücksichtung von Schubverformungen, *Die Bautechnik*, 47.

Rostovtsev, G.G. (1940). Calculation of a thin plate sheeting supported by rods (in Russian) Tondy, Leningrad, Inst. Juzkererov, Grazhdanskogo Vasdaghnogo Flota, No. 20.

Rostovtsev, G.G. (1968). in Anisitropic plates by Leknitskii, S.G., Gordon and Breach, p. 291.

Schaechterle and Leonhardt (1936). Leichte Fahrbahndecken auf stählernen Straßenbrücken, *Die Bautechnik*, p. 246.

Sedlacek, G. (1972). Bemerkenswerte Straßenbrücken aus Stahl der letzten 10 Jahre, *Technishe Mitteilungen Krupp*, p. S. 53.

Sedlacek, G. (1982). Zweiachsige Biegung und Torsion, *Stahlbau Handbuch Band 1*, Köln.

Sedlacek, G. (1992). Orthotropic Plate Bridge Decks, In Dowling, P.J., Harding, J.E. and Bjorhovde, R., editors: Construction Steel Design. An International Guide, Elsevier Applied Science, London and New York.

Sedlacek, G. and Bild, S. (1984). Simplified rules for the determination of the effective width of bridge decks caused by shear lag ″Verba volant, scripta manent″ Imprimeries Cérés s.p.r.-Liége, pp. 333-348.

Sedlacek, G. and Merzenich, G. (1991). Gutachten zu den Lastannahmen für die Verbreiterung der Rheinbrücke Mainz-Weisenau, RWTH Aachen (unpublished).

Skaloud, M. and Novotny, R. (1965). Post-critical behaviour ofan initially curved uniformly compressed panel, reinforced in its middle by longitudinal stiffener (in German), *Acta Tech.*, ČSAV, No. 2

Skaloud, M. (1970). Post-buckled behaviour of stiffened webs, Academia Nakladatelstoi Ceskoslovenske Akademie VED, Prague

Szabó, J. and Visontai, J. (1962). Válogatott fejezetek a tartók sztatikája köréből (in Hungarian), Tankönyvkiadó, Budapest.

Tesar, A. (1977), Kovové konštrukcie a mosty, *Moderné ocel'ové mosty, II. čast'* (in Slovak), ES SVŠT, Bratislava.

Troitsky, M.S. (1976). Stiffened Plates: Bending, Stability and Vibrations, Elsevier Scientific Publishing Company, Amsterdam-Oxford-New York, pp. 114-122.

Troitsky, M.S. (1987). Orthotropic Bridges. Theory and Design, The James F. Lincoln Arc Weld Found, Cleveland, Ohio.

Visontai, J. (1965). V. Ortotrop lemezek számításának menete (in Hungarian) (Dénes E., Korányi I., Tóth B., Visontai J.: Acélhidak), Mérnöki Továbbképző Intézet Kiadványa, Tankönyvkiadó, Budapest, pp. 145-170.

Weitz, F.-R. (1966). Entwicklungstendenzen des Stahlbrückenbaus am Beispiel der Rheinbrücke Wiesbaden-Schierstein, *Der Stahlbau*, Vol. 35, No. 10, pp. 289-301, Vol. 12. pp. 357-365.

Weitz, F.-R. (1974). Neuzeitliche Gesichtspunkte im schweiβenden Brückenbau, *Der Stahlbau*, Vol. 43, No. 3, pp. 73-81.

Weitz, F.-R. (1975). Entwurfsgrundlangen und Entscheidungskriterien für Konstruktionssysteme im Groβbrückenbau unter besonderer Berücksichtigung der Fertigung, *Dissertation*, Darmstadt.

Voigt, W. (1910). Lehrbuch der Kristallphysik, Lepzig

Wolchuk, R. (1990). Lessons from weld cracks in orthotropic decks on three European bridges. *Journal of Structural. Engineering*, 75.

Wolmir, A.S. (1962). Flexibile plates and shells (in German), VEB für Bauwesen, Berlin

Zienkiewicz, O.C. and Cheung, Y.K. (1964). The Finite Element Method for Analysis of Elastic Isotropic and Orthotropic Slabs, Proc. Int. Civ. Eng., London, Vol. 28, August 1964.